Maggots and Wound Healing: the Effects of *Lucilia sericata* Larval Secretions upon Interactions between Human Dermal Fibroblasts and Extracellular Matrix Proteins

Adele Jayne Horobin MSc, BSc (Hons)

Thesis submitted to the University of Nottingham for the degree of Doctor of Philosophy

October 2004

Results presented in this thesis are featured in the following publications:

Horobin A.J., Shakesheff K.M. and Pritchard D.I. (2004). Maggots and wound healing: an investigation of the effects of secretions from *Lucilia sericata* larvae upon the migration of human dermal fibroblasts over a fibronectin-coated surface. *Wound Rep. Reg.* [in press].

Horobin A.J., Shakesheff K.M., Woodrow S., Robinson C. and Pritchard D.I. (2003). Maggots and wound healing: an investigation of the effects of secretions from *Lucilia sericata* larvae upon interactions between human dermal fibroblasts and extracellular matrix components. *Br. J. Dermatol.* **148** (5): 923-933.

Horobin A.J., Pritchard D.I. and Shakesheff K.M. How do larvae of *Lucilia sericata* initiate human wound healing? *Eur. Cells Mat.* 2002; **4** suppl. 2: 69.

CONTENTS

CD-ROM featuring time-lapse movies of the two-dimensional assays described within Chapter 4:

'0-1ugmlFN' - Fibroblast migration over a 0.1 μg/ml fibronectin-coated surface.
'1ugmlFN' - Fibroblast migration over a 1 μg/ml fibronectin-coated surface.
'10ugmlFN' - Fibroblast migration over a 10 μg/ml fibronectin-coated surface.
'100ugmlFN' - Fibroblast migration over a 100 μg/ml fibronectin-coated surface.
'1000ugmlFN'- Fibroblast migration over a 1000 μg/ml fibronectin-coated surface.

'10ugmlFN10ES' - Fibroblast migration over a 10 μg/ml fibronectin-coated surface in the presence of 10 μg/ml ES.

'100ugmlFN0-1ES' - Fibroblast migration over a 100 μg/ml fibronectin-coated surface in the presence of 0.1 μg/ml ES.

FIGURES

TABLES

ABBREVIATIONS

AMP	Adenosine monophosphate
ATP	Adenosine triphosphate
bFGF	Basic fibroblast growth factor
BSA	Bovine serum albumin
CAS	Crk-associated substrate
CMFDA	5-chloromethylfluoresceine diacetate
DABCO	1-4 diazabicyclo-2-2-2-octane
DMEM	Dulbecco's modified Eagles medium
DMSO	Dimethyl sulphoxide
DNA	Deoxyribonucleic acid
ECM	Extracellular matrix
EDTA	Ethylenediaminetetraacetic acid
EGF	Epidermal growth factor
ES	Excretions/secretions
FAK	Focal adhesion kinase
FCS	Foetal calf serum
FGF	Fibroblast growth factor
FITC	Fluorescein isothiocyanate
GAG	Glycosaminoglycan
GM-CSF	Granulocyte-macrophage colony-stimulating factor
GTP	Guanosine triphosphate
HA	Hyaluronic acid
HDNF	Human dermal neonatal fibroblasts
HEPES	N-(2-hydroxyethyl)piperazine-N'-(2-ethanesulphonic acid); 4-(2-hydroxyethyl)piperazine-1-ethanesulphonic acid
HPA	Health Protection Agency
IGF	Insulin-like growth factor
IL-1	Interleukin-1
IL-6	Interleukin-6
KGF	Keratinocyte growth factor
MMP	Matrix metalloproteinase
MRSA	Methicillin resistant *Staphylococcus aureus*
MWCO	Molecular weight cut-off
NNIS	National Nosocomial Infections Surveillance
PAI-1	Plasminogen activator inhibitor type 1
PAR	Proteinase activator receptor
Pax	Paxillin
PBS	Phosphate buffered saline
PDGF	Platelet-derived growth factor
PG	Proteoglycan

PI	Propidium iodide
PPi	Inorganic phosphate
RT	Room temperature
SDS	Sodium dodecyl sulphate
SDS-PAGE	Sodium dodecyl sulphate-polyacrylamide gel electrophoresis
Src	Serine family kinase
Tal	Talin
TCA	Trichloroacetic acid
TGF-α or -β	Transforming growth factor-alpha or -beta
TIMP	Tissue inhibitor of matrix metalloproteinase
TNF-α	Tumour necrosis factor-alpha
tPA	Tissue plasminogen activator
uPA	Urokinase plasminogen activator
uPAR	Urokinase plasminogen activator receptor
v/v	Volume per unit volume
VEGF	Vascular endothelial growth factor
Vin	Vinculin

ABSTRACT

The introduction of necrophagous fly larvae (maggots) into chronic wounds for the purpose of inducing healing is an ancient practice that has recently undergone a renaissance in Western medicine. Through clinical observations, maggots are broadly recognised to debride the wound of necrotic tissue, cleanse the wound of infection and promote granulation tissue formation. Despite such recognition, little research at the biological level has been undertaken to identify the mechanisms by which maggots accomplish such feats.

The dermal fibroblast is a major cellular component of granulation tissue and as such, its migration into the wound plays a vital role in new tissue growth. Fibroblast migration is directed by the composition of the extracellular matrix. Maggot secretions contain proteolytic enzymes that are active against a variety of extracellular matrix proteins which are present at the wound site. Hence, this thesis focused upon the effects of maggot secretions on human dermal fibroblast adhesion and migration in the presence of common extracellular matrix proteins. This was with the aim of elucidating the mechanisms by which maggots stimulate tissue formation within the wound and from there, developing new products that may be used to promote wound healing.

Experiments showed that maggot secretions modulated fibroblast adhesion to tissue culture plastic surfaces and to surfaces coated with collagen and particularly fibronectin. Modification of the protein-coated surface by enzymes present within the secretion appeared to play a role. Fibroblast migration upon a fibronectin-coated surface was enhanced in the presence of maggot secretions. The same also occurred in the presence of a higher concentration of secretions when the cells were located within a three-dimensional environment comprising collagen gel and fibronectin. Evidence suggested that this may have been associated with enhanced matrix re-modelling.

ACKNOWLEDGEMENTS

First and foremost I would like to thank my supervisors, Professor Kevin Shakesheff and Professor David Pritchard, for their support, encouragement and guidance throughout the course of my PhD. I would also like to acknowledge the Engineering and Physical Sciences Research Council whose funding made this project possible. Many thanks go to Dr Susan Anderson of Nottingham University's School of Biomedical Sciences for her invaluable expertise with the confocal microscope. I would also like to thank Mr Ian Ward for compiling my confocal images. Thanks also go to past and present members of the Tissue Engineering group for their friendship and advice. In particular, I would like to thank Dr Richard Pearson for assisting me with microscopy and image analysis, Dr Sarah Dexter for introducing me to the ATP assay, Dr Lisa Riccalton-Banks for training me in cell culture and Dr Felicity Rose for her advice and guidance. Special thanks go to Dr Sandra Woodrow for introducing me to the delights of maggot wrangling!

I would also like to thank my family for their support and encouragement. I would especially like to thank Edward for being a willing proof-reader and for unwittingly lending me his computer for a year. At last, you can upgrade it to XP and we can go on holiday again!

CHAPTER 1

Introduction

It has been recognised for hundreds of years that wounds infested with necrophagous fly larvae (maggots), tend to heal more quickly and with less complications than non-infested wounds (Thomas *et al.*, 1996; Hinshaw, 2000). Although reports of the deliberate introduction of maggots into infected and gangrenous wounds followed by successful healing date back to ancient times, Western medicine has only adopted this practice since the mid-nineteenth century (Thomas *et al.*, 1996; Root-Bernstein and Root-Bernstein, 1999; Hinshaw, 2000). Sterile larvae of the *Calliphoridae* family, specifically *Lucilia sericata* (greenbottle blowfly) and *Phormia regina* (blackbottle blowfly), are used in hospitals today (Hinshaw, 2000) in what is now euphemistically referred to as 'larval therapy', 'maggot debridement therapy' or 'biosurgery' (Sherman *et al.*, 2000).

Clinical observations of such larvae stimulating wound healing are widespread (Thomas *et al.*, 1996; Church, 1999; Wolff and Hansson, 1999; Bonn, 2000; Sherman, 2000; Sherman, Hall and Thomas, 2000; Mumcuoglu, 2001; Wollina *et al.*, 2002). However, little research at the biological level has been undertaken to identify the mechanisms by which larvae accomplish this. In conducting this area of research, extensive knowledge is required of skin anatomy and physiology, the normal wound healing process and the reasons behind impaired healing. These areas are introduced below in conjunction with a discussion on the role and function of the human, dermal fibroblast and its interactions with the external environment. As will be shown, this thesis focused on the effects of *L. sericata* larval-derived products upon fibroblasts, as this cell-type plays an influential role in wound healing. Also included is an overview of the methods available for

treating wounds. Current knowledge concerning the effects of 'biosurgery' and the compositions of larval secretions is also presented.

1.1 Anatomy and physiology of the skin

The skin is the largest organ of the body and provides protection against aqueous, chemical and mechanical assaults; bacterial and viral pathogens and ultra-violet (UV) radiation (Wysocki, 2000). It also prevents excessive fluid and electrolyte loss and is responsible for thermoregulation through controlling vasoconstriction, vasodilation and perspiration (Wysocki, 2000). A typical cross-section of skin is composed of three layers: the outer epidermis, which consists of continuous sheets of epithelial cells; the dermis, composed of cells enmeshed within a supportive connective tissue or extracellular matrix (ECM); and the subcutis, consisting of adipose tissue within a framework of fibrous tissue (Fig.1.1) (Maize, 1998).

1.1.1 The epidermis

The epidermis is typically about 75 to 150 μm thick and principally consists of two layers of keratinocytes, that are noted for containing intermediate keratin filaments termed tonofibrils (Cleary, 1996). The lower basal layer consists of cuboidal or columnar-shaped cells from which other cells of the epidermis germinate. The upper layer is composed of stratified sheets of keratinocytes derived from the basal layer, which are held together by desmosomal junctions and continually displaced outwards as new sheets are produced. During their passage to the outer epidermal surface these cells differentiate, becoming progressively cornified, until they are eventually shed by a process called desquamation (Cleary, 1996). By this stage the cells are flat, anucleate, primarily composed of the interfilamentous protein filaggrin and are contained within a chemically resistant, highly insoluble envelope (Cleary, 1996). In this way the body is bestowed with some degree of protection from the outside and water loss from the skin is minimised. The cells are only shed when their desmosome connections with other cells are degraded. Lipid sheets and proteoglycans (PGs) are also found within the

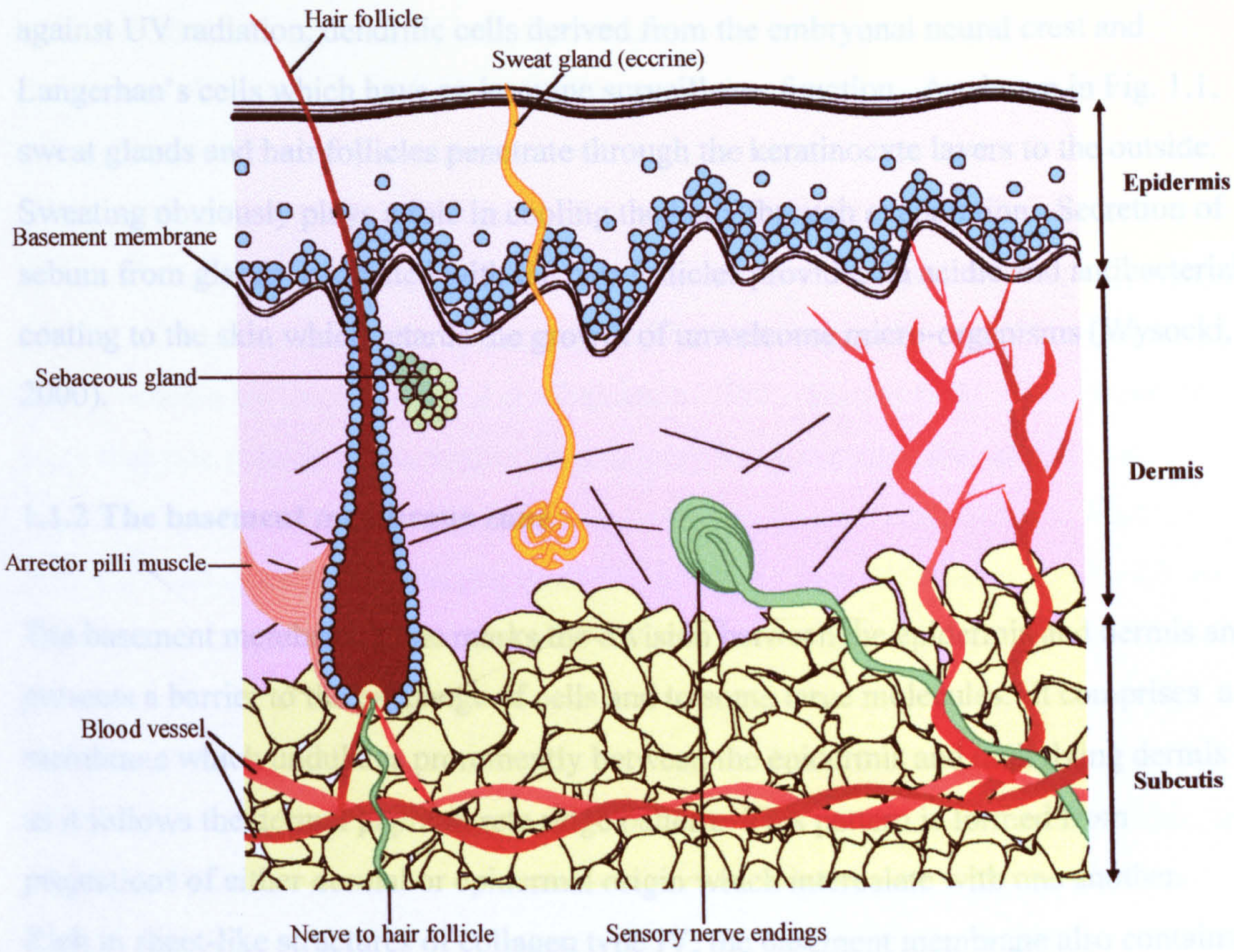

Figure 1.1 Schematic cross-section of the skin, highlighting its three principle divisions of the epidermis, dermis and subcutis. Common structures found within the skin are also shown.

epidermis. Other cells present include melanocytes, which produce pigment to protect against UV radiation, dendritic cells derived from the embryonal neural crest and Langerhan's cells which have an immune surveillance function. As shown in Fig. 1.1, sweat glands and hair follicles penetrate through the keratinocyte layers to the outside. Sweating obviously plays a role in cooling the body through evaporation. Secretion of sebum from glands associated with the hair follicles provides an acidic and antibacterial coating to the skin which retards the growth of unwelcome micro-organisms (Wysocki, 2000).

1.1.2 The basement membrane zone

The basement membrane zone marks the division between the epidermis and dermis and presents a barrier to the exchange of cells and to some large molecules. It comprises a membrane which undulates prominently between the epidermis and underlying dermis as it follows the dermal papillae-rete ridge pattern. This pattern is formed from projections of either dermal or epidermal origin which intercalate with one another. Rich in sheet-like structures of collagen type IV, the basement membrane also contains the glycoprotein laminin, heparan sulphate PG (perlecan) and chondroitin 6-sulphate PG (Timpl *et al.*, 1981; Fine and Couchman, 1988; Cleary, 1996). Basal keratinocytes adhere to this membrane through attachment plaques called hemidesmosomes. When overlying the dermal papillae, these cells also present numerous finger-like membrane projections, termed serrations, at the epidermal-dermal interface, which not only strengthen their attachment but also play a major role in anchoring the epidermis to the dermis (Cleary, 1996). The basement membrane itself is attached to the underlying dermis via bundles of elastin-like microfibrils which are continuous with elastic fibres in the dermis. Anchoring fibrils composed of collagen type VII reinforce the membrane's attachment with the dermis.

1.1.3 The dermis

The dermis is the thickest layer of the skin, ranging from 2 to 4 mm in depth (Wysocki, 2000). In comparison with the densely cellularised epidermal layer, the dermis is sparsely populated with cells, and as shown in Fig. 1.1, is vascularised and innervated (Wysocki, 2000). It is composed of a network of ECM proteins, in which collagen is

predominant. Collagen is made primarily of proline, glycine, hydroxyproline and hydroxylysine and forms triple helical structures owing to repetitive Gly-X-Y motifs, common to all collagens (Eckes, Aumailley and Krieg, 1996). So far, 19 different collagen types have been identified according to their chain lengths, number of collagenous domains (the repetitive motifs) and their content of noncollagenous regions (Eckes, Aumailley and Krieg, 1996). Endowing the skin with tensile strength, the fibrillar collagens form fibres, each composed of three long, uninterrupted protein chains which adopt a triple helical conformation. Each chain or fibril is composed of more than one collagen type, with collagen type I being the principal component, contributing around 85 % to 90 % of dermal collagen (Smith, Holbrook and Madri, 1986). Lesser amounts of collagen types III (8 % to 11 % contribution) and V (2 % to 4 % contribution) are also present (Smith, Holbrook and Madri, 1986). Very small quantities of other collagens are associated with the fibrils but do not share the long, uninterrupted triple helices of the fibrillar collagens. These include collagens type XII and type XIV (Smith, 2001). Elastin is another fibril-forming protein present within the matrix. Like collagen, elastin contains high amounts of proline and glycine, but does not however contain significant amounts of hydroxyproline (Wysocki, 2000). As such, elastin takes on a different structure, adopting coil or spring-like formations which can be stretched and, when released, returned to their original conformations (Wysocki, 2000). This characteristic provides the skin with its elastic recoil and prevents it from being permanently reshaped.

Within the dermis, proteoglycans (PGs) comprise what is often referred to as 'ground substance', or the matrix occupying the space between collagen and elastin fibres (Wysocki, 2000). The varieties of PGs present display a number of different glycosaminoglycan (GAG) chains, including heparan sulphate, chondroitin sulphates A, B and C, and keratan sulphate (Gallo, 2000). The core proteins of the PGs locate the GAG chains to specific locations, which are orientated according to the positioning of cells. For example, syndecan is a cell membrane-intercalated proteoglycan which carries both heparan sulphate and chondroitin sulphate chains (Harris, Leigh and Navsaria, 2001). Small leucine-rich decorins, which carry dermatan sulphate and chondroitin sulphate (Iozzo, 1998), are located within the extracellular spaces (Gallo, 2000). The collagen-proteoglycan-elastin network is interlinked and reinforced by a large and complex group of glycoproteins, of which the most common is fibronectin

(Wolfe, 1995). Fibronectin is widespread throughout the ECM and through its multiple binding sites (Fig. 1.2) forms extensive networks among the collagens and PGs.

The dermis can be divided into papillary and reticular regions. The papillary dermis lies immediately beneath the epidermis and is so named because of its projections which fit in between opposing projections from the epidermis, so forming the papillae rete-ridge pattern. The dermal papillae contain capillary loops which provide oxygen and nutrients to the epidermis via the basement membrane zone. Although the demarcation between regions is not distinct, the papillary region contains smaller collagen and elastin fibres and a greater proportion of ground substance than the reticular region (Wysocki, 2000). The reticular region forms the base of the dermis and is extensively vascularised (Wysocki, 2000).

The fibroblast is the predominant cell-type resident within the dermis. This cell synthesises dermal collagens, PGs, elastin and other ECM proteins and has an extensive role in wound healing. Other cells present include phagocytic dendritic cells which contain antigenic markers. Macrophages, derived from circulating monocytes, are also present and when activated they partake in various immune functions. They also play an important role in mediating many aspects of wound healing. Lymphocytes and mast cells which contain histamine and heparin as well as function in a host of dermal inflammatory processes are also present. (Maize, 1998).

1.1.4 The subcutis

The subcutis or hypodermis attaches the dermis to underlying structures and provides blood vessels which lead on to the dermis. Composed primarily of adipose tissue, the subcutis also provides insulation for the body, energy reserves and cushioning from external mechanical impacts. In addition, it adds to the mobility of the skin over underlying structures such as muscle and bone.

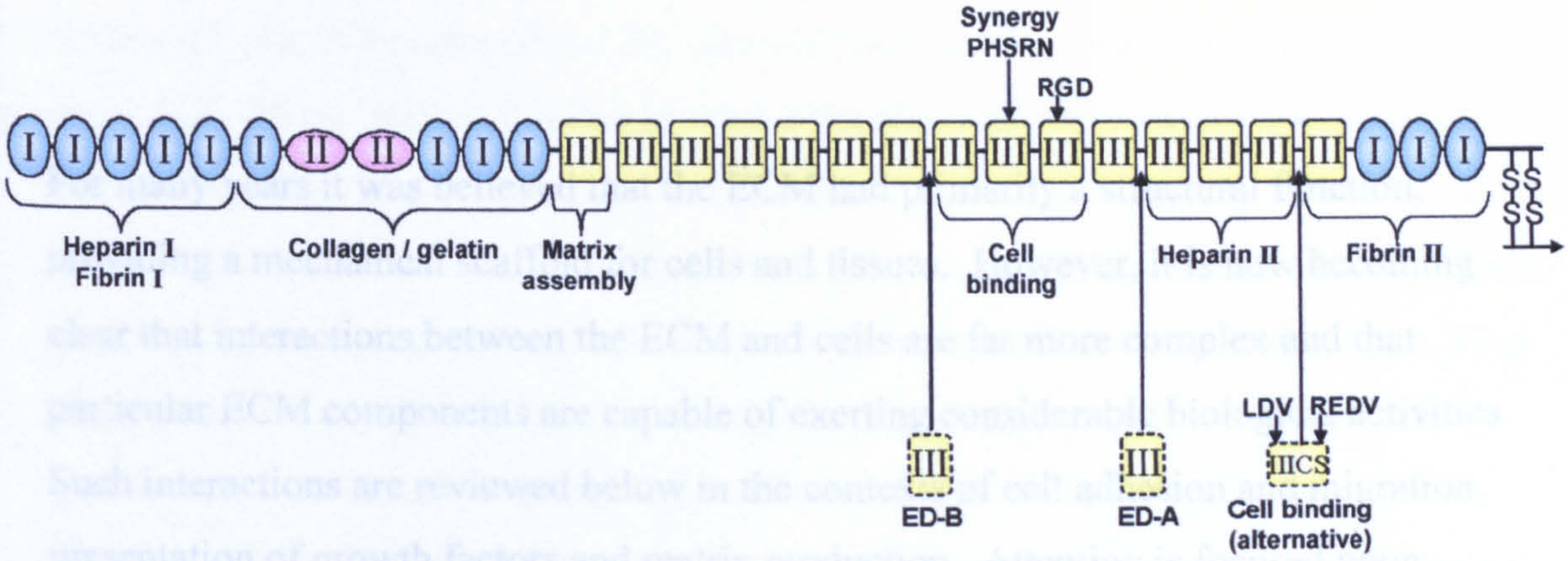

Figure 1.2 Structural map of fibronectin showing homologous repeats. Fibronectin is dimer, with each subunit linked via a pair of carboxyl-terminal disulphide bonds. Each subunit is composed of multiple repeats of three types of structural modules termed types I, II or III. Functional binding domains are as indicated. As shown, fibronectin can bind to heparin via either of two functional domains. These also bind to heparan sulphate GAG chains located on cell membranes. The strongest heparin binding site is located towards the carboxyl-terminal end of the molecule (Heparin II). The heparin I domain also interacts with fibrin and together with the Fibrin II domain, allows high concentrations of fibronectin to be located within the fibrin clot. The close association between fibrin and fibronectin is thought to facilitate cellular interaction with fibrin. The collagen domain binds to native collagen and with higher affinity to the denatured or unravelled regions of the collagen molecule (gelatin). The matrix assembly domain facilitates fibronectin fibrillogenesis. The cell binding domain contains the Arg-Gly-Asp-Ser (RGDS) sequence (of which RGD is the most crucial) which binds most cells. Cell binding to RGD is enhanced by interactions with neighbouring synergy sequences such as Pro-His-Ser-Arg-Asn (PHSRN). Units with dotted outlines are inserted within the molecule, where indicated, as a result of alternative splicing of mRNA. These units are type III modules, one of which comprises a portion of the IIICS region. This contains the CS-1 sequence, comprising Leu-Asp-Val (LDV) and the weaker Arg-Glu-Asp-Val (REDV) sequences which are recognised by the $\alpha 4\beta 1$ receptor in fibroblasts. Splice variants tend to be lacking in plasma fibronectin, but are produced by wound macrophages and are believed to modulate fibroblast phenotype (refer to Chapter 6.4). (Taken from Yamada and Clark, 1996).

1.2 Interactions between cells and the extracellular matrix

For many years it was believed that the ECM had primarily a structural function, providing a mechanical scaffold for cells and tissues. However, it is now becoming clear that interactions between the ECM and cells are far more complex and that particular ECM components are capable of exerting considerable biological activities. Such interactions are reviewed below in the contexts of cell adhesion and migration, presentation of growth factors and matrix production. Attention is focused upon interactions involving human, dermal fibroblasts.

1.2.1 Cell adhesion and migration

The survival of 'anchorage-dependent' cells is dependent on their adhesion to suitable protein substrates (Stoker *et al.*, 1968; Benecke *et al.*, 1978). Within the skin, anchorage-dependent cells such as dermal fibroblasts and basal keratinocytes adhere to and migrate along ECM structural proteins such as collagen, fibronectin, laminin and vitronectin. Cell adherence is principally mediated through the integrin family of cell surface receptors. Integrins are composed of two transmembrane glycoprotein subunits, alpha (α) and beta (β), which are non-covalently bonded on the extracellular side, forming a heterodimer. There are a number of different isoforms for each subunit owing to alternative splicing of the precursor mRNA molecules (Yamada, Gailit and Clark, 1996). Binding is dependent on the recognition of short peptide sequences (ligands) present within the protein substrate. For example, the cell binding domain of fibronectin contains the tetrapeptide Arg-Gly-Asp-Ser (RGDS) sequence, which is the primary ligand for fibroblast attachment via the $\alpha_5\beta_1$ integrin (Fig. 1.2) (Pierschbacher and Ruoslahti, 1984; Ruoslahti and Pierschbacher, 1986; Obara, Kang and Yamada, 1988). Binding is also influenced by the three-dimensional configuration of the protein. For example, fibroblasts bind to collagen primarily through $\alpha_1\beta_1$ and $\alpha_2\beta_1$ integrins (Eckes *et al.*, 2000). However, these integrins only recognise the collagen ligand sequence, thought to be Gly-Phe-Hyp-Gly-Glu-Arg (GFOGER), when the protein is within its native, triple helical conformation (Knight *et al.*, 2000).

Once bound to a ligand, the integrin uses its transmembrane organisation to transmit signals into the cytoplasm (Fig. 1.3). Termed 'outside-in' signalling (Yamada, Gailit and Clark, 1996), integrin binding promotes the clustering of integrins and, through associating with various adapter proteins, directs the assembly of actin filaments into larger stress fibres. In turn this initiates more integrin clustering, thus enhancing matrix binding and the strength of cell adhesion in a positive feedback loop. As a result, focal adhesions are formed where aggregates of ECM proteins, integrins and cytoskeletal proteins are assembled (Giancotti and Ruoslahti, 1999). This process is subject to a regulatory force termed 'inside-out' signalling. This is where the tails of the integrin receptors, which are located within the cell cytoplasm, determine the affinity of ligand binding through controlling the assembly of cytoskeletal linkages in response to signals from the outside. The more cytoskeletal linkages that become associated with attachments to the ECM, the more likely it will be that focal adhesions will form and cell adhesive strength will increase (Yamada, Gailit and Clark, 1996).

In addition to organising the cell cytoskeleton around contacts with the outside, integrin clustering also initiates the formation of integrin-growth factor receptor complexes. This results in the partial activation of the growth factor receptors, thus enhancing the cell's response to growth factors such as platelet-derived growth factor (PDGF), epidermal growth factor (EGF) and vascular endothelial growth factor (VEGF) (Porter and Hogg, 1998; Giancotti and Ruoslahti, 1999). There is also evidence to suggest that integrins interact in *cis* with other kinds of transmembrane receptors, which together influence aspects of cell adhesion, motility, metastasis or growth (Porter and Hogg, 1998). Of particular interest is research which suggests that integrins, depending on their state of activation, may form complexes with urokinase plasminogen activator receptor (uPAR) (Porter and Hogg, 1998). uPAR is the cell surface receptor for the serine proteinase urokinase-type plasminogen activator (uPA). Upon binding to uPAR, uPA is activated to convert plasminogen into plasmin (Mignatti *et al.*, 1996). In turn, plasmin degrades fibrin and other ECM proteins and also activates matrix metalloproteinases (MMPs) (Mignatti *et al.*, 1996). Such degradation and activation of other enzymes, particularly if it is localised around bound integrin receptors may promote cell migration through modifying cell adhesion. Indeed, research has shown uPAR to co-localise with integrins at the leading edge of migrating cells (Andreasen *et al.*, 1997), helping the cells to create a path for directed movement through the matrix

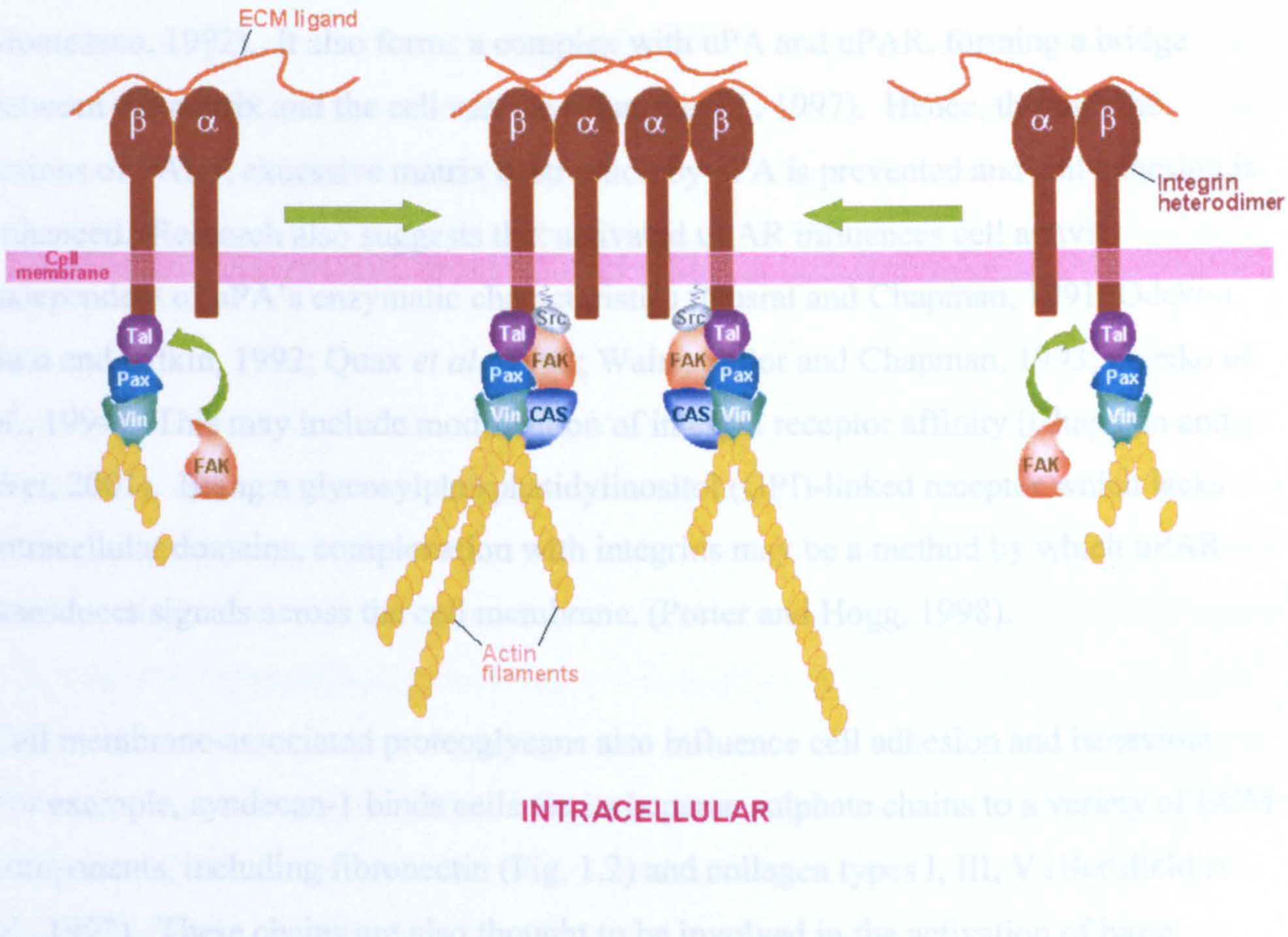

Figure 1.3 Schematic diagram showing the integrin heterodimer and the 'outside-in' signalling generated upon the integrin's binding to a recognised ECM ligand. As integrins bind to the ECM they become clustered in the plane of the cell membrane and associate with a cytoskeletal and signalling complex, which includes and activates various kinases involved in promoting the assembly of actin filaments. The re-organisation of actin filaments into larger stress fibres, in turn, causes more integrin clustering, thus enhancing matrix binding and integrin organisation in a positive feedback loop. Proteins involved in the signalling complex include: Tal, talin; Pax, paxillin; Vin, vinculin; FAK, focal adhesion kinase; CAS, $p130^{CAS}$; Src, serine family kinase. (Adapted from Giancotti and Ruoslahti, 1999).

(Murphy and Gavrilovic, 1999). The matrix does however, attenuate such degradation through storing and presenting plasminogen activator inhibitor type-1 (PAI-1). This molecule has been shown to inhibit the catalytic activity of uPA (Pepper and Montesano, 1992). It also forms a complex with uPA and uPAR, forming a bridge between the matrix and the cell surface (Planus *et al.*, 1997). Hence, through the actions of PAI-1, excessive matrix destruction by uPA is prevented and cell adhesion is enhanced. Research also suggests that activated uPAR influences cell activity independent of uPA's enzymatic characteristics (Nusrat and Chapman, 1991; Odekon, Sato and Rifkin, 1992; Quax *et al.*, 1992; Waltz, Sailor and Chapman, 1993; Gyetko *et al.*, 1994). This may include modification of integrin receptor affinity (Chapman and Wei, 2001). Being a glycosylphosphatidylinositol (GPI)-linked receptor which lacks intracellular domains, complexation with integrins may be a method by which uPAR transduces signals across the cell membrane. (Porter and Hogg, 1998).

Cell membrane-associated proteoglycans also influence cell adhesion and behaviour. For example, syndecan-1 binds cells via its heparan sulphate chains to a variety of ECM components, including fibronectin (Fig. 1.2) and collagen types I, III, V (Bernfield *et al.*, 1992). These chains are also thought to be involved in the activation of basic fibroblast growth factor (bFGF) at the cell surface and are believed to act as co-receptors with integrins (Rapraeger, Krufka and Olwin, 1991; Bernfield *et al.*, 1992; Oksala *et al.*, 1995; Woods and Couchman, 1998; Turnbull, Powell and Guimond, 2001). Dermatan sulphate is also involved in activating cellular response to bFGF and has been implicated in fibroblast proliferation, indicating roles for other GAG side chains in modifying cell behaviour (Penc *et al.*, 1998; Denholm *et al.*, 2000).

Successful cell migration through the ECM involves a fine balance between matrix degradation and re-modelling, allowing a path to be forged, and maintenance of the matrix fibrillar structure, providing a substrate upon which cells can adhere and generate leverage for movement. Too much degradation yields a matrix which is lacking in points of adhesion and the scaffold necessary for directing cell movement. Too little degradation, and the cells are held fast to the substrate, unable to release themselves from the matrix. Cells such as fibroblasts express a number of different proteolytic enzymes to modify the surrounding matrix. These include serine proteinases such as uPA, which as discussed above, activates plasminogen and MMPs (Ellis *et al.*,

1993; Behrendt *et al.*, 1993). uPA is secreted as an inactive zymogen (pro-uPA) which is activated by trace amounts of plasmin (Mignatti *et al.*, 1996). Once activated, a positive feedback loop is initiated, where uPA generates more plasmin, which in turn, activates more pro-uPA. This zymogen also binds to cell-bound uPAR, where it is then activated, thus localising matrix degradation around the cell. As the actions of uPAs are regulated by the uPA/uPAR/PAI-1 complex (Planus *et al.*, 1997) and cells which secrete uPA also secrete its inhibitor (Mignatti *et al.*, 1996), serine proteinase activity is under fine control.

Fibroblasts also secrete MMPs to modify the matrix. MMPs are a family of genetically-related zinc-dependent proteases that collectively degrade most components of the ECM, with distinct specificities (Lambert *et al.*, 2001). Hence, the collagenases target native collagens in triple helical conformations, while the gelatinases degrade collagens following their unravelling by the actions of collagenases. The stromelysins target the basement membrane, including glycoproteins and proteoglycans. The matrilysins have a very broad specificity, while the metalloelastases target elastin (Mignatti *et al.*, 1996). Like uPA, MMPs are secreted as inactive zymogens which are then activated either auto-catalytically, by other MMPs or by a number of serine proteinases including plasmin, trypsin, neutrophil elastase and mast cell chymase (Mignatti *et al.*, 1996; Lambert *et al.*, 2001). Tissue-derived inhibitors (TIMPs) block the actions of MMPs, thus providing a method of controlling proteolysis.

Release of proteolytic enzymes not only facilitates the cell to alter its adhesion to the matrix and forge a path for movement. The resulting controlled degradation of the matrix also releases peptides which display various bioactive properties, affecting cell adhesion, migration and proliferation. For example, RGD peptides cleaved from fibronectin display independent cell adhesive properties (Pierschbacher and Ruoslahti, 1984), while a peptide from the carboxy-terminal heparin-binding domain of fibronectin promotes focal adhesion formation (Woods *et al.*, 1993). A fibronectin peptide containing the PHSRN sequence, which acts synergistically with the RGD sequence in cell binding (Fig. 1.2), appears to exert a chemotactic response from fibroblasts, enhancing ECM invasion within the wound (Livant *et al.*, 2000). Migration-promoting properties have also been observed with the gelatin binding domain of fibronectin (Schor *et al.*, 1996). Cathepsin D digests of fibronectin have been shown to promote

deoxyribonucleic acid (DNA) synthesis, thereby stimulating proliferation (Humphries and Ayad, 1983). In addition, actions of bacterial and mammalian collagenases have been shown to release peptides from collagen which exhibit chemotactic activity for fibroblasts and other cells (Postlethwaite, Seyer and Kang, 1978; Albini and Adelmann-Grill, 1985). Modification of the ECM by cell-derived proteolytic enzymes therefore has far-reaching consequences for cell behaviour.

Upon being stimulated to migrate, cells such as fibroblasts polarise and extend protrusions in the direction of migration. These protrusions are driven by actin polymerisation and develop into large, broad lamellipodia or narrow and pointed filopodia. Lamellipodia form when the cytoskeleton extends a branching 'dendritic' network of actin filaments. These structures are particularly suited to push along a broad length of plasma membrane and provide the basis for directional migration. In filopodia, the actin filaments are organised into long, parallel bundles and these structures may well serve as sensors to explore the local environment (Ridley *et al.*, 2003). Cell protrusion is regulated by the Rho family of small guanosine triphosphate (GTP)-binding proteins (GTPases), including Rac, CDc42, RhoA and RhoG (Ridley *et al.*, 2003). The strength of cell adhesion also regulates cell protrusion, by applying a resistance to flow and by modulating the activity of the GTPase proteins via the transduction of signals from the $\alpha_5\beta_1$ integrin receptor (Cox, Sastry and Huttenlocher, 2001). In order for locomotion to be achieved, the protrusions that the cell makes must be stabilised by attachment to the substratum, allowing traction to be exerted. Areas lying opposite to the protrusion must then detach, allowing further exploration to take place. Hence, the cell must become polarised in its behaviour. Because migrating cells must be able to detach from and exert traction on the substratum, the speed of migration is a biphasic function of the strength of cell adhesion (Ridley *et al.*, 2003). In turn, cell adhesion is determined by the density of adhesive ligands on the substrate (Gaudet *et al.*, 2003), the density of integrin receptors that are expressed and the affinity of these receptors for the substrate ligand (Ridley *et al.*, 2003). It therefore follows that researchers have found intermediate concentrations of adhesive substrate coatings such as collagen or fibronectin to be most favourable for migration (DiMilla *et al.*, 1993; Gaudet *et al.*, 2003).

Studies undertaken by Pelham and Wang (1999), Beningo *et al.* (2001), Munevar, Wang and Dembo (2001a and b), Petroll, Ma and Jester (2003) reveal that migrating cells exert the greatest tractional forces on their substratum attachments near the leading cell edge. These then pull on adhesions towards the rear of the cell, fitting a 'frontal towing model' of cell migration. In fibroblasts, the rearmost adhesions often tether the cell strongly to the substratum, resulting in a long tail to the site of anchorage (Munevar, Wang and Dembo, 2001b; Ridley *et al.*, 2003). The tension that becomes focused at the tail is sometimes sufficient to physically break the linkage between integrin and the actin cytoskeleton, leaving the integrin behind as the cell moves on (Ridley *et al.*, 2003). It may therefore be suggested that the release of cell trailing edges, particularly for fibroblasts, represents a rate-limiting step of migration.

1.2.2 Growth factor presentation and effect

In addition to partially activating growth factor receptors via integrin clustering, the ECM exerts other mechanisms by which it may influence the response of cells to growth factors. Owing to their flexibility and polyanionic character, GAG chains attached to PGs have the ability to bind many different ligands (Gallo and Bernfield, 1996). Such characteristics may not only contribute to heparan sulphate's involvement in activating bFGF at the cell surface (see section 1.2.1). but also allows the ECM to act as a storage depot or reservoir for growth factors. Evidence for this occurring has been found with FGF and TGF-β (Ruoslahti and Yamaguchi, 1991; Vlodavsky *et al.*, 1991; Witt and Lander, 1994). In this way, the presentation of growth factors is controlled by the composition of the matrix. As cells release proteolytic enzymes to remodel the matrix, particularly upon being stimulated to migrate, it therefore follows that the matrix confers a regulatory effect upon cell behaviour through the subsequent presentation of growth factors.

The ECM not only controls the presentation of growth factors but also influences the levels of growth factor expression and how the cells react to growth factor stimulation. For example, the presence of basement membrane down-regulates epithelial cell expression of TGF-β1 (Streuli *et al.*, 1993). The reaction of fibroblasts to PDGF has been shown to be dependent on the composition of the ECM. Xu and Clark (1995)

found that PDGF maximally stimulated α_3 and α_5 integrin subunits, comprising receptors for fibrin and fibronectin ligands, when the cells were embedded within a predominantly fibrin or fibronectin matrix. However, when the cells were within a collagen gel, PDGF stimulated α_2 subunits which recognise collagen ligands.

1.2.3 Production of extracellular matrix

As shown in section 1.2.1 and 1.2.2, the ECM exerts a considerable influence over fibroblast behaviour. However, dermal fibroblasts are responsible for synthesising matrix components and are therefore able to exert control over the composition of the matrix that affects them. Nevertheless, the composition of the matrix present at the time may partly determine which components are subsequently synthesised, thus participating in a dynamic and reciprocal relationship with the cells. For example, during wound healing, the presence of TGF-β initially stimulates fibroblasts to synthesise collagen (Ignotz and Massague, 1986). However, as the collagen matrix becomes abundant, the cells down-regulate collagen synthesis despite the continued presence of stimulating factors such as TGF-β (Clark *et al.*, 1995). The presence of collagen is not the only factor involved in down-regulating collagen production. Studies have shown that the mechanical forces the cells experience within the collagen matrix also exerts an influence, providing an added dimension to fibroblast-ECM interactions (Grinnell, 1994).

1.3 Wound Healing

Wounds that proceed to heal normally are referred to as acute wounds. Wounds that fail to heal or display a considerable delay in healing are referred to as chronic wounds. The characteristics of each type of wound are summarised below.

1.3.1 The acute wound

Normal wound healing involves the co-ordination of a number of dynamic, interactive processes which serve to minimise blood loss, eliminate infection, stimulate dermal and epidermal cells to proliferate, migrate into the wound space, and form new tissue. These may be summarised into three overlapping phases: inflammation, tissue formation and tissue re-modelling (Clark, 1996; Singer and Clark, 1999).

1.3.1.1 Inflammation

Severe tissue injury causes blood vessel disruption, with extravasation of blood constituents (Clark, 1996; Singer and Clark, 1999). This results in the stimulation of blood clotting which occurs following the activation of intrinsic and extrinsic pathways of enzymatic cascades. Here, the activated form of one clotting factor catalyses the activation of the next (Stryer, 1995). The intrinsic pathway begins with the surface activation of Hageman factor (factor XII), following its contact with exposed collagen, basement membrane or negatively-charged surfaces such as heparin or dextran sulphate. The extrinsic pathway is triggered by tissue damage which causes the release of tissue procoagulant factor (Stryer, 1995). These two pathways converge on a sequence of final steps, whereby thrombin is activated to cleave the plasma protein fibrinogen into fibrin. This protein then forms an insoluble cross-linked network, blocking further blood loss and providing a scaffold for cell migration into the wound. As shown in Fig. 1.4, the fibrin clot also entraps platelets which, in addition to providing several clotting factors, also release adhesive proteins, chemotactic factors for blood leukocytes and growth factors such as PDGF and TGF-α and -β to stimulate endothelial, dermal and epidermal cell invasion (Clark, 1996). Once activated, many of the clotting factors stimulate the complement cascade, resulting in the infiltration of inflammatory neutrophils (Fig. 1.4) (Iocono *et al.*, 1998). These cells release enzymes and cytotoxic oxygen free-radicals to remove bacteria and foreign particles. They also release chemotactic factors for recruiting more neutrophils. Further leukocyte chemotactic factors originate from formyl methionyl peptides cleaved from bacterial proteins, products released from damaged cells, and the release of fibrinopeptides as thrombin cleaves fibrinogen to produce fibrin (Clark, 1996).

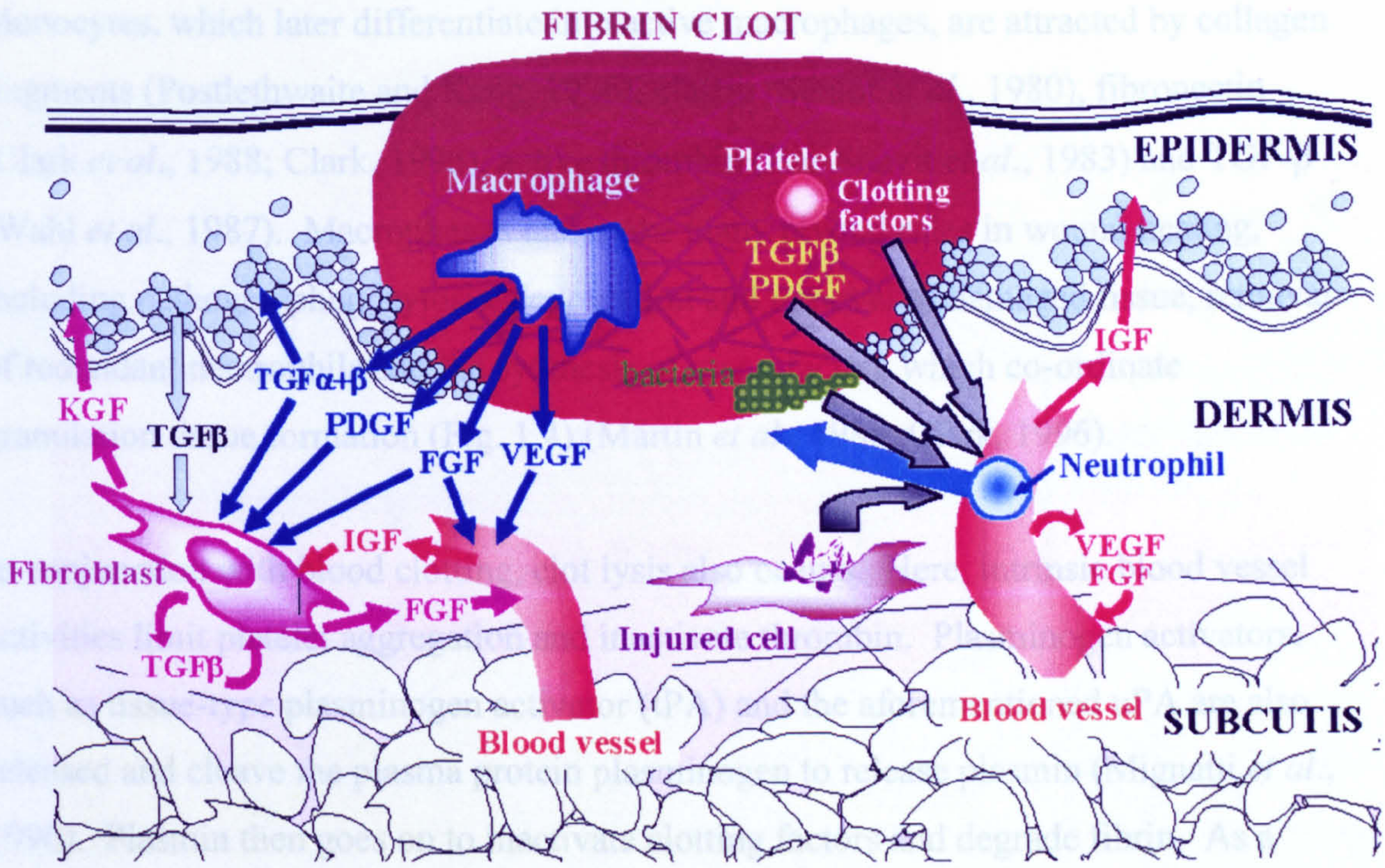

Figure 1.4 Schematic diagram illustrating the main features of the inflammatory phase of wound healing including the fibrin clot, infiltration of neutrophils and macrophages. Also featured are growth factors and clotting factors which are derived from the sources indicated. These stimulate angiogenesis, neutrophil infiltration, and the proliferation and migration of fibroblasts and keratinocytes. FGF, fibroblast growth factor; IGF, insulin-like growth factor; KGF, keratinocyte growth factor; PDGF platelet-derived growth factor; TGFα and β, transforming growth factor alpha and beta; VEGF, vascular endothelial growth factor. Note that re-epithelialisation is beginning to occur, the path dissecting between fibrin clot and underlying dermis.

Monocytes, which later differentiate into active macrophages, are attracted by collagen fragments (Postlethwaite and Kang, 1976), elastin (Senior *et al.*, 1980), fibronectin (Clark *et al.*, 1988; Clark, 1996), active thrombin (Bar-Shavit *et al.*, 1983) and TGF-β (Wahl *et al.*, 1987). Macrophages undertake many pivotal roles in wound healing, including pathogen phagocytosis, degradation and removal of damaged tissue, removal of redundant neutrophils and the synthesis of many factors which co-ordinate granulation tissue formation (Fig. 1.4) (Martin *et al.*, 1988; Clark, 1996).

In conjunction with blood clotting, clot lysis also occurs. Here, intrinsic blood vessel activities limit platelet aggregation and inactivate thrombin. Plasminogen activators, such as tissue-type plasminogen activator (tPA) and the aforementioned uPA are also released and cleave the plasma protein plasminogen to release plasmin (Mignatti *et al.*, 1996). Plasmin then goes on to inactivate clotting factors and degrade fibrin. As a result, clotting remains localised to the wound and vessels remain permeable to immune cells. In addition, the release of fibrin degradation products stimulates further neutrophil and monocyte invasion of the wound (Clark, 1996).

1.3.1.2 Tissue formation

Summarised in Fig. 1.5, tissue formation consists of re-epithelialisation of the wound and the formation of new stroma or granulation tissue. During re-epithelialisation, basal keratinocytes from the wound edge and from skin appendages such as hair follicles undergo marked phenotypic alteration to increase their mobility. Changes include the retraction of intracellular keratin tonofilaments (Clark, 1996; Paladini *et al.*, 1996; Singer and Clark, 1999) and the dissolution of most intercellular desmosomes, releasing physical connections between cells. The cells also develop peripheral actin filaments and dissolve hemidesmosomal links with the basement membrane in order to facilitate movement. All these changes may be stimulated by local release of growth factors such as epidermal growth factor (EGF), TGF-α and keratinocyte growth factor (KGF) as well as the increased expression of growth factor receptors (Singer and Clark, 1999).

Once a migratory phenotype has been adopted, the keratinocytes express collagenase and plasminogen activator to modify the ECM. Migrating along fibronectin and vitronectin glycoproteins, the cells then proceed to locate across the wound space as a

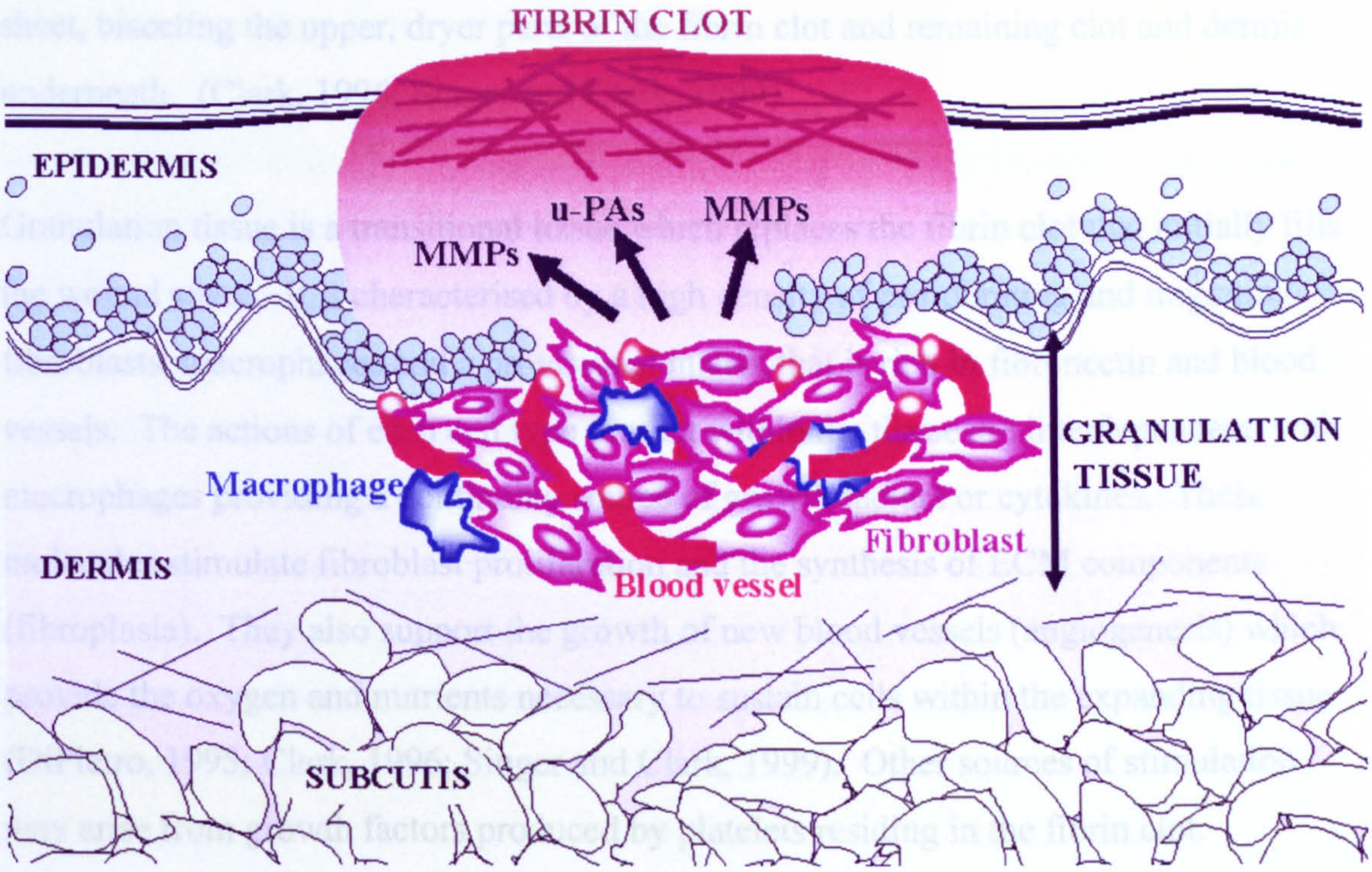

Figure 1.5 Schematic diagram illustrating the main features of the tissue formation phase of wound healing following disinfection of the wound. Included is the degradation of the fibrin clot, thus allowing the influx of new tissue, granulation tissue growth and re-epithelialisation. MMP, matrix metalloproteinase; u-PA, urokinase-type plasminogen activator.

sheet, bisecting the upper, dryer parts of the fibrin clot and remaining clot and dermis underneath. (Clark, 1996; Singer and Clark, 1999).

Granulation tissue is a transitional tissue which replaces the fibrin clot that initially fills the wound space. It is characterised by a high density of proliferating and migrating fibroblasts, macrophages and a provisional matrix that is rich in fibronectin and blood vessels. The actions of each cell type present within the tissue are interdependent, with macrophages providing a continuing source of growth factors or cytokines. These molecules stimulate fibroblast proliferation and the synthesis of ECM components (fibroplasia). They also support the growth of new blood vessels (angiogenesis) which provide the oxygen and nutrients necessary to sustain cells within the expanding tissue (DiPietro, 1995; Clark, 1996; Singer and Clark, 1999). Other sources of stimulation may arise from growth factors produced by platelets residing in the fibrin clot. Fibroblasts also directly contribute, expressing fibroblast growth factor (FGF) which stimulates angiogenesis and an autocrine response.

The newly formed provisional matrix provides a scaffold of fibrin, fibronectin and hyaluronic acid for assisting cell migration (Clark, 1996; Singer and Clark, 1999). As with epidermal cells, plasminogen activators and certain matrix metalloproteinases, such as interstitial collagenase (MMP-1), gelatinase (MMP-2) and stromelysin (MMP-3), are produced by the leading edge of the granulation tissue to cleave a path for cell migration into the fibrin clot (Clark, 1996). As discussed previously (section 1.2.1), the activities of these enzymes against the fibrin and fibronectin-rich matrix of the clot and the granulation tissue may also release bio-active peptides to further enhance fibroblast proliferation and migration, thus promoting the advancement of new tissue into the wound (Humphries and Ayad, 1983; Pierschbacher and Ruoslahti, 1984; Woods *et al.*, 1993; Schor *et al.*, 1996; Livant *et al.*, 2000).

As shown in Fig. 1.4, there is considerable interaction between dermal fibroblasts and the keratinocytes of the epidermis. Both cell types express growth factors to influence the other's behaviour. There is also evidence to suggest that they co-ordinate to re-establish the basement membrane (Hansbrough, 2001).

1.3.1.3 Tissue re-modelling

As keratinocytes migrate from the wound edges and re-form the basement membrane, thus forming a viable epidermis, the underlying granulation tissue undergoes re-modelling. Occurring first at the wound edges, re-modelling incurs a reduction in the density of macrophages and fibroblasts in the granulation tissue through apoptosis. The outgrowth of capillaries is also inhibited, reducing blood flow to the area (Iocono *et al.*, 1998). Some remaining fibroblasts also transform into myofibroblasts. Expressing α-smooth muscle actin, characteristic of contractile smooth muscle cells, myofibroblasts co-ordinate to contract the wound edges together (Clark, 1996). Concurrently, cells within the new epidermis differentiate to form stratified, cornified, keratinocyte layers, thus restoring the permeability barrier (Clark, 1996).

The tissue re-modelling phase also incorporates the transformation of the provisional matrix of the granulation tissue into a more collagenous matrix, as the fine collagen fibre bundles of the granulation tissue are consolidated into thicker masses (Iocono *et al.*, 1998). This is orchestrated by the dermal fibroblast in response to cues from the composition of the matrix itself and from growth factors such as TGF-β (Ignotz and Massague, 1986; Clark *et al.*, 1995). Following the completion of healing, this process leaves behind a relatively acellular, collagenous scar, with reduced need for blood supply (Clark, 1996).

1.3.2 The chronic wound

Impaired healing results in the formation of an open, ulcerated, chronic wound, generally agreed to be hypoxic (Herrick *et al.*, 1996) (Fig. 1.6). Ulcers may be caused by a failure to clear virulent infections. Wound infection prolongs the inflammatory phase of healing, prevents epithelialisation, delays collagen synthesis and increases the production of inflammatory cytokines which may cause further tissue damage (Waldrop and Doughty, 2000). Ulcers may also be caused by diabetes, a condition that is becoming a growing problem in Western societies. Here, wounds may be characterised by reduced collagen synthesis, decreased wound-breaking strength and impaired leukocyte function. These characteristics may be partially explained by increased levels of gelatinases and decreased levels of growth factors, particularly insulin growth factor

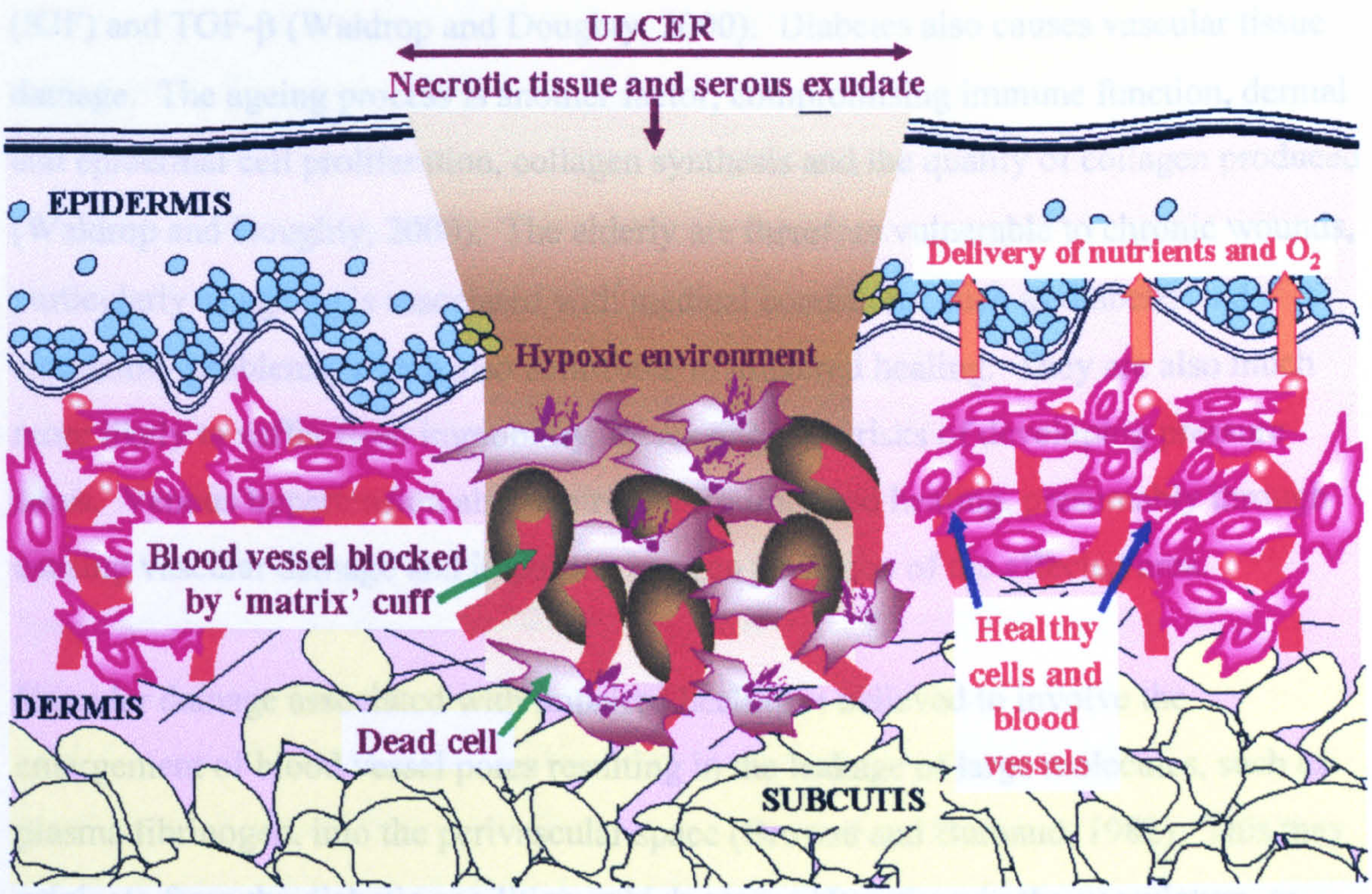

Figure 1.6 Schematic diagram illustrating the main features of the chronic, non-healing wound. The ulcer that forms, contains necrotic tissue and serous exudate. It may also be infected and the tissue is deprived of oxygen and nutrients because the blood vessels have become blocked by matrix cuffs. These cuffs contain polymerised fibrin, fibronectin, laminin and type IV collagen (Herrick *et al*., 1992).

(IGF) and TGF-β (Waldrop and Doughty, 2000). Diabetes also causes vascular tissue damage. The ageing process is another factor, compromising immune function, dermal and epidermal cell proliferation, collagen synthesis and the quality of collagen produced (Waldrop and Doughty, 2000). The elderly are therefore vulnerable to chronic wounds, particularly as ageing is associated with medical conditions, such as diabetes and circulatory problems, which also contribute to impaired healing. They are also much more likely to suffer from immobility, increasing their risks of developing pressure sores. Venous hypertension also contributes to impaired healing, presumably through causing vascular damage and impairing oxygen perfusion of the affected area.

Vascular damage associated with impaired healing is believed to involve the enlargement of blood vessel pores resulting in the leakage of large molecules, such as plasma fibrinogen, into the perivascular space (Browse and Burnaud, 1982). This may originate from the diabetic condition, which causes alterations in the vasculature, or from excessive venous back-pressure. Another theory is that leakage is caused by the accumulation of leukocytes in response to venous stasis, which then release toxic metabolites and proteolytic enzymes, damaging the capillaries (Coleridge Smith *et al.*, 1988). Once leaked from the vessels, fibrinogen is polymerised to fibrin by the plasmin present in the area, producing cuffs around individual capillaries. These cuffs are proposed to inhibit diffusion of oxygen from the blood vessels to the tissue, thus impeding repair (Browse and Burnaud, 1982). However, this has not been conclusively demonstrated (Herrick *et al.*, 1992; Yamada and Clark, 1996) and histological studies show that fibrin cuffs are discontinuous (Pardes *et al.*, 1990), making it unlikely that they inhibit oxygen diffusion alone (Yamada and Clark, 1996). However, fibrin cuffs may become highly cross-linked (Mosesson *et al.*, 1989; Shainoff, Urbanic and DiBello, 1991; Siebenlist and Mosesson, 1992). As a consequence, their porosity may be reduced, decreasing the structures' susceptibility to fibrinolysis and altering fibrin's interactions with cells and cytokines (Yamada and Clark, 1996). In this respect, evidence exists that old venous thrombi become highly cross-linked and resist fibrinolysis (Brommer and van Brocke, 1992).

It has been proposed that fibrin cuffs entrap growth factors, thus inhibiting their perfusion into the wound (Falanga and Eaglestein, 1993) and inducing localised cell proliferation around blood vessels. Indeed, evidence from Pardes *et al.* (1990) and

Herrick *et al.* (1992) suggest that continuous cuffs of mesenchymal cells embedded within fibrin, fibronectin, laminin and type IV collagen, exist around the microvasculature of venous ulcers. Thus, it appears that composite matrix cuffs inhibit diffusion of oxygen, growth factors and other nutrients into the wound, causing cell death and the build up of necrotic tissue and exudate (Fig. 1.6).

In addition to vascular problems, there is considerable evidence to suggest that fibroblast phenotype may also play an important role in impaired healing. For example, other anomolies of ulcerated and chronic wounds include the presence of high levels of fibroblast-derived collagenases (MMP-1) and gelatinases (MMP-2) and low levels of neutral serine proteinases in chronic leg ulcer exudate, compared with normal, acute wound fluids (Weckroth *et al.*, 1996). However, Cook *et al.* (2000) claim that in comparison to normal fibroblasts those excised from chronic wounds produce higher levels of tissue inhibitors of MMP-1 and MMP-2, resulting in decreased levels of active metalloproteinases. Also, when cultured in collagen lattices, these fibroblasts exhibit impaired ECM reorganisation, based on reduced lattice shrinkage. Chronic wound fibroblasts also demonstrate impaired collagen synthesis (Herrick *et al.*, 1996). Here, tissue hypoxia may be partially responsible through inhibiting the hydroxylation of proline residues. Buckley *et al.* (2001) propose that fibroblasts regulate the switch from acute, resolving inflammation, to adaptive immunity and tissue repair. As a result, chronic inflammation occurs when the fibroblasts fail to make this switch, due to disordered behaviour, thus prolonging the survival and retention of inflammatory leukocytes.

1.4 Wound healing therapies

In addition to biosurgery (reviewed in section 1.5), there a number of other treatments that may be applied to chronic wounds in order to facilitate healing. Firstly, debridement is indicated for any wound where necrotic tissue or foreign bodies are present or indeed, if the wound is infected (Ramundo and Wells, 2000). Debridement or the removal of non-viable tissue and foreign matter helps control or reduce the risk of

infection, facilitates visualisation of the wound wall and base, thus aiding wound assessment and may prompt the chronic wound to adjust protease and cytokine levels to those of the acute wound (Ramundo and Wells, 2000). Methods for debridement include the application of exogenous enzymes. For example, collagenases are used to dissolve collagen fibres that secure the slough (moist devitalised tissue) or eschar (dry, firm devitalised tissue) to the underlying wound bed. Papain and its activator urea are used in combination to directly digest the necrotic tissue. Fibrinolysin and a deoxyribonuclease are used together (sometimes in combination with a topical antibiotic) to degrade fibrin and DNA found in the slough (Ramundo and Wells, 2000). Dakin's solution (dilute sodium hypochlorite) may also be used in debridement, denaturing protein to aid its removal by other means (Ramundo and Wells, 2000). Wet-to-dry debridement consists of applying saline-moistened gauze to the wound bed and leaving it to dry, trapping debris from the wound as it does so. However, both Dakin's solution and wet-to-dry debridement represent non-selective treatments, affecting both non-viable and healthy epithelial and granulation tissue. Surgical debridement (removal of necrotic tissue using forceps, scissors or scalpel) is more selective, but some viable tissue may also be removed.

Once it has been cleaned, a variety of different dressings may be applied to the wound, providing an environment to maximise the healing response and prevent contamination. The type of dressing used is dependent on the characteristics of the wound. Although it is necessary to keep the wound moist, thus aiding re-epithelialisation and promoting debridement by autolysis (the body's own normal inflammatory process for removing necrotic tissue), it is sometimes necessary to apply absorbent pads, alginates or foams to wounds producing large amounts of exudate (Dealey, 1999). In so doing, excessive moisture is removed, thus preventing maceration of the surrounding skin. Hydrocolloid dressings made from cellulose, gelatins and pectins swell and become gel-like as they absorb moisture, thus protecting the wound from drying out (Dealey, 1999). Hydrogels, made from insoluble polymers have a large water content and are able to hydrate dry wounds, aiding the removal of eschar (Dealey, 1999).

Recent innovations in wound care include the application of growth factors, as there is evidence to suggest that chronic wounds are deficient in these signalling molecules (Falanga and Eaglestein, 1993). PDGF was the first, and up until 2001, the only

recombinant growth factor to be approved by the United States Food and Drug administration (FDA) for topical application to wounds (Robson and Smith, 2001). Other growth factors including TGF-β, bFGF, EGF, granulocyte-macrophage colony-stimulating factor (GM-CSF) have been tested in clinical trials with varying degrees of success. However, as yet, evidence for the effectiveness of growth factor therapy are limited (Robson and Smith, 2001). This may be due to poor clinical trial design and difficulties in extrapolating laboratory animal data to human patients. Once applied, the chronic wound itself may inactivate the growth factors. For example, tissue hypoxia may inhibit their activities while excess proteolytic activity may destroy them (Robson and Smith, 2001).

Other topical agents that have been applied to wounds with some success include the fibrinolysis promoter tPA, to enhance fibrin removal in venous ulcers (Falanga *et al.*, 1996). Hyaluronic acid (HA) has also been applied using various delivery vehicles (Romanelli, 2001). HA is an important component of the provisional matrix, aiding the migration of fibroblasts within the granulation tissue, promoting the proliferation of keratinocytes and maintaining an extracellular hydrated space in the epidermis (Oksala *et al.*, 1995; Chen and Abatangelo, 1999).

Other developments include the use of skin replacements. Cadaver allograft skin may be applied as a temporary cover, encouraging vascularisation of the wound bed (Hansbrough, 2001). Unfortunately, allograft skin is rejected after a few weeks, is in limited supply, of variable quality and may carry a risk of transferring viruses to the patient (Hansbrough, 2001). It can however, better prepare the wound for accepting subsequent skin autografts. Patient skin biopsies may also be taken, from which keratinocytes may be harvested and then cultured in the laboratory. These can then be grafted back on to the patient's wound as thin sheets of cells or as cells supported on a biocompatible and biodegradeable membrane, some of which contain HA esters (Hansbrough, 2001; Lobmann *et al.*, 2003). However, such grafts do not always take (Kakibuchi *et al.*, 1996), are fragile (Hansbrough, 2001) and the technique requires considerable time for growing the cells up in culture.

Perhaps a more sophisticated approach to skin replacements involves the combined use of fibroblasts, embedded within a supportive matrix, and keratinocytes, creating an

epidermal-dermal composite graft. In full-thickness wounds, it is preferable to supply both epidermal and dermal structures because by definition, full-thickness wounds lack dermis. Supplying a dermal replacement will therefore increase the chances of applied cultured epithelial sheets taking successfully. Human fibroblasts, in contrast to epidermal cells are relatively non-antigenic (Hansbrough, 2001). Allogeneic fibroblasts seeded within a biodegradable synthetic matrix have been applied to wounds with some success, supporting the take of subsequently applied conventional skin grafts (Hansbrough, Doré and Hansbrough, 1992). The cells may do this as they produce matrix proteins and numerous cytokines, encouraging vascularisation of the skin graft (Hansbrough, 2001). The presence of a fibroblast-populated dermal matrix below a layer of keratinocytes has also been shown to promote the formation of basement membrane (Hansbrough, 2001). Epidermal-dermal composites are currently in development (Ghosh *et al.*, 1997; Chakrabarty *et al.*, 2001; Hansbrough, 2001; Bhargava *et al.*, 2004; Huang *et al.*, 2004).

1.5 The use of maggots in wound healing

Currently, the use of maggots in the procedure termed 'biosurgery' is indicated for necrotic and sloughy wounds that have not responded to conventional methods of debridement (Dealey, 1999; Ramundo and Wells, 2000). Biosurgery is broadly recognised to exert the following beneficial effects upon wounds: debridement or the elimination of necrotic tissue; disinfection of the wound through microbial killing; and the active promotion of wound healing (Thomas *et al.*, 1996; Church, 1999; Wolff and Hansson, 1999; Bonn, 2000; Sherman, Hall and Thomas, 2000; Mumcuoglu, 2001; Wollina *et al.*, 2002). Larvae of *Calliphoridae*, such as *L. sericata*, are used in biosurgery because they select only dead tissue for ingestion. Presumably this is related to the fact that in their natural habitat, the adult flies typically lay their eggs on corpses (Root-Bernstein and Root-Bernstein, 1999). Due to this characteristic, *L. sericata* larvae are very effective at debriding the wound. The larvae perform this function via the release of proteolytic enzymes in their excretions/secretions (ES), which degrade and liquefy the necrotic tissue, allowing the larvae to ingest it. As the larvae are very

specific in their targeting of dead tissue and are small enough to reach into most areas of the wound, they may actually debride the wound far more efficiently and precisely than what is achieved through conventional surgical debridement. In addition, it is believed that the continual removal of liquefied tissue and serous exudate by the larvae also aids debridement (Sherman, Hall and Thomas, 2000).

It has long been realised that the natural habitats of *Calliphoridae* larvae, which include corpses and excrement, are saturated with bacteria. Hence, they must be able to tolerate or even eradicate resident pathogens in order to compete and survive (Sherman, Hall and Thomas, 2000). There are a number of ways in which it is believed larvae disinfect wounds. Firstly, they actively ingest bacteria which are then lysed in the gut (Robinson and Norwood, 1933, 1934; Mumcuoglu *et al.*, 2001). Secondly, it has been proposed that ammonia secreted by larvae may be responsible for wound disinfection, as fluids from wounds undergoing 'biosurgery' are alkaline (Bonn, 2000; Sherman, Hall and Thomas, 2000). Another theory is that the copious amounts of exudate that are produced in response to mechanical stimulation by crawling larvae may help flush the wound of some bacteria (Sherman, Hall and Thomas, 2000). In addition, recent studies by Thomas *et al.*(1999) have shown that *L. sericata* larval ES contains anti-microbial activity. This may also be capable of eliminating multi-drug resistant strains of *Staphyloccocus aureus* such as the methicillin-resistant strain (MRSA). In this respect, both Bonn (2000) and Dissemond *et al.* (2002) report that wounds previously infected with MRSA were free of the resistant strain following biosurgery. This is of particular interest because infections caused by antibiotic-resistant strains of certain bacteria are becoming increasingly commonplace. For example, the UK's Health Protection Agency (HPA) has reported an increase in the proportion of patients incubating methicillin-resistant strains of *S. aureus*, from 3 % in 1992 to 43 % in 2002 (HPA, 2003). The US-based National Nosocomial Infections Surveillance (NNIS) System report states that the occurrence of resistant strains of *Enterococci, S. aureus* and *Pseudomonas aeruginosa* in intensive care patients was 47 %, 43 % and 49 % higher in 1999 compared with resistance rates from the preceding five years (NNIS, 1999).

It has been observed by clinical practioners that 'biosurgery' appears to actively stimulate the production of granulation tissue, increasing the rate at which wounds heal (Buchman and Blair, 1932; Wilson, Doan and Miller, 1932; Reames, Christensen and

Luce, 1988; Thomas *et al.*, 1996; Wolff and Hansson, 1999; Sherman, Hall and Thomas, 2000; Mumcuoglu, 2001; Wollina *et al.*, 2002.). This may simply be due to the removal of debris and infection that may have been impairing healing. For example, the proteolytic enzymes that have shown to be produced by larvae, may not only liquefy necrotic tissue for ingestion, but may also degrade ECM elements of composite fibrin cuffs found within ulcerated wounds. This may then initiate the removal of capillary blockages, aid wound perfusion and reduce tissue hypoxia. Indeed, research has demonstrated *L. sericata* larval ES to degrade fibrin, fibronectin, laminin and collagens I, III, IV and V (Chambers *et al.*, 2003). However, many people believe that larvae do actively stimulate wound healing (Sherman, Hall and Thomas, 2000). It has been proposed that granulation tissue responds positively to the physical stimulation of larvae crawling over the wound (Sherman, Hall and Thomas, 2000). The variety of enzymes, allantoin, urea and ammonium bicarbonate by-products of metabolism that the larvae exude may also exert bioactivities upon the wound bed (Robinson, 1937, 1940; Sherman, Hall and Thomas, 2000). For example, trypsin-like enzymes that have been discovered within ES (Chambers *et al.*, 2003) may influence healing through activating membrane-bound protease-activated receptors (PARs). Part of the G-protein-coupled receptor family (Déry and Bunnett, 1999) and expressed by fibroblasts, keratinocytes, endothelial cells and platelets, PARs are activated when their attached ligands are cleaved by trypsin-like enzymes such as thrombin. Once activated, PARs may participate in a number of processes involved in wound healing (Déry and Bunnett, 1999). The proven degradative activity of larval ES enzymes against many ECM components may also influence the wound through the release of bioactive peptides. For example, fibrinopeptides behave as chemotactic factors for neutrophils (Clark, 1996).

Research by Prete (1997) has shown that human fibroblast proliferation actually increases in the presence of *L. sericata* haemolymph and alimentary secretion. In addition, these larval extracts appeared to enhance proliferation of fibroblasts already stimulated by the mitogens EGF and interleukin-6 (IL-6). It may be possible that, in addition to its own direct actions, larval ES may act synergistically with mitogenic factors produced by the body, thus accelerating granulation tissue formation.

1.6 Aims and objectives

As indicated in section 1.3, fibroblasts play many roles in wound healing. They also appear to be implicated in impaired healing. Chronic wounds that have been treated with maggots often demonstrate an improvement in granulation tissue formation. Due to the roles of fibroblasts in tissue formation and impaired healing, this observed effect may at least in part be explained by an alteration in fibroblast activity. Increasing the rate at which fibroblasts migrate into the wound space may be one way by which the advancement of granulation tissue may be improved. As shown in section 1.2.1, the speed of cell migration is related to the strength of cell adhesion to the surface. Hence, the influence of *L. sericata* larval ES upon fibroblast adhesion and migration was investigated in both two-dimensional and three-dimensional environments. This was with the aim of elucidating the mechanisms by which *L. sericata* larvae stimulate tissue formation within the wound and from there, developing new products that may be used to promote wound healing.

CHAPTER 2

Materials and Methods

From the materials and methods utilised for this study, those which were regarded as involving the practice of standard, well-established techniques are included within this chapter. This encompasses mammalian cell culture and passage, microscopy, fluorescent staining of cells for microscopic examination, gel electrophoresis and the coating of surfaces with adhesive, extracellular matrix proteins. Additionally, this chapter includes a description of how *L. sericata* larval excretions/secretions (ES) were collected and characterised, as this applies to all of the impending chapters which present and discuss the results that were obtained during the period of study. Novel methods that were developed for particular pieces of research and therefore not described here are presented in the appropriate chapter.

2.1 Materials

Human, dermal, neonatal fibroblasts were provided by TCS Cellworks®, Claydon, Buckinghamshire, UK and sterile, first instar *Lucilia sericata* larvae were obtained from LarvE™, Surgical Materials Testing Laboratory, Cardiff, UK. Throughout all experimental work, tissue culture grade plastic dishes, plates and flasks were supplied by Nunc, Life Technologies Ltd, Paisley, UK. All other substances were supplied by Sigma®, Poole, Dorset, UK, unless otherwise stated.

2.2 Methods

2.2.1 Fibroblast cell culture

Human, dermal, neonatal fibroblast cells were monolayer cultured within T75 flasks containing standard cell culture medium (Dulbecco's Modified Eagle's Medium (DMEM) (Gibco™ Invitrogen Ltd, Paisley, UK), 10 % foetal calf serum (FCS), antibiotic/antimycotic solution (100 units/ml penicillin G, 100 μg/ml streptomycin sulphate and 0.25 μg/ml amphotericin B) and 2 mM L-glutamine). Cells were incubated at 37°C in a 5 % (v/v) CO_2 humidified atmosphere and cell culture medium was replaced three times a week. Typically, cells were passaged once every 7 to 10 days, when they were approximately 70 % to 80 % confluent. This was undertaken by suspending the cells, using 0.25 % trypsin/ethylenediaminetetraacetic acid (EDTA) (0.02 %), before splitting them 1 in 10 or 1 in 20 within the standard cell culture medium described above. Occasionally, cells were cryopreserved for long term storage. This was achieved by re-suspending freshly trypsinised cells within FCS containing 10 % dimethyl sulphoxide (DMSO). Following re-suspension, cells were immediately transferred to an appropriate freezer and left overnight to reach -80°C. The frozen cells were then stored in liquid nitrogen until required. Cells between passage numbers 5 and 10 were used for experiments.

For experiments, fibroblasts were suspended within serum-free medium. This was to ensure that any larval ES subsequently added to the medium retained its full activity, as explained in section 2.2.2. The cells were also counted, using an Improved Neubauer double cell haemocytometer (Weber Scientific International, W. Sussex, UK), and their viability determined by Trypan blue exclusion. First they were trypsinised, as previously mentioned, and then suspended within standard cell culture medium containing 10 % FCS to neutralise the trypsin. The cells were then pelleted by centrifugation at 180 *g*, using a Sigma® 3K15 laboratory centrifuge. Medium supernatant was then aspirated and cells washed in sterile, phosphate buffered saline (PBS) (pH 7.3) (for formula, see Appendix). Subsequently, cells were pelleted again by centrifugation as before. PBS supernatant was removed and the cells re-suspended

within 5 ml of serum-free cell culture medium. This suspension (20 µl) was then mixed with 60 µl serum-free cell culture medium and 20 µl Trypan blue before being placed into the haemocytometer. Those cells that had absorbed the blue dye were considered non-viable. Minimum acceptable cell viability of the population was taken as 80 %. Once the number and viability of the cells suspended within the serum-free medium had been assessed, an appropriate volume of the cell suspension was taken according to how many viable cells were required. This sample was then diluted with further serum-free cell culture medium to the requisite cell density.

2.2.2 *Lucilia sericata* larval excretion/secretion collection and characterisation

Secretions (hereon in referred to as excretions/secretions (ES) as the methods by which the larvae extrude these substances are uncertain) were collected from sterile, freshly hatched *Lucilia sericata* larvae in an aseptic environment. Approximately four hundred larvae were washed, two to four times, in 1 ml of PBS for 30 minutes at room temperature (RT) to recover ES products. Larvae were rested for one hour between washings. ES collections were pooled and passed through a 0.2 µm pore diameter Minisart high flow syringe filter (Sartorius AG, Goettingen, Germany) before use and stored at -20°C.

The protein concentration and proteolytic activity of each batch of ES collected was determined. Protein content was estimated using the Bio-Rad (Hercules, CA, USA) protein colorimetric assay based upon the Bradford method (Bradford, 1976). Here, a sample of ES was removed from storage and thawed at RT. Bovine serum albumin (BSA), serially diluted with PBS, was also prepared. The ES and each BSA sample were then individually diluted 1 in 10 with PBS, containing 22 % Bio-Rad protein assay dye reagent concentrate, and left for 5 minutes at RT. Absorbance at 595 nm wavelength by each sample was then measured, using a Dynex MRX microtitre plate spectrophotometer, and the results from the BSA samples used to plot a protein standard curve. ES protein concentration was determined by comparison with the standard curve (Fig. 2.1 and Table 2.1). ES proteolytic activity was assessed through the employment of a fluorescein isothiocyanate (FITC)-casein digest assay (Twining, 1984). Here, a sample of the ES collected was diluted 1 in 20 with 0.1 M Tris-HCl buffer (pH 8.5)

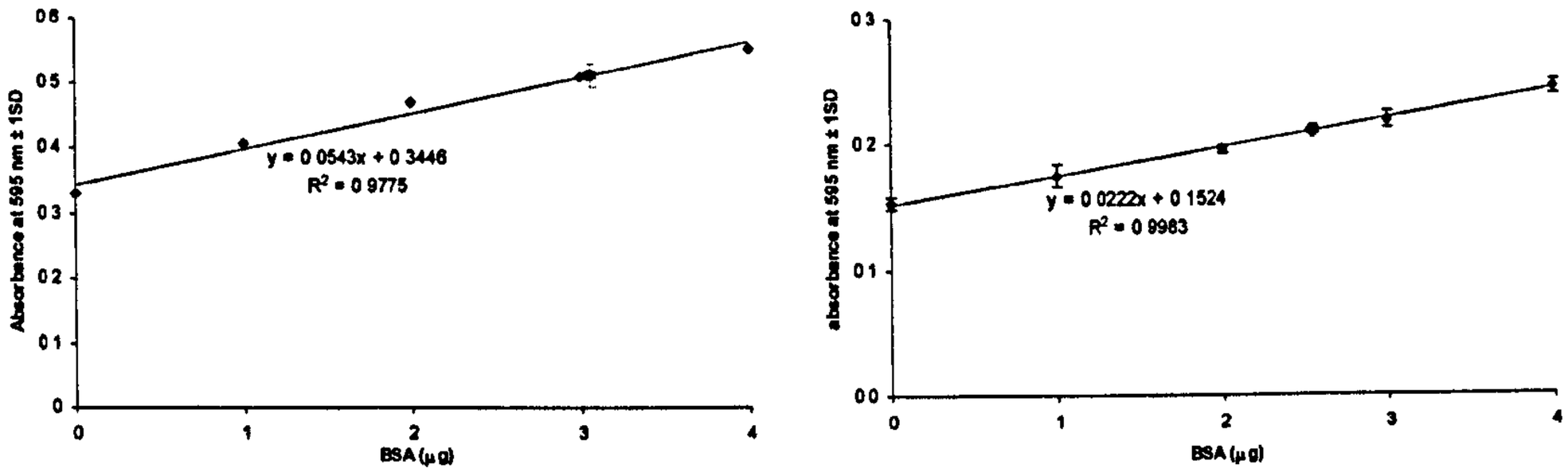

Figure 2.1 Bovine serum albumin (BSA) standard curves used to calculate *L. sericata* larval ES protein concentration. ES batch tested is as indicated above each graph. With the exception of the BSA samples relevant to ES batch A (where only one sample at each BSA concentration was tested), means and standard deviations from three replicates are shown. The equation shown for each linear trendline fitted to each set of BSA standard values was used to calculate mean ES protein concentration. R^2 values for each trendline is shown to illustrate how closely the BSA standard values fitted a linear relationship. Black diamonds refer to BSA absorbance at 595 nm. Grey circles refer to ES absorbance at 595 nm.

ES batch	Mean ES protein concentration (μg/ml)	FITC-casein digest: fluorescence caused by ES activity	ES specific activity (fluorescence/mg ES protein)
A	61.28	273.51	7.14×10^6
B	51.26	247.28	7.72×10^6
C	50.64	208.23	6.58×10^6
D	47.98	295.87	9.87×10^6
E	161.74	610.36	6.04×10^6

Table 2.1 Characterisation of batches of ES collected separately and from different consignments of *L. sericata* larvae. Details include the mean protein concentration of each batch, as estimated using the Bio-Rad protein colorimetric assay. The specific proteolytic activity of the ES collected is also shown. This was calculated using the known protein concentration and the fluorescence generated from the digestion of FITC-casein conjugates. For example, ES batch D yielded a mean fluorescence of 295.87 from FITC-casein digestion. The amount of ES protein responsible for the fluorescence detected, as calculated from the volume of the sample measured, was 0.030 μg. Hence, the fluorescence/mg ES protein was equal to $[1 / (3 \times 10^{-5})] \times 295.87 = 9.87 \times 10^6$.

containing 5.3 % FITC-casein conjugate, made up as previously described (Sarath *et al.*, 1989) (see Appendix), and incubated at 37°C for two hours. 5 % trichloroacetic acid (TCA) was then added and incubated for 1 hour at RT to precipitate undigested protein. Protein precipitate was pelleted and a sample of the supernatant mixed 1 in 10 with 0.5 M Tris-HCl (pH 8.8). Fluorescence was measured using a Dynex MFX microtitre plate fluorometer (485 nm excitation/538 nm emission wavelengths). Fluorescence detected from an ES blank sample was subtracted. The specific activity (fluorescence/mg protein) of the batch of ES tested was then calculated. The results are shown in Table 2.1.

The effect of FCS upon the proteolytic activity of larval ES was also assessed. Here, serum-free cell culture medium was prepared. Cell culture medium containing 20 % FCS was also prepared and then serially diluted at a ratio of 1 : 1 in serum-free medium. 80 µl of each serial dilution or serum-free medium was then mixed with 20 µl of serum-free medium which contained enough ES (from stock A) to provide 1 µg ES protein. For each sample, this yielded final concentrations of 10 µg/ml ES and either 16 %, 8 %, 4 %, 2 %, 1 % or 0 % FCS. This procedure was repeated three times to provide three replicate samples for each FCS percentage tested. The proteolytic activity of ES exposed to each FCS percentage concentration was then measured by following the FITC-casein digest assay protocol described above. For this purpose, each replicate sample was diluted 1 in 20 with 0.1 M Tris-HCl buffer (pH 8.5) containing 5.3 % FITC-casein conjugate (Appendix). As shown in Fig. 2.2, ES exposed to 0.5 % FCS displayed 31.6 % of its proteolytic activity when not exposed to FCS. ES exposed to 8 % and 16 % FCS exhibited 2.1 % and 1.4 % activity respectively, indicating a near-complete inhibition of activity. It was therefore decided to conduct experiments, concerning the effects of ES upon human dermal fibroblasts, in serum-free conditions. This measure was taken to ensure that the cells would be exposed to the full activity of ES.

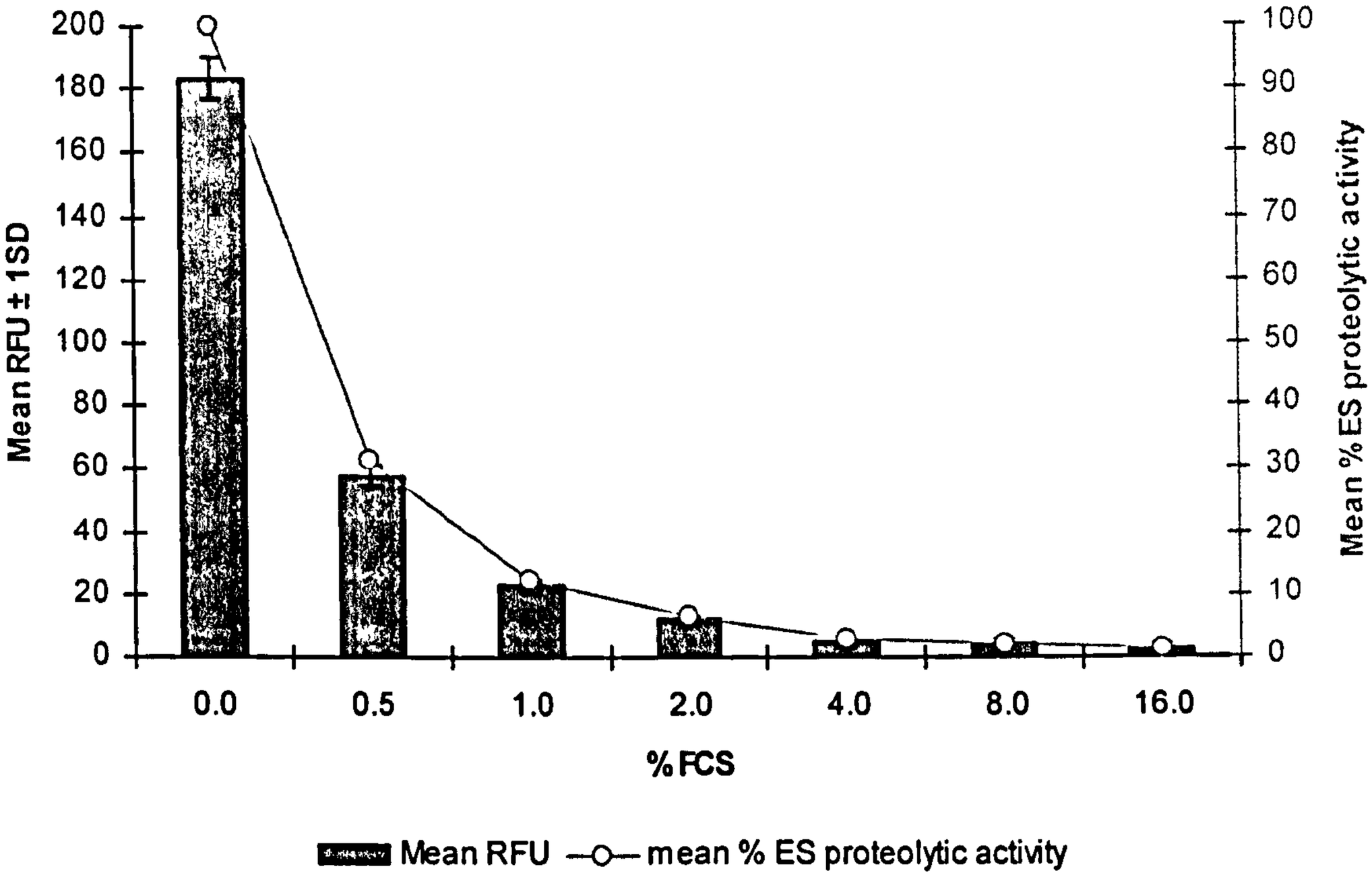

Figure 2.2 Effect of FCS upon ES proteolytic activity, as measured using the FITC-casein assay. Columns refer to the y axis on the left hand side of the graph which plots the relative fluorescence resulting from the proteolytic degradation of FITC-casein due to the actions of ES. The line refers to the y axis on the right hand side of the graph which plots the percentage activity of ES in relation to its activity in the absence of FCS.

2.2.3 Extracellular matrix protein coating of surfaces

Bovine fibronectin from a 0.1 % solution stock or acid solubilised rat-tail collagen type I (Upstate®, Buckingham, UK) from a 0.37 % solution stock was used to coat tissue culture grade plastic well plates. Following dilution with PBS to an appropriate concentration, the protein solution indicated was added to each well and incubated overnight at 37°C. Wells were then aspirated of remaining solution and washed with PBS. Prior to collagen coating, wells were first incubated with 0.01 % poly-L-lysine solution for 15 minutes at RT, before being aspirated, washed twice with PBS and left to air dry.

2.2.4 Microscopy

Within two-dimensional assays, cells were observed through an inverted Leica (Cambridge, UK) DM IRB or DM IRBE microscope, using phase contrast or fluorescence. Images were captured by an attached digital camera (Leica DC 200 or JVC TK C1380) and analysed by Leica Qwin software.

When fluorescence was used, cells were stained with 5-chloromethylfluorescein diacetate (Celltracker™ green CMFDA, Molecular Probes, Eugene, OR), before being incorporated into experiments. Once in contact with a cell, Celltracker™ freely diffuses through the cell membrane and undergoes what is thought to be a glutathione *S*-transferase-mediated reaction within the live cell cytoplasm (refer to company literature). This results in the production of membrane-impermeant glutathione-fluorescent dye adducts and hence the emission of a fluorescent signal that illuminates the whole cell when viewed through standard fluorescein filters. In order to stain the cells, 50 μg of lyophilised Celltracker™ was warmed to RT and then reconstituted in DMSO to 10 mM. Cell culture medium that had been aspirated from a flask of confluent cells to be stained was then added, diluting Celltracker™ to 10 μM. The medium containing the dye was then returned to the cells and incubated for 45 minutes at 37°C in a 5 % (v/v) CO_2 humidified atmosphere. The medium was then replaced with fresh, standard cell culture medium and cells incubated for a further 45 minutes. After this period, the medium was aspirated and the cells washed twice with PBS. They were then trypsinised in the usual way and incorporated into the experiment.

Within three-dimensional assays, cells were observed, as before, through an inverted Leica (Cambridge, UK) DM IRB microscope using phase contrast. They were also imaged using a confocal Leica TCS4D system incorporating a Leica DMRBE upright fluorescence microscope. For this purpose, cells were fixed in 4 % paraformaldehyde (Appendix) for 20 minutes. If they had not already been stained with Celltracker™ green CMFDA, as outlined above, the cells were then stained with FITC-phalloidin conjugate and propidium iodide (PI). This was to allow for confocal imaging of the cytoskeletal actin and nuclei respectively. Staining was achieved by first incubating the fixed cells in ice-cold permeabilising solution for 10 minutes. Next, a 10 µl aliquot of a FITC-phalloidin stock solution was diluted 1 in 100 with PBS containing 1 % BSA. This was then added to the samples. After 30 minutes, 1 % BSA/PBS containing 10 µg/ml PI was added and left for 1 minute. Assays were washed 3 times with 1 % BSA/PBS before and after each of the above steps. Refer to the Appendix for further details of the solutions used. Before imaging, samples were mounted with a coverslip as stated.

2.2.5 Sodium dodecyl sulphate polyacrylamide gel electrophoresis (SDS-PAGE)

SDS-PAGE, undertaken according to the method of Laemmli (1970), was used to investigate the proteolytic activity of ES upon fibronectin and collagen. ES/ECM protein samples, prepared as outlined in the text, were diluted 1 in 10 with ice-cold acetone and left overnight at -20°C to precipitate the protein. The precipitate present within each sample was then pelleted by centrifugation. Subsequently, the supernatant was removed from each sample and replaced with 20 µl reducing sample buffer (Appendix). 10 µl of SDS 6H molecular weight standards was then obtained. The standards and the prepared samples were incubated at 99°C for ~5 minutes. The samples and standards were then loaded into a 4 % acrylamide stacking gel in preparation for resolving through a 12 % acrylamide gel. The stacking and resolving gels had previously been prepared according to the recipes outlined in the Appendix and polymerised between plates within Bio-Rad Mini-Protean II cell apparatus. A current of 20 mA was applied across each gel in order to separate any fragments within each sample. Resulting protein bands were then stained with Coomassie blue and their positions compared with those of each of the molecular weight standards.

2.2.6 Statistical analysis

Data were analysed for statistically significant differences using GraphPad Instat® or GraphPad Prism™ software. Throughout, data were tested for normal distribution before pursuing further analysis. If necessary, the data were transformed, by logging or square rooting, in order to generate normal distribution. The appropriate parametric or non-parametric tests were then applied. Statistical significance was taken as $P \leq 0.05$.

CHAPTER 3

Fibroblast Adhesion to Extracellular Matrix Proteins

3.1 Introduction

Impaired healing results in the formation of an open, ulcerated, chronic wound. *Lucilia sericata* larvae, or greenbottle fly maggots are sometimes applied to such wounds where conventional treatments have failed. It may be deduced from clinical observations that the larvae aid wound healing by removing necrotic tissue, disinfecting the wound and actively promoting granulation tissue formation (Thomas *et al.*, 1996; Church, 1999; Wolff and Hansson, 1999; Bonn, 2000; Sherman, Hall and Thomas, 2000; Mumcuoglu, 2001; Wollina *et al.*, 2002). Despite such observations being widespread, little research at the biological level has been undertaken to identify the mechanisms by which larvae accomplish this. However, recently it has been found that *L. sericata* larval excretions/secretions (ES), which are continually exuded into the wound as part of the larva's feeding strategy, contains high levels of proteolytic activity. Such activity has been shown to act upon common dermal extracellular matrix (ECM) components (Chambers *et al.*, 2003). As such, the larvae may inadvertently aid healing by introducing proteinases into the wound, which then proceed to initiate changes in the healing response. Hence, the bio-active properties of ES were examined. Attention was paid to the effects of ES upon human dermal fibroblast behaviour in the presence of some common adhesive ECM proteins that have been found liable to ES proteolytic activity.

The human, dermal fibroblast was chosen for investigation because it plays a central role in orchestrating successful wound healing. As a major cellular constituent of the

dermis, fibroblasts are responsible for re-modelling the existing dermal matrix and synthesising new matrix (Clark, 1996). They are also responsible for releasing growth factors and cytokines to stimulate neighbouring fibroblasts and to orchestrate re-epithelialisation and angiogenesis (Clark, 1996). As such, fibroblasts play a pivotal role in the expansion of granulation tissue into the wound space. They are also responsible for contracting the wound edges together, facilitating wound closure (Tomasek *et al.*, 2002). Studies have revealed some age-related changes in fibroblast behaviour (Albini *et al.*, 1988; Dimri *et al.*, 1995; Ballas and Davidson, 2001) which may contribute to impaired healing, particularly when considering that the elderly are prone to non-healing wounds. Other studies have described phenotypic differences in fibroblasts taken from chronic wounds when compared to those taken from healthy skin (Herrick *et al.*, 1996; Hehenberger *et al.*, 1998; Mendez *et al.*, 1998; Ongenae *et al.*, 2000; Raffetto *et al.*, 2001; Stanley and Osler, 2001), while others have described differences in the behaviour of fibroblasts when exposed to chronic wound fluids (Mendez *et al.*, 1999; Malinda and Wysocki, 2000; Weckroth *et al.*, 2001). Further studies have described imbalances in the matrix metalloproteinase (MMP) activity within fluids taken from chronic wounds (Vaalamo *et al.*, 1996; Weckroth *et al.*, 1996; Cook *et al.*, 2000). As fibroblasts release MMPs and their inhibitors, these cells may contribute to such imbalances (West, Pereira-Smith and Smith, 1989; Bizot-Foulon *et al.*, 1995; Ashcroft *et al.*, 1997). In addition, it has been proposed that fibroblasts regulate the switch from acute resolving inflammation to adaptive immunity and tissue repair (Buckley *et al.*, 2001). Hence, if fibroblasts fail to make this switch, then chronic inflammation and impaired healing may result.

Fibronectin and collagen are two common ECM proteins, both of which are prevalent within the wound. Within the dermis, fibroblasts adhere to and migrate along these structural proteins, which form a meshwork of fibrils. Fibronectin has been shown to facilitate the directional migration of cells into the fibrin clot (Greiling and Clark, 1997). In *in vitro* culture, fibroblasts adhere to surfaces coated with these proteins. Studies have shown that the strength of adhesion to these surfaces determines fibroblast morphology and motility (Dembo and Bell, 1987; DiMilla *et al.* 1993; Puschel *et al.*, 1995; Maheshwari *et al.*, 1999; Gaudet *et al.*, 2003). In addition, studies have also shown that fibroblasts are unable to proliferate unless attached to a suitable substratum (and are therefore termed anchorage-dependent) (Stoker *et al.*, 1968; Benecke *et al.*,

1978). Moreover, the expression of MMPs by fibroblasts has been shown to at least in part be regulated by the mechanical stress that the cell experiences, this being imparted by the rigidity of the substrate that the cell is attached to (Mauch *et al.*, 1989; Lambert *et al.*, 1992, 1998, 2001). Hence, the effect of larval ES upon the adhesion of fibroblasts to fibronectin- and collagen-coated surfaces was examined.

3.2 Methods

3.2.1 Preliminary observations of fibroblasts exposed to larval ES

Before any experiments were undertaken, fibroblasts were exposed to larval ES and observations recorded. For this purpose, cells were trypsinised and transferred into cell culture medium (4.5 % FCS). Following cell counting using a haemocytometer, cells were diluted further to a concentration of 90,000 cells/ml. Cell suspension (150 µl) containing 13,500 cells was then transferred to each well of a clear, flat-bottomed 48-well tissue culture plate. Medium (150 µl, 4.5 % FCS) containing either 10 µg/ml ES (taken from ES batch A) or ES blank (an equivalent volume of PBS) was added to each well immediately afterwards. Phase contrast images were then taken of the centre of each well, using an inverted light microscope, following 72 hours incubation at 37°C.

3.2.2 Assessment of cellular and larval ES response to filtered cell culture medium containing 10 % FCS

In most experiments, fibroblasts were suspended within serum-free cell culture medium before being exposed to larval ES. This is because previous studies, as described in Chapter 2.2.2, revealed FCS to inhibit ES proteolytic activity. In some cases, where cells were to be seeded upon tissue culture plastic surfaces that had not been pre-coated with any adhesive protein, fibroblasts were suspended in medium containing 10 % FCS in order to facilitate their adhesion to the surface. However, the medium had first been filtered through a centrifugal filter unit containing a 10,000 molecular weight cut-off (MWCO) membrane (Millipore™), in an attempt to remove any protease inhibitors. In

addition, the cells had been pre-adapted to low serum conditions (2 % FCS) through reducing the serum present within the medium by 2 % at each passage. In order to assess the cells' response to this filtered medium, 1 ml or 100 µl of filtered medium containing 45,000 cells/ml was added to each well of a clear 12-well tissue culture plate or white, opaque 96-well plate respectively. They were then incubated at 37°C for 72 hours before the medium was aspirated from the wells and replaced with fresh, filtered medium. Cells within the 12-well plate were then observed using phase contrast light microscopy, while those within the 96-well plate were subjected to the ATP assay in order to estimate adhered cell number (see section 3.2.4). In both cases, comparisons were made with cells that had been incubated in unfiltered medium containing 5 % FCS. The proteolytic activity of ES exposed to the filtered medium was also assessed using the FITC-casein assay, as described in Chapter 2.2.2.

3.2.3 Heat treatment of larval ES

In order to eliminate the proteolytic activity displayed by larval ES, a sample of ES was incubated at 100°C for 30 minutes. The solution was then diluted to 10 µg/ml with PBS, and its proteolytic activity estimated using the FITC-casein assay, as described in Chapter 2.2.2. A comparison was made with the proteolytic activity of untreated ES that had been taken from the same batch and had also been diluted to 10 µg/ml using PBS.

3.2.4 Adenosine triphosphate assay

The ATPLite™-M assay system (PerkinElmer®, Boston, USA) monitors adenosine triphosphate (ATP) levels by utilising the reaction of ATP present within a sample with added luciferase and D-luciferin. As shown in Equation 3.1, such a reaction results in the production of light. Hence, the intensity of luminescence from a sample assayed using this system reflects the amount of ATP present.

Equation 3.1

$$\text{ATP} + \text{D-luciferin} + O_2 \xrightarrow[Mg^{2+}]{\text{LUCIFERASE}} \text{Oxyluciferin} + \text{AMP} + \text{PPi} + CO_2 + \text{Light}$$

(where: ATP = adenosine triphosphate; AMP = adenosine monophosphate; PPi = inorganic phosphate)

As living cells produce ATP, this assay kit can be used to estimate the number of cells within a sample according to the concentration of ATP present. Here, this assay was used to quantify the number of cells adhering to a surface. The standard assay procedures were followed as outlined in Fig. 3.1.

3.2.4.1 ATP and cell number standard curves

To validate the assay, ATP and cell number standard curves were established using the ATPLite™-M assay in order to confirm that the luminescence detected displayed a linear relationship with the known ATP concentration or cell number present. For the ATP standard curves, a vial of lyophilised ATP (provided with the kit) was reconstituted with 1170 µl water to obtain 10 mM stock solution. An aliquot was diluted in series, using water, to give ATP concentrations ranging from 0.625 µM to 20 µM. The procedure for assaying ATP standards, as outlined in Fig. 3.1a, was then followed. The luminescence emanating from each well was detected using a FL600 fluorimeter and luminometer (Labtech International). Initially, ATP standard curves were established to validate the assay system. They were also used in cell adhesion experiments so that relative luminescence readings from samples could be converted to ATP concentration values. Hence, an ATP dilution series was assayed at each time-point within the experiment performed. For the cell number standard curves, 100 µl of cell culture medium (5 % FCS) containing cell densities of between 1,500 and 150,000 cells/ml were added to wells of a white, opaque 96-well tissue culture plate and incubated for the time stated. The procedure for assaying cell adhesion, as outlined in Fig. 3.1b, was then followed from stages ii to iv.

3.2.5 Cellular nucleic acid assay

The CyQUANT® assay kit (Molecular Probes) quantifies the number of cells present in a sample according to the levels of cellular nucleic acids present. This is achieved through the use of a green fluorescent dye (CyQUANT GR) which exhibits an enhancement of fluorescence when bound to cellular nucleic acids. Here, this assay was used to quantify the number of cells adhering to a surface, providing complementary results to those obtained using the ATP assay.

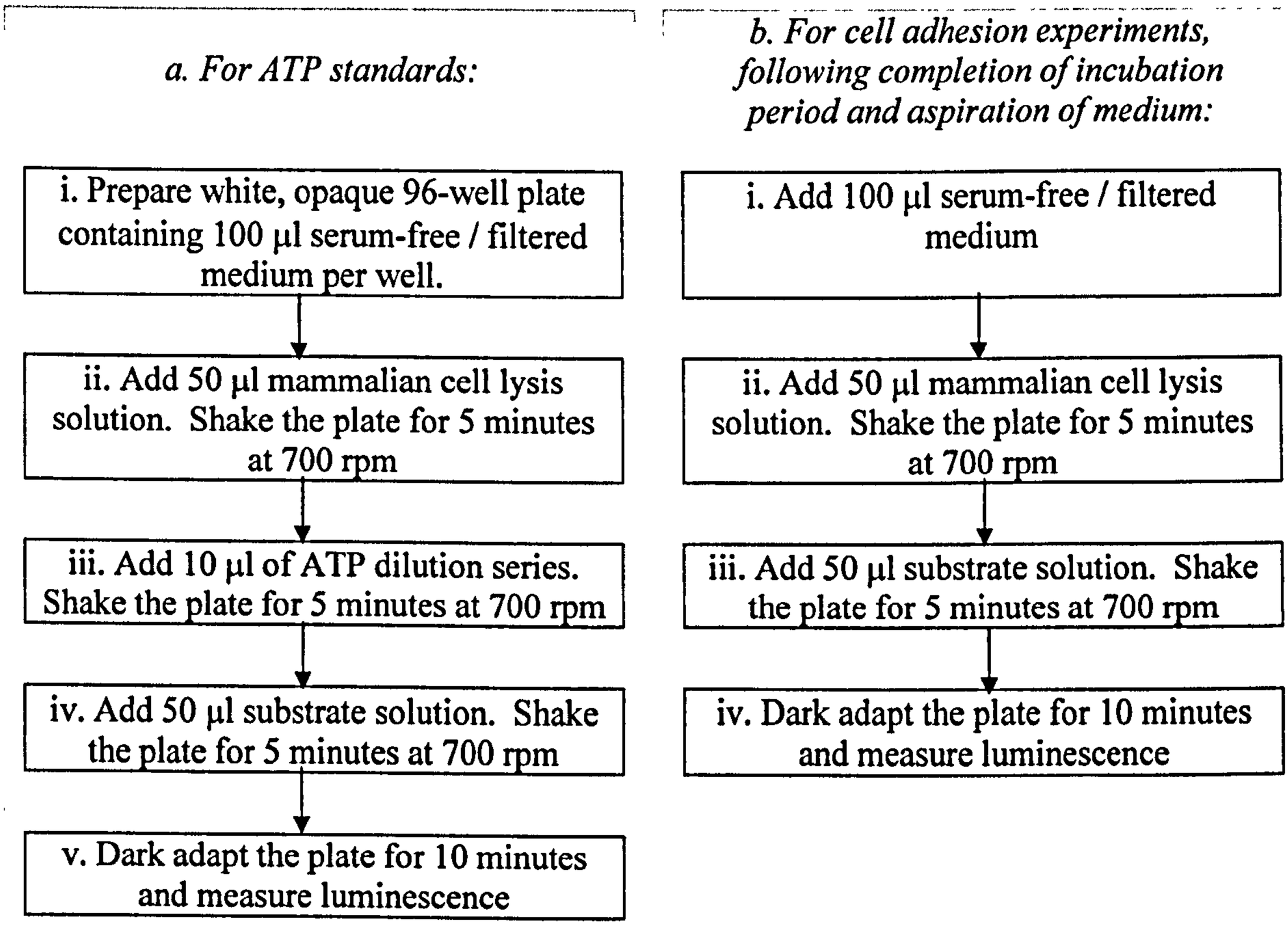

Figure 3.1 Standard ATP assay procedures.

3.2.5.1 Cell number standard curves

Cell number standard curves were established using the CyQUANT® assay in order to confirm that the fluorescence emitted by the CyQUANT GR dye displayed a linear relationship with the known cell number present. Initially, serial dilutions of cell suspensions, from 244 cells/ml to 500,000 cells/ml, were tested in order to validate the assay system. Here, 100 µl of cell suspension was added to each well of a black 96-well plate. The plate was then frozen and stored at -80°C until required. Following thawing of the plate at RT, 200 µl of distilled water containing 7.5 % cell lysis buffer (provided in the assay kit) and 0.4 % CyQUANT GR dye was added to each well. The fluorescence emitted from each well was then detected using the FL600 fluorimeter and luminometer (485 ± 20 nm excitation/590 ± 35 nm emission wavelengths). Following validation, standard curves of 244 cells/ml to 250,000 cells/ml were used for the conversion of relative fluorescence readings from samples within cell adhesion experiments to cell densities.

3.2.6 Quantification of fibroblast adhesion in response to larval ES

Confluent fibroblasts (70 % – 80 %) were trypsinised and suspended in cell culture medium containing 10 % FCS, to neutralise remaining trypsin. The serum was then removed, as it had already been shown to inhibit ES proteolytic activity (see Chapter 2.2.2). This was undertaken as described in Chapter 2.2.1, leaving cells re-suspended within serum-free cell culture medium or where specified, within medium containing 10 % FCS which had previously been filtered through a 10,000 MWCO membrane (refer to section 3.2.2). The cells were then counted using a haemocytometer and diluted with further serum-free or filtered medium to 90,000 cells/ml. Meanwhile, heat-treated or untreated ES from the designated batch was diluted to the required concentration using serum-free or filtered medium. This was then mixed at a ratio of 1:1 with the cell suspension, leaving a final cell density of 45,000 cells/ml and the ES concentration indicated. Aliquots (100 µl) were then added to each well of a white, opaque 96-well tissue culture plate (for ATP assay) or each well of a black 96-well tissue culture plate (for CyQUANT® assay) and incubated at 37°C for the time stated. Where indicated, the wells had previously been coated with either 10 µg/ml fibronectin (1 µg added per well)

or 30 μg/ml collagen type I (3 μg added per well), following the procedure outlined in Chapter 2.2.3. In some instances before the addition of cells, fibronectin- or collagen-coated wells were exposed to either 10 μg/ml untreated ES or ES blank (PBS substitute) at 37°C for the time stated, and then washed three times with PBS. These samples therefore consisted of ECM protein-coated surfaces pre-exposed to ES and cells which remained naïve to ES.

Following the indicated period of incubation, wells within the white 96-well tissue culture plates were aspirated of medium, to remove non-adherent cells, and then assayed for ATP content, using the ATPLite™-M assay kit. The procedure followed was as outlined in Fig. 3.1b. Resulting luminescence readings were converted to ATP concentration using the appropriate ATP standard curve. Cells plated within the black 96-well tissue culture plates were aspirated of medium, frozen at -80°C and then thawed at RT when required. After they had been thawed, 200 μl of distilled water containing 7.5 % cell lysis buffer (provided in the assay kit) and 0.4 % CyQUANT GR dye was added to each well. As with the cell number standard curves (section 3.2.5.1), the fluorescence emitted from each well was then detected using the FL600 fluorimeter and luminometer (485 ± 20 nm excitation/590 ± 35 nm emission wavelengths). Resulting fluorescence readings were converted to cell numbers using the appropriate cell number standard curve.

3.2.7 Effect of larval ES upon fibroblast cell morphology and spreading over ECM protein-coated surfaces

Here, the visible alterations in fibroblast morphology caused by the presence of ES were quantified. Firstly, wells of a 48-well tissue culture plate were coated with either 10 μg/ml fibronectin (3 μg added per well) or 30 μg/ml collagen type I (9 μg added per well), following the procedure outlined in Chapter 2.2.3. A flask of 70 % – 80 % confluent fibroblasts, pre-stained with Celltracker™ green CMFDA as outlined in Chapter 2.2.4, were trypsinised and the cells suspended in 10 % FCS to neutralise the trypsin. The cells were then re-suspended within serum-free cell culture medium at a density of 10,000 cells/ml. Meanwhile, untreated or heat-treated ES from batch D was diluted to 20 μg/ml within serum-free medium. Alternatively, an equivalent volume of

PBS was added to serum-free medium (control). Medium containing either the specified ES or PBS was then mixed at a ratio of 1:1 with the cell suspension. Aliquots (300 µl) were then added to each of three fibronectin- or collagen-coated wells, such that 1,500 cells were added to each well in the presence or absence of 10 µg/ml ES. The cells were then incubated for 4 hours at 37°C. Using fluorescence microscopy, 10 random images were taken of each well, providing a total of 30 images of cells exposed to each condition. The images were then analysed using Leica QUIPS software (Leica Microsystems UK, Milton Keynes, UK) to assess the following morphological parameters of each cell that was fully visible: area, length, breadth, perimeter and roundness. This procedure involved using the appropriate tools within the software programme to hand-draw around the circumference of each cell, thus marking its shape and size for computational analysis. Roundness was defined as a shape factor, which gives a minimum value of unity for a perfect circle. The shape factor was calculated as [cell perimeter^2 ($4\pi \times$ cell area $\times$ 1.064)$^{-1}$], where 1.064 is the digitisation adjustment factor to correct for the corners produced by the digitisation of the cell perimeter.

3.2.8 Proteolytic degradation of ECM proteins by larval ES: investigation using SDS-PAGE

Here, ES containing-medium that was used to pre-incubate fibronectin- or collagen-coated surfaces before the addition of cells, as described in section 3.2.6, was prepared and resolved through a 12 % acrylamide gel, as outlined in Chapter 2.2.5. Samples containing fibronectin or collagen alone were also run through the gel for comparison. In a separate experiment, 1 mg/ml bovine fibronectin stock was diluted with PBS containing either untreated or heat-treated ES from batch D, such that final concentrations of 100 µg/ml fibronectin and 0.1 µg/ml ES were achieved. This was then incubated at 37°C for the time stated. The samples were then prepared for gel electrophoresis as outlined in Chapter 2.2.5 and resolved through a 12 % acrylamide gel. Samples containing only 100 µg/ml fibronectin or 0.1 µg/ml ES were also subjected to electrophoresis for comparison. In all cases, resulting bands were visualised by staining with Coomassie blue.

3.2.9 Statistical analysis

Cell adhesion data (estimations of ATP content or cell number) were analysed for statistically significant differences using GraphPad Prism™ software. Here, whole datasets were initially tested using two-way ANOVA. Data from each time-point were then compared using one-way ANOVA and Tukey-Kramer's multiple comparison tests. Cell morphological data (resulting from QUIPS analysis) were not normally distributed and were therefore compared using the non-parametric analysis of variance equivalent of Kruskal-Wallis ANOVA and Dunn's multiple comparisons test. Again, GraphPad Prism™ software was used. Throughout, statistical significance was taken as $P \leq 0.05$.

3.3 Results

The findings of Chambers and colleagues (2003) demonstrate larval ES to be rich in proteolytic activity, including trypsin-like and chymotrypsin-like serine proteinase activity. They also demonstrate the ability of ES to degrade common dermal ECM proteins, including collagen and fibronectin. Fibroblasts are known to adhere to such proteins within the dermis. In addition, porcine-derived trypsin, in combination with EDTA, is used to detach cells from tissue culture grade plastic surfaces during standard cell passage procedures (see Chapter 2.2.1). The influence of ES upon fibroblast adhesion and morphology in the presence of these ECM proteins was therefore examined.

3.3.1 Preliminary observations of fibroblasts exposed to larval ES

Preliminary studies, concerning the observation of fibroblasts plated upon tissue culture grade plastic surfaces in low serum conditions, revealed that the presence of 10 μg/ml ES altered fibroblast morphology. As shown in Fig. 3.2, after 72 hours incubation in medium containing ES, cells appeared less elongated than those incubated in the absence of ES. Many had also aggregated, while some were floating in suspension.

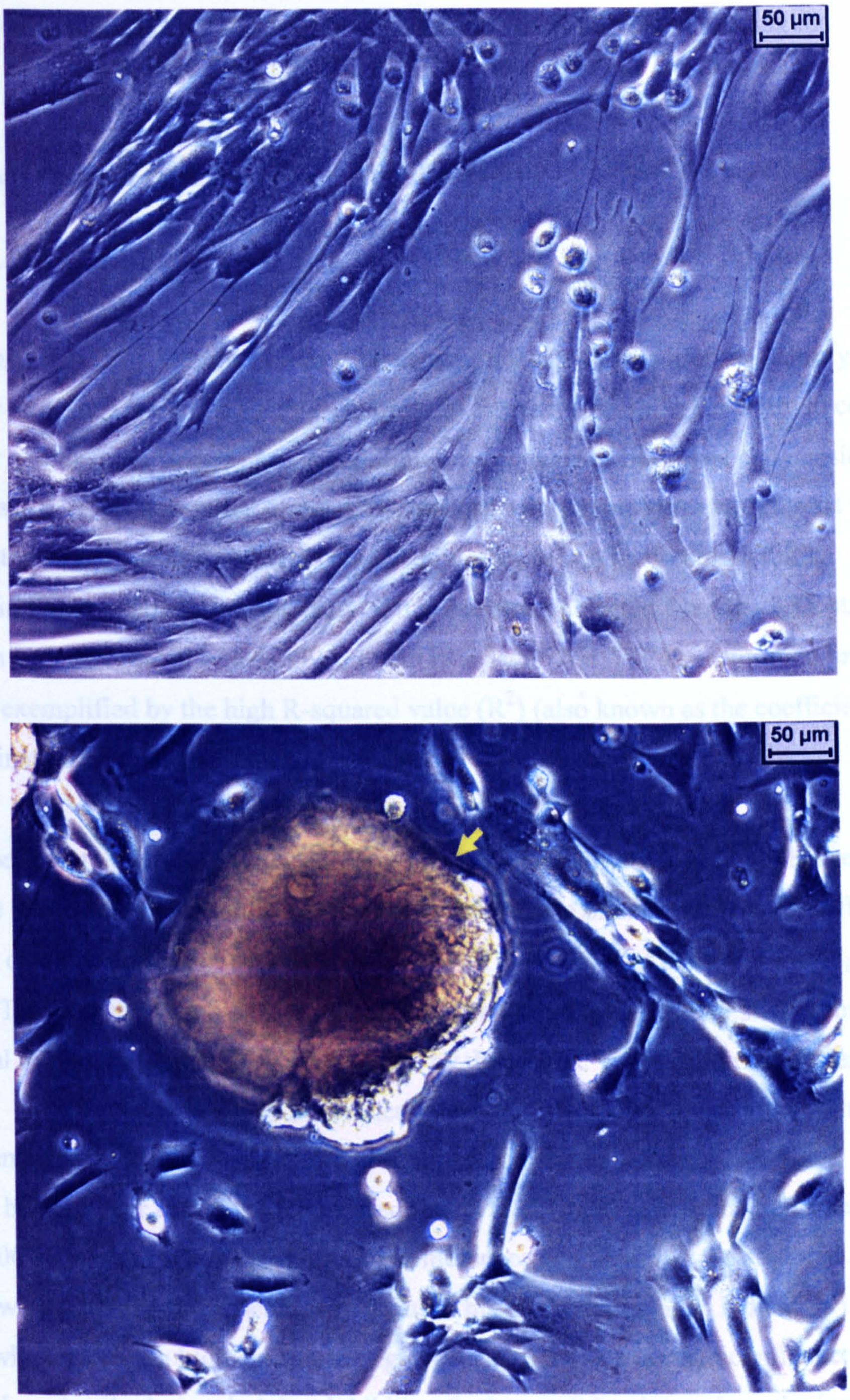

Figure 3.2 Representative images of fibroblast cells following 72 hours incubation in the absence (*top*) or presence of ES (10 µg/ml) (*bottom*). Cell culture medium contained 2.5% FCS. The presence of ES inhibited fibroblast spreading across the surface. As indicated by the arrow, large multi-cellular aggregates also formed, indicating inhibition of cell adhesion to the surface.

These observations lead to the development of assays capable of quantifying the number of cells adhering to various surfaces.

3.3.2 Validation of quantitative cell adhesion assays

3.3.2.1 ATP assay

Here, the ATPLite™-M luminescent ATP detection assay kit was used to quantify the number of cells present in a sample. In order to assess the assay's sensitivity to cell number and linearity of response, serial dilutions of a known fibroblast cell density were tested. A dilution series of the ATP standard solution provided with the kit was also tested. These procedures were repeated in order to confirm reproducibility. As shown in Fig. 3.3 the relative intensity of luminescence detected from the ATP standard dilution series exhibited a close linear relationship with the ATP concentration present. This is exemplified by the high R-squared value (R^2) (also known as the coefficient of determination) for the linear trendline drawn.

An experiment undertaken to assess the ATP assay's sensitivity to cell number revealed that the relative luminescence detected from each sample of cells immediately after plating displayed a strong linear relationship with the density of cells present (Fig. 3.4a). This was the case for the entire range of cell seeding densities tested, from 1,500 cells/ml to 150,000 cells/ml, as exemplified by the high R^2 value of the linear trendline drawn. However, following 48 hours incubation (Fig. 3.4b), the linear relationship between initial cell-seeding density and luminescence was considerably weaker, as shown by the lower R^2 value. It appeared that at the higher cell seeding densities (120,000 cells/ml to 150,000 cells/ml), luminescence and therefore the assumed ATP levels were levelling off, reaching a plateau. This may have been an indication that the cells, which were at a high density to begin with, had rapidly reached confluence over the 48 hour incubation period thus inhibiting further proliferation and continuing rises in ATP levels. Luminescence intensities and therefore ATP levels across the lowest cell seeding densities (1,500 cells/ml to 15,000 cells/ml) appeared to be similar. In fact, as shown in Fig. 3.4c, the intensity of luminescence detected after 48 hours was actually slightly lower than the values recorded at 0 hours. As the cells were seeded at such low

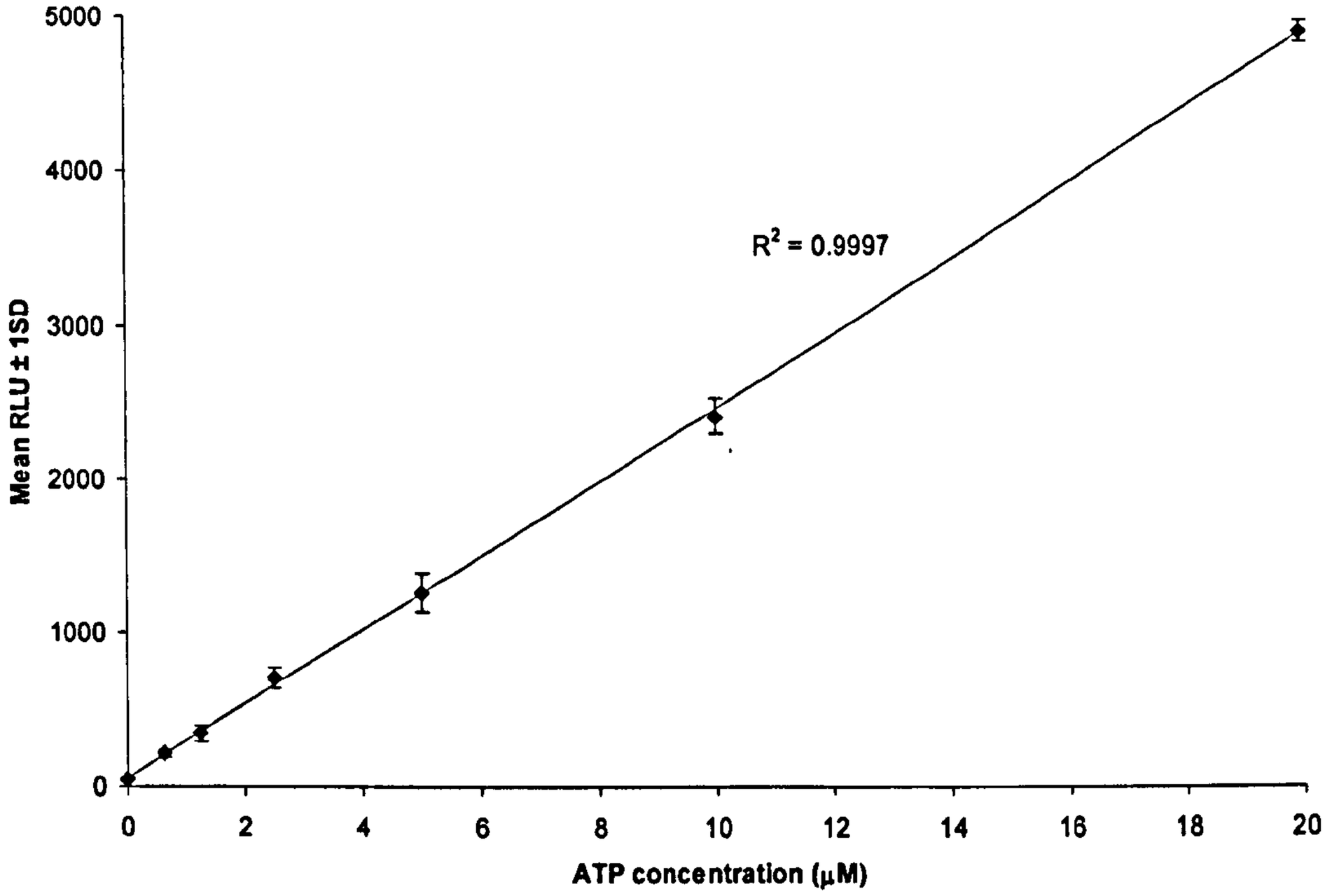

Figure 3.3 Representative ATP standard curve. Each data point represents the mean value of three replicate samples. R^2 value of the linear trendline shown.

a.

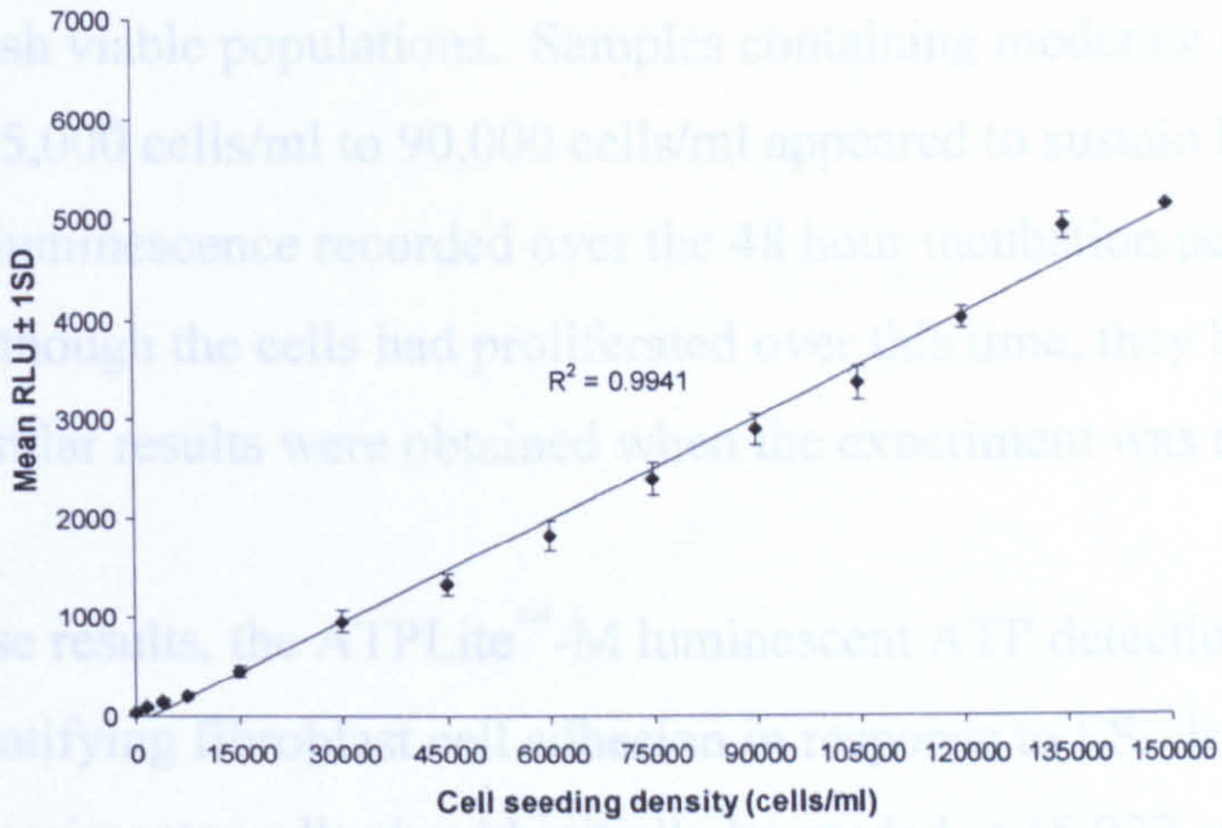

b.

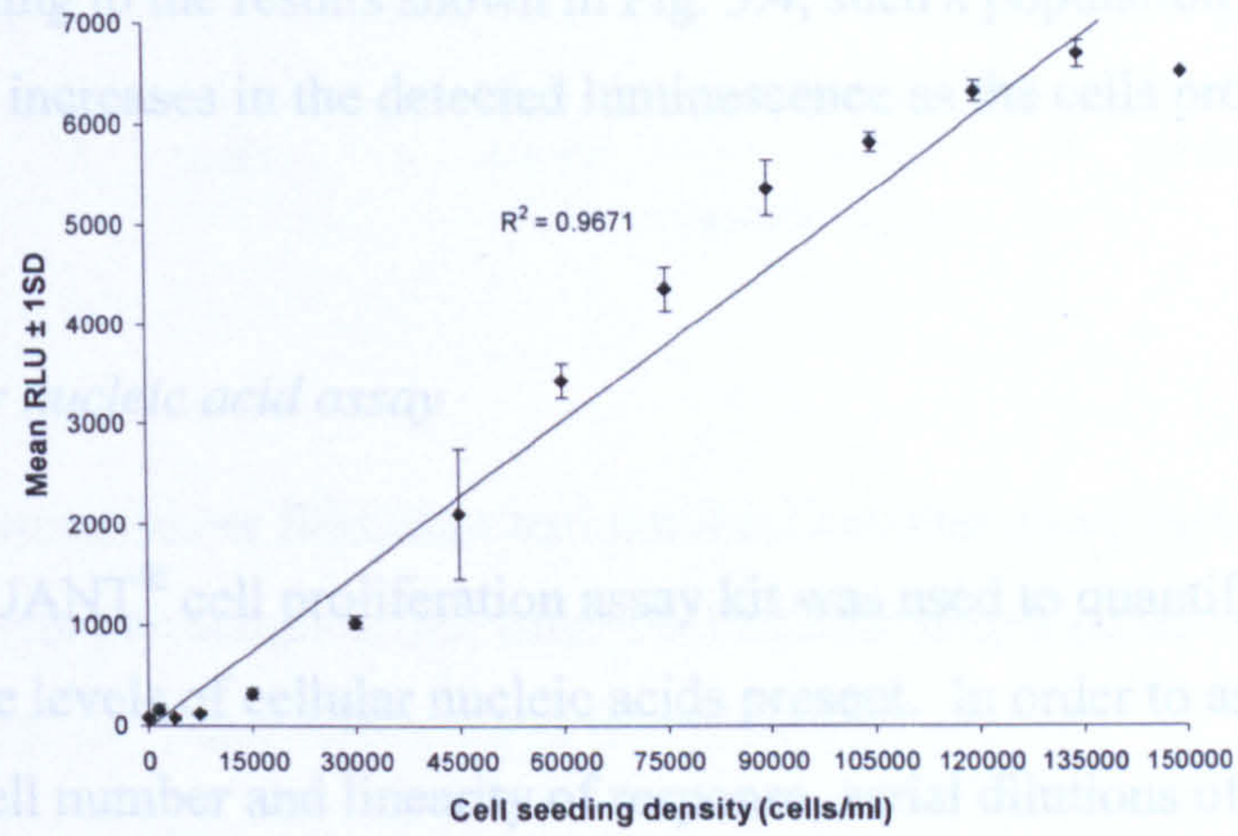

c.

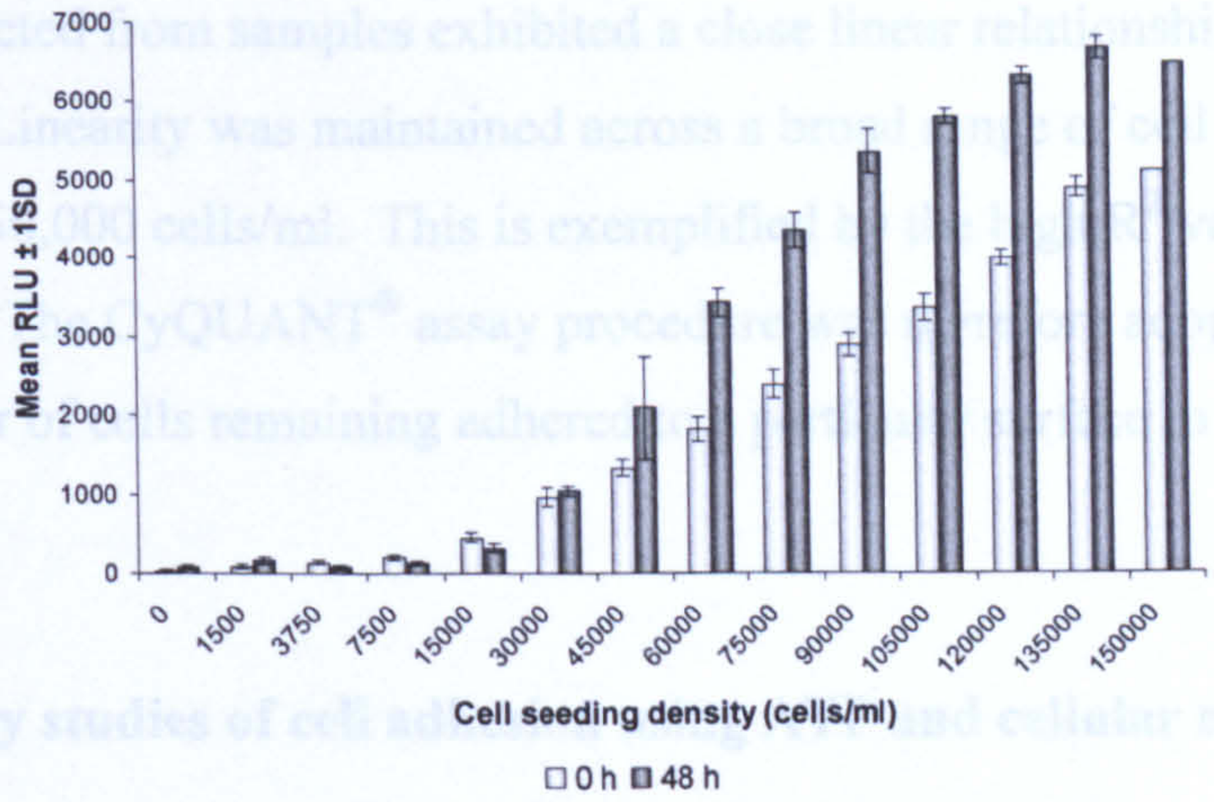

Figure 3.4 A representation of the relationship between fibroblast cell seeding density and luminescence intensity resulting from application of the ATP assay after 0 hours incubation (a) and 48 hours incubation (b). Comparison between results from a. and b. is shown in c. Data points represent the mean value of three replicate samples. R^2 value of each linear trendline is shown.

seeding densities, the decrease in luminescence may have been indicative of the cells failing to establish viable populations. Samples containing moderate cell seeding densities from 45,000 cells/ml to 90,000 cells/ml appeared to sustain linear increases in the intensity of luminescence recorded over the 48 hour incubation period. This indicated that although the cells had proliferated over this time, they had not attained confluency. Similar results were obtained when the experiment was repeated.

Based upon these results, the ATPLite™-M luminescent ATP detection assay kit was adopted for quantifying fibroblast cell adhesion in response to ES. It was also decided that for such experiments, cells should initially be seeded at 45,000 cells/ml. This is because, according to the results shown in Fig. 3.4, such a population density should allow for linear increases in the detected luminescence as the cells proliferate over 48 hours.

3.3.2.2 Cellular nucleic acid assay

Here, the CyQUANT® cell proliferation assay kit was used to quantify cell numbers according to the levels of cellular nucleic acids present. In order to assess the assay's sensitivity to cell number and linearity of response, serial dilutions of a known fibroblast cell density were tested. As shown in Fig. 3.5, the relative intensity of fluorescence detected from samples exhibited a close linear relationship with the cell density present. Linearity was maintained across a broad range of cell densities, from 244 cells/ml to 250,000 cells/ml. This is exemplified by the high R^2 value for the linear trendline drawn. The CyQUANT® assay procedure was therefore adopted in order to assess the number of cells remaining adhered to a particular surface in the presence of ES.

3.3.3 Preliminary studies of cell adhesion using ATP and cellular nucleic acid assays

Use of the ATP and CyQUANT® assays initially involved investigating the adhesion of cells upon tissue culture plastic surfaces in the presence of different protein concentrations of ES (batch B). As the presence of serum within the medium inhibits

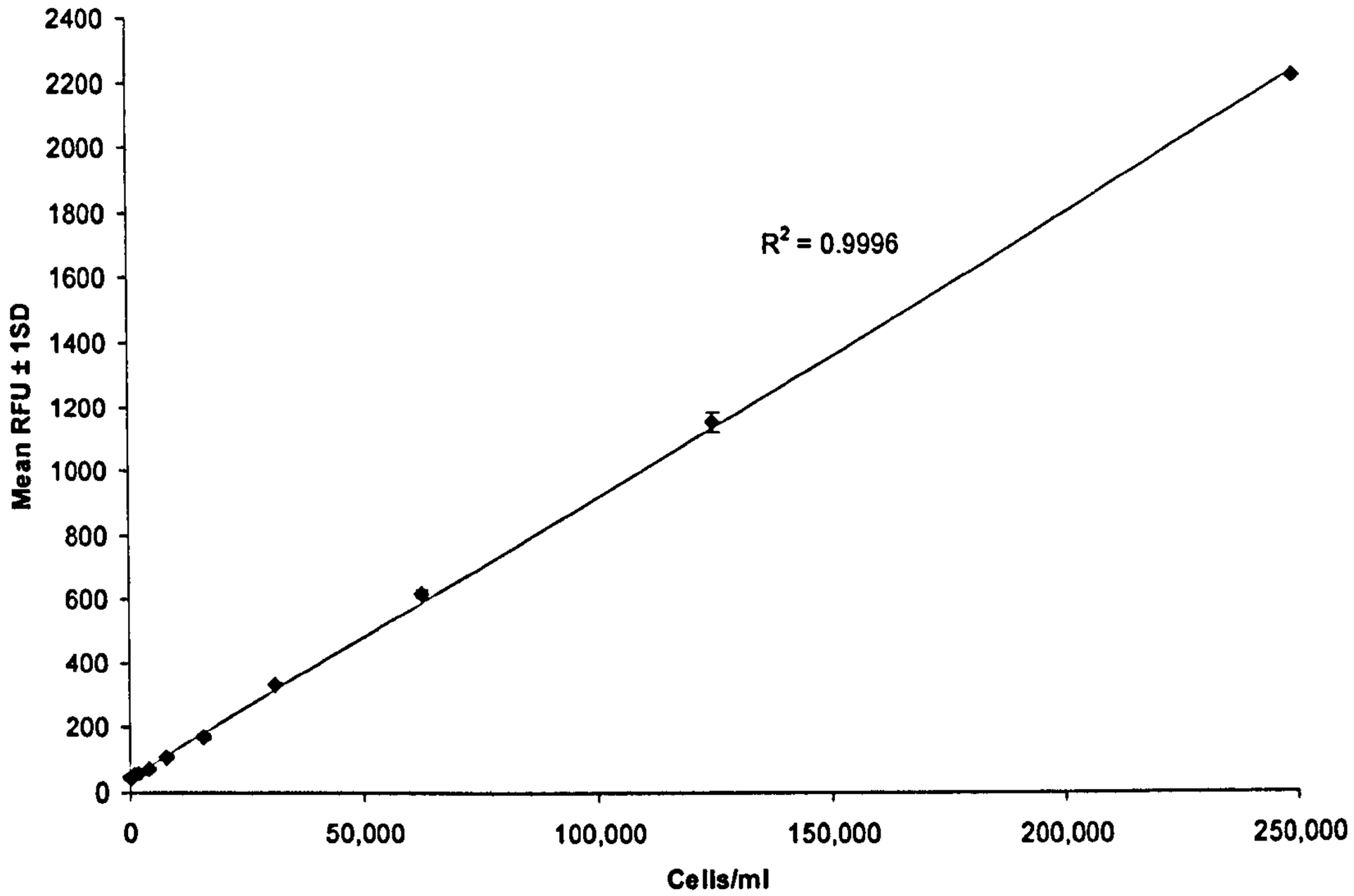

Figure 3.5 Representative fibroblast cell number standard curve derived using the CyQUANT® assay procedure. Each data point represents the mean value of three replicate samples. R^2 value of the linear trendline shown.

ES proteolytic activity (Fig. 2.2), the existence of serum-free conditions would therefore have been ideal. However, a concern was that cell adhesion to the bare, plastic surface would have been severely curtailed in a serum-free environment as there would have been no proteins present to provide an adhesive coating over the plastic. It was conjectured that the protease inhibitors present within serum are of a large size. For example, the protease inhibitor α_2 macroglobulin is a 772 kDa serum protein which displays an almost universal specificity for various proteolytic enzymes (Abe, Shinmei and Nagai, 1973; Neurath, 1989). Hence, in an attempt to remove such inhibitors, medium containing 10 % FCS was filtered through a 10,000 MWCO membrane before being introduced to the cells. As shown in Fig. 3.6, filtration of medium containing FCS eliminated its inhibitory activity over the larval ES proteinases. Although curtailed in their growth and adhesion (Fig. 3.7), many fibroblasts that had previously been adapted to low-serum conditions succeeded in adhering to the plastic surface whilst within the 10,000 MWCO filtered medium (Fig. 3.8). However, it must be noted that here a control for the absence of FCS was missing. Hence, the benefit of using filtered medium over medium in which serum is absent could not be substantiated. In addition, the filtered and unfiltered media should have contained the same percentage of FCS before their respective treatments. Nevertheless, ATP and CyQUANT® assays that were undertaken to quantify the effect of ES upon cell adhesion to uncoated tissue culture plastic were conducted in the presence of filtered medium. As shown in Fig. 3.9a, levels of ATP within samples displayed a dose response to the concentration of ES present. As the concentration of ES increased, the levels of ATP decreased. Results from the CyQUANT® assay displayed a similar trend in total nucleic acid content, confirming a dose-dependent decrease in cell adhesion (Fig. 3.9b). In both assays, 10 µg/ml ES clearly elicited a substantial decrease in cell adhesion. Hence, this concentration of ES was included within subsequent experiments, as described below.

3.3.4 Heat treatment of larval ES to eradicate proteolytic activity

Before undertaking work to investigate the effect of ES upon fibroblast behaviour, a sample of ES was heat-treated, as described in section 3.2.3, to eradicate its proteolytic activity through protein denaturation. Thus, in comparing heat-treated ES with the untreated native ES, the contribution of ES proteolytic activity towards any observed effect upon cells or protein-coated surfaces could be discerned. Results from the FITC-

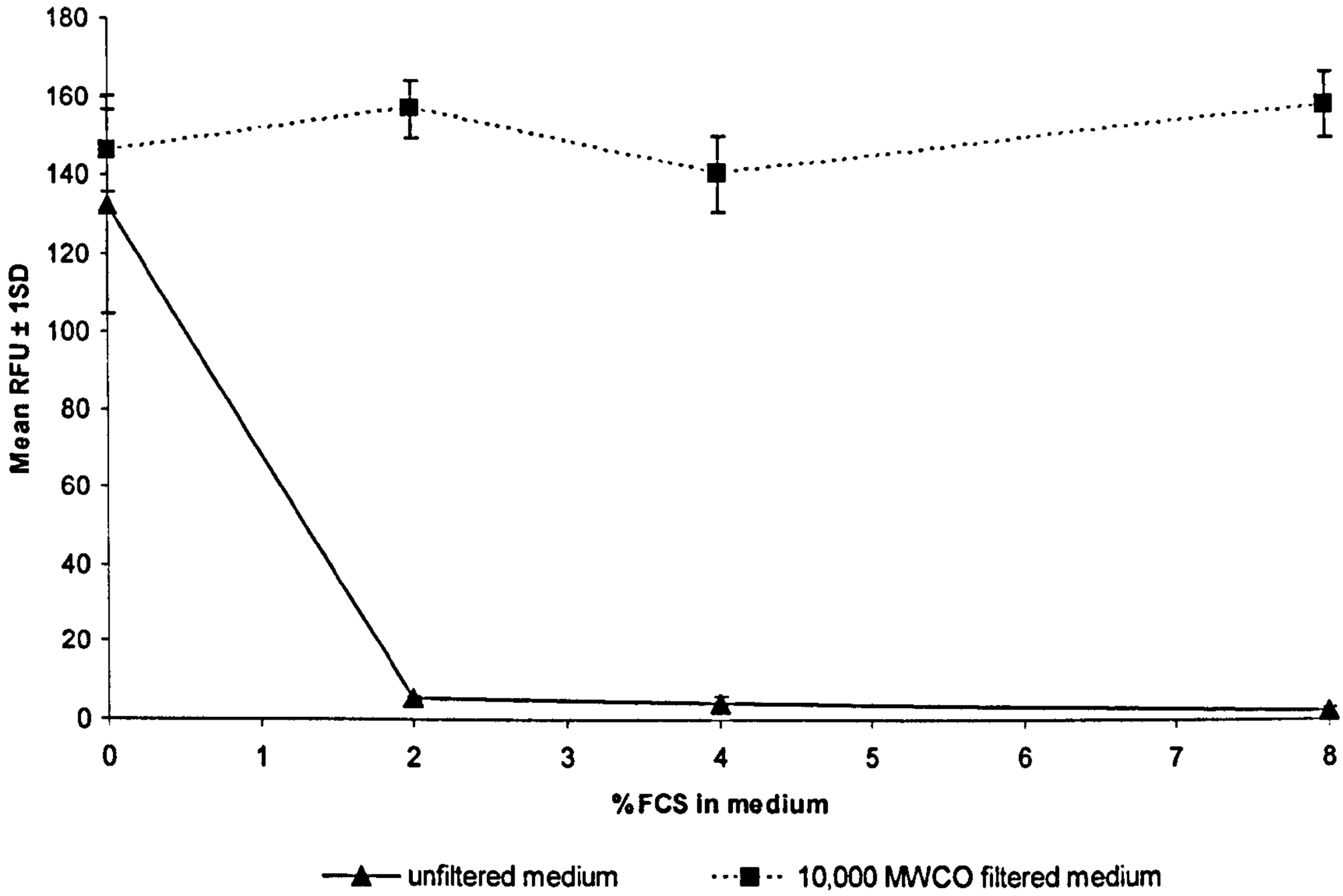

Figure 3.6 Proteolytic activity of ES (taken from batch B – refer to Table 2.1) in the presence of media containing different concentrations of FCS, pre- and post-filtration through a 10,000 molecular weight cut-off (MWCO) membrane. Activity measured using the FITC-casein assay as described in Chapter 2.2.2. Each value represents the mean of three replicate samples.

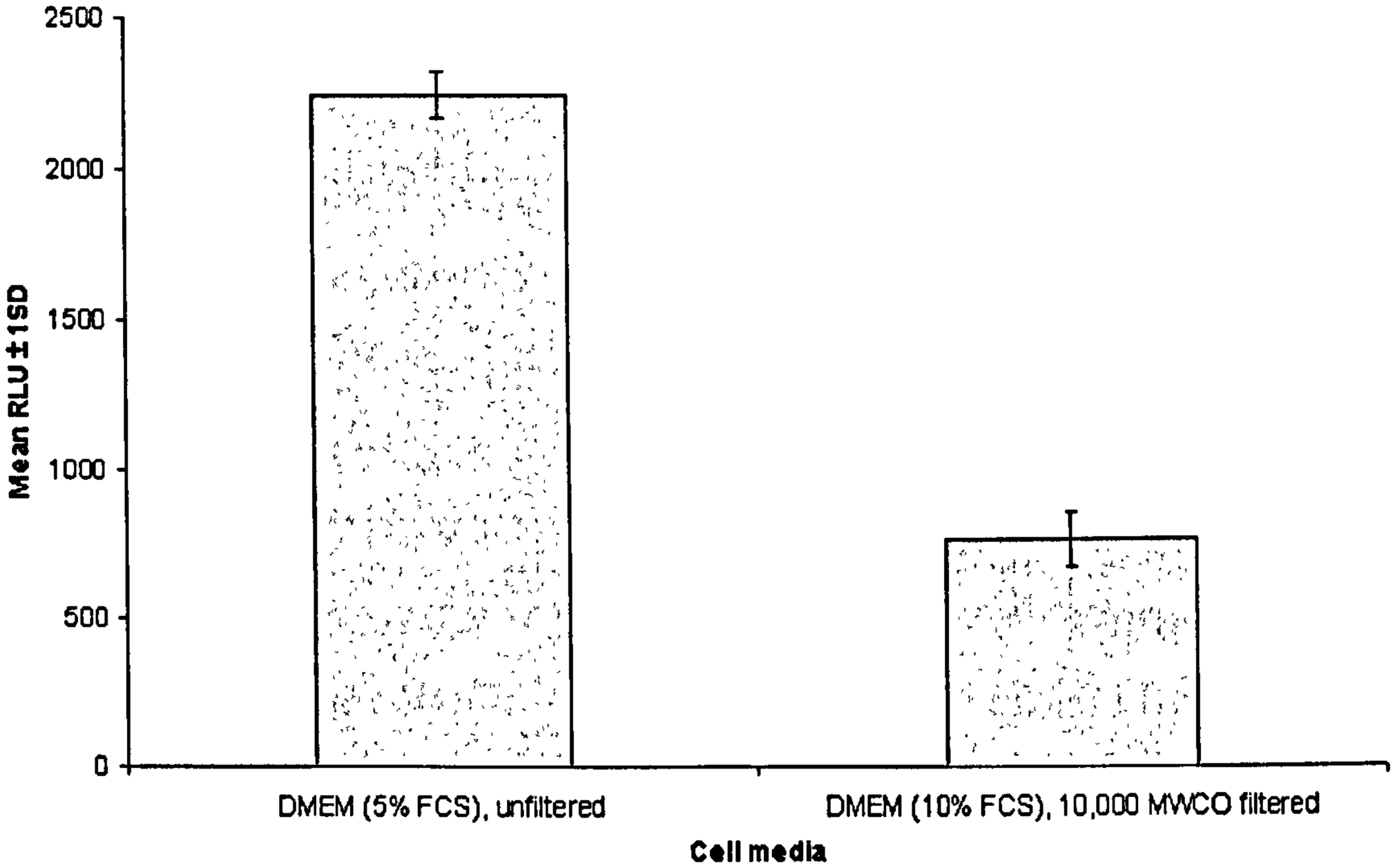

Figure 3.7 Luminescence intensities representing the relative numbers of fibroblasts adhered to tissue culture plastic, as measured using the ATP assay. Measurements taken following 72 hours incubation of the cells in medium (percentage FCS content indicated) that was unfiltered or filtered through a 10,000 MWCO membrane. Each value represents the mean of three replicate samples.

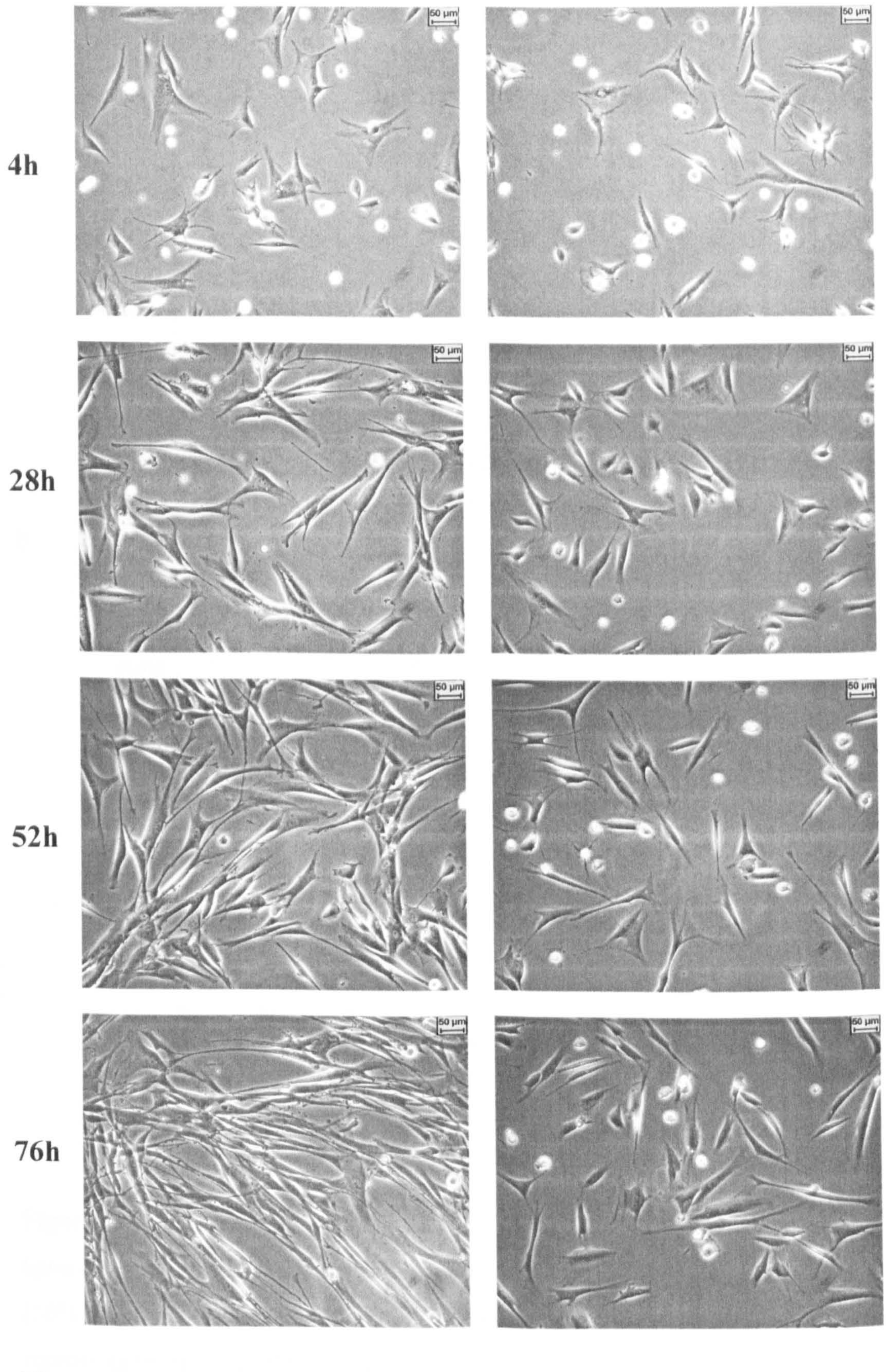

Figure 3.8 Representative images of fibroblasts adhered to tissue culture plastic in the medium indicated and for the times indicated. Medium containing 10% FCS was filtered through a 10,000 MWCO membrane.

a.

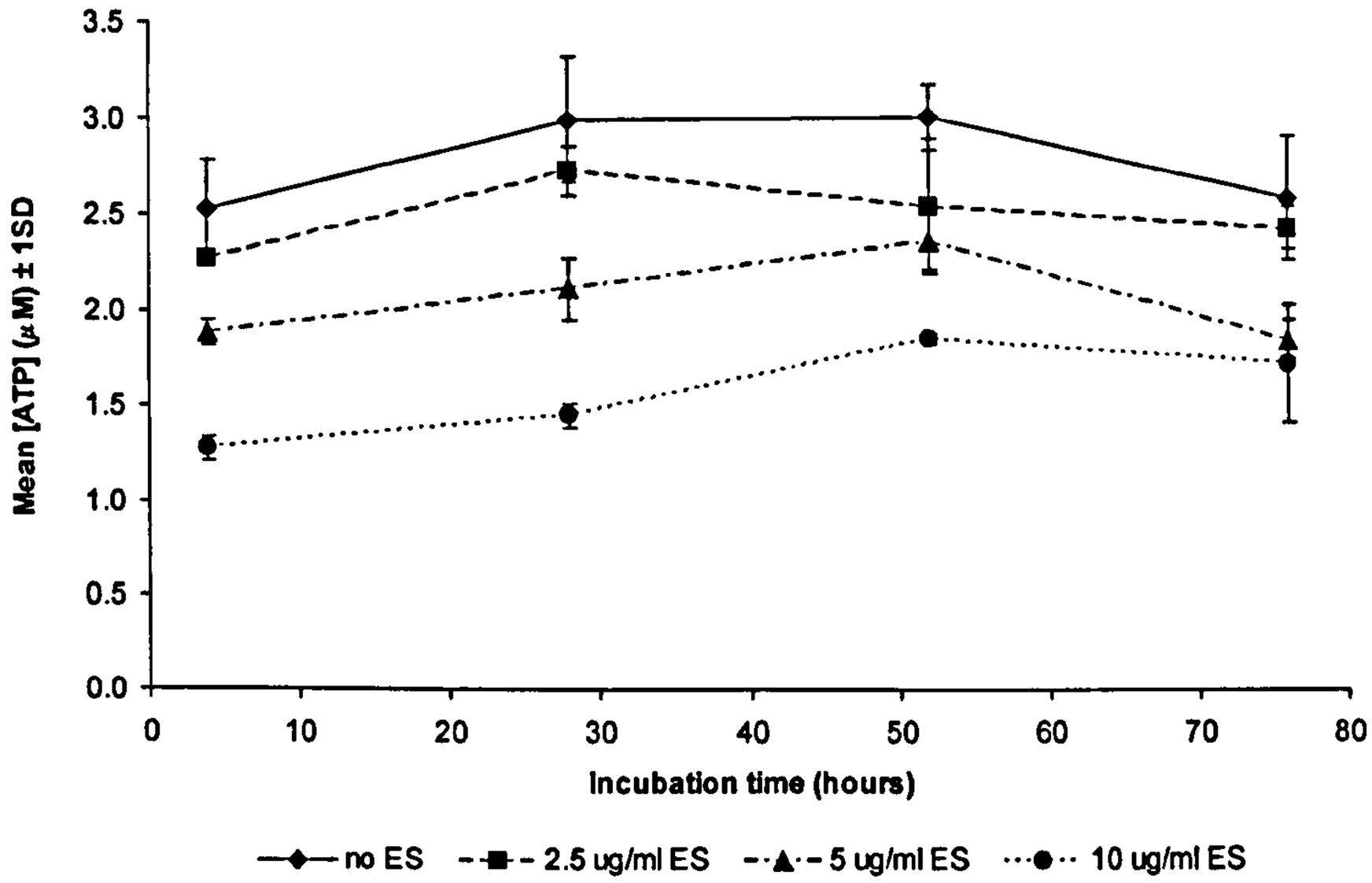

b.

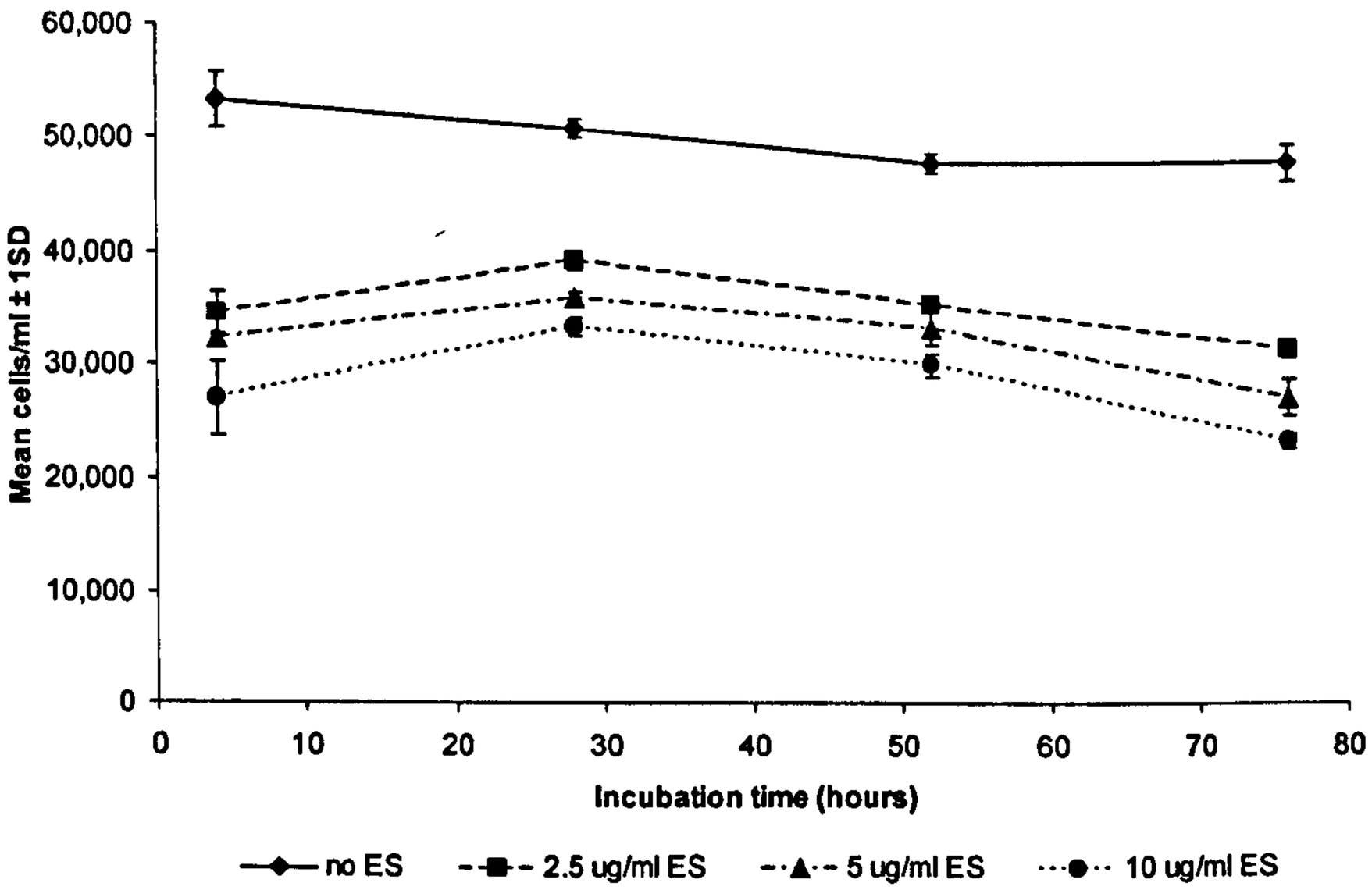

Figure 3.9 ATPLite™-M assay (a) and CyQUANT® assay (b) results from cells seeded upon a tissue culture plastic surface in the presence of 10,000 MWCO filtered medium (10% FCS) and the concentration of ES indicated (ES from batch B). Each value represents the mean of three replicate samples.

casein assay revealed that heat-treated ES possessed negligible proteolytic activity against the substrate (Fig. 3.10). As shown, supernatant from FITC-casein exposed to heat-treated ES exhibited similarly low levels of fluorescence to that taken from substrate exposed to an ES blank solution (PBS replacement). Supernatant from substrate exposed to untreated ES exhibited substantially higher levels of relative fluorescence.

3.3.5 Effect of larval ES upon fibroblast adhesion to fibronectin

3.3.5.1 ATP and cellular nucleic acid assays

The effects of larval ES (from batch C) upon fibroblast cell adhesion to a fibronectin-coated surface was first examined using the ATPLite™-M and CyQUANT® assays. Following coating of wells of a 96-well plate with bovine fibronectin, serum-free medium containing 4.5×10^3 fibroblasts and either 10 µg/ml larval ES (whole, untreated or heat-treated) or ES blank (PBS replacement) was added to each well. Following the specified period of incubation, wells were aspirated of medium to remove detached cells and the number of remaining adhered cells estimated using the indicated assay.

ATP assay results (Fig. 3.11) revealed lower ATP concentrations within wells exposed to untreated ES, indicating the presence of a lower number of cells when compared to the control (ES absent) over the time course of the experiment. This difference was apparent after only 4 hours incubation, up to which point there had been a limited time for cell proliferation to take place under either condition. This suggested that the initial number of cells adhering to the fibronectin-coated surface was lower in the presence of untreated ES. At 24 hours incubation, ATP levels of adhered cells in the presence of untreated ES remained similar to the levels recorded at 4 hours incubation. A slight dip in the ATP level was recorded at 48 hours incubation, indicating a small loss in cell viability or a decrease in the number of cells remaining adhered. Although wells exposed to heat-treated ES displayed higher ATP levels than those exposed to the untreated ES, they were still appreciably lower throughout the incubation period than those measured in the control wells. Differences were noticeable from 4 hours

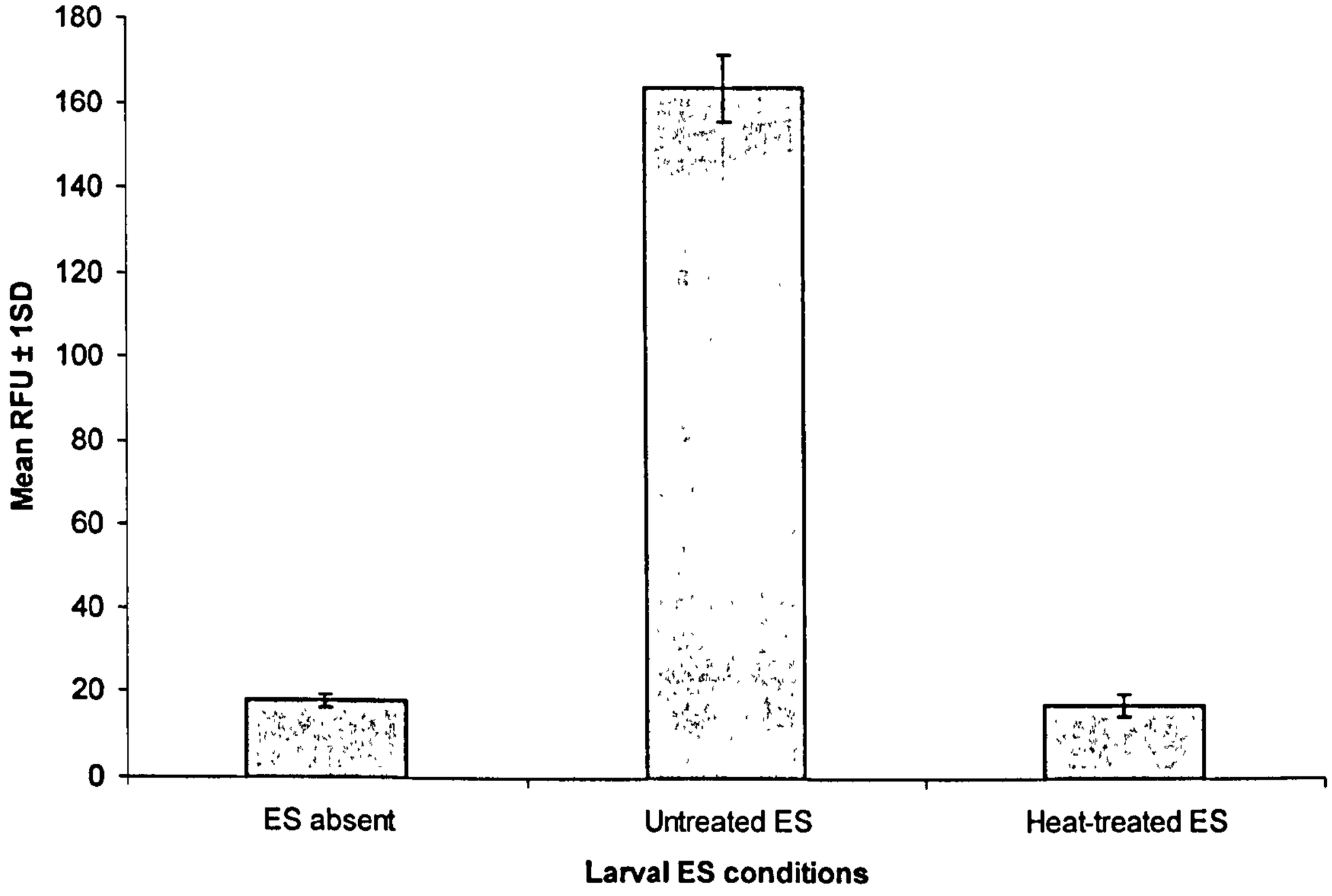

Figure 3.10 FITC-casein assay demonstrating the effect of heat-treatment upon larval ES proteolytic activity. Fluorescence resulting from FITC-casein hydrolysis in the absence of ES (PBS replacement) or in the presence of 10 μg/ml untreated ES or 10 μg/ml heat-treated ES. In both instances, ES was taken from ES batch D (refer to Table 2.1). Each value represents the mean from three replicate samples.

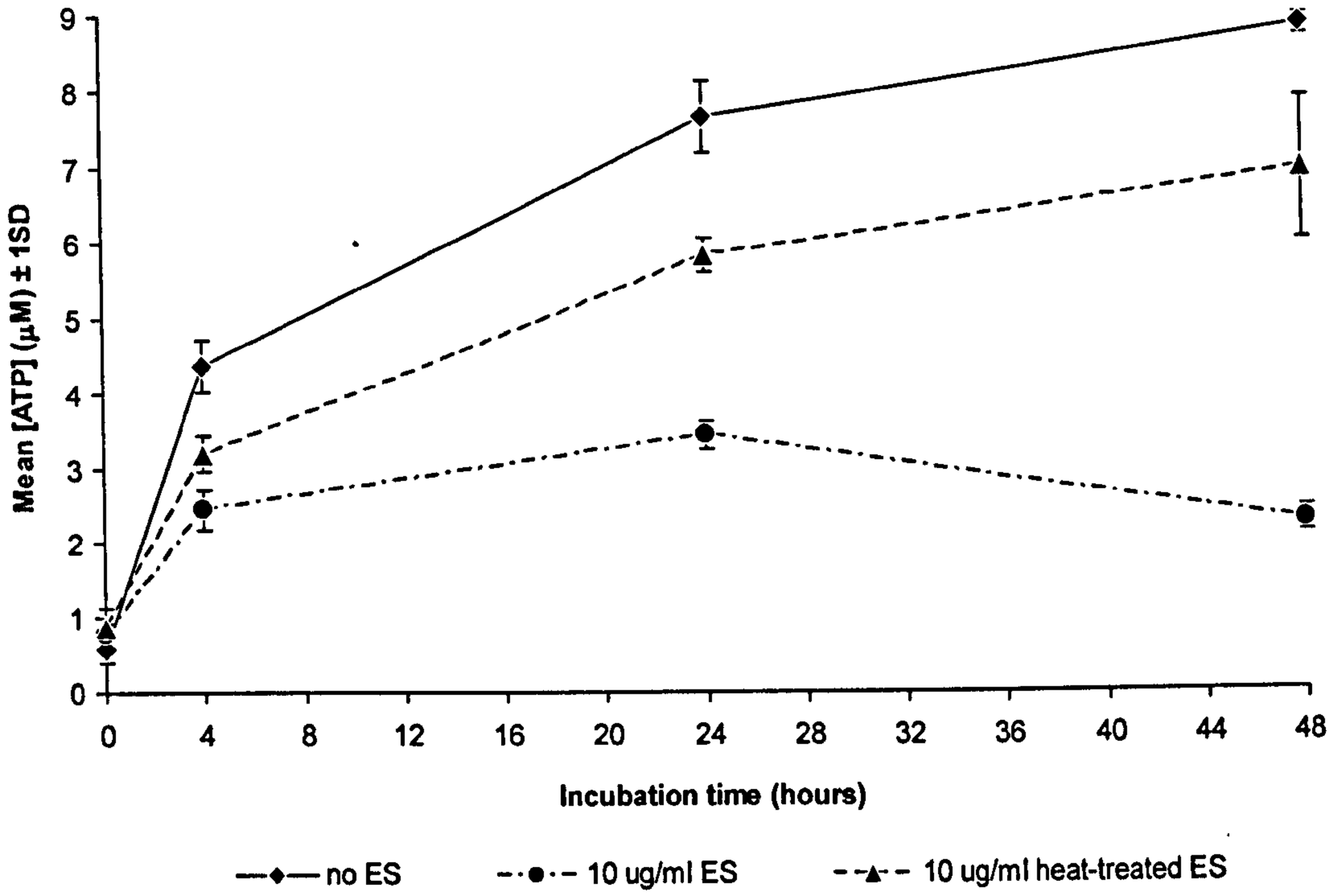

Figure 3.11 Mean ATP concentration derived from fibroblasts seeded upon a fibronectin-coated surface in the absence (no ES) or presence of 10 μg/ml larval ES (untreated or heat-treated) over the incubation period indicated. Each value represents the mean of three replicate samples.

incubation onwards, indicating that although heat treatment reduced the influence of ES, it did not abolish its effects completely. Statistical analysis of all the assay data, across all time-points, revealed significant differences between datasets (two-way ANOVA, $P < 0.0001$). Examining data at each time-point revealed that significant differences occurred from 4 hours incubation onwards. One-way ANOVA and Tukey-Kramer's multiple comparison tests of data collected at 4 hours incubation revealed significant differences between ATP levels contained within: control and untreated ES wells ($P < 0.001$); control and heat-treated ES wells ($P < 0.01$); untreated ES and heat-treated ES wells ($P < 0.05$).

Cellular nucleic acid assay (CyQUANT®) results revealed lower nucleic acid concentrations within wells exposed to heat-treated ES and in particular, untreated ES, indicating the presence of a lower number of cells when compared to the control (ES absent) (Fig. 3.12). However, no appreciable differences were seen until 48 hours incubation. Statistical analysis of all the assay data, across all time-points revealed significant differences between datasets (two-way ANOVA, $P < 0.0001$). These differences were only apparent from 48 hours incubation. Here, one-way ANOVA and Tukey-Kramer's multiple comparison tests exposed significant differences between numbers of cells contained within: control and untreated ES wells ($P < 0.001$); control and heat-treated ES wells ($P < 0.05$); untreated ES and heat-treated ES wells ($P < 0.01$). As the ATP assay results revealed clear differences from 4 hours incubation onwards, this suggests that the presence of ES may have also reduced cellular metabolic activity and hence, cell viability, in addition to decreasing cell adhesion.

3.3.5.2 Examination of cell morphology

Fibroblasts pre-stained with Celltracker™ green CMFDA were seeded upon a fibronectin-coated surface in the presence or absence of 10 μg/ml ES (heat-treated or untreated). After 4 hours incubation, random images were taken of the cells using fluorescence microscopy. These were then examined with Leica QUIPS software to assess various morphological features of the cells observed. Table 3.1 states the total number of cells that were fully visible within the images taken and hence the number of cells that were analysed for the morphological characteristics described. Statistical

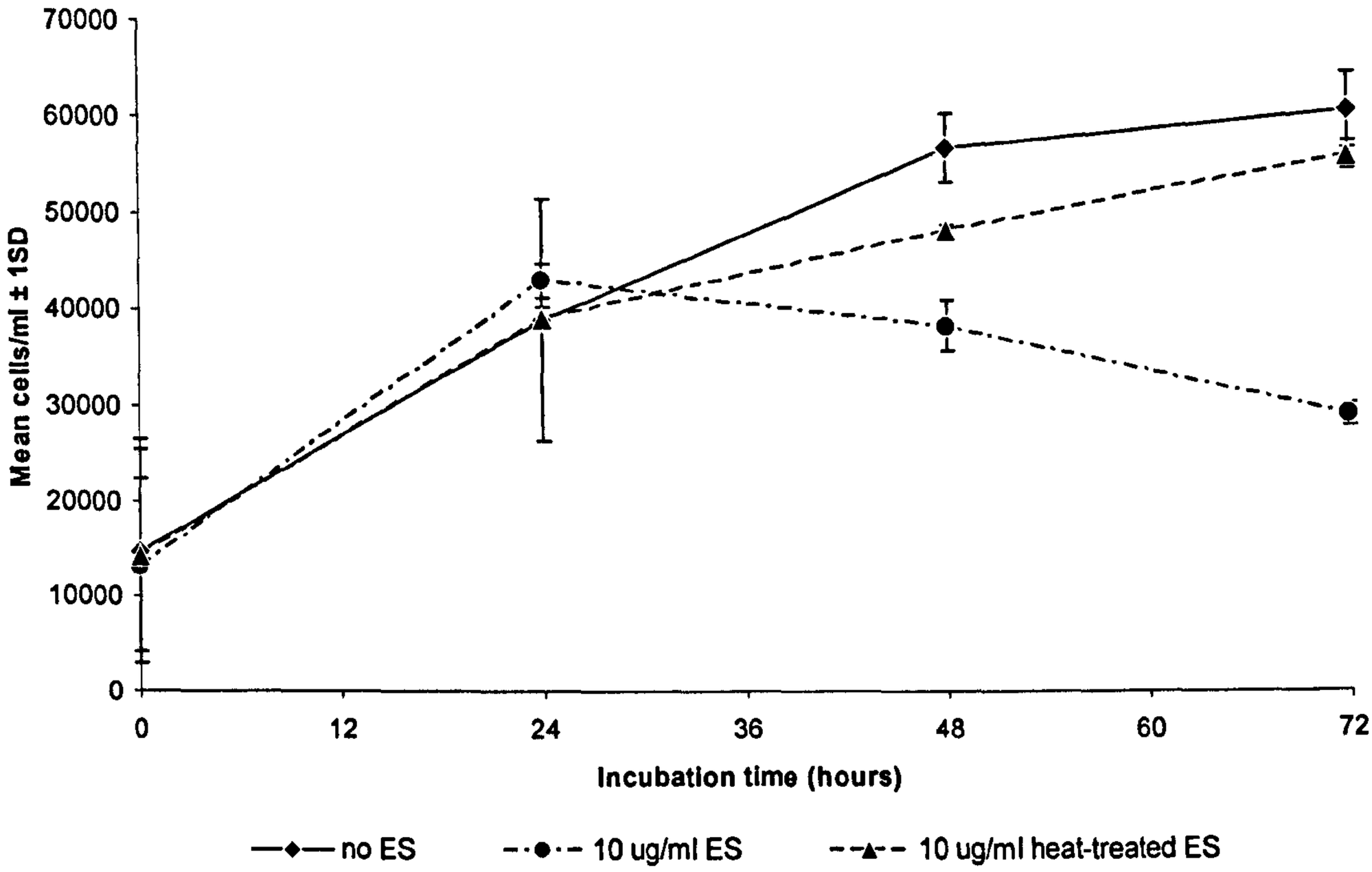

Figure 3.12 Mean number of adherent fibroblast cells seeded upon a fibronectin-coated surface in the absence (no ES) or presence of 10 μg/ml larval ES (untreated or heat-treated) over the incubation period indicated. Numbers measured using the CyQUANT® assay. Each value represents the mean of three replicate samples.

Cell morphological characteristic	ES absent	Untreated ES	Heat-treated ES
Area (μm^2)	1539.37	572.28	843.13
Length (μm)	56.92	28.73	38.04
Breadth (μm)	40.43	26.07	30.86
Perimeter (μm)	170.24	92.04	116.77
Roundness	1.38	1.10	1.22
Number of cells analysed	255	322	306

Table 3.1 Measurements of morphological characteristics of cells that had been seeded upon a fibronectin-coated surface and incubated for 4 hours in the absence of ES or in the presence of 10 μg/ml untreated ES or 10 μg/ml heat-treated ES. Median values are presented. The number of cells that were analysed is also shown. Roundness refers to a shape factor, where a perfect circle = 1. The shape factor was calculated as [cell perimeter^2 ($4\pi \times$ cell area $\times$ 1.064)$^{-1}$], where 1.064 is the digitisation adjustment factor to correct for the corners produced by the digitisation of the cell perimeter.

analysis of the data revealed that they were not normally distributed. Hence, the results are presented in terms of the median values calculated.

As shown in the representative images in Fig. 3.13, cells in untreated ES remained smaller and more rounded than those in the absence of ES, which by 4 hours incubation had started to spread over the surface. Cells exposed to the heat-treated ES were either well spread or had remained small and rounded. This indicated that heat treatment had reduced the influence of ES upon cell morphology. These differences were reflected in the data that were obtained. As shown in Table 3.1 the presence of untreated ES, and to a more limited extent heat-treated ES, reduced the median cell area, length, breadth and perimeter calculated. Median shape factor values were also reduced, indicating cells to be more rounded in the presence of ES. Application of the Kruskal-Wallis ANOVA and Dunn's multiple comparisons test revealed all of these reductions to be significant. Highly significant differences ($P < 0.001$) between all cell culture conditions for all the morphological features measured were detected. Differences between the surface areas of individual cells are shown in Fig. 3.14. As deduced from the percentage frequency distributions displayed, the presence of ES decreased cell surface area, skewing the peak of the frequency distribution curve to the left (lower cell area ranges). This was particularly so with the untreated ES.

3.3.6 Effect of larval ES upon fibroblast adhesion to collagen

3.3.6.1 ATP and cellular nucleic acid assays

The effects of larval ES (from batch C) upon fibroblast cell adhesion to a collagen-coated surface was first examined using the ATPLite™-M and CyQUANT® biochemical assay kits. Following a similar procedure to when fibronectin was used, cells were incubated in the presence or absence of 10 μg/ml larval ES (untreated or heat-treated) within wells coated with collagen. Following the specified period of incubation, wells were aspirated of medium to remove detached cells and the number of remaining adhered cells estimated using the indicated assay.

ATP assay results (Fig. 3.15) revealed a similar trend to when cells were adhered to fibronectin. However, the differences observed between treatments were less

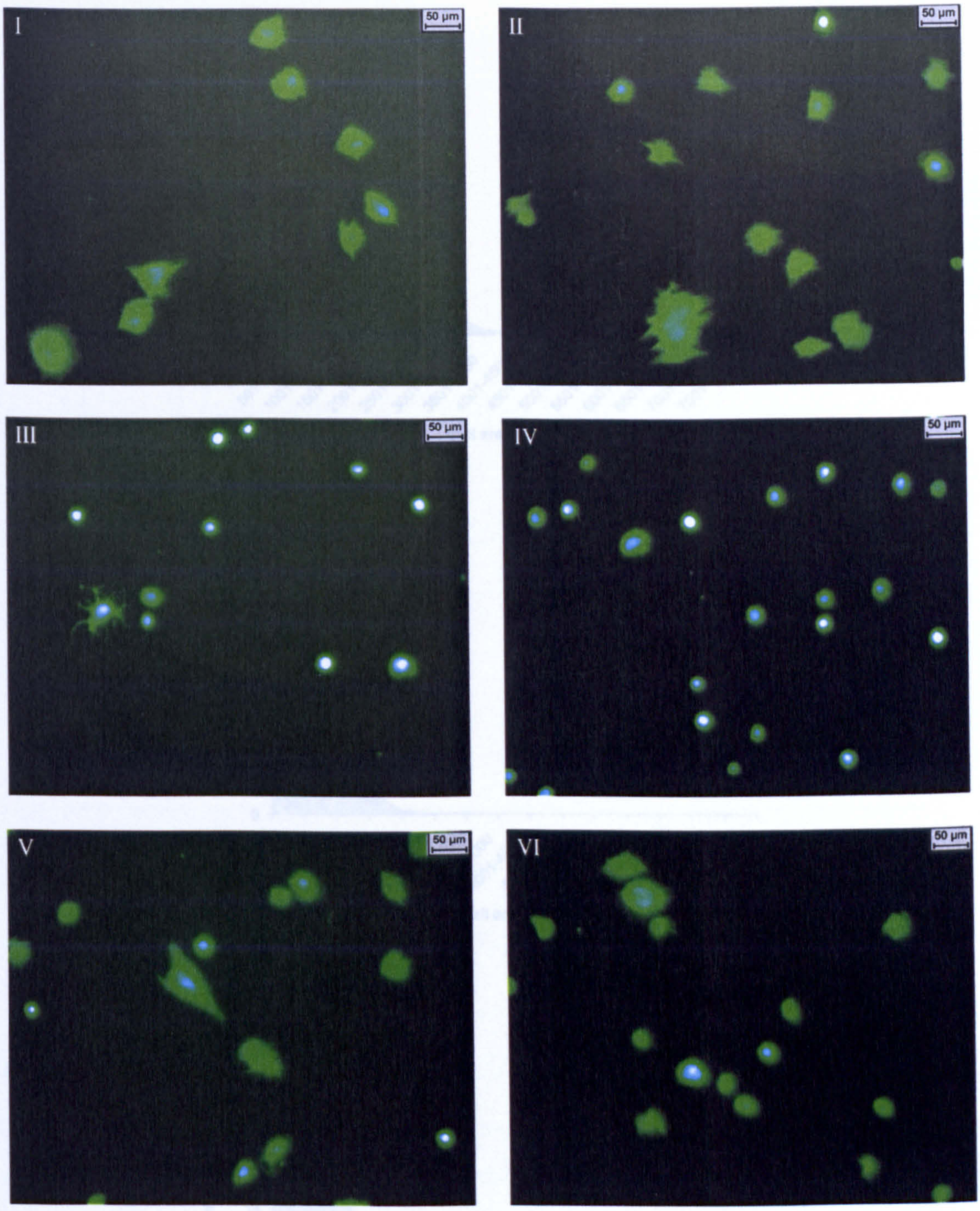

Figure 3.13 Representative images of fibroblasts following 4 hours incubation upon a fibronectin-coated surface in the absence of ES (I and II) or in the presence of 10 µg/ml untreated ES (III and IV) or 10 µg/ml heat-treated ES (V and VI). Images illustrate the morphological differences shown quantitatively in Table 3.1 and reflect results of the relevant statistical analysis described in section 3.3.5.2.

a.

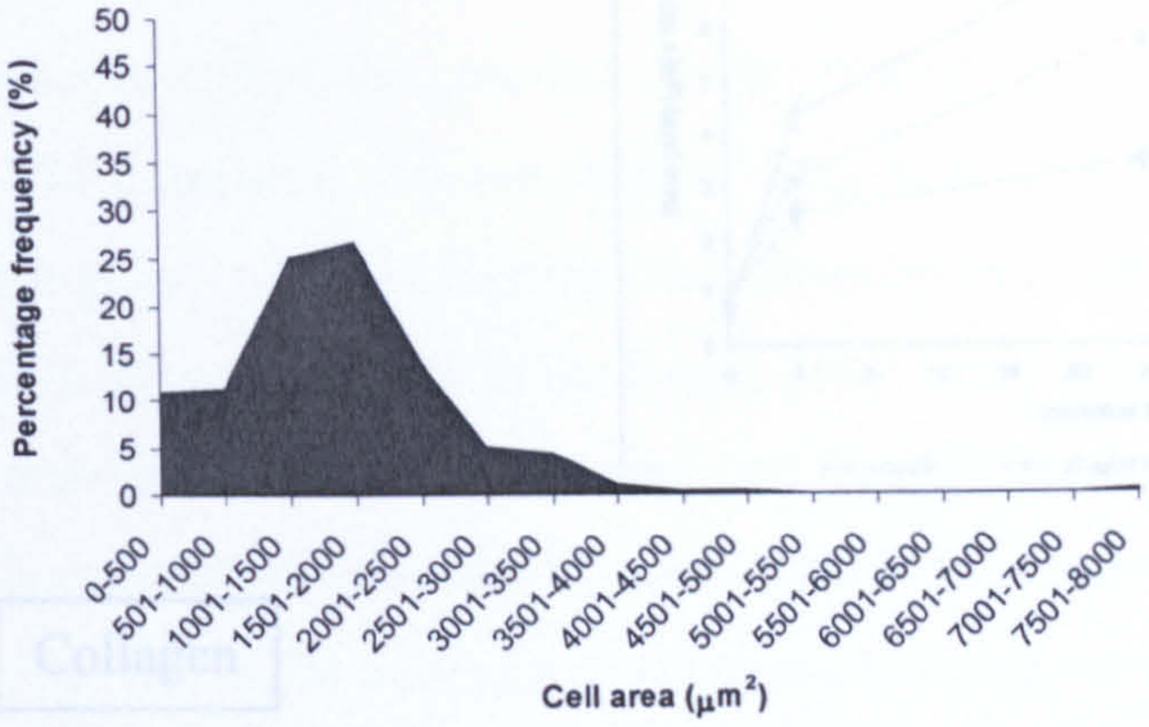

b.

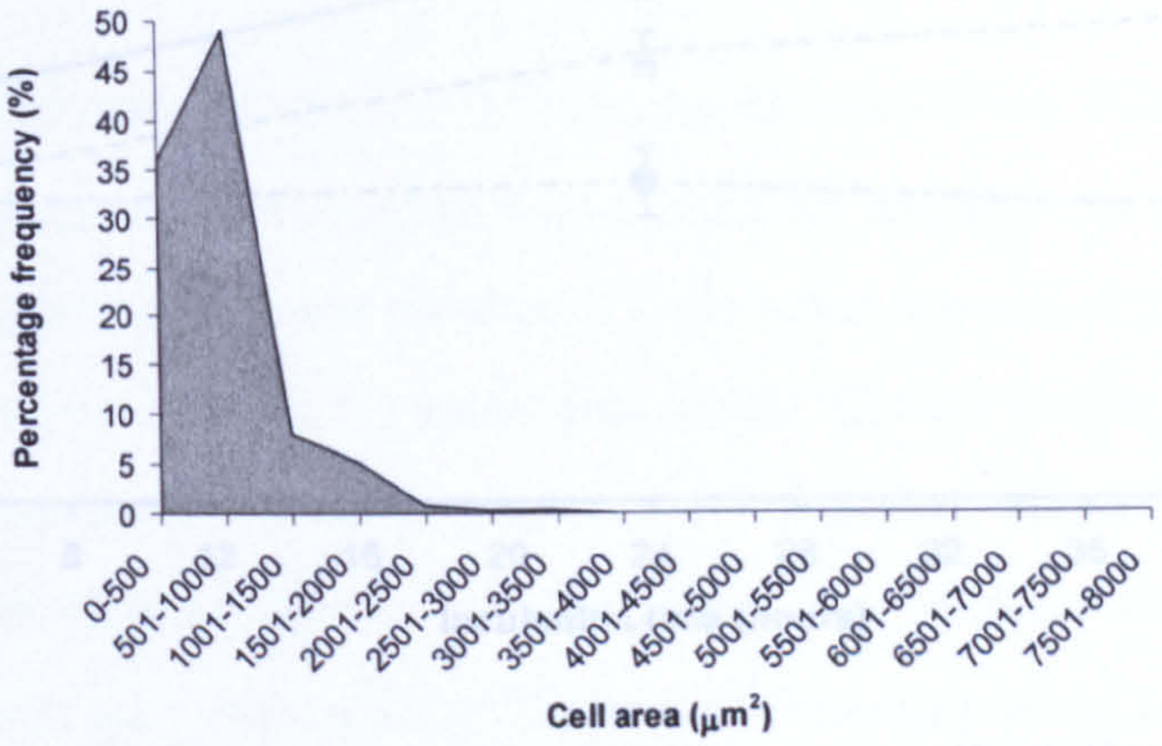

c.

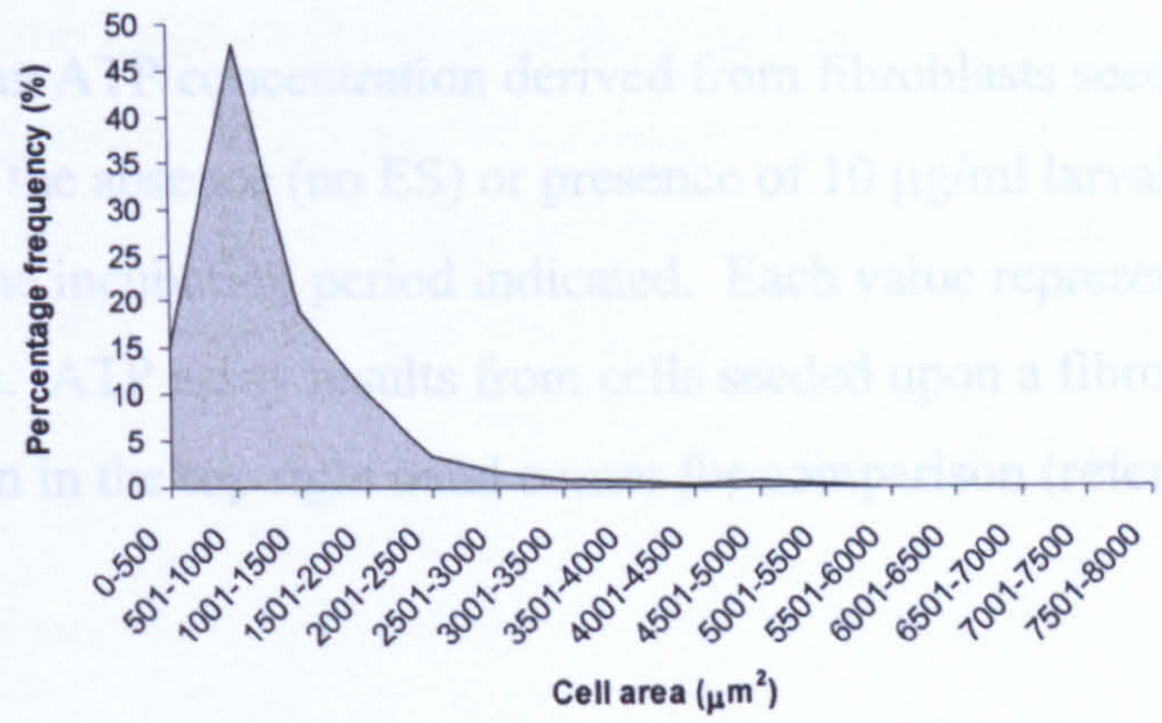

Figure 3.14 Percentage frequency distribution of fibroblast cell area, as measured using Leica QUIPS software. Taken from images of cells after they had been incubated for 4 hours upon a fibronectin-coated surface in the absence (a) or presence of 10 μg/ml untreated ES (b) or 10 μg/ml heat-treated ES (c).

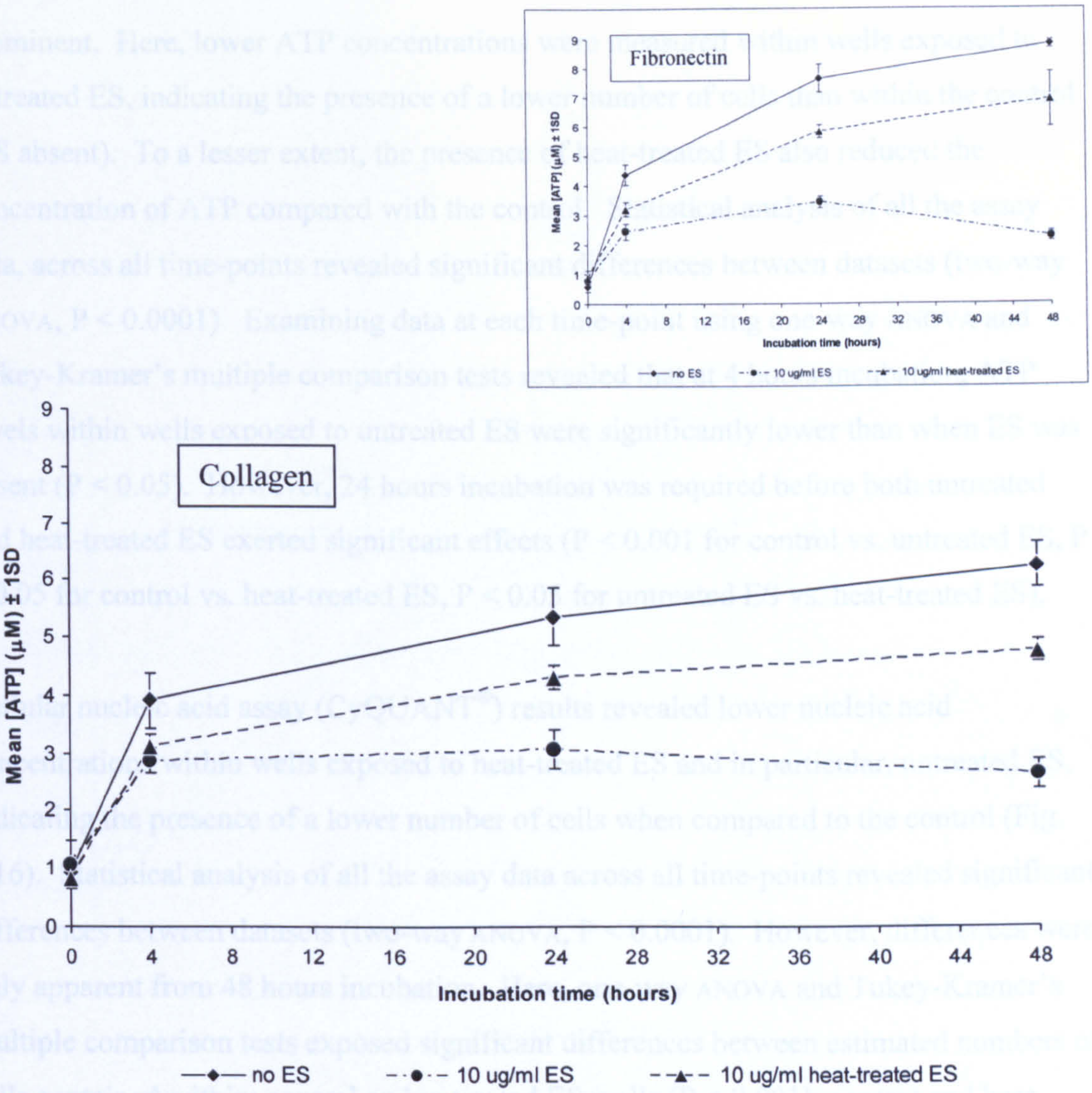

Figure 3.15 Mean ATP concentration derived from fibroblasts seeded upon a collagen-coated surface in the absence (no ES) or presence of 10 µg/ml larval ES (heat-treated or untreated) over the incubation period indicated. Each value represents the mean of three replicate samples. ATP assay results from cells seeded upon a fibronectin-coated surface are shown in the top right hand corner for comparison (refer to Fig. 3.11).

prominent. Here, lower ATP concentrations were measured within wells exposed to untreated ES, indicating the presence of a lower number of cells than within the control (ES absent). To a lesser extent, the presence of heat-treated ES also reduced the concentration of ATP compared with the control. Statistical analysis of all the assay data, across all time-points revealed significant differences between datasets (two-way ANOVA, $P < 0.0001$). Examining data at each time-point using one-way ANOVA and Tukey-Kramer's multiple comparison tests revealed that at 4 hours incubation, ATP levels within wells exposed to untreated ES were significantly lower than when ES was absent ($P < 0.05$). However, 24 hours incubation was required before both untreated and heat-treated ES exerted significant effects ($P < 0.001$ for control vs. untreated ES, $P < 0.05$ for control vs. heat-treated ES, $P < 0.05$ for untreated ES vs. heat-treated ES).

Cellular nucleic acid assay (CyQUANT®) results revealed lower nucleic acid concentrations within wells exposed to heat-treated ES and in particular, untreated ES, indicating the presence of a lower number of cells when compared to the control (Fig. 3.16). Statistical analysis of all the assay data across all time-points revealed significant differences between datasets (two-way ANOVA, $P < 0.0001$). However, differences were only apparent from 48 hours incubation. Here, one-way ANOVA and Tukey-Kramer's multiple comparison tests exposed significant differences between estimated numbers of cells contained within: control and untreated ES wells ($P < 0.001$); control and heat-treated ES wells ($P < 0.01$); untreated ES and heat-treated ES wells ($P < 0.05$). As the ATP assay results revealed clear differences from 4 hours incubation onwards, this suggests that the presence of ES may have also reduced cellular metabolic activity and hence, cell viability, in addition to decreasing cell adhesion. Similar conclusions were drawn when fibronectin-coated wells were used.

3.3.6.2 Examination of cell morphology

In a procedure similar to that used to examine cell morphology whilst the cells were in contact with a fibronectin-coated surface, fibroblasts that had been pre-stained with Celltracker™ green CMFDA were seeded upon a collagen-coated surface in the presence or absence of 10 μg/ml ES (heat-treated or untreated). After 4 hours incubation, random images were taken of the cells using fluorescence microscopy.

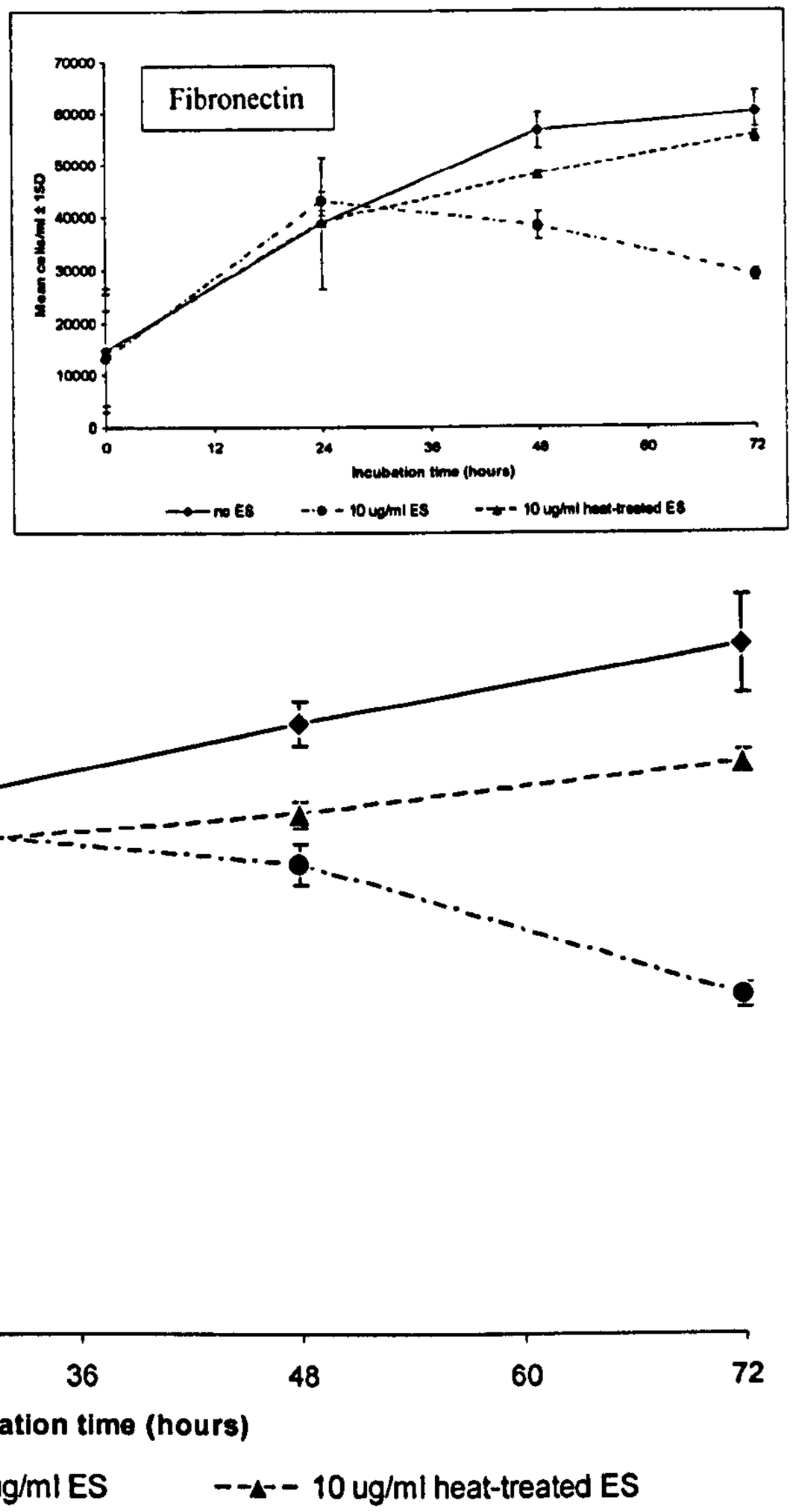

Figure 3.16 Mean number of adherent fibroblast cells seeded upon a collagen-coated surface in the absence (no ES) or presence of 10 μg/ml larval ES (heat-treated or untreated) over the incubation period indicated. Numbers measured using the CyQUANT® assay. Each value represents the mean of three replicate samples. Adherent cell number results from cells seeded upon a fibronectin-coated surface are shown in the top right hand corner for comparison (refer to Fig. 3.12).

These were then examined with Leica QUIPS software. Table 3.2 states the total number of cells that were fully visible within the images and hence the number of cells that were analysed. As with fibronectin, statistical analysis of the data revealed that they were not normally distributed. Hence, the results are presented here in terms of the median values calculated.

As shown in the representative images in Fig. 3.17, differences in the morphologies of cells exposed to different conditions were slight or undetectable. Cells in untreated ES were only marginally smaller and more rounded than those in the absence of ES. Cells exposed to the heat-treated ES appeared quite similar to those in the control. These conclusions were reflected in the data that were obtained. As shown in Table 3.2, the presence of untreated ES slightly reduced the median cell area, length, breadth and perimeter calculated. The median shape factor was also slightly reduced, indicating cells to be more rounded in the presence of ES. Application of the Kruskal-Wallis ANOVA and Dunn's multiple comparisons test revealed all of these reductions to be significant ($P < 0.001$). Median values for cells in the presence of heat-treated ES were only very slightly lower than those for cells in the control. Kruskal-Wallis ANOVA and Dunn's multiple comparisons test revealed no significant differences in cell area or cell breadth ($P < 0.05$), although significant differences in cell length ($P < 0.01$), perimeter ($P < 0.05$) and roundness ($P < 0.001$) were detected. However, despite these significant results, it may be concluded that heat-treated ES exerted a negligible effect over the 4 hour incubation period. This is because it was difficult to visually distinguish any differences within the images between cells exposed to each condition. In addition, the differences in the median values were very small. Also, not all of the morphological feature comparisons yielded significant results. As each feature is related to each other (for instance, cell area will play a role in determining cell length and breadth, while cell roundness will affect cell perimeter distance), only firm positive conclusions concerning the existence of scientifically important differences could be made if all the comparisons provided significant P values. Differences between the surface areas of individual cells are shown in Fig. 3.18. As deduced from the graphs displayed, the presence of untreated ES increased the percentage frequency of measurements lying within the 0 to 500 μm^2 range. Heat-treated ES had a minimal effect upon shifting the percentage frequency distribution to the left, towards the lower cell area ranges.

Cell morphological characteristic	ES absent	Untreated ES	Heat-treated ES
Area (μm^2)	679.54	525.86	627.18
Length (μm)	32.45	27.66	30.32
Breadth (μm)	27.664	25.00	26.60
Perimeter (μm)	102.68	87.25	96.03
Roundness	1.12	1.09	1.09
Number of cells analysed	297	276	292

Table 3.2 Measurements of morphological characteristics of cells that had been seeded upon a collagen-coated surface and incubated for 4 hours in the presence or absence of 10 μg/ml ES (untreated or heat-treated). Median values are presented. The number of cells that were analysed is also shown. The shape factor was calculated as [cell perimeter^2 ($4\pi \times$ cell area $\times$ 1.064)$^{-1}$], where 1.064 is the digitisation adjustment factor to correct for the corners produced by the digitisation of the cell perimeter.

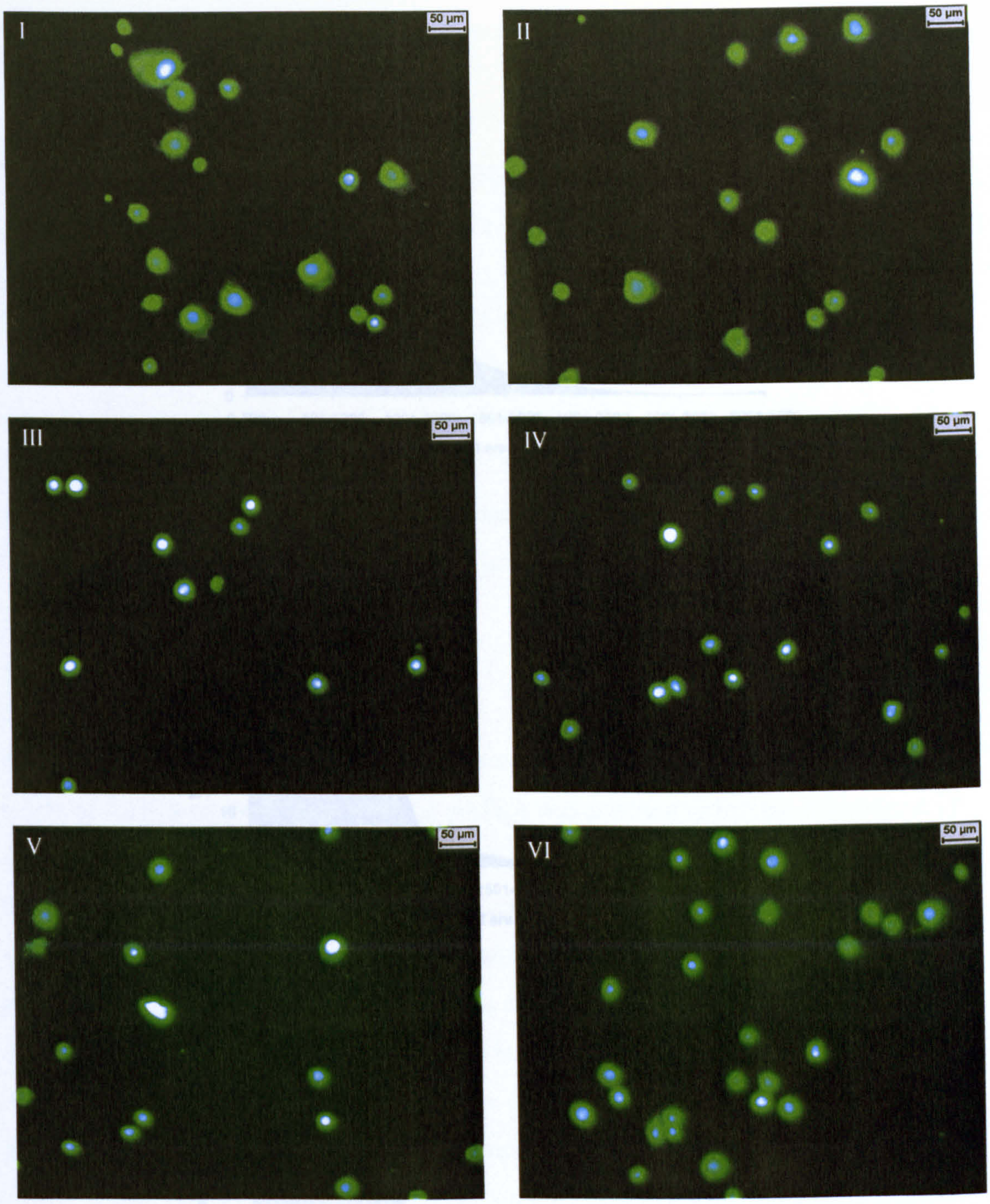

Figure 3.17 Representative images of fibroblasts following 4 hours incubation upon a collagen-coated surface in the absence of ES (I and II) or in the presence of 10 µg/ml untreated ES (III and IV) or 10 µg/ml heat-treated ES (V and VI). Images illustrate the morphological differences shown quantitatively in Table 3.2 and reflect results of the relevant statistical analysis described in section 3.3.6.2.

a.

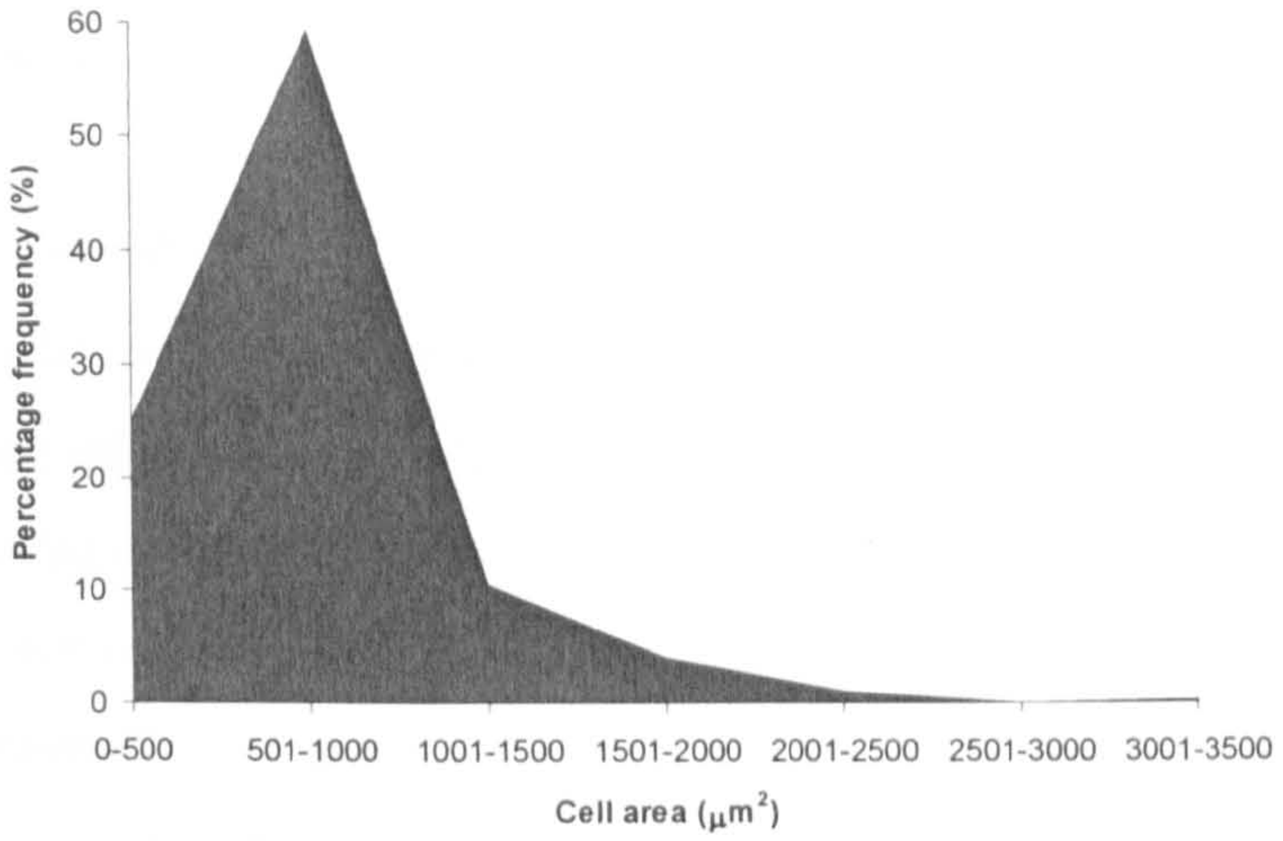

b.

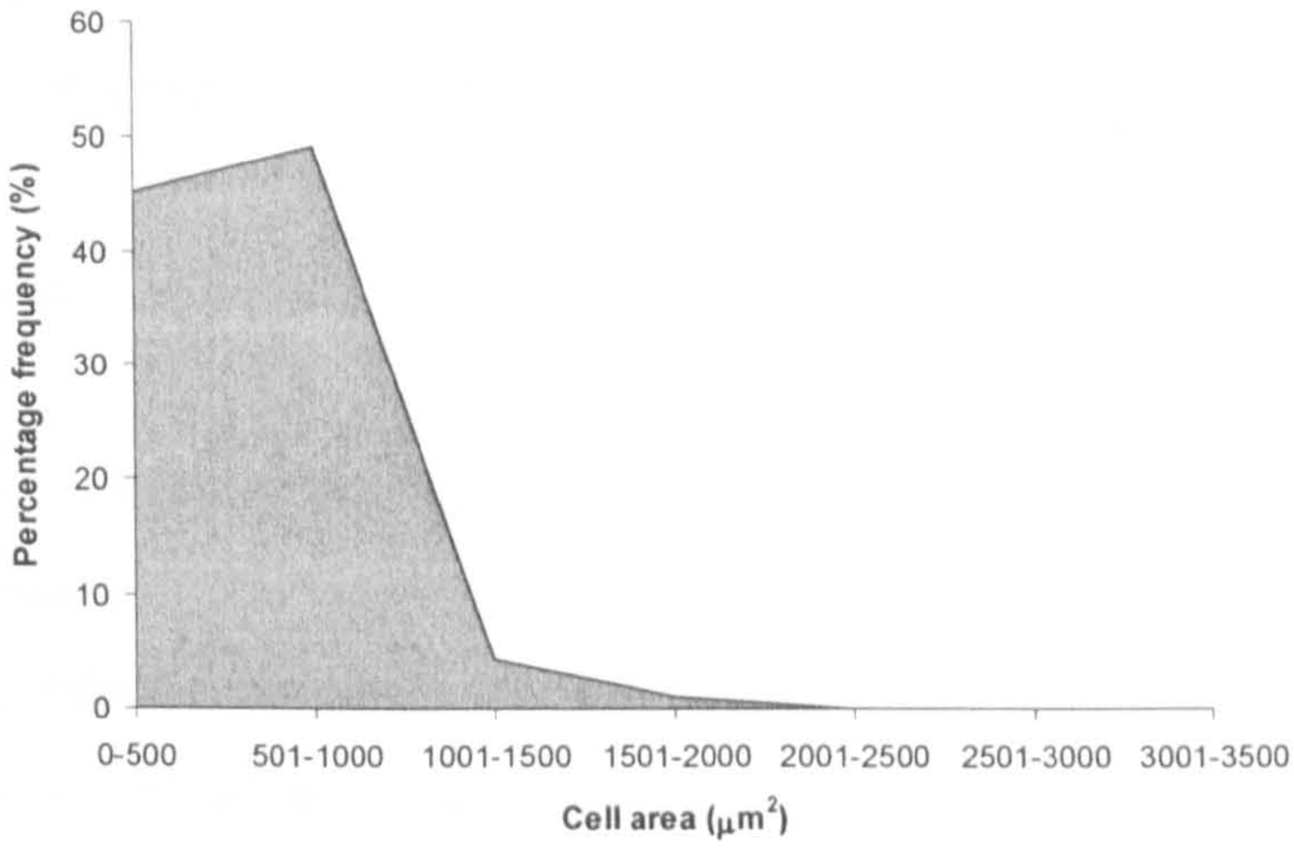

c.

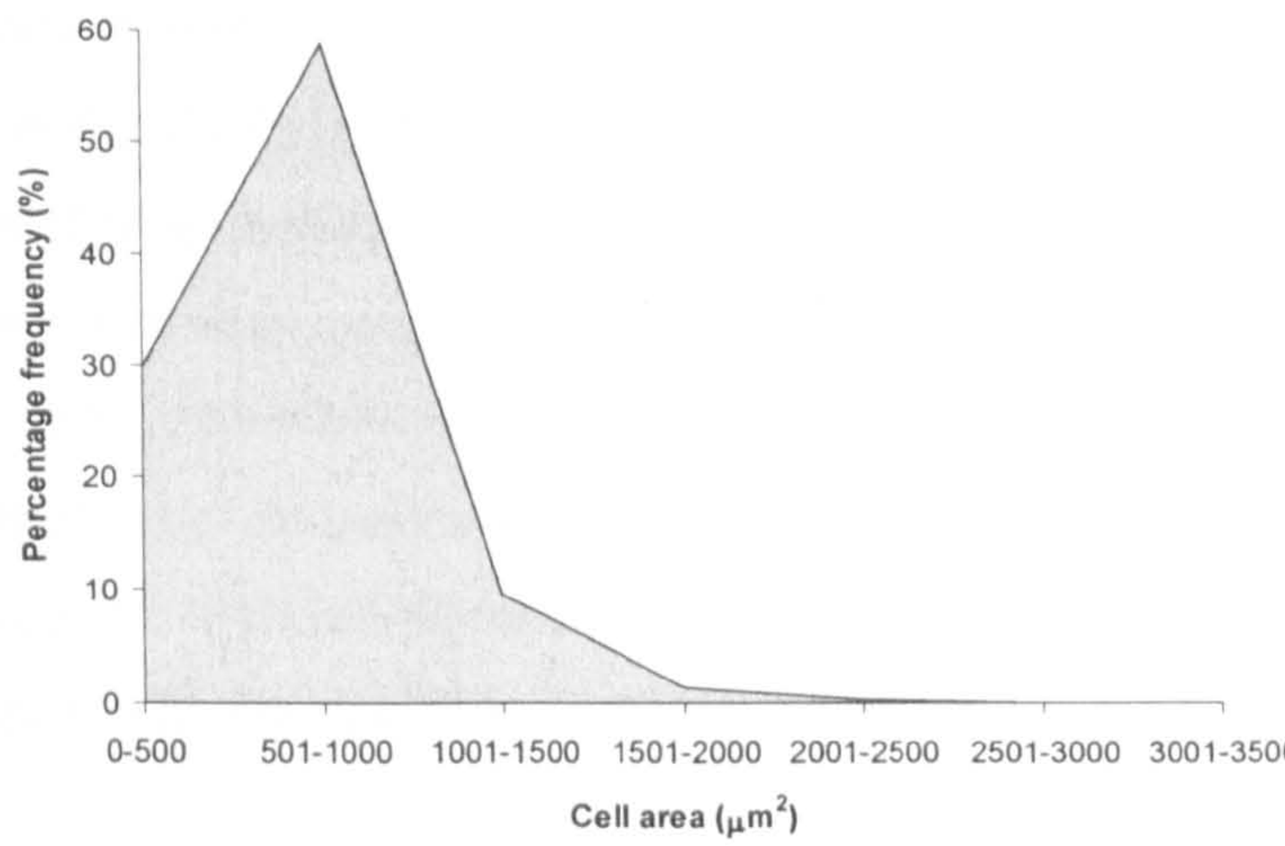

Figure 3.18 Percentage frequency distribution of fibroblast cell area, as measured using Leica QUIPS software. Taken from images of cells after they had been incubated for 4 hours upon a collagen-coated surface in the absence (a) or presence of 10 μg/ml untreated ES (b) or 10 μg/ml heat-treated ES (c).

3.3.7 Effect of larval ES upon the ECM protein-coated surface: influence upon fibroblast adhesion

Previous studies have shown larval ES to degrade common ECM proteins such as fibronectin and collagen. Other studies have shown that the concentration of the protein coating the surface influences cell adhesion. Hence, the effect of pre-exposing the fibronectin- or collagen-coated surface to ES (taken from batch D) before the addition of cells was therefore examined. ATP and CyQUANT® assays similar to those conducted in sections 3.3.5.1 and 3.3.6.1 were undertaken to estimate the number of cells adhering to the pre-exposed surfaces. Comparisons were made with the levels of cell adhesion that occurred upon surfaces that had not been pre-exposed to ES, but were then subsequently exposed to 10 μg/ml ES or PBS upon the inclusion of cells.

3.3.7.1 Fibronectin

As shown in Fig. 3.19, pre-exposing the fibronectin-coated surface to ES modified the levels of ATP detected. The longer the surface was exposed to ES, the lower the ATP levels measured, indicating an inverse relationship between exposure to ES and subsequent levels of cell adhesion and cell viability. Application of the one-way ANOVA and Tukey-Kramer's multiple comparison tests upon data collated at each time-point revealed significant differences in the levels of ATP and therefore the estimated levels of cell adhesion and viability (Table 3.3). Firstly, at 4, 24 and 48 hour time-points, cell adhesion and viability upon the surfaces pre-exposed for 24 and 48 hours was significantly lower than that upon the surface which was not exposed to ES at any time (the ES blank control), either before or upon the addition of cells. As the pre-exposed surfaces were aspirated of all medium containing ES and washed three times with PBS before the addition of cells, such significant differences indicate that ES exerted an indirect effect upon cell adhesion and viability by altering the surface.

There were also significant differences in cell adhesion and viability between samples containing the pre-exposed surfaces (pre-exposed to ES for either 4, 24 or 48 hours) and those containing surfaces that had been simultaneously seeded with cells and exposed to ES (the 10 μg/ml ES control). However, it is interesting to note that there were no significant differences when comparing cell adhesion upon surfaces that had been

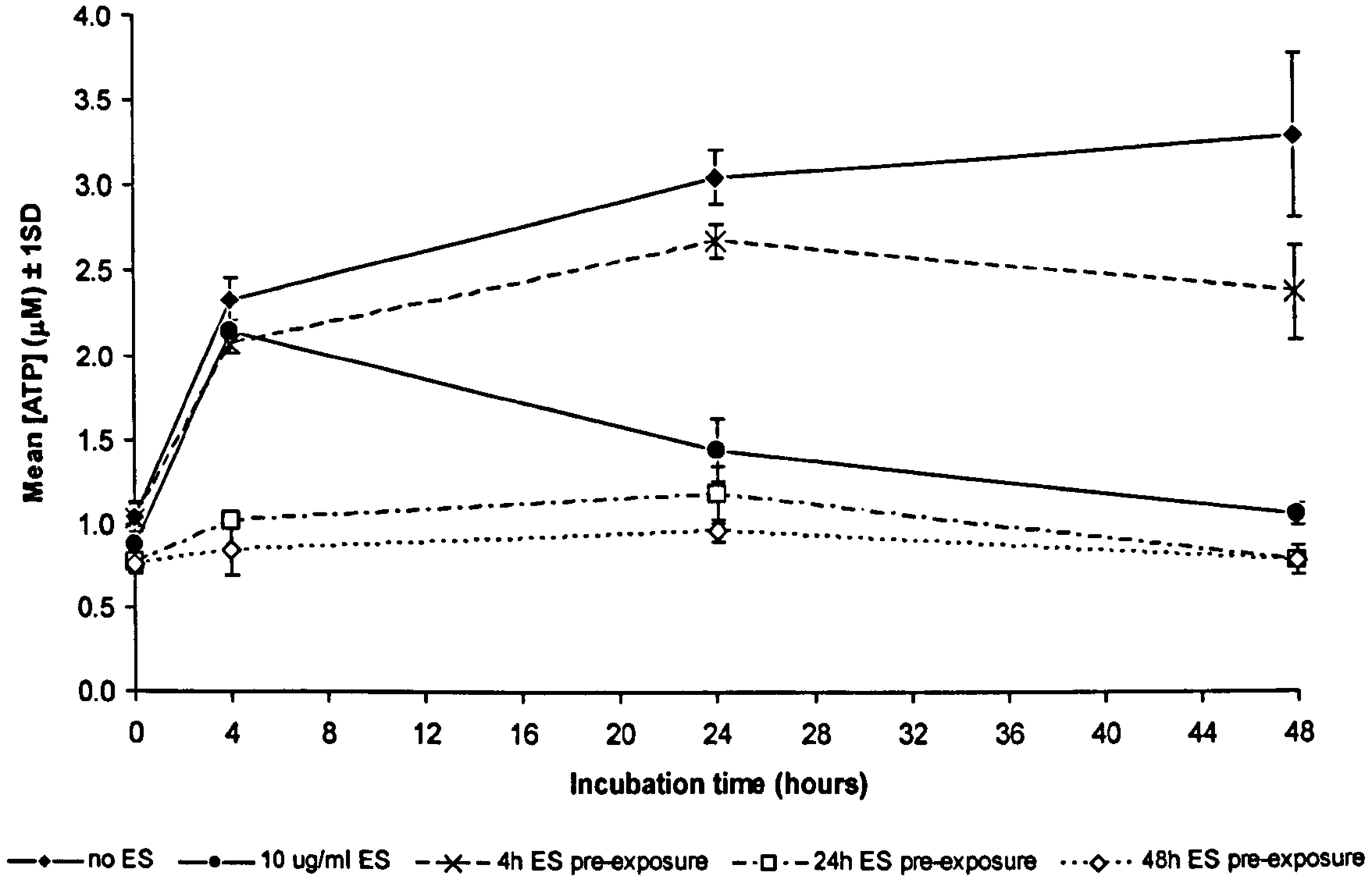

Figure 3.19 Mean ATP concentration derived from fibroblasts seeded upon a fibronectin-coated surface in the absence or presence of 10 µg/ml ES. Where indicated, the surface had first been pre-exposed to 10 µg/ml larval ES for 4, 24 or 48 hours before the addition of cells in ES-free medium. Each value represents the mean of three replicate samples.

4 Hours One-way ANOVA: $P < 0.0001$.

	ES blank control	10 µg/ml ES control	4h pre-exposed	24h pre-exposed	48h pre-exposed
ES blank	-	-	-	-	-
10 µg/ml ES	ns	-	-	-	-
4h pre-exposed	ns	ns	-	-	-
24h pre-exposed	$P < 0.001$	$P < 0.001$	$P < 0.001$	-	-
48h pre-exposed	$P < 0.001$	$P < 0.001$	$P < 0.001$	ns	-

24 Hours One-way ANOVA: $P < 0.0001$.

	ES blank control	10 µg/ml ES control	4h pre-exposed	24h pre-exposed	48h pre-exposed
ES blank	-	-	-	-	-
10 µg/ml ES	$P < 0.001$	-	-	-	-
4h pre-exposed	ns	$P < 0.001$	-	-	-
24h pre-exposed	$P < 0.001$	ns	$P < 0.001$	-	-
48h pre-exposed	$P < 0.001$	$P < 0.001$	$P < 0.001$	ns	-

48 Hours One-way ANOVA: $P < 0.0001$.

	ES blank control	10 µg/ml ES control	4h pre-exposed	24h pre-exposed	48h pre-exposed
ES blank	-	-	-	-	-
10 µg/ml ES	$P < 0.001$	-	-	-	-
4h pre-exposed	$P < 0.01$	$P < 0.001$	-	-	-
24h pre-exposed	$P < 0.001$	ns	$P < 0.001$	-	-
48h pre-exposed	$P < 0.001$	ns	$P < 0.001$	ns	-

Table 3.3 Analysis of cell adhesion/viability upon a fibronectin-coated surface, as estimated using the ATP assay. Results of one-way ANOVA and Tukey-Kramer's multiple comparison tests upon data collated at each time-point of a 48 hour incubation period. As shown by the results highlighted in yellow, there were no significant differences in cell adhesion/viability upon surfaces that had been exposed to ES for the same length of time, either before the addition of cells (the pre-exposed surfaces) or from when cells had been added (10 µg/ml ES control).

exposed to ES for the same length of time, either before the addition of cells (the pre-exposed surfaces) or from when cells had been added (10 μg/ml ES control). This indicated that modification of the fibronectin-coated surface by ES played a primary role in altering cell adhesion and viability.

In a similar experiment, the CyQUANT® assay was applied to determine the total number of adherent cells within samples. Here, pre-exposing the fibronectin-coated surface to ES was shown to modify cell number estimates (Fig. 3.20). As with the ATP assay, results demonstrated that the longer the surface was exposed to ES, the lower the cell numbers measured, indicating an inverse relationship between exposure to ES and subsequent levels of cell adhesion. Indeed, application of the one-way ANOVA and Tukey-Kramer's multiple comparison tests revealed that cell number estimates within samples containing the pre-exposed surfaces were significantly lower than within those containing surfaces that had not been exposed to ES at any time (the ES blank control) (Table 3.4). However, as can be seen in Fig. 3.20, the differences were much smaller than those estimated by the ATP assay. In addition, cell adhesion in the presence of ES (10 μg/ml ES control) was significantly lower than the levels of cell adhesion that had occurred upon the pre-exposed surfaces. It therefore appeared that although pre-exposing the fibronectin-coated surface to ES subsequently influenced fibroblast adhesion, the effect was not as great as when the cells were actually exposed to ES upon their introduction to the surface.

3.3.7.2 Collagen

As shown in Fig. 3.21, pre-exposing the collagen-coated surface to ES modified the levels of ATP detected. In common with the results described in the previous section (3.3.6.1), there appeared to be an inverse relationship between length of pre-exposure to ES and subsequent levels of cell adhesion and viability. However, differences between samples were smaller and were not deemed to be significant at the 24 hour time-point (Table 3.5). Indeed, none of the data measured at 24 hours displayed any significant differences. In comparison to when the surfaces were coated with fibronectin, the results here were less conclusive. However, pre-exposing the collagen-coated surface to ES did appear to exert a limited effect upon the cells.

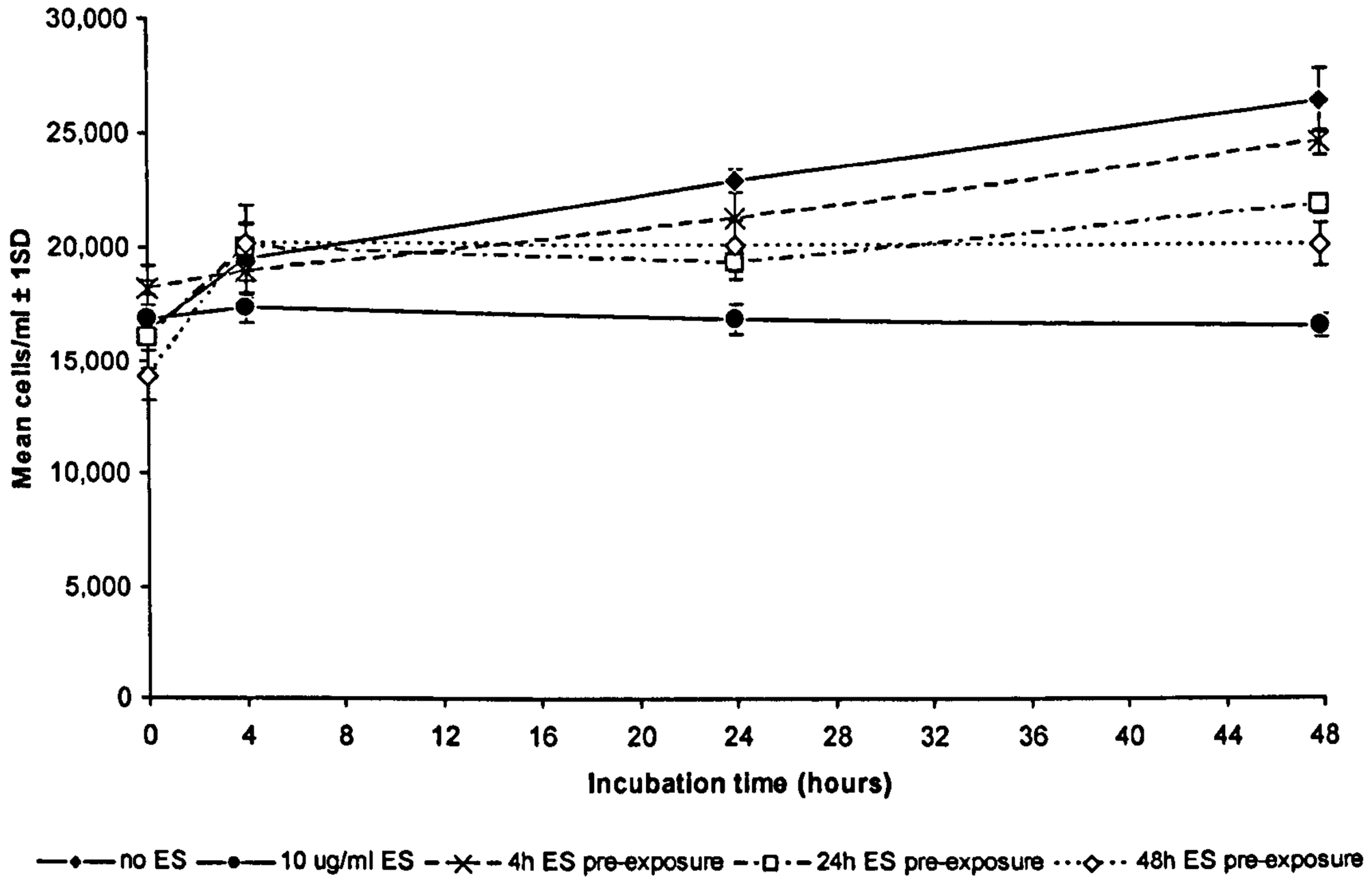

Figure 3.20 Mean number of adherent fibroblast cells seeded upon a fibronectin-coated surface in the absence or presence of 10 μg/ml ES. Where indicated, the surface had first been pre-exposed to 10 μg/ml larval ES for 4, 24 or 48 hours before the addition of cells in ES-free medium. Each value represents the mean of three replicate samples.

4 Hours One-way ANOVA: P = 0.1151 (not significant).

	ES blank control	10 μg/ml ES control	4h pre-exposed	24h pre-exposed	48h pre-exposed
ES blank	-	-	-	-	-
10 μg/ml ES	ns	-	-	-	-
4h pre-exposed	ns	ns	-	-	-
24h pre-exposed	ns	ns	ns	-	-
48h pre-exposed	ns	ns	ns	ns	-

24 Hours One-way ANOVA: P = 0.0002.

	ES blank control	10 μg/ml ES control	4h pre-exposed	24h pre-exposed	48h pre-exposed
ES blank	-	-	-	-	-
10 μg/ml ES	P < 0.001	-	-	-	-
4h pre-exposed	ns	P < 0.01	-	-	-
24h pre-exposed	P < 0.01	ns	ns	-	-
48h pre-exposed	P < 0.05	P < 0.05	ns	ns	-

48 Hours One-way ANOVA: P < 0.0001.

	ES blank control	10 μg/ml ES control	4h pre-exposed	24h pre-exposed	48h pre-exposed
ES blank	-	-	-	-	-
10 μg/ml ES	P < 0.001	-	-	-	-
4h pre-exposed	ns	P < 0.001	-	-	-
24h pre-exposed	P < 0.001	P < 0.001	P < 0.05	-	-
48h pre-exposed	P < 0.001	P < 0.01	P < 0.001	ns	-

Table 3.4 Analysis of cell adhesion upon a fibronectin-coated surface, as estimated using the CyQUANT® assay. Results of one-way ANOVA and Tukey-Kramer's multiple comparison tests upon data collated at each time-point of a 48 hour incubation period.

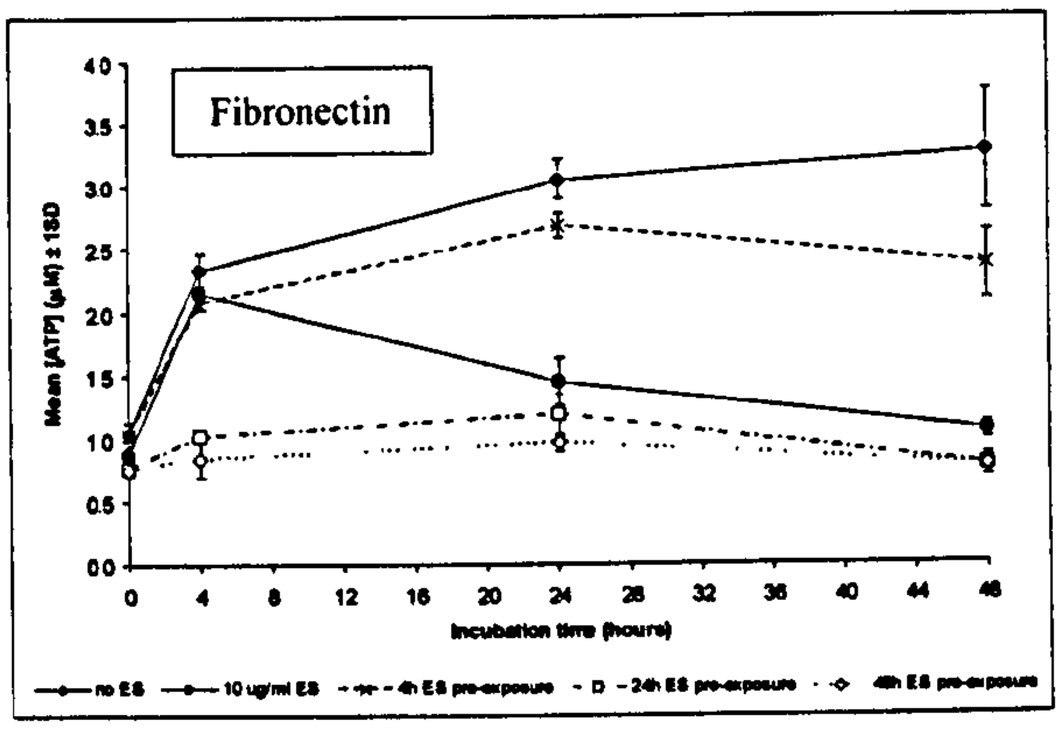

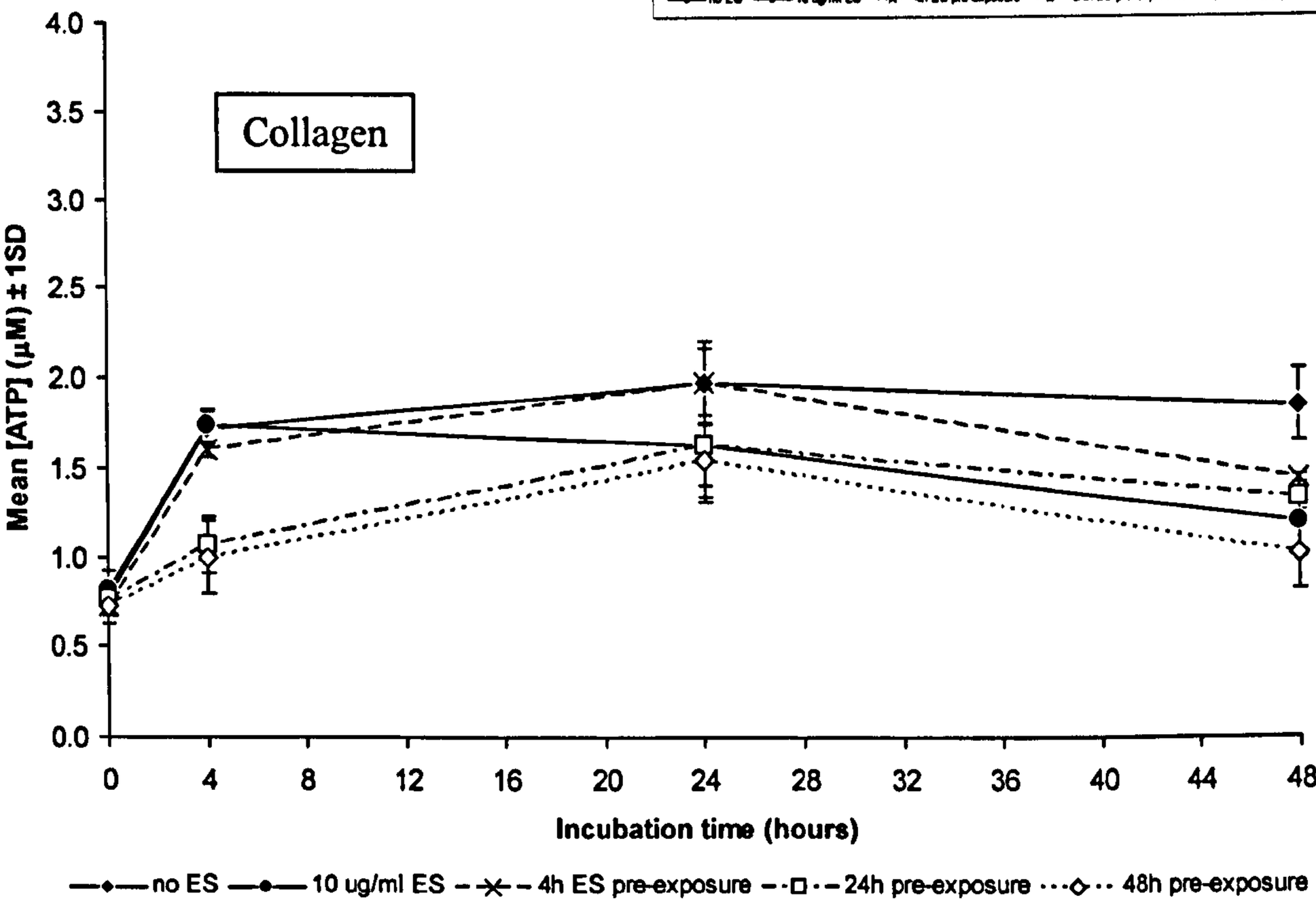

Figure 3.21 Mean ATP concentration derived from fibroblasts seeded upon a collagen-coated surface in the absence or presence of 10 µg/ml ES. Where indicated, the surface had first been pre-exposed to 10 µg/ml larval ES for 4, 24 or 48 hours before the addition of cells in ES-free medium. Each value represents the mean of three replicate samples. ATP assay results from cells seeded upon a fibronectin-coated surface are shown in the top right hand corner for comparison (refer to Fig. 3.19).

4 Hours One-way ANOVA: P < 0.0001.

	ES blank control	10 µg/ml ES control	4h pre-exposed	24h pre-exposed	48h pre-exposed
ES blank	-	-	-	-	-
10 µg/ml ES	ns	-	-	-	-
4h pre-exposed	ns	ns	-	-	-
24h pre-exposed	P < 0.001	P < 0.001	P < 0.01	-	-
48h pre-exposed	P < 0.001	P < 0.001	P < 0.01	ns	-

24 Hours One-way ANOVA: P = 0.0749 (not significant).

	ES blank control	10 µg/ml ES control	4h pre-exposed	24h pre-exposed	48h pre-exposed
ES blank	-	-	-	-	-
10 µg/ml ES	ns	-	-	-	-
4h pre-exposed	ns	ns	-	-	-
24h pre-exposed	ns	ns	ns	-	-
48h pre-exposed	ns	ns	ns	ns	-

48 Hours One-way ANOVA: P = 0.0002.

	ES blank control	10 µg/ml ES control	4h pre-exposed	24h pre-exposed	48h pre-exposed
ES blank	-	-	-	-	-
10 µg/ml ES	P < 0.01	-	-	-	-
4h pre-exposed	P < 0.05	ns	-	-	-
24h pre-exposed	P < 0.01	ns	ns	-	-
48h pre-exposed	P < 0.001	ns	P < 0.05	ns	-

Table 3.5 Analysis of cell adhesion/viability upon a collagen-coated surface, as estimated using the ATP assay. Results of one-way ANOVA and Tukey-Kramer's multiple comparison tests upon data collated at each time-point of a 48 hour incubation period.

Results from a similar experiment in which the CyQUANT® assay was applied, were less conclusive than comparative results from when fibronectin was used. As shown in Fig. 3.22, pre-exposing the collagen-coated surface to ES before the addition of cells appeared to exert little effect upon subsequent cell adhesion. Results were similar to those taken from samples containing surfaces that had not been exposed to ES at any time (the ES blank control). In addition, cell adhesion in the presence of ES (10 μg/ml ES control) was significantly lower than the levels of adhesion which occurred upon the pre-exposed surfaces at all the time-points measured (Table 3.6). Although lower numbers of cells were found upon 48 hour pre-exposed surfaces than upon surfaces pre-exposed for 4 hours, the differences were small and not significantly different. There was therefore insufficient evidence to suggest that the length of pre-exposure to ES displayed an inverse relationship with subsequent levels of cell adhesion. However, as shown with the ATP assay results, cell viability may have been slightly affected.

3.3.8 Proteolytic degradation of ECM proteins by larval ES: investigation using SDS-PAGE.

A previous study has established that larval ES degrades fibronectin and other ECM proteins (Chambers *et al.*, 2003). However, this conclusion was based upon experiments in which larval ES was incubated with ECM proteins that were in solution, rather than as coatings over a plastic surface. In the cell adhesion experiments (section 3.3.5 to 3.3.7), the ES that was used only came into contact with fibronectin or collagen surface coatings. The ability of larval ES to release proteolytic fragments from such coatings was therefore investigated. Hence, the solution of ES (10 μg/ml) that was exposed to the fibronectin- or collagen-coated surfaces, as described in section 3.3.7, was separated into its component peptides using SDS-PAGE. As shown in Fig. 3.23, there appeared to be little evidence for the existence of fibronectin or collagen proteolytic fragments within the solutions. It may therefore be concluded that no proteolytic degradation took place. However, it is also possible that ES degraded the ECM protein present on the surface but the resulting fragments remained adhered to that surface. In such a scenario, the solution of ES removed at the end of the pre-exposure time would not have contained any proteolytic fragments. In addition, the solution of ES tested was only in contact with the ECM-coated surface for 4 hours. It is possible that the solutions that remained in contact with the surface for longer may have

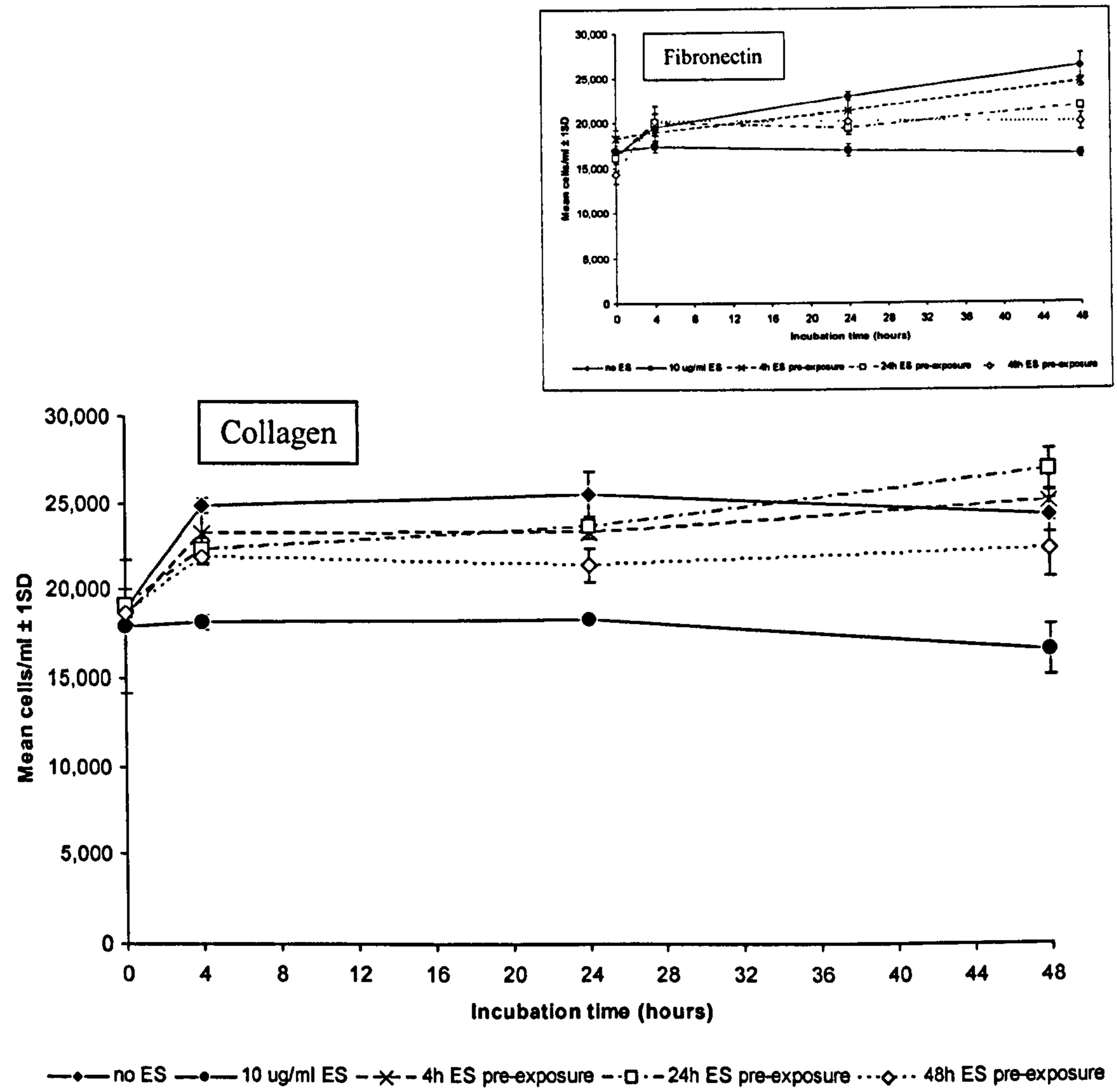

Figure 3.22 Mean number of adherent fibroblast cells seeded upon a collagen-coated surface in the absence or presence of 10 μg/ml ES. Where indicated, the surface had first been pre-exposed to 10 μg/ml larval ES for 4, 24 or 48 hours before the addition of cells in ES-free medium. Each value represents the mean of three replicate samples. Adherent cell number results from cells seeded upon a fibronectin-coated surface are shown in the top right hand corner for comparison (refer to Fig. 3.20).

4 Hours One-way ANOVA: $P < 0.0001$.

	ES blank control	10 μg/ml ES control	4h pre-exposed	24h pre-exposed	48h pre-exposed
ES blank	-	-	-	-	-
10 μg/ml ES	$P < 0.001$	-	-	-	-
4h pre-exposed	ns	$P < 0.001$	-	-	-
24h pre-exposed	$P < 0.01$	$P < 0.001$	ns	-	-
48h pre-exposed	$P < 0.01$	$P < 0.001$	ns	ns	-

24 Hours One-way ANOVA: $P < 0.0001$.

	ES blank control	10 μg/ml ES control	4h pre-exposed	24h pre-exposed	48h pre-exposed
ES blank	-	-	-	-	-
10 μg/ml ES	$P < 0.001$	-	-	-	-
4h pre-exposed	$P < 0.05$	$P < 0.001$	-	-	-
24h pre-exposed	ns	$P < 0.001$	ns	-	-
48h pre-exposed	$P < 0.001$	$P < 0.01$	ns	$P < 0.05$	-

48 Hours One-way ANOVA: $P < 0.0001$.

	ES blank control	10 μg/ml ES control	4h pre-exposed	24h pre-exposed	48h pre-exposed
ES blank	-	-	-	-	-
10 μg/ml ES	$P < 0.001$	-	-	-	-
4h pre-exposed	ns	$P < 0.001$	-	-	-
24h pre-exposed	ns	$P < 0.001$	ns	-	-
48h pre-exposed	ns	$P < 0.01$	ns	$P < 0.01$	-

Table 3.6 Analysis of cell adhesion upon a collagen-coated surface, as estimated using the CyQUANT® assay. Results of one-way ANOVA and Tukey-Kramer's multiple comparison tests upon data collated at each time-point of a 48 hour incubation period.

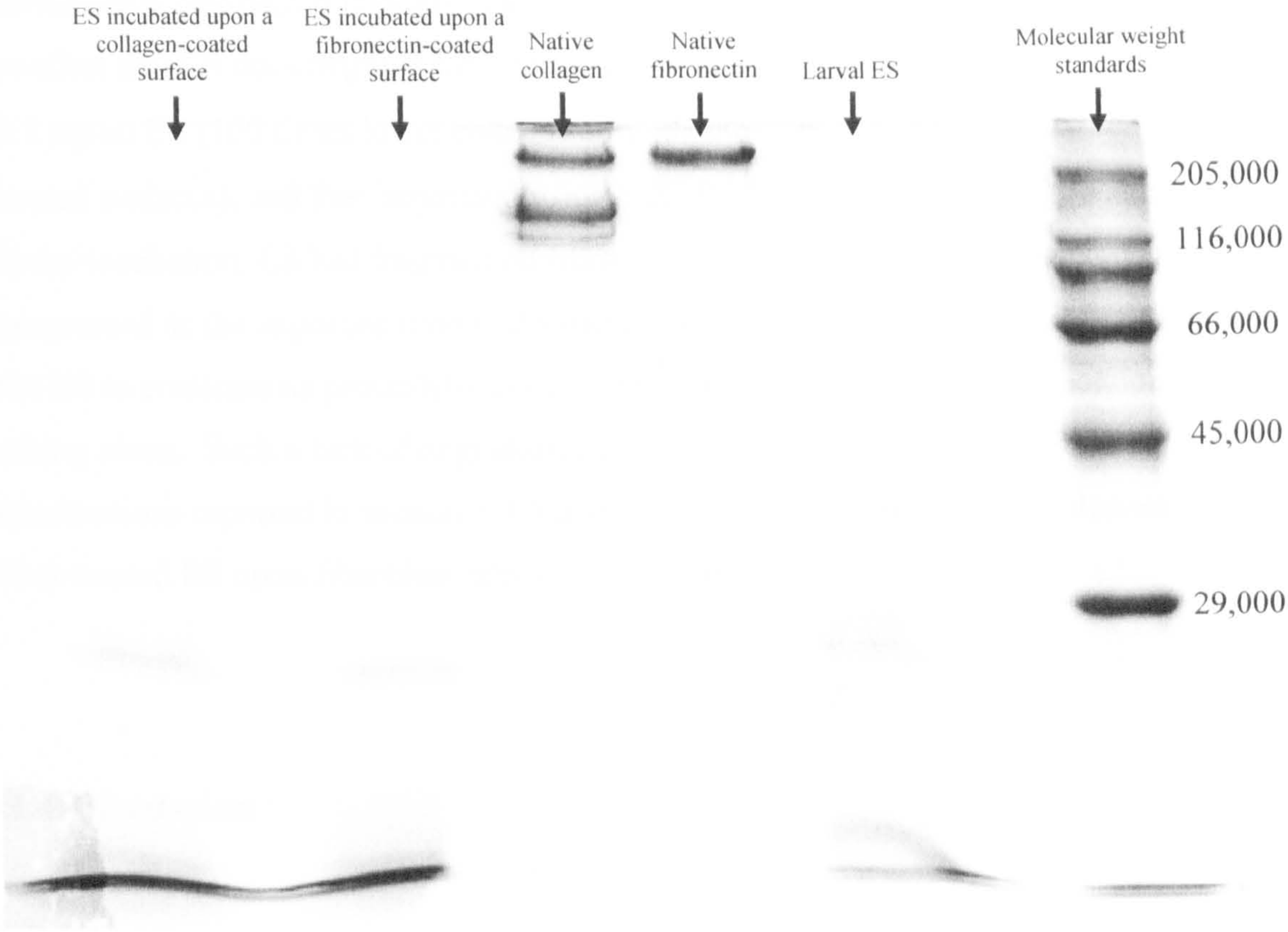

Figure 3.23 SDS-PAGE gel (12%) showing separation of the contents within a larval ES solution incubated upon a fibronectin- or collagen-coated surface for 4 hours. Solutions containing native fibronectin, native collagen or larval ES alone are also separated on the gel, to provide a comparison. Numbers superimposed on the right hand side of the gel refer to the molecular weight standard bands (Da).

contained proteolytic fragments. However, a separate experiment was undertaken to confirm that ES does degrade fibronectin in solution. Here, fibronectin was exposed to 0.1 μg/ml ES (100 times lower concentration than that used to pre-expose the ECM-coated surfaces), and then separated using SDS-PAGE. As shown in Fig. 3.24a, by 4 hours incubation, ES had fragmented fibronectin. It also appeared that such degradation progressed as the exposure time to ES increased. Fig. 3.24b confirms that heat-treating the ES to eradicate its proteolytic activity prevented any fibronectin degradation from taking place. Such a lack of degradative activity may have contributed to the observations reported in section 3.3.5 and 3.3.6 concerning the weaker influence of heat-treated ES upon fibroblast adhesion in comparison with the untreated ES.

3.4 Discussion

Initial observations showed that fibroblasts, in the presence of 10 μg/ml larval ES, displayed altered morphologies. Further studies revealed that fibroblast adhesion to the tissue culture surface was modified in the presence of ES. As the concentration of ES increased, the number of fibroblasts successfully adhering to the surface decreased, indicating a dose-dependent, direct effect upon the cell surface receptors (integrins) or their connections with the surface. The presence of larval ES also reduced fibroblast adhesion to fibronectin- and collagen-coated surfaces. Results also suggested that cell viability may have been reduced as well. In addition, ES induced changes in the morphology of cells adhering to these surfaces. Here, studies revealed that cells in the presence of ES adopted more compact, rounded morphologies, indicating a lower number of receptor-mediated interactions with the surface in question. Interestingly, heat-treated ES, which was shown to have negligible proteolytic activity, did not influence cell adhesion, viability and morphology as much as the untreated ES. This suggests that ES proteinases were involved in modifying fibroblast behaviour. In both the cell adhesion and morphology studies, differences between treatments were more profound in the presence of fibronectin than collagen, indicating that the properties of the surface-coating were involved in the ES-mediated changes in fibroblast behaviour. Evidence which supports this hypothesis was provided by studies which showed that

a.

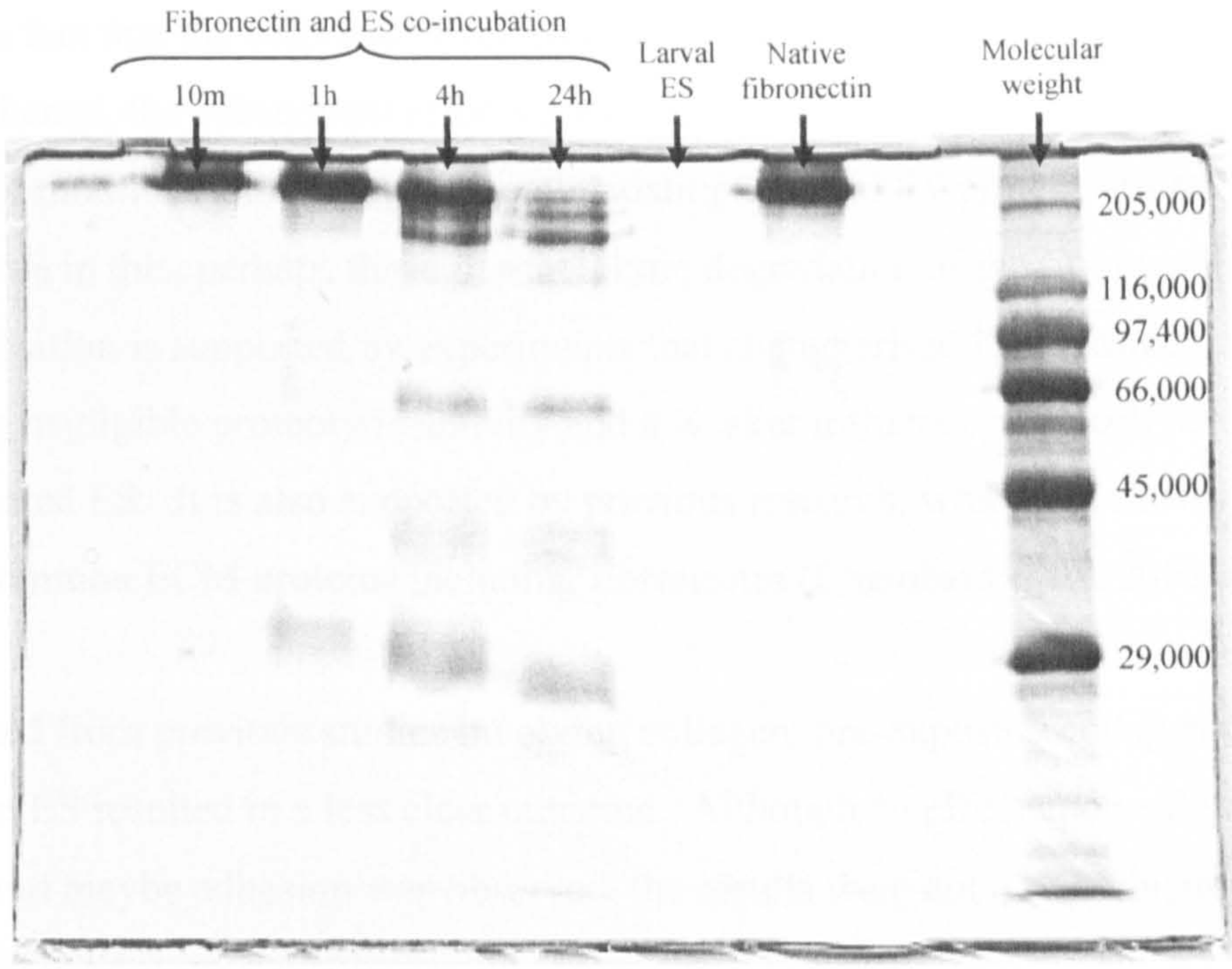

b.

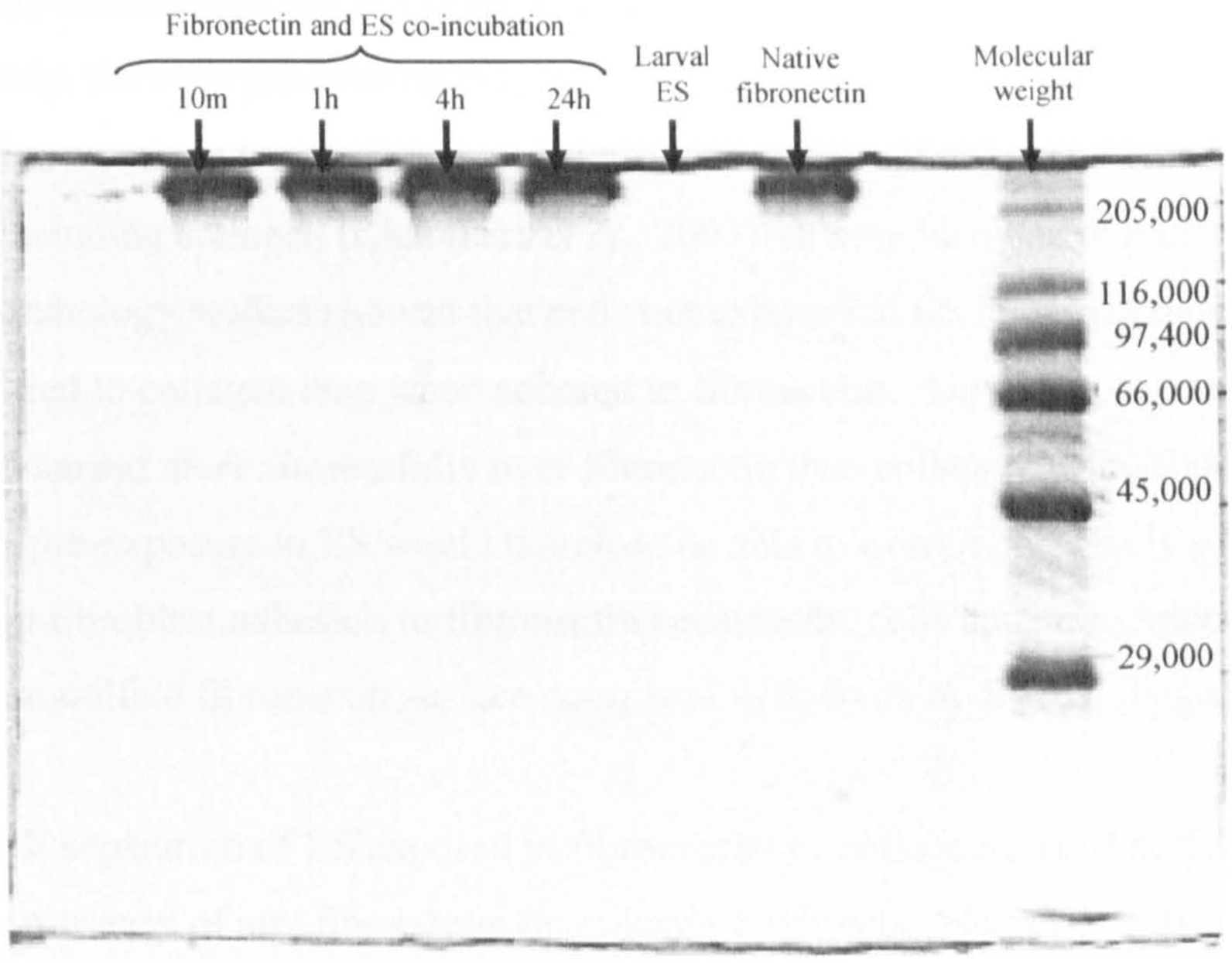

Figure 3.24 SDS-PAGE gel (12%) showing degradation of fibronectin (100 μg/ml) following exposure to either 0.1 μg/ml untreated ES (a) or 0.1 μg/ml heat-treated ES (b) for the times indicated. Native fibronectin and larval ES alone are also separated on the gel, to provide a comparison. Numbers superimposed on the right hand side of the gel refer to the molecular weight standard bands (Da). Larval ES failed to stain, indicating low protein concentration relative to its high specific enzymatic activity.

pre-exposing the fibronectin-coated surface to ES resulted in modified cell adhesion, despite the fact that the cells had never come into contact with ES. As the pre-exposure time lengthened, the subsequent effects upon cell adhesion increased, indicating a progressive modification of the fibronectin coating. Larval ES proteinases may have played a role in this, perhaps through proteolytic degradation of the fibronectin surface. This supposition is supported by experiments that characterised heat-treated ES as containing negligible proteolytic activity and a weaker influence upon cell adhesion than untreated ES. It is also supported by previous research, which has shown ES to degrade common ECM proteins including fibronectin (Chambers *et al.*, 2003).

As expected from previous studies involving collagen, pre-exposing collagen-coated surfaces to ES resulted in a less clear outcome. Although an effect upon subsequent cell viability and maybe adhesion was observed, the results were not as convincing as those recorded in the presence of fibronectin. Here, any modification of the collagen coating that ES may have caused did not exert as great an influence upon cell behaviour. Alternatively, the collagen coating may have been more resistant to modification. However, as mentioned, previous research has revealed ES to degrade common ECM proteins, including collagen (Chambers *et al.*, 2003). It may be noted that images taken for the morphology studies showed that cells not exposed to ES remained more rounded when adhered to collagen than when adhered to fibronectin. This suggests that fibroblasts spread more successfully over fibronectin than collagen. Modification of the surface by pre-exposure to ES would therefore be able to exert a potentially greater effect upon fibroblast adhesion to fibronectin because the cells appear to interact more with an unmodified fibronectin surface compared with an unmodified collagen surface.

SDS-PAGE separation of ES exposed to fibronectin- or collagen-coated surfaces did not reveal the presence of any fibronectin or collagen fragments. However, separation of ES diluted within a solution of fibronectin did confirm the presence of proteolytic fragments of fibronectin. The ECM protein was fragmented in a progressive, time-dependent manner. It therefore appears likely that ES had fragmented the fibronectin surface and possibly the collagen surface. However, fragments may not have showed as visible bands on the gel because the concentration of the protein may not have been high enough. Alternatively, any fragments released from the proteins may have remained adhered to the tissue culture surface. Any role that the modification of the

protein surface may have played in altering fibroblast adhesion is emphasised by the negligible effect that heat-treated ES exerted upon fibronectin in solution. Using SDS-PAGE, no fragmentation of fibronectin was observed at any time-point. The apparent inability of heat-treated ES to alter fibronectin may perhaps explain why it exerted only a modest effect upon fibroblast behaviour. The fact that heat-treated ES exerted any effect at all may have due to some low level residual proteolytic activity which was too low to be detected by the FITC-casein assay used to assess proteolytic activity. While this level of activity may have been too weak to break the FITC-casein bond or fragment fibronectin, it may still have been able to affect integrin receptors or their connections directly. Alternatively, the presence of some non-proteolytic heat-stable agent may have been responsible.

It may therefore be concluded from these results that ES at a concentration of 10 µg/ml reduces the extent of fibroblast adhesion, affects cell viability and induces a more rounded morphology by altering integrin receptor interactions with the surface. Proteinases within ES appear to be responsible and may act to alter adhesion by targeting the receptors directly, degrading their extracellular domains or surface connections. These actions may also be responsible for reducing cell viability as fibroblasts are anchorage-dependent cells (Stoker *et al.*, 1968; Benecke *et al.*, 1978). As such, their metabolic activity and survival is dependent upon their adhesion to suitable protein substrates. ES proteinases may also influence cell adhesion and viability through modifying, where present, the fibronectin-coated surface, reducing its adhesive properties. The discrete adhesive sites present within this molecule may explain why modification of the fibronectin surface may play a role in altering cell adhesion and morphology. Research has found that fibronectin contains a number of functional domains, which include binding sites for cells, various ECM proteins or molecules from a variety of other sources (Mohri, 1997), as shown in Fig. 1.2 in Chapter 1. The primary cell attachment site consists of a tetrapeptide of Arg-Gly-Asp-Ser (RGDS) located within the cell-binding domain of fibronectin (Pierschbacher and Ruoslahti, 1984; Ruoslahti and Pierschbacher, 1986; Obara, Kang and Yamada, 1988). In fibroblasts, the $\alpha_5\beta_1$ integrin is the main receptor for this site. However, other receptors are believed to be involved, both with this attachment site and neighbouring sites, which are thought to act synergistically in inducing cell attachment (Aota, Nagai and Yamada, 1991; Aota, Nomizu and Yamada, 1994; Bowditch *et al.*, 1994). These include the

integrin receptors $\alpha_3\beta_1$, $\alpha_v\beta_1$, $\alpha_v\beta_3$ and $\alpha_v\beta_6$ (Gailit and Clark, 1996). Several peptides from the heparin-binding domain (heparin II in Fig. 1.2 in Chapter 1) also support cell attachment via interaction with cell membrane-associated proteoglycans such as the syndecans (McCarthy *et al.*, 1988, 1990; Drake *et al.*, 1992; Woods *et al.*, 1993). One study has shown focal adhesion formation in fibroblasts to be dependent upon their binding to the heparin-binding domain of fibronectin (Woods *et al.*, 2000). Additional cell binding sites have been located on the carboxyl-terminal side of the heparin-binding domain. Termed the connecting segment (site IIICS), this region contains the $\alpha_4\beta_1$ receptor-binding sites CS-1 and CS-5 (Huhtala *et al.*, 1995). The CS-1 sequence binds with high affinity to the $\alpha_4\beta_1$ receptor and is also recognised by the $\alpha_4\beta_7$ receptor. Such findings suggest that the spatial configuration and co-operation of a number of ligand-bound integrins, facilitated by additional interactions between fibronectin and cell membrane-associated proteoglycans, determines the strength of cell adhesion achieved. Hence, the deletion of any of these binding sites by the actions of ES will weaken the association of the fibroblasts with the surface. For example, even if the primary RGDS cell attachment site remained intact upon the fibronectin coating, the re-location of neighbouring attachment sites would prevent the full adhesion activity of this site. Such rearrangement of the positioning of binding sites may occur if the fibronectin coating the surface was fragmented by the proteolytic actions of ES. Alternatively, binding sequences may be destroyed completely by proteolysis, depending on how long the fibronectin was exposed to ES and what concentration of ES was used.

The destruction of cell-binding sites by ES would inevitably alter the density of adhesive sites available to the cell. Evidence has shown that the density of particular attachment sites available influences the strength of cell adhesion. For example, Wang and Ingber (1994) found that raising the density of a fibronectin RGD peptide coating over ferromagnetic microbeads promoted the spreading of attached endothelial cells. It also altered the mechanical properties of the attached cells' cytoskeletons, increasing cytoskeletal stiffness, apparent viscosity and permanent deformation in response to an applied stress. Goldstein and DiMilla (2002) found, through using a radial-flow chamber, that the strength of hydrodynamic shear required to detach cells increased as the concentration of fibronectin coating the surface also increased. Garcia, Ducheyne and Boettiger (1997) found that cell adhesive strength increased linearly with adsorbed

fibronectin surface density. Collectively, these results suggest that increasing the concentration of ECM proteins promotes integrin-ligand binding and the formation of molecular links with the cytoskeleton, thus increasing the strength by which cells are held in place. These findings are in accordance with the 'receptor saturation model' originally presented by Dembo and Bell (1987) and later by Gaudet *et al.* (2003) (Fig. 3.25a). Based upon thermodynamic analysis of cell adhesion, this model explains the influence of the substrate surface upon cell spreading in terms of the number of adhesive sites available to the cell. As the substrate surface concentration increases, the adhesive sites become denser and cell adhesion increases as the number of integrin receptors binding to the substrate becomes higher. Concurrently, cell spreading also increases because the cell is able to make more contacts with the substrate. However, assuming that integrins are expressed in finite numbers (Akiyama and Yamada, 1985), there will come a point where the integrin receptors become saturated by available adhesive sites. As the number of adhesive sites increases above the saturation point, cell spreading starts to decrease because the integrin receptors become saturated over a smaller distance. According to the 'receptor saturation model', the addition of ES, which reduces cell adhesion and causes a more rounded cell morphology must be inducing a reduction in the availability of adhesive sites (Fig. 3.25b). Results show that this reduction may be caused by both modification of the surface and direct degradation of the integrin receptor connections with the surface.

Another possible mechanism by which ES alters fibroblast adhesion and viability may involve the modification of fibroblast-mediated proteolysis of the fibronectin substrate. Research by Huhtala *et al.* (1995) has shown that when fibroblasts are seeded upon a chymotryptic 120 kD fragment of fibronectin containing the RGDS cell binding sequence, the cells upregulate collagenase (MMP-1), gelatinase B (MMP-9) and stomelysin-1 (MMP-3) expression. The additional presence of the IIICS connecting segment (or more particularly the CS-1 binding sequence) results in the suppression of MMP levels back to those detected when intact fibronectin is used. As mentioned in the previous paragraph, the RGDS cell-binding sequence in fibronectin is targeted by the $\alpha_5\beta_1$ receptor, whereas the $\alpha_4\beta_1$ integrin receptor targets CS-1 and CS-5 sites within the IIICS connecting segment. These results therefore indicate that co-operative signalling by $\alpha_5\beta_1$ and $\alpha_4\beta_1$ integrin receptors regulates MMP gene expression in fibroblasts. In addition, Huhtala *et al.* (1995) found that peptide V (located within the heparin-binding

a.

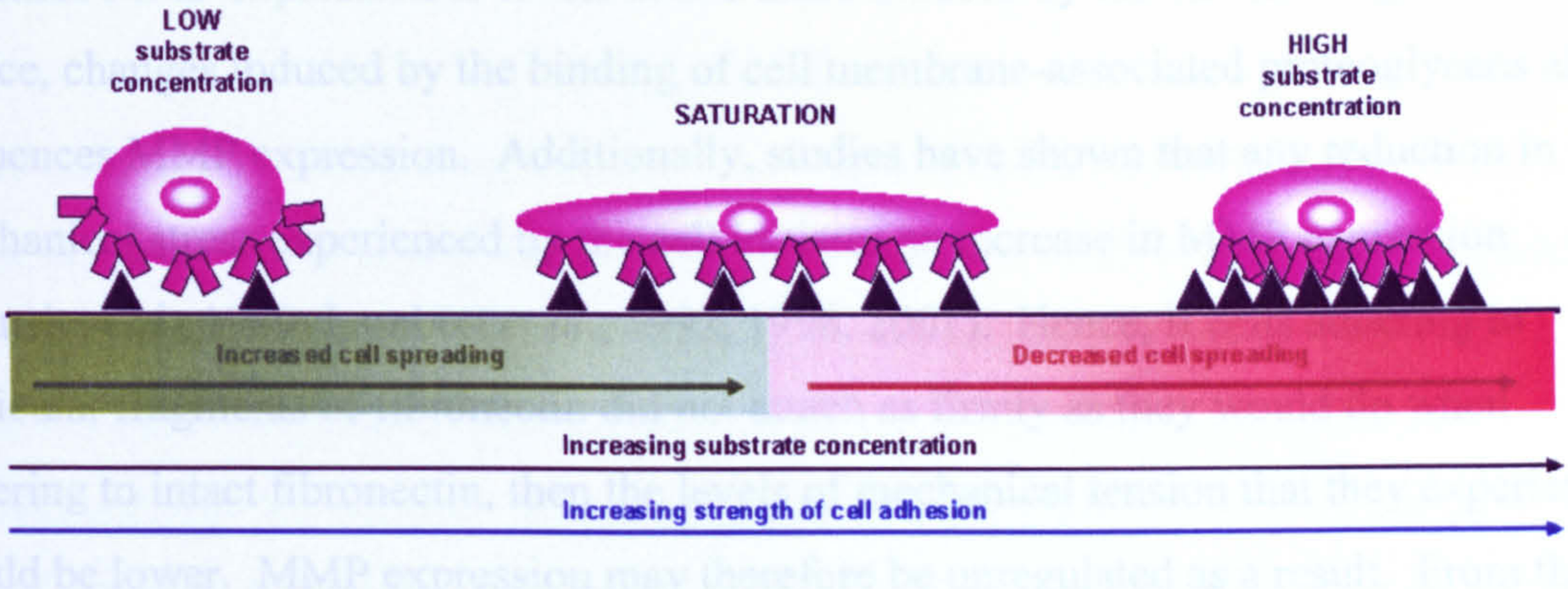

b.

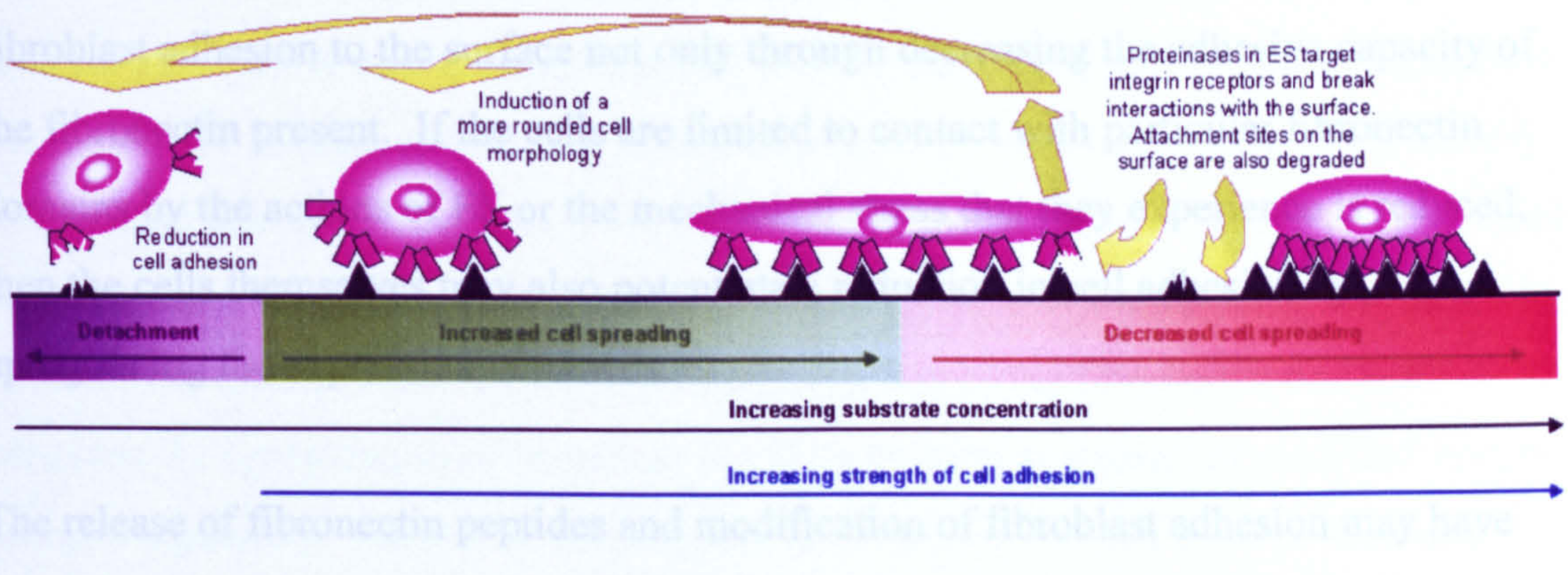

Figure 3.25 Receptor saturation model showing the relationship between substrate concentration, cell adhesion, cell spreading and the influence of larval ES. **a.** At low substrate concentrations, the number of available adhesive sites are low. Hence, the cell is unable to spread fully. As the substrate concentration rises, cell spreading and the strength of cell adhesion increases as the cell comes into contact with more adhesive sites. At the 'saturation' point, the number of available integrin receptors within the cell are approximately equal to the number of adhesive sites that the cell can reach. If the substrate concentration rises further, adhesive sites become denser. Cell spreading therefore starts to decrease as the integrin receptors become saturated by adhesive sites over a smaller area. However, the strength of cell adhesion continues to rise as the anchorage within a given area becomes stronger. **b.** The effect of the presence of untreated larval ES. Here, ES reduces the availability of adhesive sites through proteolytic modification of the surface. Integrin receptor-ligand bonds may also be directly targeted. As a consequence, cell spreading and adhesion is reduced. Cells may also become detached. Figures adapted from Gaudet *et al*. (2003).

domain of the fibronectin molecule), in conjunction with the 120 kD fragment, increases MMP expression to levels above those induced by the 120 kD fragment alone. Hence, changes induced by the binding of cell membrane-associated proteoglycans also influences MMP expression. Additionally, studies have shown that any reduction in mechanical stress experienced by the cell initiates an increase in MMP expression (Mauch *et al.*, 1989; Lambert *et al.*, 1992, 1998, 2001). Hence, if cells adhering to particular fragments of fibronectin did not attach as firmly as they would do when adhering to intact fibronectin, then the levels of mechanical tension that they experience would be lower. MMP expression may therefore be upregulated as a result. From the evidence presented by Mauch *et al.*, 1989; Huhtala *et al.*, 1995 and Lambert *et al.*, 1992, 1998, 2001, it may therefore be proposed that ES mediates the strength of fibroblast adhesion to the surface not only through decreasing the adhesive capacity of the fibronectin present. If the cells are limited to contact with particular fibronectin domains by the actions of ES or the mechanical stress that they experience is reduced, then the cells themselves may also potentiate a reduction in cell adhesion by upregulating the expression of MMPs.

The release of fibronectin peptides and modification of fibroblast adhesion may have consequences for other aspects of fibroblast behaviour. For example, certain fibronectin peptides have been shown to possess chemotactic properties (Postlethwaite *et al.*, 1981 Livant *et al.*, 2000). Cell attachment has been shown to control fibronectin and $\alpha_5\beta_1$ integrin expression (Dalton, Marcantonio and Assoian, 1992). Integrins have been shown to associate with other receptors, altering their affinity for specific ligands (Porter and Hogg, 1998). As described in Chapter 1.2.1, they have also been shown to co-localise with urokinase plasminogen activator receptor (uPAR), together with urokinase plasminogen activator (uPA) and its inhibitor (uPAI-1), forming an integrin-protease complex to promote migration and modulate cell adhesion (Planus *et al.*, 1997; Porter and Hogg, 1998). There is also evidence to suggest that the strength of cell adhesion and the density of adhesive sites determine the speed of cell migration (Dembo and Bell, 1987; DiMilla *et al.*, 1993; Puschel *et al.*, 1995; Maheshwari *et al.*, 1999; Cox, Sastry and Huttenlocher, 2001; Gaudet *et al.*, 2003). It is therefore possible that if ES modifies fibroblast adhesion to proteins such as collagen and particularly fibronectin, it may also influence fibroblast migration.

3.5 Conclusions

L. sericata larval ES at a concentration of 10 μg/ml was found to reduce the extent of fibroblast adhesion to both tissue culture plastic and fibronectin- and collagen-coated surfaces. It also appeared to reduce cell viability and induce a more rounded cell morphology, in accordance with a reduction in the number of receptor-mediated interactions with the surface. Such modifications in fibroblast-surface interactions were dose-dependent and reliant upon the proteolytic activity present within ES. Proteinases within ES appeared to act by targeting the cell surface receptors directly, degrading their extracellular domains or surface connections, and also by modifying the protein-coated surface, particularly when fibronectin was used. Possible implications originating from the proteolytic modification of the fibronectin surface include a decrease in the density of available adhesive sites, which in concert with a less favourable spatial orientation of adhesive sites, causes a reduction in the adhesive capacity of the surface. Another possible implication resulting from the fragmentation of the fibronectin molecule concerns the upregulation of fibroblast MMP expression as a result of modified integrin receptor signalling. As will be investigated in Chapter 4, modification of fibroblast adhesion may have consequences for fibroblast migration and the progression of wound healing.

CHAPTER 4

Fibroblast Migration in Two Dimensions

4.1 Introduction

In the previous chapter *L. sericata* ES was shown to modify fibroblast adhesion and spreading upon fibronectin and to a lesser extent, collagen. It was also shown to fragment fibronectin by proteolytic degradation. These results suggest that ES is capable of influencing fibroblast-ECM interactions. The ability to exert such influences may have important consequences in many physiological processes, including wound healing. For instance, a major feature of wound healing in which fibroblasts play a vital role, is the formation of granulation tissue (discussed within Chapter 1). As part of this process, fibroblasts migrate into the wound space (Chen, 1981, Clark, 1996; Maheshwari *et al.*, 1999). Fibroblast migration has been shown to be controlled in part by the composition and structure of the ECM environment surrounding the cells. For example, penetration of the fibrin clot is believed to be assisted by the presence of fibronectin as the cells have been shown to use this protein as a scaffold for 'contact guidance' (Hsieh and Chen, 1983; Clark, 1996). There is also evidence to suggest that the matrix itself drives the translocation of cells towards other areas of the matrix containing higher concentrations of fibronectin (Newman, Frenz and Tomasek, 1985; Hocking, Sottile and Langenbach, 2000). Believed to be associated with matrix fibrillogenesis, this has also been shown with non-living particles, indicating the influence that the composition of the matrix can independently exert upon cell movement. Another theory is that the matrix acts as a reservoir for growth factors, controlling their presentation to the cells (Nathan and Sporn, 1991, Eckes *et al.*, 2000). In addition to the ECM exerting control over fibroblast migration, there is evidence to

suggest that cells reciprocate. Firstly, fibroblasts in response to pro-inflammatory mediators such as interleukin-1 (IL-1) and tumour necrosis factor-alpha (TNF-α) secrete various MMPs and plasminogen activator to break down the surrounding matrix, so easing their translocation into other areas (Grant *et al.*, 1987; Wilhelm *et al.*, 1987; Saus *et al.*, 1988; Stetler-Stevenson *et al.*, 1989; Mauviel, 1993; Woessner, 1991; Bizot-Foulon *et al.*, 1995. They also synthesise new matrix components, thus altering the character of the matrix and, in so doing, modifying the signals that they receive from their environment (Welch *et al.*, 1990; Clark, 1996; Eckes *et al.*, 2000).

It is therefore clear that modification of fibroblast-ECM interactions by the actions of substances released by *L. sericata* larvae may provide a mechanism by which biosurgery influences wound healing. An indication that this may be occurring is provided by numerous clinical observations which suggest that wounds treated with larvae demonstrate enhanced granulation tissue development (Buchman and Blair, 1932; Wilson, Doan and Miller, 1932; Reames, Christensen and Luce, 1988; Thomas *et al.*, 1996; Wolff and Hansson, 1999; Sherman, Hall and Thomas, 2000; Mumcuoglu, 2001; Wollina *et al.*, 2002.). Modification of fibroblast migration may play a significant part in this because new tissue formation is dependent upon fibroblast movement into the wound space. Fibroblast motility is also subject to interactions with the ECM. Investigations into the effects of ES upon fibroblast migration were therefore undertaken.

Cell migration has been observed in a variety of two-dimensional assays. These assays have employed methods ranging from tracking the movement and membrane activity of individual cells (Maheshwari *et al.*, 1999; Raffetto *et al.*, 2001) to monitoring the rate at which a gap, surrounded by areas of confluent cells, is filled by invading cells (Malinda and Wysocki, 2000). Other assays have involved studying the mechanical forces generated by cells when they migrate across flexible substrata (reviewed by Beningo and Wang, 2002). The impact of coating surfaces with ECM components, including collagen, laminin and fibronectin has also been investigated (Dean and Blankenship, 1997). In addition, various studies examining the influence of ECM-derived proteolytic degradation products upon cell migration have been performed (Schor *et al.*,1996; Livant *et al.*, 2000).

Here, the effect of ES upon fibroblast migration was investigated using a novel, two-dimensional *in vitro* wound assay. This involved seeding fibroblasts onto a fibronectin-coated surface and then monitoring their migration, using time-lapse digital photography, into a cell-free area. It was hypothesised that the presence of ES would increase the rate at which the leading cell edge migrated into the free-space.

4.2 Methods

4.2.1 Two-dimensional *in vitro* wound assay

A 35 mm tissue culture dish containing 2 ml of bovine fibronectin at 0.1, 1.0, 10, 100 or 1000 µg/ml concentration was incubated overnight at 37°C. The fibronectin solution was then aspirated and a sterile, glass cloning cylinder, of 4.7 mm internal diameter, was placed upright in the middle of the dish. A flask of 70 % – 80 % confluent fibroblasts were then trypsinised, as described in Chapter 2.2.1 and suspended in cell culture medium containing 10 % FCS, to neutralise remaining trypsin. The serum was then removed, as it had already been shown to inhibit ES proteolytic activity (see Chapter 2.2.2). This was undertaken as described in Chapter 2.2.1, leaving cells suspended within serum-free cell culture medium. Following cell counting using a haemocytometer, 1×10^6 fibroblasts were taken and suspended within 2 ml of serum-free cell culture medium. This contained either 0.1 µg/ml ES (taken from batch D) or an equivalent volume of PBS (PBS blank). In one assay, 10 µg/ml ES was added to the medium. The cells were then seeded around the outside of the cylinder within the dish. Cell culture medium, which was identical to that used to suspend the cells, was then added to the inside of the cylinder to ensure consistent exposure of the whole fibronectin surface. The dish was then incubated for 4 hours at 37°C.

Following incubation the cloning cylinder was removed, taking cares not to disturb the confluent cell layer that had formed around it. The dish was then immediately placed under an inverted microscope and positioned so that the inner boundary of the cell layer was viewed in a vertical orientation and approximately a third of the field of view was

taken up by cells. In the assay containing 10 μg/ml ES, the cell boundary was viewed in a diagonal orientation. For all the assays a temperature of 37°C was maintained using a heated, perspex incubation chamber surrounding the stage and sterile filtered 5 % (v/v) CO_2 was perfused over the dish. Phase contrast images were then taken of the same field of view every three minutes for 48 hours, using Lida time-lapse software. The images were then sorted in ascending chronological order and compiled into a Microsoft AVI movie format using Adobe Premiere 5.1. Movies are available for viewing on the enclosed CD-ROM.

4.2.2 Analysis of results

In addition to qualitative analysis of the time-lapse movies, images were also analysed quantitatively for the extent of cell migration into the free space created by the cloning cylinder. This was undertaken by first selecting the images that pictured the progress of the cell boundary after 0, 24 and 48 hours incubation. An area within each image was then selected. This contained the edge of the original cell boundary and part of the initially cell-free space (Fig. 4.1). For consistency, the area selected for analysis was kept at the same size for all images analysed and in the same position for each image derived from the same experiment. Initially, the total area of this selected region was calculated. This was performed using Leica QUIPS software. The area within this region that was covered by cells was also measured using the same software. Here, the perimeter of each cell or group of confluent cells lying within the selected region was outlined and the enclosed area measured in μm^2. All the measurements were then added together and the total expressed as a percentage of the total area analysed (Fig. 4.2). The increase in percentage cell surface area coverage over time was then determined by subtracting the percentage coverage at 0 hours from the percentage coverage at 24 or 48 hours. This method made sure that the percentages calculated at 0 hours were negligible for all experiments, thus ensuring that differences in the initial positioning of the cell boundary in the field of view did not affect the values obtained. It also ensured that only cell migration into the un-seeded, cell-free area was quantified. The complete field of view in each image was also analysed to quantify the percentage increase in cell surface area coverage of the whole image after 24 and 48 hours incubation. This was undertaken using Leica QUIPS software as before. The data generated were then compared with those obtained when the methods outlined in Fig. 4.1 and 4.2 were used.

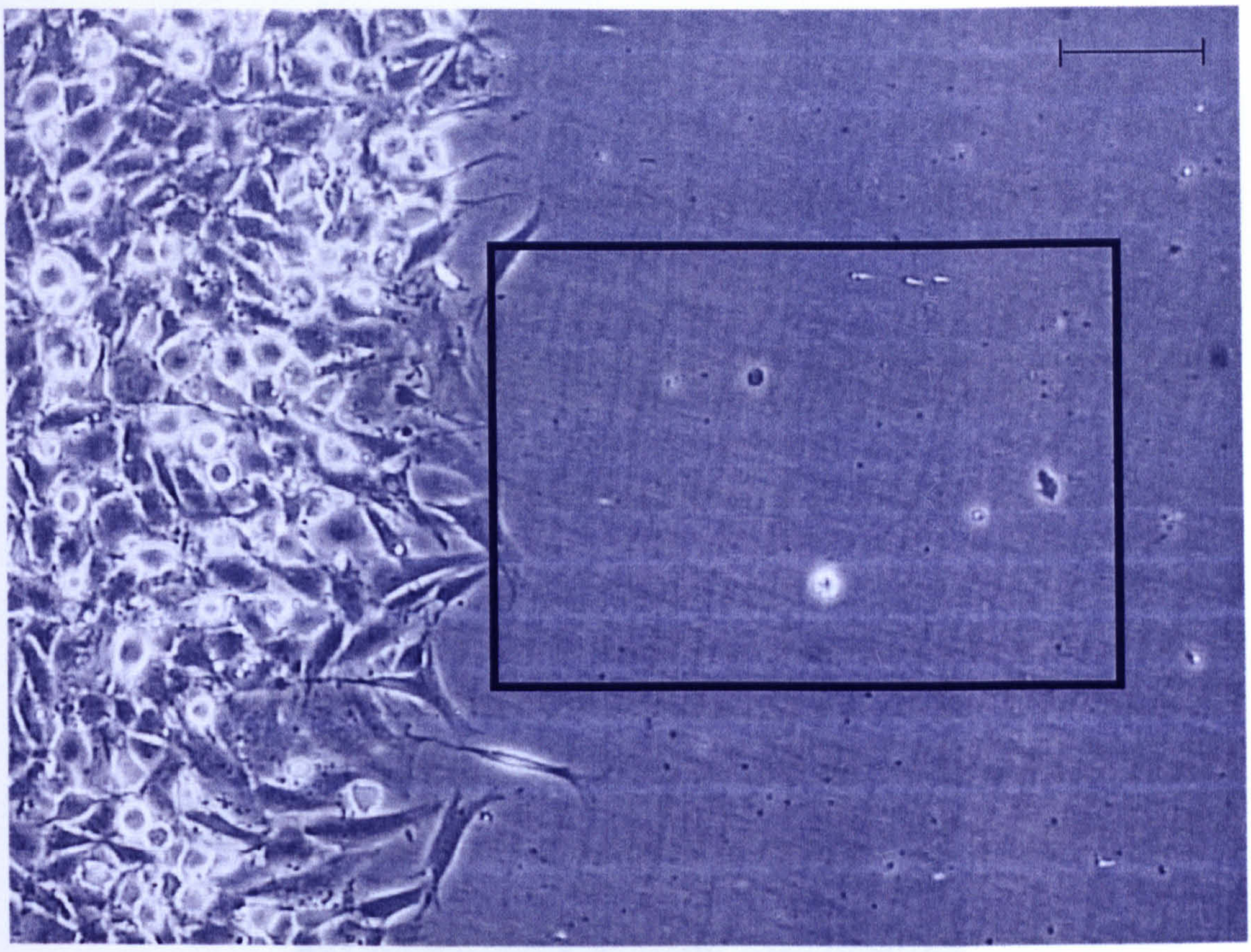

Figure 4.1 A representation of how images generated from the two-dimensional *in vitro* wound assay were analysed quantitatively for the extent of cell migration into the free space. An area within the image, taken from the position of the cell boundary at time 0 hours into the initially cell-free area, was defined as shown here, enclosed within a black rectangle. This area was then analysed for cell surface area coverage. Micron bar represents 100 μm.

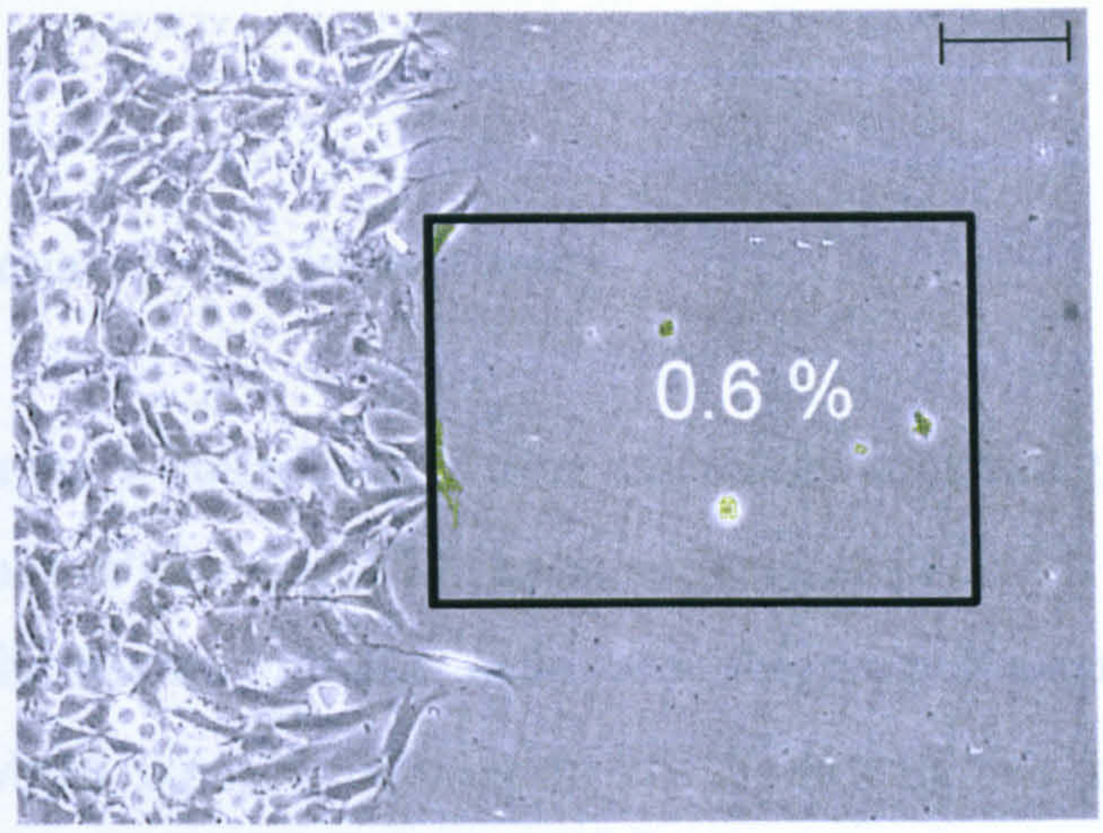

Figure 4.2 Quantitative analysis of cell migration. A region within each image, outlined by a black rectangle, was analysed for fibroblast cell surface area coverage. The perimeter of each cell or group of confluent cells lying within the selected region was outlined and the enclosed area (shown in green for illustrative purposes) measured in μm^2. All the measurements were then added together and the total expressed as a percentage of the total area analysed. Micron bar represents 100 μm.

4.3 Results

4.3.1 Two-dimensional *in vitro* wound assay

Two-dimensional *in vitro* wound assays were assembled containing 1×10^6 fibroblasts, seeded in the presence or absence of ES, upon surfaces coated with different concentrations of fibronectin. Initially, cells were observed on a surface coated with 10 μg/ml fibronectin whilst exposed to 10 μg/ml ES. Following this preliminary study, cells were seeded upon surfaces coated with 0.1, 1.0, 10, 100 or 1000 μg/ml fibronectin without any ES. In an additional study, where 100 μg/ml fibronectin was used to coat the surface, 0.1 μg/ml ES was also added at the time of cell seeding. For each assay, fibroblast migration into the cell-free area was recorded through the use of time-lapse digital photography (see enclosed CD-ROM).

Cells that were placed on a 10 μg/ml fibronectin surface whilst exposed to 10 μg/ml ES had difficulty in adhering to the surface (Fig. 4.3). Even at the beginning of this preliminary study, where cells had not been exposed to ES for very long, many of the cells were floating in the medium or else had adhered to the surface but failed to spread. Over the 48 hour observation period, many of the adhered cells became either detached, inhibited from spreading further or more rounded in morphology. One cell which is highlighted within part of the movie by a red circle, demonstrates the apparent difficulty that the cells had in maintaining adhesions with the surface. At the beginning of the movie, the cell was rounded. It was then observed to express short, but broad, lamellipodial extensions. However, over time these extensions were reduced to short, slender, finger-like projections or filopodia. The projections were then lost as the cell rounded-up. It appeared that some of these projections were physically detached from the cell. By around 24 hours (half-way through the movie), the cell started to make a recovery and began to spread out again. Indeed, by approximately two thirds of the way through the observation period, the cell appeared quite well spread. It was also longer and less rounded, resembling a polarised morphology. However, before very long the cell rapidly lost its connections with the surface. The projections became very thin and the cell adopted a smaller and more rounded morphology. By the end of the 48 hour period, the cell appeared fully rounded again. Another cell, highlighted within part of

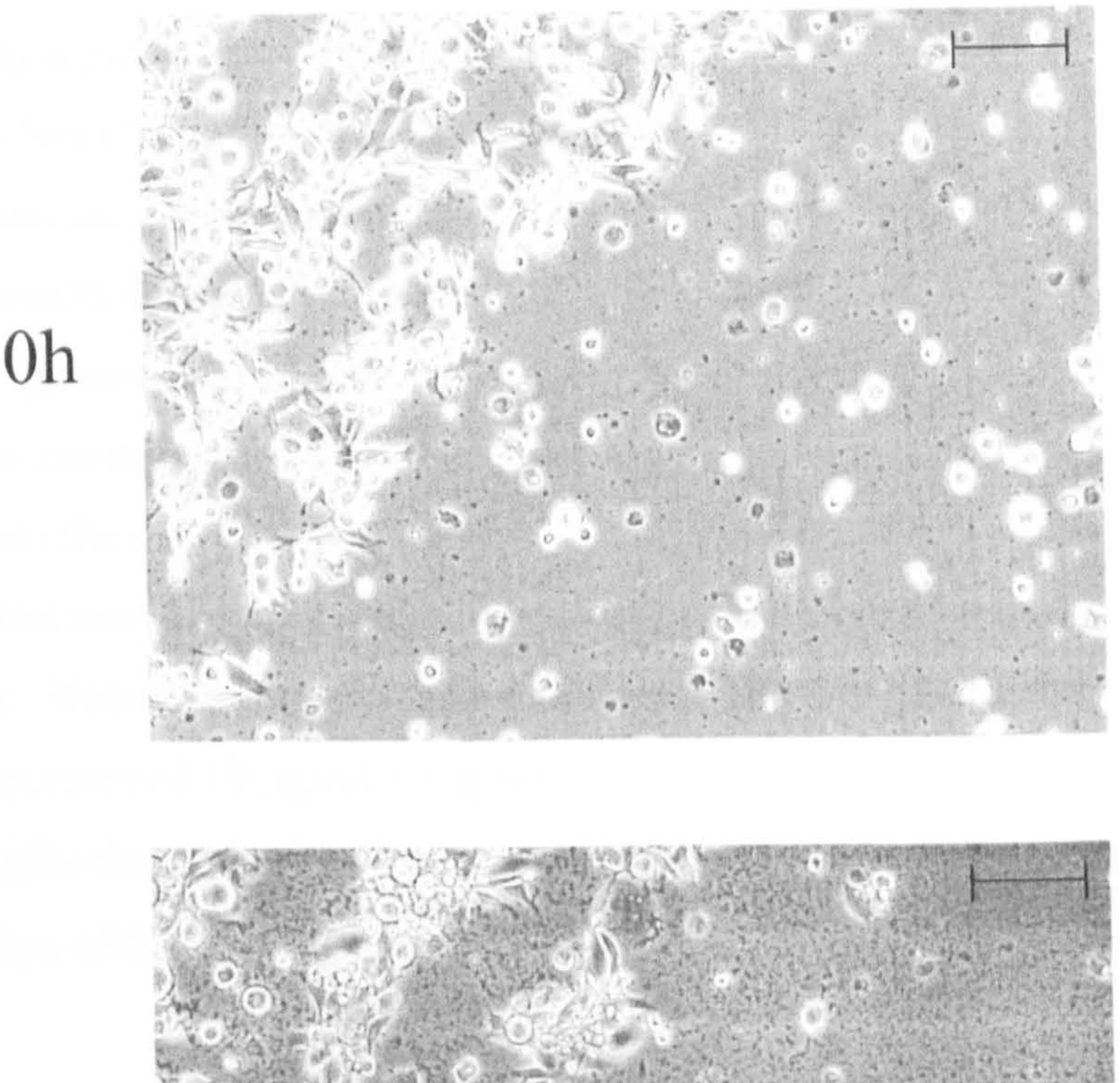

Figure 4.3 Fibroblast cell migration over 48 hours, whilst exposed to 10 μg/ml ES, upon a surface coated with 10 μg/ml fibronectin. Many of the cells shown are unattached and floating in the medium. Micron bar represents 100 μm.

the movie by a green circle, briefly demonstrates migration as it can be observed to move away from the group of cells where it was originally located. However, this cell failed to maintain a well-spread morphology throughout the observation period. None of the other cells demonstrated any significant migration. In addition, extracellular debris was observed. This debris, viewed as black or dark grey static or floating marks, appeared to increase as the period of incubation lengthened. It is possible that the debris resulted from the destruction of cells. The fact that the cell encircled in red periodically lost its spread morphology because its extensions became severed suggests that this may be possible. However, further investigations are required to confirm this. Whatever the case, the presence of 10 μg/ml ES appeared to be deleterious to the cells, inhibiting fibroblast adhesion and migration. It was therefore decided to apply a much lower concentration of 0.1 μg/ml ES in further studies.

After the preliminary study described above, cell migration in response to different concentrations of fibronectin was assessed. The movies, and selected stills contained within them, demonstrated that cell behaviour within the serum-free conditions of the assay was influenced by the concentration of fibronectin present upon the surface (Fig. 4.4a). Initially, cells were able to adhere and spread upon the surface coated with 0.1 μg/ml fibronectin. However, the majority failed to adhere for very long and returned to suspension over the 48 hour incubation period. As a consequence, few cells were able to migrate and the original cell boundary receded during this time. In contrast, cells adhered and spread well over the surface coated with 1 μg/ml fibronectin. Over 48 hours, they migrated into the un-seeded, cell-free area, thus expanding the cell boundary further into the observed field of view. Cells were also seen to adhere and spread over the surfaces coated with 10, 100 and 1000 μg/ml fibronectin. As with the 1 μg/ml fibronectin-coated surface, the cells also migrated into the initially cell-free area, thus expanding the cell boundary. However, the motility of the cells exposed to the 1000 μg/ml fibronectin-coated surface appeared to be lower. Here, the distance that the cell boundary travelled into the un-seeded area was less than that seen when 1 to 100 μg/ml fibronectin was present. As a consequence, more of the un-seeded area within the field of view was left exposed by the end of the observed 48 hour incubation period. The movies and selected still images also demonstrated that the presence of 0.1 μg/ml ES

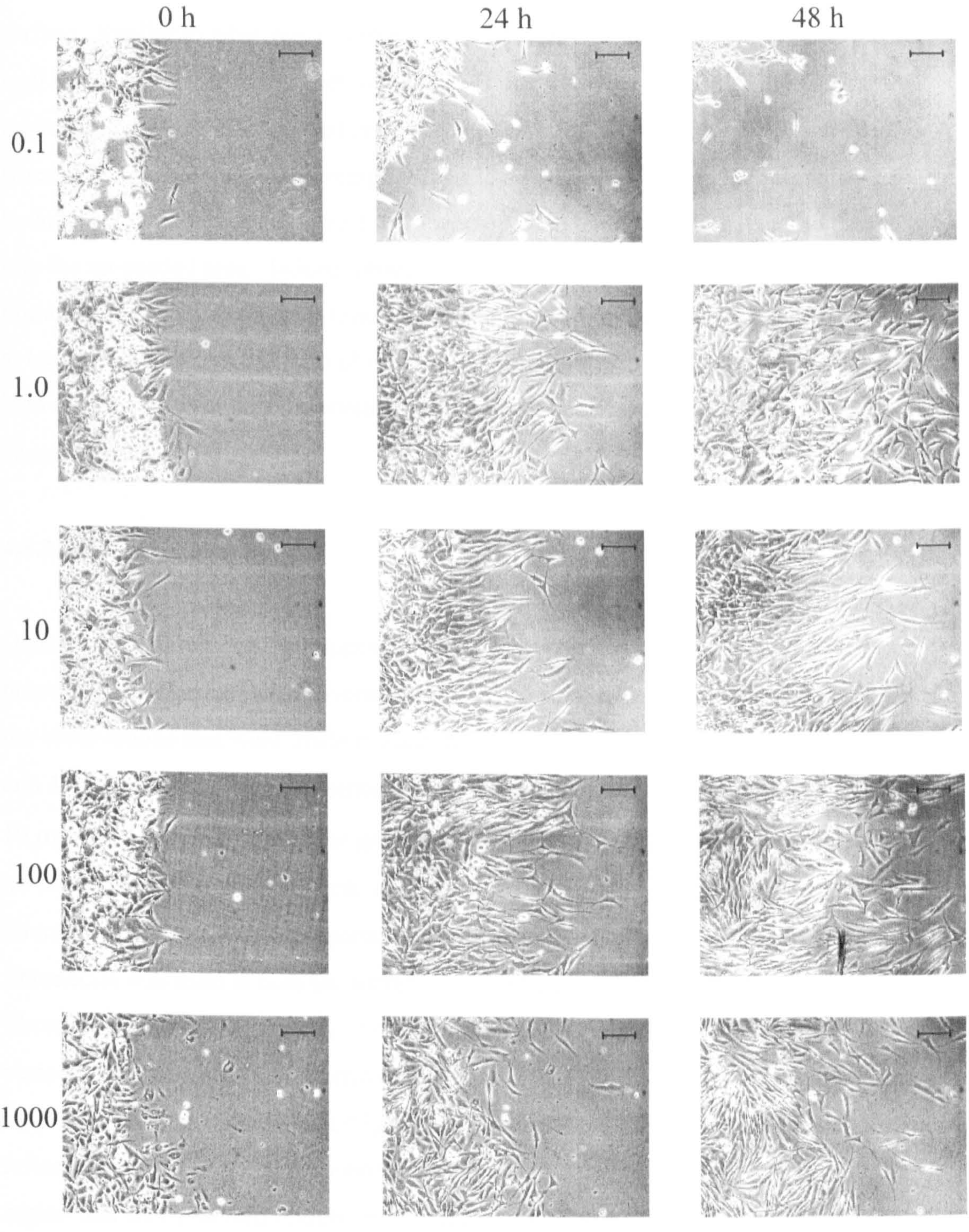

Figure 4.4a Fibroblast cell migration over 48 hours upon a fibronectin-coated surface. Concentration of fibronectin is indicated, in μg/ml, on the left hand side of each series of images. Micron bar represents 100 μm.

accelerated the level of cell migration that was achieved within the assay (Fig. 4.4b). Here, ES was added to cells that were then seeded upon a 100 μg/ml fibronectin-coated surface. Similar to what was observed when ES was absent, cells adhered and spread well upon the surface. However, over the ensuing 48 hours the cells were observed to move rapidly into the un-seeded area, filling the entire field of view far earlier than when ES was omitted. The corresponding movie also showed that the migrating cell boundary moved through and past the observed field of view during its rapid progress into the un-seeded area. Indeed, observations that were made at a lower magnification immediately after the 48-hour time period had elapsed, indicated that cells had migrated at least twice as far as the field of view visible within the time-lapse movie. This result is in contrast to what was observed when cells were exposed to the higher ES concentration of 10 μg/ml.

4.3.2 Analysis of results

Quantitative analysis of the images shown in Fig. 4.4a and b, in which the total percentage cell surface area coverage within each image was assessed, concurred with the observations that were made in section 4.3.1. Use of the method outlined in Fig. 4.1 and 4.2 revealed that in the absence of ES, surfaces coated with 1.0 μg/ml fibronectin or 10 μg/ml fibronectin yielded the greatest increase in cell surface area coverage of the un-seeded, initially cell-free area, with values of 37 % and 36 % respectively after 48 hours (Fig. 4.5a). This is compared with an increase of only 14 % when 1000 μg/ml fibronectin was used to coat the surface, thus indicating that the higher concentration of fibronectin inhibited migration. An increase of 0.2 % was calculated over the 48 hour period when 0.1 μg/ml fibronectin coated the surface. While such a negligible increase may show that the cells did not migrate successfully into the un-seeded area, it does not reflect the retreat of the cell boundary from its original position. This is because the region that was analysed within each image covered only the unseeded area and the edge of the original cell boundary. The assays containing surfaces coated with 100 μg/ml fibronectin revealed that, in the absence of ES, cell surface area coverage increased by 19 % after 24 hours and 30 % after 48 hours. However, coverage attained in the presence of 0.1 μg/ml ES reached 51 % by 24 hours and 56 % by 48 hours. These values were 2.6 times and 1.9 times higher respectively than the coverage

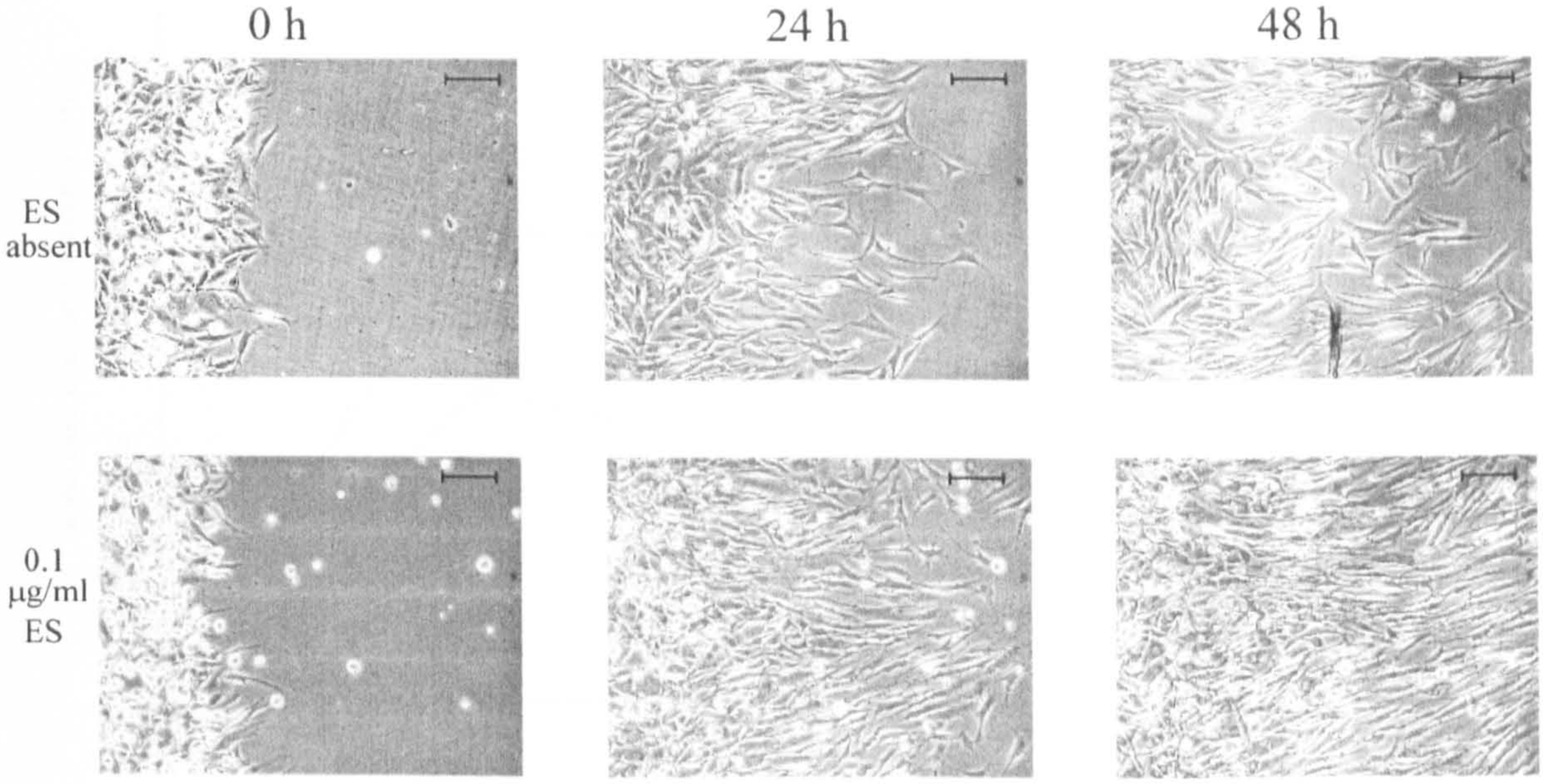

Figure 4.4b Fibroblast cell migration over 48 hours upon a 100 μg/ml fibronectin-coated surface in the absence of ES (*top*) or in the presence of 0.1 μg/ml ES (*bottom*). Micron bar represents 100 μm.

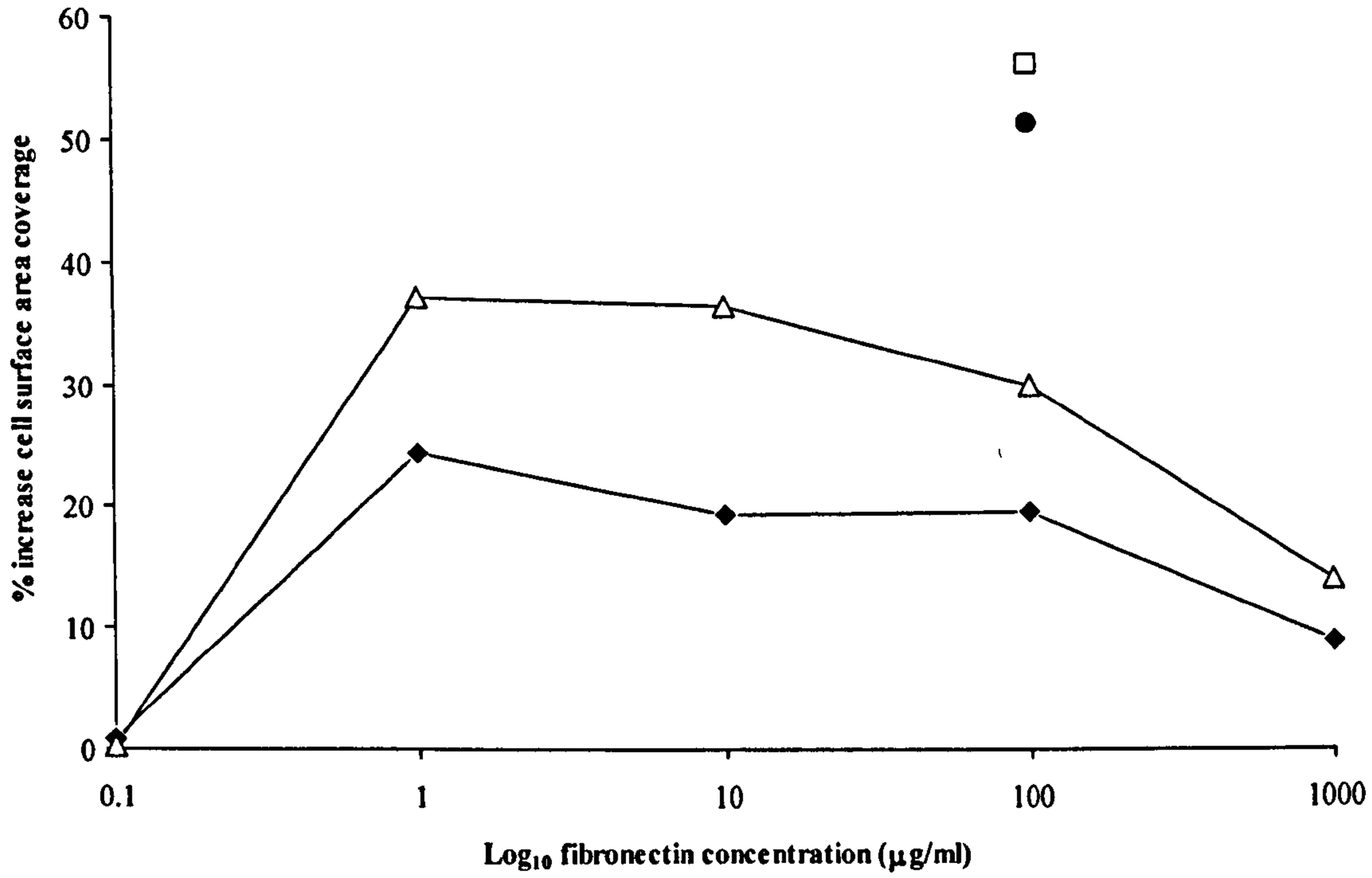

Figure 4.5a Migration of fibroblasts across a cell-free area: percentage increase in total cell surface area coverage of a fibronectin-coated surface, as calculated using the methods outlined in Fig. 4.1 and 4.2. Concentration of fibronectin used to coat surface varied from 0.1 to 1000 µg/ml, as indicated. Cellular response to the presence of 0.1 µg/ml ES whilst upon a 100 µg/ml fibronectin surface is also shown. Percentage increases in cell surface area coverage over 24 hours in the absence of ES (◆) or in the presence of 0.1 µg/ml ES (●). Percentage increases in cell surface area coverage over 48 hours in the absence of ES (△) or in the presence of 0.1 µg/ml ES (□).

attained by cells when ES was omitted. This analysis therefore confirmed that the presence of ES accelerated cell migration.

In addition to the analysis described above, which was performed upon a selected region within each image, the whole field of view within each image was also analysed. This method included analysis of both the un-seeded, initially cell-free area and all of the visible, cell-seeded area. As such, this allowed for quantifying the extent to which the boundary of cells, that had been seeded upon the 0.1 μg/ml fibronectin-coated surface, receded over the 48 hours. Here, calculations revealed that total cell surface area coverage had changed by -11 % after 24 hours incubation and -23 % after 48 hours incubation (Fig. 4.5b). In contrast, cell coverage over the 1.0 μg/ml fibronectin-coated surface was shown to have increased by 13 % over 48 hours, compared with 23 % when the surface had been coated with 10 μg/ml fibronectin. As with the alternative method of analysis, cells on the surface coated with 1000 μg/ml fibronectin demonstrated only a small increase in total cell coverage. By 48 hours, a maximum increase of only 5 % had been attained. Cells on the 100 μg/ml fibronectin-coated surface showed an increase in total surface area coverage. By 24 hours, coverage was 16 % greater than at the beginning of the incubation period. However, by 48 hours this difference had dropped to 9 %. This may have been due to an overall sparser distribution of cells by 48 hours, including those within the original cell-seeded area. In contrast, when ES was present, the change in total cell surface area coverage was far greater, increasing by 34 % after 24 hours and 40 % after 48 hours. Thus, calculations drawn from both methods of data analysis support the hypothesis that ES promotes fibroblast migration across fibronectin surfaces. They also confirm that the concentration of fibronectin present upon the surface influenced cell adhesion and the rate of migration.

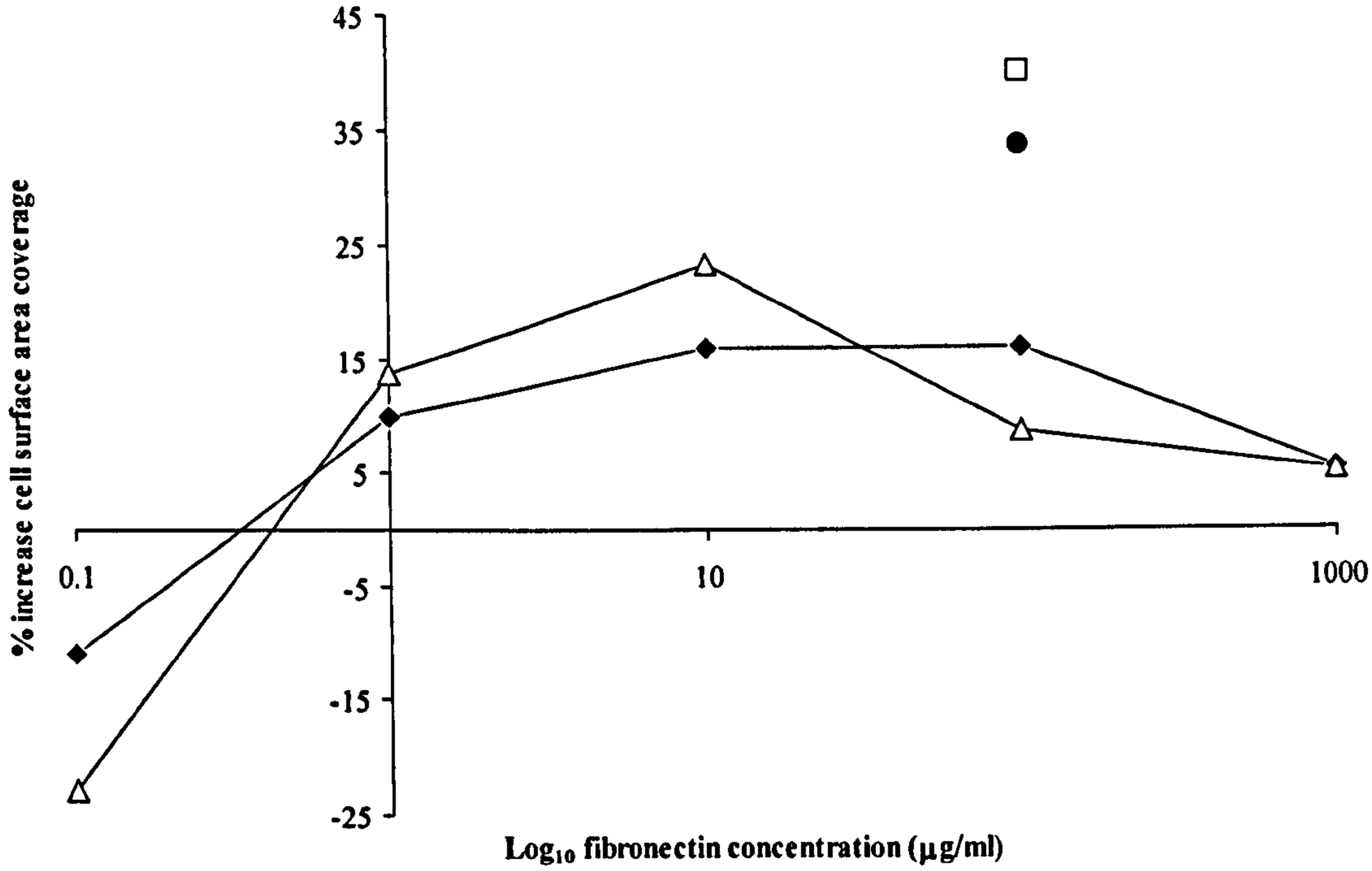

Figure 4.5b Migration of fibroblasts across a cell-free area: percentage increase in total cell surface area coverage of a fibronectin-coated surface. Data derived from analysis of the whole field of view. Concentration of fibronectin used to coat surface varied from 0.1 to 1000 µg/ml, as indicated. Cellular response to the presence of 0.1 µg/ml ES whilst upon a 100 µg/ml fibronectin surface is also shown. Percentage increases in cell surface area coverage over 24 hours in the absence of ES (◆) or in the presence of 0.1 µg/ml ES (●). Percentage increases in cell surface area coverage over 48 hours in the absence of ES (△)or in the presence of 0.1 µg/ml ES (□).

4.4 Discussion

The results presented within Chapter 3 demonstrate that *L. sericata* larval ES modifies fibroblast adhesion to ECM-coated surfaces, particularly fibronectin (Horobin *et al.*, 2003). Such an influence over fibroblast behaviour could have implications upon fibroblast motility. Hence, the effect of ES upon human, dermal fibroblast migration within two-dimensional *in vitro* wound assays was investigated. Initially, 10 μg/ml ES was included within the assay because this same concentration had been applied to experiments presented within Chapter 3. Results from this preliminary study indicated that the majority of cells were prevented from adhering and migrating across the 10 μg/ml fibronectin-coated surface. This effect was not due to the concentration of fibronectin present, as cells were shown to spread and migrate well over this surface when ES was absent. It may therefore be concluded that the presence of ES was responsible. Hence, the results from this preliminary study complement those that were obtained in the previous chapter, where various assays showed that 10 μg/ml ES also reduced fibroblast adhesion to fibronectin. Additionally however, the preliminary time-lapse study provides an indication as to the possible consequences of such a reduction in fibroblast adhesion. Here, this action was shown to have a deleterious effect upon the cells, inhibiting their attachment to the substratum, preventing migration and possibly causing the destruction of cellular extensions.

Further time-lapse studies showed that in contrast, the addition of ES at the much lower concentration of 0.1 μg/ml enhanced fibroblast migration upon fibronectin. Although these results must be treated with caution because no replicate samples were tested and therefore no statistical analysis performed, the margin by which 0.1 μg/ml ES increased migration allows for tentative conclusions to be drawn. It may be proposed that this concentration of ES hastened the rate of cell migration by altering the fibronectin-coated surface. This hypothesis is based upon results from the previous chapter where it was shown that over a similar period of time and at the same concentration, ES modified fibronectin, degrading it into separate peptides (see Fig. 3.24a). Such an alteration in the character of the fibronectin surface may have caused a reduction in the strength of

fibroblast adhesion, without, as was observed with the higher ES concentration, inhibiting cell attachment. In turn, this may have contributed to accelerated migration.

The supposition that ES assisted migration by reducing the strength of cell adhesion is supported by the results that were obtained when different concentrations of fibronectin were tested in the absence of ES. The lowest fibronectin surface concentration tested (0.1 μg/ml) was insufficient to sustain prolonged cell adherence, thus inhibiting migration. Intermediate fibronectin concentrations (1 and 10 μg/ml) provided for optimal migration, while the highest concentrations (100 and 1000 μg/ml) reduced migration. These results are consistent with the 'receptor saturation model' originally presented by Dembo and Bell in 1987 and later by Gaudet *et al.* (2003). Based upon thermodynamic analysis of cell adhesion, this model explains the influence of the substrate surface upon cell spreading in terms of the number of adhesive sites available to the cell. Used in Chapter 3.4 to explain why fibroblasts exposed to 10 μg/ml ES exhibited a more rounded morphology (Fig. 3.25), this model may also be used to explain the effects of cell adhesion upon migration (Fig. 4.6). As the substrate surface concentration increases there will come a point where the integrin receptors, assuming they are expressed in finite numbers (Akiyama and Yamada, 1985), become saturated by available adhesive sites. Below the saturation point, cell spreading increases with a rise in the density of adhesive sites because the cell is able to make more contacts with the substrate. However, above the saturation point, cell spreading decreases with a continuing rise in the density of adhesive sites because the integrin receptors become saturated over a smaller distance. Hence, the saturation point coincides with a transition in the response of cells to increasing substrate concentration. Gaudet *et al.* (2003) found that at collagen surface concentrations far below the saturation point, BALB/c 3T3 fibroblast cell migration was negligible. However as the collagen surface concentration increased to near saturation point, a more motile cell phenotype became prominent. Cell migration then increased as the collagen concentration increased. At the highest collagen concentrations tested, cell migration became inhibited. According to Gaudet *et al.* (2003) 'it is generally accepted that this inhibition occurs because the substrate becomes overly adhesive and the contractility of the cell is unable to overcome the adhesive attachments'. This theory is consistent with the 'receptor saturation model' because integrin receptor-ligand bonds that occur when the adhesive sites are

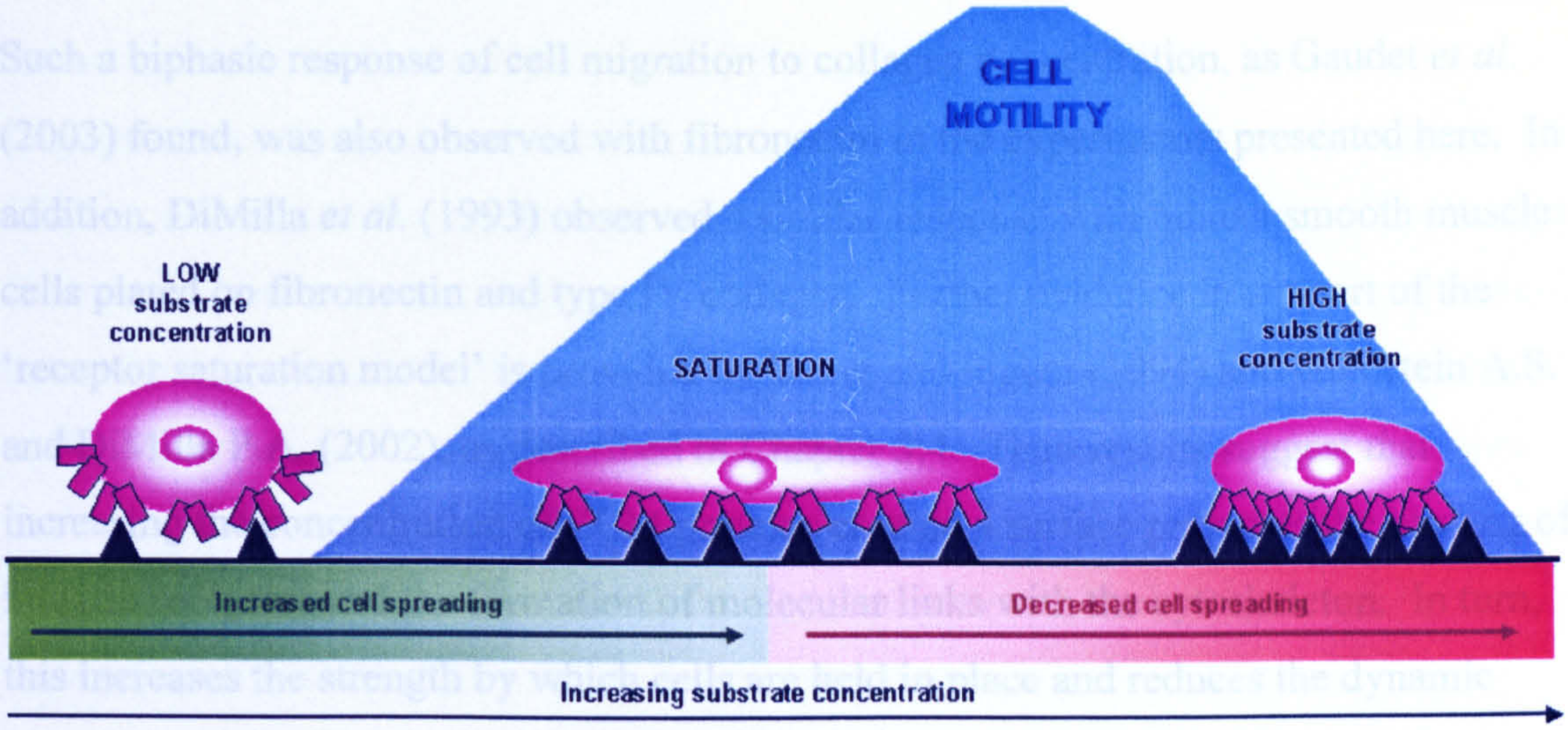

Figure 4.6 Receptor saturation model showing the relationship between substrate concentration, cell adhesion, spreading and migration. At low substrate concentrations, the number of available adhesive sites are low. Hence, the cell is unable to spread fully. Migration is inhibited because the cell is unable to maintain sufficient contact with the substrate to generate traction forces. As the substrate concentration rises, cell spreading increases as the cell comes into contact with more adhesive sites. Cell movement also becomes possible. At the 'saturation' point, the number of available integrin receptors within the cell are approximately equal to the number of adhesive sites that the cell can reach. Cell motility continues to increase as a greater number of adhesive sites become accessible. If the substrate concentration rises further, adhesive sites become denser. Thus, cell spreading begins to decrease as the integrin receptors become saturated by adhesive sites over a smaller area. Eventually, adhesive sites become so dense that the substrate becomes excessively adhesive. Here, cell traction forces can no longer overcome the strength of cell adhesion. Thus, cell motility is decreased. Figure adapted from Gaudet *et al*. (2003).

very dense, tend to be clustered together and are therefore more able to resist mechanical loads that promote detachment.

Such a biphasic response of cell migration to collagen concentration, as Gaudet *et al.* (2003) found, was also observed with fibronectin in the experiments presented here. In addition, DiMilla *et al.* (1993) observed a similar response with human smooth muscle cells plated on fibronectin and type IV collagen. Further evidence in support of the 'receptor saturation model' is provided by Wang and Ingber (1994) and Goldstein A.S. and DiMilla P.A. (2002), as described in Chapter 3.4. Their results suggest that increasing the concentration of ECM proteins coating a surface promotes the binding of integrin receptors and the formation of molecular links with the cytoskeleton. In turn, this increases the strength by which cells are held in place and reduces the dynamic responsiveness of cells to external stimuli. More evidence is provided by Puschel *et al.* (1995). These researchers found that fibroblasts taken from elderly volunteers (aged between 80 and 92 years old) adhered more strongly to fibronectin than those taken from younger individuals (aged between 20 to 30 years old). The authors hypothesised that the increased adhesive capacity of older fibroblasts contributes to impaired healing in the elderly by slowing the rate at which the cells can migrate through the surrounding matrix and into the wound space. Yet further evidence suggests that $\alpha_5\beta_1$ integrin-mediated adhesion to high fibronectin concentrations induces a 'stop' signal for cell migration via activating the GTPase protein RhoA, which stimulates focal adhesion formation (Cox, Sastry and Huttenlocher, 2001). The authors found that as RhoA activity increased with increasing fibronectin, the activity of other GTPase proteins, CDc42 and Rac1, both of which co-ordinate to promote cell polarisation and protrusion, actually decreased. Hence according to these findings, an increase in the strength of cell adhesion above a certain point causes a decrease in the protrusion of cells into new territory. Inducement of 'stop' signals may therefore be another method by which high substrate concentrations inhibit migration.

In order to fully appreciate how the fibronectin surface concentration and the presence of ES influenced fibroblast migration, it is necessary to discuss the mechanisms by which cells migrate. Studies undertaken by Pelham and Wang (1999), Beningo *et al.* (2001), Munevar, Wang and Dembo (2001a and b), Petroll, Ma and Jester (2003) reveal that cells migrate via the exertion of tractional forces near the leading cell edge,

while adhesions located at the back of the cell serve as passive anchors. Discussed in more detail within Chapter 1, these results concur with "a frontal towing model of cell migration, in which the frontal regions serve as the 'engine' that tows an adhesive cargo consisting of the cell body and the tail" (Beningo and Wang, 2002). This adhesive cargo produces dragging forces which, according to Munevar, Wang and Dembo (2001b), sometimes show a strong focus at the tail-end of the cell. As these forces resist forward movement, it may be suggested that the release of cell trailing edges represents a rate-limiting step of migration. If this is so, the high fibronectin concentrations tested within the experiments presented here may have inhibited migration. This is because the high density of adhesive sites may have caused clustering of integrin receptor-ligand bonds at the trailing edge of the cell. Stronger tractional forces would therefore have been necessary to effect forward motion because a greater number of bonds would needed to have been disrupted and reformed. In accordance with this theory, Gaudet *et al* (2003) found that traction per unit area exerted by migrating cells was greater at high substrate concentration.

Considering how cells migrate, the presence of 0.1 μg/ml ES may have increased fibroblast migration by assisting the detachment of cell trailing edges, without compromising the cells' abilities to exert tractional forces. Generation of such differential effects across the geography of the cell may be possible when considering the general shape of migrating cells. As shown by various migration studies and within the time-lapse movies recorded here, the leading edge of a cell is generally broader than its trailing edge. The trailing edge can on occasion extend, becoming exceptionally long and thin as the cell body moves while the end of the trailing edge fails to release from the surface. In this case, the trailing edge would be attached to a smaller area of fibronectin than the leading edge. If the fibronectin surface had been altered by the proteolytic actions of ES, reducing its surface adhesion capacity, then the trailing edge would be more vulnerable to losing grip than the leading edge. This is particularly so when considering that clustering of receptor-ligand bonds at the trailing edge of the cell is less likely to occur when adhesive sites are more sparse. Thus, migration would be enhanced. In accordance with the 'receptor saturation model', a similar mechanism of promoting migration may be involved when cells are exposed to a lower concentration of substrate.

Another possible explanation as to how 0.1 μg/ml ES accelerated migration is also based upon the shape of migrating cells. A broad leading edge, located a short distance from the thicker cell body, and an extended long, thin trailing cell edge would result in a situation where the trailing edge possessed a much higher surface area to volume ratio than the main cell body or indeed, the broader lamellipodial leading edge. As a consequence, the trailing edge of the cell and its receptor-surface interactions would be more exposed to the surrounding medium. Presumably, this would result in the trailing edge being more vulnerable to direct attack from the proteolytic agents present with ES. Hence, substrate adhesions located at the rear of the cell may be more likely to be destroyed by proteolysis than those located towards the cell front. Possible evidence for the destruction of cell trailing edge adhesions, and maybe of the cytoplasmic extensions themselves, may be observed in the time-lapse movie showing cells exposed to 10 μg/ml ES. Here, it appears that thin cytoplasmic extensions may be being broken off, resulting in the failure of the cells to spread. Differences in the character of the adhesions found at the cell front compared with the rear of the cell may also contribute to differential effects of ES across the cell. As discussed within Chapter 1.2.1, focal adhesions which form at the leading cell edge, generate the most traction to drive migration. As they mature, the adhesions become larger and are relocated backwards, into the cell body and towards the trailing cell edge, becoming focal adhesion plaques. It may be the case that these more mature focal adhesions are more liable to protelytic action than their younger counterparts, or that they are less able to react dynamically to a changing environment.

Thus, in considering the effect of ES upon fibroblast migration in terms of the 'receptor saturation model', 0.1 μg/ml ES may have promoted migration on a surface coated with a relatively high concentration of fibronectin (100 μg/ml) by reducing the density of adhesive sites (Fig. 4.7a). The higher ES concentration of 10 μg/ml may have reduced migration on the surface coated with an intermediate concentration of fibronectin (10 μg/ml), by the same means. However, a reduction in the density of adhesive sites may have occurred to such an extent that the cells could not maintain enough bonds with the surface to allow spreading or indeed to remain attached (Fig. 4.7b). This is in agreement with what was observed in the relevant time-lapse movie. As the

a.

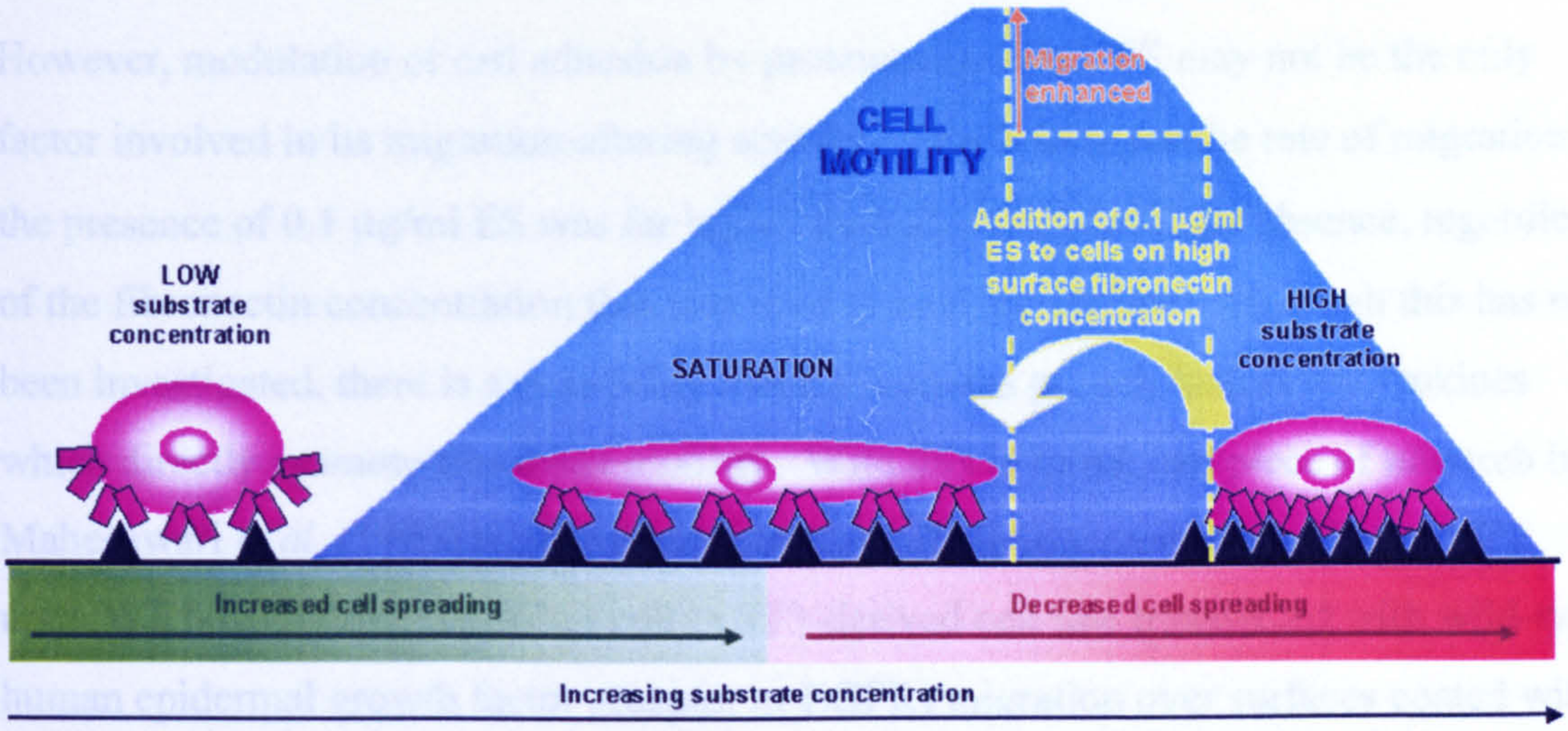

b.

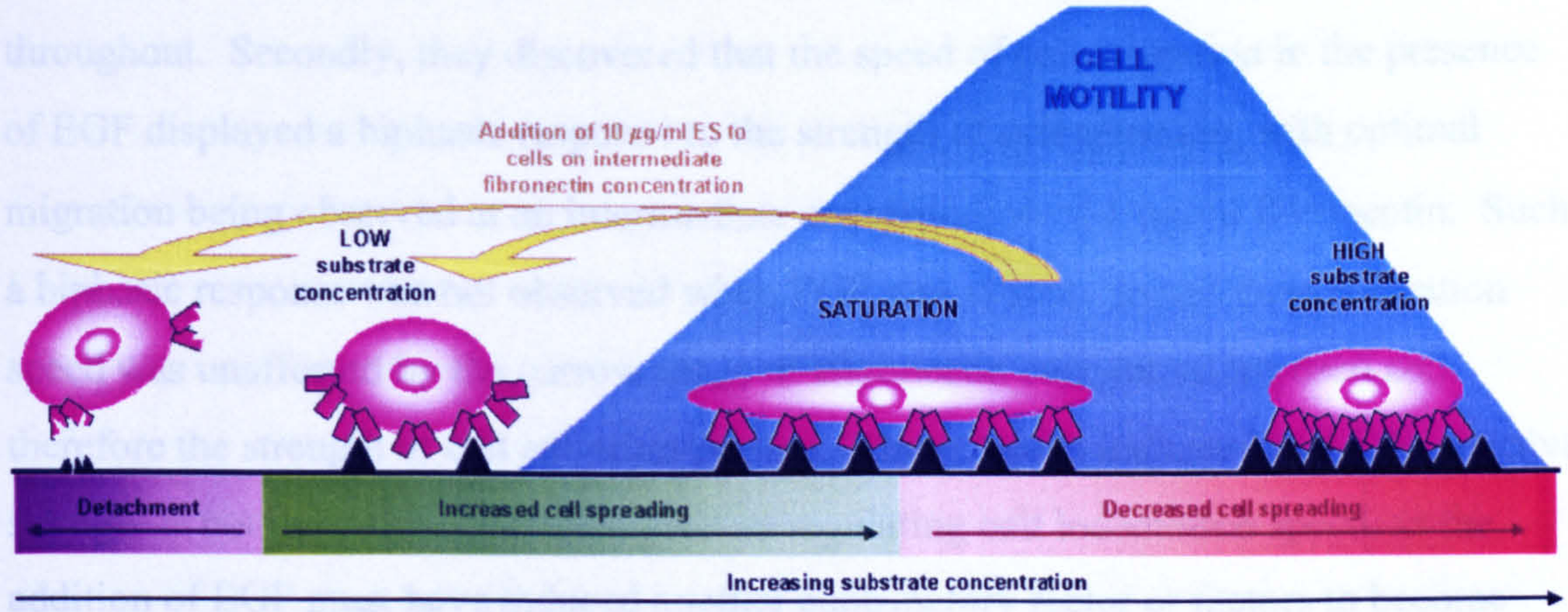

Figure 4.7 Receptor saturation model demonstrating the proposed impact that the presence of larval ES has upon cell adhesion, spreading and migration. **a.** The effect of 0.1 µg/ml ES upon cells seeded on a relatively high concentration of fibronectin. This concentration of ES alters the fibronectin surface, reducing the density of adhesive sites and therefore promoting cell spreading and migration. **b.** The effect of 10 µg/ml ES upon cells seeded on an intermediate fibronectin concentration. Through the high proteolytic activity of ES, adhesive sites are reduced, inhibiting cell spreading and migration. Integrin receptor-ligand bonds that remain may also be degraded and the cells become detached.

concentration of ES was so high, direct proteolytic degradation of receptor-ligand bonds may also have played a major role.

However, modulation of cell adhesion by proteinases within ES may not be the only factor involved in its migration-altering activity. This is because the rate of migration in the presence of 0.1 μg/ml ES was far higher than any recorded in its absence, regardless of the fibronectin concentration that was used to coat the surface. Although this has not been investigated, there is a possibility that ES contains growth factors or cytokines which directly promote fibroblast motility. With this in mind, one piece of research by Maheshwari *et al.* (1999) is of particular interest. This concerned the effect of EGF upon WT NR6 murine fibroblast cell (a 3T3-derived cell line transfected with wild-type human epidermal growth factor receptor or EGFR) migration over surfaces coated with 0.1 to 3 μg/ml fibronectin. The authors found that firstly, cell adhesion increased as the concentration of the fibronectin coating increased, both in the presence and absence of EGF. However, in the presence of EGF, the strength of adhesion was relatively lower throughout. Secondly, they discovered that the speed of cell migration in the presence of EGF displayed a biphasic response to the strength of cell adhesion, with optimal migration being observed at an intermediate concentration of 1 μg/ml fibronectin. Such a biphasic response was not observed when EGF was absent. In this case, migration speed was unaffected by the narrow range of fibronectin concentrations used and therefore the strength of cell adhesion present. These results indicated that cell adhesive strength is not the only biophysical process regulating cell locomotion speed, as the addition of EGF must have induced another contributory factor or factors to become involved.

In continuation of this research, Maheshwari *et al.* (1999) also examined cell membrane activity in terms of fractional membrane protrusion. This was determined by first calculating the area extended by a cell over a given time in order to find the average rate of change of cell protrusion area. This data was then normalised to account for differences in average cell area. The results revealed that with increasing fibronectin coating concentration and concomitant cell adhesive strength, EGF first decreased membrane activity compared with the control, then increased it and then finally had no effect. Here, maximum membrane activity was observed at 0.3 and 1 μg/ml fibronectin

concentration. Thus, EGF not only elicited a bi-phasic response to fibronectin in terms of cell migration speed, it also elicited a bi-phasic response in terms of cell membrane activity. Further examination of these results revealed that the response curves representing migration speed and membrane activity did not precisely run parallel with each other when plotted against fibronectin concentration. At 0.3 μg/ml fibronectin, EGF enhanced cell membrane activity but failed to promote the speed of cell locomotion above the level observed in the control. This indicated that membrane activity, although influential, was not the only controlling factor involved in cell migration. The researchers therefore concluded that in the presence of EGF, both cell membrane activity and cell adhesive strength (and therefore fibronectin concentration) affect cell migration.

With these conclusions in mind, it would be interesting to observe the effect of ES upon fibroblast cell membrane activity. How ES affects cell migration upon surfaces coated with different concentrations of fibronectin would also be of interest. Here, in the absence of these results, some parallels may be drawn against the effects that EGF was shown to exert upon the cells, as demonstrated by Maheshwari *et al.* (1999). ES like EGF has been shown to reduce cell adhesion to fibronectin (Chapter 3), albeit perhaps by different mechanisms. It may therefore be speculated that at low concentrations of fibronectin, ES may actually inhibit cell migration. This is because Maheshwari *et al.* (1999) found that at the lowest fibronectin concentration tested (0.1 μg/ml), EGF inhibited cell membrane activity and migration. The authors hypothesised that this was due to EGF reducing cell adhesion to a surface that already had a low surface adhesion capacity. This in turn would have prevented the EGF-stimulated cells from being able to establish any stable attachments. ES may therefore prove to exert the same effect. Higher concentrations of ES may also exert a similar effect at higher concentrations of fibronectin. This was indeed observed when cells were exposed to 10 μg/ml ES, as shown in the relevant time-lapse movie.

It may also be speculated that at very high concentrations of fibronectin, ES at just 0.1 μg/ml may not be able to exert such a dramatic effect upon migration. Maheshwari *et al.* (1999) found that at the highest fibronectin concentration tested (3 μg/ml), EGF had little effect upon cell membrane activity and migration. They explained this through

hypothesising that the strength of cell adhesion to this surface fibronectin concentration is overriding the influence that EGF can exert. Another theory is that high cell adhesive strength is inducing the cells to produce 'stop' signals on migration. This has indeed been observed by Cox, Sastry and Huttenlocher (2001), as discussed earlier. However, to hypothesise that the effects of ES like EGF, can be overridden by high surface fibronectin concentrations, does not take into account the proven ability of proteinases within ES to break down fibronectin (Chambers *et al.*, 2003; Horobin *et al.*, 2003) thus presumably altering surface/receptor interactions. Nor does it consider the fact that ES was shown to increase migration while cells were attached to a far higher concentration of fibronectin than was used when EGF was tested. Another factor also unaccounted for in this hypothesis concerns the consequences that may result from the liberation of peptides from fibronectin as it is degraded by the proteolytic actions of ES. Once exposed, a number of peptide sequences found within fibronectin have been shown to modulate fibroblast adhesion (Pierschbacher and Ruoslahti, 1984; Woods *et al.*, 1993), chemotaxis (Postlethwaite *et al.*, 1981) and migration (Livant *et al.*, 2000). Fibronectin fragments have also been shown to regulate matrix metalloproteinase (MMP) gene expression by fibroblasts (Huhtala *et al.*, 1995). This study showed that a 120 kDa fibronectin fragment containing the central cell-binding domain, co-ordinately induces procollagenase and its activator urokinase plasminogen activator (uPA), thus increasing matrix-degradative activity. As discussed previously, MMPs are important in tissue re-modelling during wound healing, breaking down ECM components to allow the free passage of migrating fibroblasts and therefore the advancement of granulation tissue (Clark, 1996).

Having discussed the parallels and possible differences between EGF- and ES-stimulation of fibroblast migration, it is interesting to note the findings of Prete (1997). Here, the author found that the addition of 'alimentary secretions', from late second instars of *Phaenicia sericata* larvae, augmented the mitogenic actions of EGF upon human fibroblasts. If the mitogenic activity of EGF is also influenced by the strength of cell adhesion to a surface, then ES may behave synergistically by modifying fibroblast adhesion towards a level more conducive to the actions of EGF. Alternatively, ES may also contain some form of independent, yet limited growth-promoting activity. This may be a reasonable conclusion as Prete demonstrated that cells in the presence of 10 % serum, modestly increased [^{3}H]-thymidine incorporation when exposed to 'alimentary

secretions' alone. However, the research in this thesis has found no evidence to suggest that ES in isolation, without the presence of any serum components or other sources of growth factors, conveys mitogenic action. It may therefore be assumed that the promotion of cell proliferation by ES requires cells to interact with other mitogenic stimuli.

Despite the lack of evidence to suggest that ES stimulates fibroblast proliferation independently, it may be argued that any increase in the rate at which a confluent layer of cells expands its borders, is due to enhanced cell proliferation. However, the advantage of observing cells in real-time as they migrate across a surface, is that the progress of individual cells can be visibly tracked. In addition, any cell division can also be observed. With this in mind, it may be concluded that after viewing the time-lapse movies recorded in these experiments, ES enhanced the progression of the leading cell edge by stimulating cell locomotion and not cell proliferation. The visual tracking of individual cells exposed to 0.1 μg/ml ES revealed them to be moving much more rapidly than cells migrating in the absence of ES. In addition, cell division did not appear to be more frequent.

4.5 Conclusions

In summary, larval ES at 0.1 μg/ml, appears to enhance the rate at which fibroblasts migrate across a fibronectin-coated surface. Much higher concentrations of ES, such as 10 μg/ml, induce the opposite effect, indicating a dose-dependent response. ES proteinases and/or the actions of other as yet unknown agents within ES may be responsible. These results were obtained while observing cells in a two-dimensional environment. *In vivo* however, cells interact within a three-dimensional environment. As will be discussed in the next chapter, several studies have shown the behaviour of fibroblasts to be dependent upon whether they are exposed to two-dimensional or three-dimensional environments. With this in mind, research was directed towards developing a more physiologically-relevant, three-dimensional, *in vitro* wound assay, in which the effects of larval ES upon fibroblast migration could be observed.

CHAPTER 5

Fibroblast Migration in Three Dimensions: Method Development

5.1 Introduction

As shown in the previous chapter, larval ES appears to modify fibroblast migratory behaviour, increasing the rate at which the cells migrate across a fibronectin-coated surface. However, as briefly discussed, cells behave differently upon planar surfaces than within the three-dimensional matrix that they experience *in vivo*. Examination of mesenchymal cells *in situ* has revealed that they adopt stellate shapes and protrude dendritic-like networks of extensions (Tamariz and Grinnell, 2002; Grinnell *et al.*, 2003). This is in contrast to their flattened, lamellar appearance on planar surfaces (Elsdale and Bard, 1972). Cells observed *in situ* also exhibit attachments to the surrounding matrix that are characteristically different to those observed in two-dimensional environments (Breathnach, 1978; Trinkaus, 1984; van Exan and Hardy, 1984; Omagari and Ogawa, 1990; Beertsen, McCulloch and Sodek, 2000; Cukierman *et al.*, 2001). Termed "3D-matrix adhesions" by their original observers, these attachments contain paxillin and α_5 integrin receptors that have co-localised and run parallel with fibronectin fibres within the ECM. This is in contrast to the associations formed in the two-dimensional environment. Here, the attachments comprise of much more discrete focal contacts and can be identified as focal adhesions, containing integrin $\alpha_v\beta_3$, paxillin, vinculin and focal adhesion kinase (FAK) (Fig. 1.3, Chapter 1), or fibrillar adhesions, which are composed of $\alpha_5\beta_1$ integrin and tensin (Zamir *et al.*, 1999; Friedl and Bröcker, 2000).

The introduction of the fibroblast-populated collagen lattice by Ehrmann and Gey (1956) signified the first attempt to observe fibroblasts *in vitro* within a three-dimensional environment. Since then, collagen gels have been widely used for *in vivo*-like cell culture (Friedl and Bröcker, 2000) and are considered to represent a fair reproduction of the biophysical architecture of the dermis, in terms of the random network-like distribution of collagen type I fibres (Friedl and Bröcker, 2000).

Cells embedded within collagen gels have been shown to adopt dendritic-like networks of extensions that share some similarity to the *in situ*-like morphology (Elsdale and Bard, 1972; Tamariz and Grinnell, 2002; Grinnell *et al.*, 2003; Cukierman *et al.*, 2001). First used quantitatively as models of wound contraction (Bell *et al*, 1979), cell motility within such gels has been shown to result in β_1 integrin receptor-mediated translocation of collagen fibrils and global matrix re-modelling (gel contraction) (Bell *et al*, 1979; Tomasek & Akiyama, 1992; Kuhn *et al.*, 2000; Cukierman *et al.*, 2001). As the extent of re-modelling appears dependent upon the density of cells present, with minimal contraction occurring below 1×10^4 cells per ml of gel, this suggests that intercellular communication plays a role (Ehrlich, Gabbiani and Meda, 2000; Ehrlich and Rittenburg, 2000). Indeed, metabolic coupling between cells where they communicate via the intercellular passage of molecules through gap junctions, has been shown to occur within collagen gels and has been found to be necessary for their contraction (Ehrlich, Gabbiani and Meda, 2000; Ehrlich and Rittenburg, 2000; Grinnell *et al.*, 2003).

Fibroblast migration within collagen gels has also been studied. In two dimensions, migration across a surface is predominantly a function of adhesion and de-adhesion events because resistance to the advancing cell body above the planar surface is lacking. Within three dimensions however, cells have to overcome resistance from the matrix that completely surrounds them. Matrix barriers force the cells to adapt their morphology, making them either change shape and/or enzymatically degrade ECM components in order to facilitate locomotion (Friedl and Bröcker, 2000; Haas, Davis and Madri, 1998). It is therefore perhaps unsurprising that the ECM exerts a considerable influence over the behaviour of cells embedded within it. For example, researchers have found that fibroblasts only up-regulate $\alpha_2\beta_1$ integrin receptor expression when they are placed within a collagen gel and not when they are attaching to a collagen-coated

surface (Klein *et al.*, 1991). This finding indicates the importance of the biomechanical architecture of the matrix in determining fibroblast behaviour.

Within gels, collagen concentrations of between 1.5 to 2 mg/ml are preferable for observing cell migration (Friedl and Bröcker, 2000). However, it has been reported that the motility of cells within gels containing collagen only, results predominantly in matrix re-organisation and contraction rather than cell locomotion (Bell *et al*, 1979; Harris, Stopak and Wild, 1981; Grinnell, 1994; Tomasek *et al.*, 2002). Within tissue, collagen is associated with a variety of ECM components including fibronectin and GAGs. This may explain why collagen gels *in vitro* are less favourable to cell adhesion, migration, proliferation and adoption of *in situ*-like morphologies, than cell-derived three-dimensional matrices (Cukierman *et al.*, 2001). Therefore, in order to observe cells within more physiologically relevant conditions, the addition of other ECM components to collagen gels is preferable. As discussed previously, fibroblasts are known to use fibronectin to assist migration into the wound space during granulation tissue formation (Hsieh and Chen, 1983; Clark, 1996). It therefore seems logical that the addition of fibronectin to collagen gels improves the migration of embedded cells. One study estimated that the addition of 30 μg/ml fibronectin provides for optimal migration (Greiling and Clark, 1997). Other studies have examined the suitability of conventional cell culture media for providing physiologically relevant conditions. These have shown that supplementing media with L-ascorbic acid 2-phosphate stimulates accumulation of dermal fibroblast-derived collagen matrix and multilayering of fibroblasts (Hata and Senoo, 1989; Ishikawa *et al.*, 1997; Ohgoda *et al.*, 1998). The addition of L-ascorbic acid 2-phosphate has also been shown to improve renal, proximal, tubular cell growth and promote *in vivo*-like function (Nowak and Schnellmann, 1996). Based upon this information, *in vitro* wound assays containing three-dimensional collagen/fibronectin matrices were developed in order to assess cell migration in three dimensions. The use of L-ascorbic acid 2-phosphate in the production of an *in vitro* three-dimensional matrix was also investigated.

5.2 Methods

5.2.1 Preparation of collagen gels

5.2.1.1 Collagen gel - 1 mg/ml

Powdered DMEM (Gibco™, Invitrogen Ltd, Paisley, UK) was dissolved in a solution containing antibiotic/antimycotic, L-glutamine, N-(2-hydroxyethyl)piperazine-N'-(2-ethanesulphonic acid); 4-(2-hydroxyethyl)piperazine-1-ethanesulphonic acid (HEPES) and $NaHCO_3$, such that all of the above components were mixed at 1.5 times the concentrations used for routine cell culture (see Appendix). Where mentioned, 0.3 mM L-ascorbic acid 2-phosphate or 45 μg/ml bovine fibronectin was also present. Following refrigeration, the stock solution was mixed on ice, at a ratio of 2:1, with a cold solution containing 3 mg/ml acid-solubilised bovine collagen type I (ICN Biomedicals, Ohio, USA). A final concentration of 1 x DMEM, 1.0 mg/ml collagen, 25 mM HEPES, 3.7 g/l $NaHCO_3$ and where present, 0.2 mM L-ascorbic acid 2-phosphate and 30 μg/ml fibronectin, was obtained.

5.2.1.2 Collagen gel - 1.5 mg/ml

As before, powdered DMEM (Gibco™, Invitrogen Ltd, Paisley, UK) was dissolved in a solution containing antibiotic/antimycotic, L-glutamine, HEPES and $NaHCO_3$. However, in this case all of the above components were mixed at twice the concentrations used for routine cell culture (see Appendix). In addition, 60 μg/ml bovine fibronectin was also present. Following refrigeration, the stock solution was mixed on ice, at a ratio of 1:1, with a cold solution of 3 mg/ml acid-solubilised bovine collagen type I. A final concentration of 1 x DMEM, 1.5 mg/ml collagen, 25 mM HEPES, 3.7 g/l $NaHCO_3$ and 30 μg/ml fibronectin was obtained.

5.2.2 Development of three-dimensional assays using the cloning cylinder

Fibroblast cells were trypsinised and suspended in cell culture medium containing 10 % FCS to neutralise the trypsin. They were then prepared in serum-free medium and counted, using a haemocytometer, as described in Chapter 2.2.1. The cells were again pelleted and re-suspended at a density of $1x10^6$ cells/ml within a specified collagen solution. The solution was kept on ice to prevent gelation and the cells were mixed by careful and slow pipetting, in order to minimise bubble formation.

A pre-cooled 35 mm dish was prepared with a cloning cylinder placed upright in its centre. The collagen solution containing the cells was then poured into this dish around the outside of the cylinder (Fig. 5.1). Following sufficient incubation at 37°C to effect gelation, the cloning cylinder was carefully removed, so as not to disturb the gel that had formed around it. Next, concentrated serum-free cell culture medium, some of which was incorporated into the collagen solution (refer to section 5.2.1), was diluted to 1 x concentration. It was ensured that where L-ascorbic acid 2-phosphate was present within the gel, the medium also contained this component. This medium (2 ml) was then added to the dish, covering the gel, and replaced every 24 hours. Cells were observed using phase contrast microscopy and/or confocal microscopy, as described in Chapter 2.2.4.

5.2.2.1 Fibroblast migration from a populated gel in the presence of L-ascorbic acid 2-phosphate

Fibroblasts were suspended as described above, within 1.5 ml or 2 ml of a 1 mg/ml collagen gel solution, containing 0.2 mM L-ascorbic acid 2-phosphate. In one case, 30 µg/ml fibronectin was also added. The assay was then prepared following the methods outlined in Fig. 5.1 and above. Cells were observed migrating out of the gel and towards the centre of the dish, across the exposed tissue culture plastic surface.

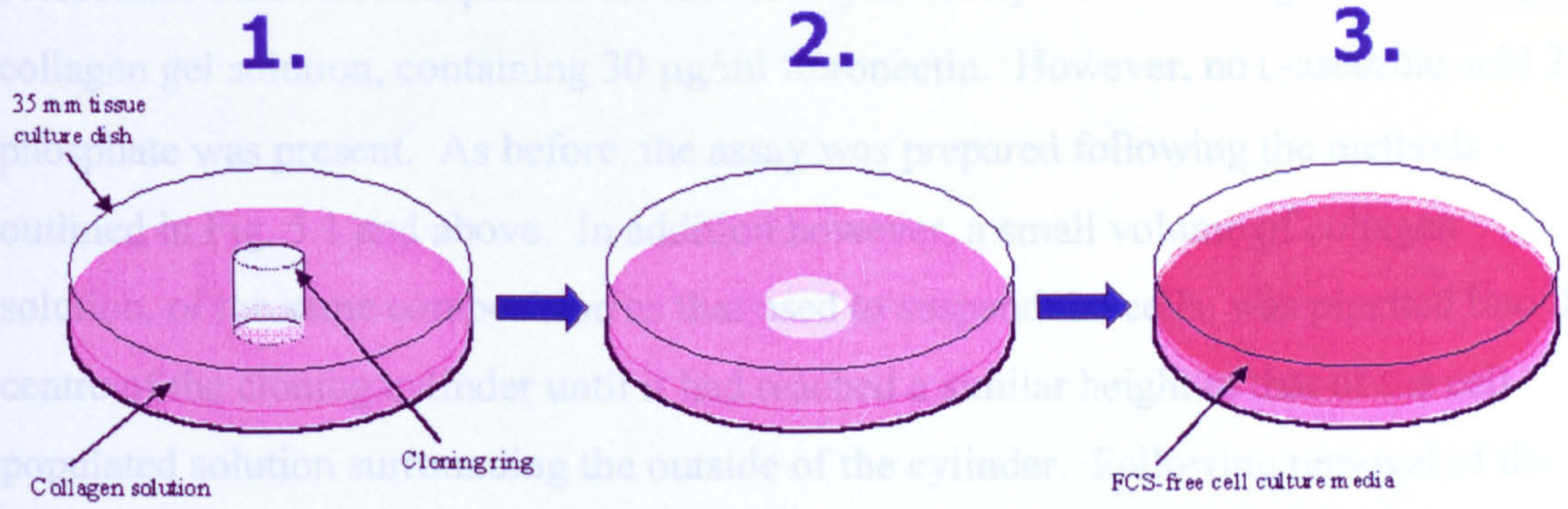

Figure 5.1 Three-dimensional *in vitro* wound assay assembled using a cloning cylinder. 1. Cloning cylinder placed upright in the centre of a 35 mm tissue culture dish. Fibroblast-seeded collagen solution poured around the outside of the cylinder. 2. After collagen gelation, the cloning cylinder is removed to leave a hole in the gel layer. 3. Cell culture medium poured on top of the gel, to cover.

5.2.2.2 Fibroblast migration from a populated gel to a cell-free gel

Fibroblasts cells were suspended as described previously within a 1 mg/ml or 1.5 mg/ml collagen gel solution, containing 30 μg/ml fibronectin. However, no L-ascorbic acid 2-phosphate was present. As before, the assay was prepared following the methods outlined in Fig. 5.1 and above. In addition however, a small volume of collagen solution, of the same composition as that used to suspend the cells, was pipetted into the centre of the cloning cylinder until it had reached a similar height to that of the cell-populated solution surrounding the outside of the cylinder. Following removal of the cylinder, cells were observed at the cell-populated/cell-free boundary using phase contrast microscopy.

In many cases, cells were also fixed and stained *in situ* in preparation for analysis by confocal microscopy. This was achieved by first aspirating the serum-free cell culture medium from the top of the gel. Enough 4 % paraformaldehyde to cover the gel was then added and left at RT for 20 minutes. The FITC-PI staining protocol, as outlined in Chapter 2.2.4, was then followed. In one case, cells were pre-stained with Celltracker™ before being embedded within the gel. Here, following fixation of the cells as described above, no further staining was required. Whatever the case, gels were stored in the dark at 4°C before being taken to the confocal microscope. Immediately prior to analysis, gels were mounted with a drop of 2.5 % 1-4 diazabicyclo-2-2-2-octane (DABCO) solution (see Appendix) and a coverslip.

5.2.3 Development of three-dimensional assays using the 'cell droplet' method

Here, a droplet of collagen solution seeded with cells were placed between two gel layers as illustrated in Fig. 5.2. Firstly, a stock of 1.5 mg/ml collagen solution, containing 30 μg/ml fibronectin was prepared (see section 5.2.1.2). Where specified, larval ES (from batch E – see Table 2.1) was added to the concentration indicated. For specified controls PBS was added in place of ES. Once prepared, 650 μl or 1000 μl of the stock solution was poured into a 35 mm or 58 mm tissue culture dish respectively and left to gel at 37°C in an even, thin, continuous layer.

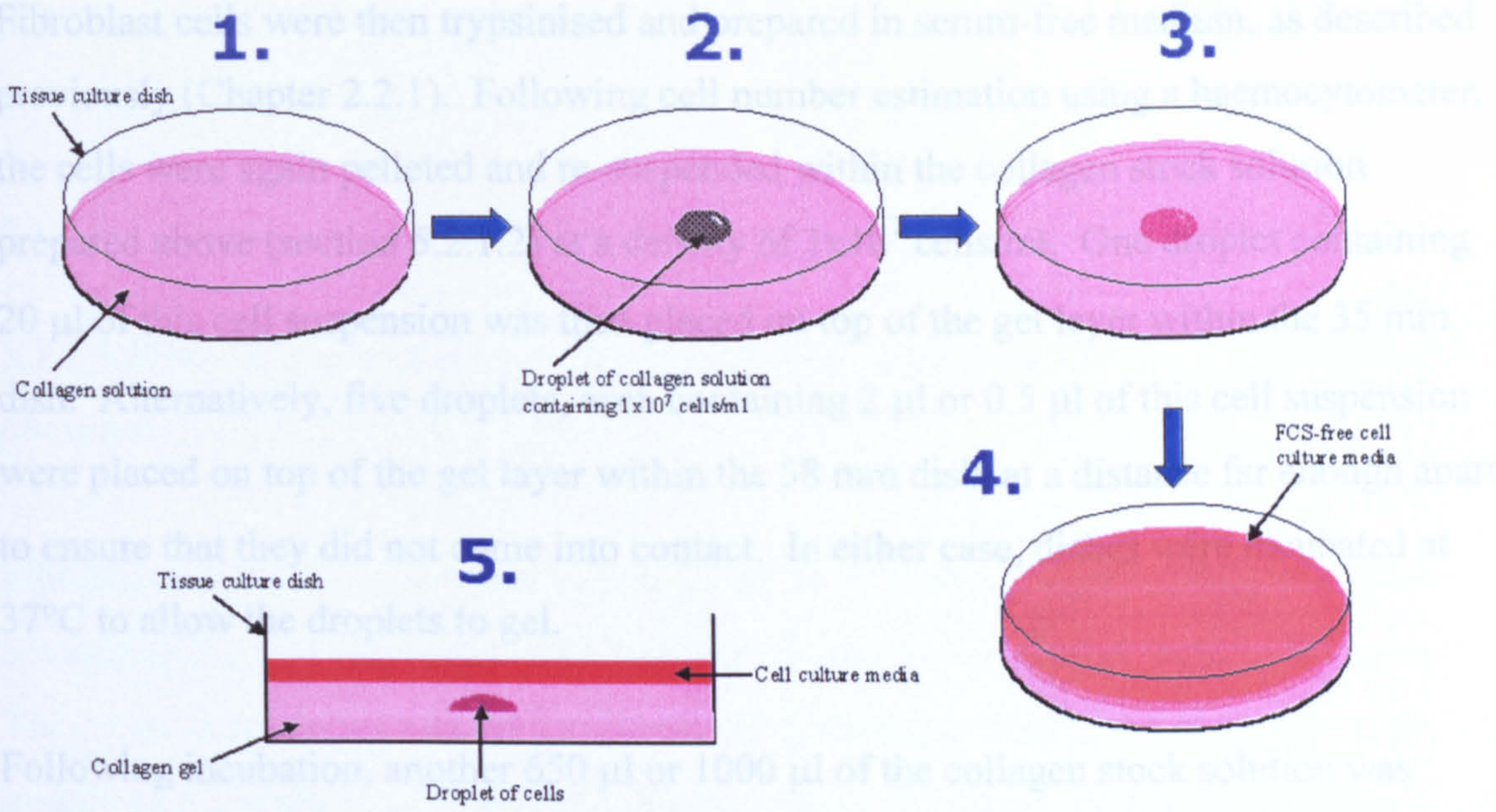

Figure 5.2 Three-dimensional *in vitro* wound assay assembled using the 'cell droplet' method. 1. Collagen solution poured into tissue culture dish and left to gel in a thin, even layer. 2. Droplet of collagen solution containing 1 x 10^7 cells/ml, placed on top of the first gel layer and left to gel. 3. Second collagen layer poured over the top of the cell droplet to cover and left to gel. 4. Cell culture medium then poured on top of the gel. 5. Fully assembled assay shown in cross-section, illustrating how all the cells within the droplet are completely surrounded by collagen gel and therefore must migrate in three dimensions.

Fibroblast cells were then trypsinised and prepared in serum-free medium, as described previously (Chapter 2.2.1). Following cell number estimation using a haemocytometer, the cells were again pelleted and re-suspended within the collagen stock solution prepared above (section 5.2.1.2) at a density of $1x10^7$ cells/ml. One droplet containing 20 µl of this cell suspension was then placed on top of the gel layer within the 35 mm dish. Alternatively, five droplets, each containing 2 µl or 0.5 µl of this cell suspension were placed on top of the gel layer within the 58 mm dish, at a distance far enough apart to ensure that they did not come into contact. In either case, dishes were incubated at 37°C to allow the droplets to gel.

Following incubation, another 650 µl or 1000 µl of the collagen stock solution was poured carefully over the top of the cell droplets located within the 35 mm or 58 mm dish respectively, to completely cover them. Dishes were then incubated at 37°C to allow gelling of the top collagen layers to occur. Finally, serum-free cell culture medium from the same stock used to make the collagen gel, was diluted to 1 x concentration and then added to each dish, until gels were covered. Where ES was present within the gels, ES was also added to the medium, to the same concentration. The assembled assays were then incubated at 37°C in a humidified 5 % CO_2 atmosphere for the time stated. Medium was replaced every 24 hours.

Cells were observed *in situ*, using both phase contrast microscopy and confocal microscopy. For the latter, cells were first fixed with 4 % paraformaldehyde and stained with FITC-phalloidin and PI within their gels, as described in Chapter 2.2.4. Immediately prior to analysis, gels were carefully drained and blotted of excess liquid, before being mounted with Bio-Rad fluorescence mounting medium and a coverslip.

5.3 Results

5.3.1 Development of three-dimensional assays using the cloning cylinder

5.3.1.1 Fibroblast migration from a populated gel in the presence of L-ascorbic acid 2-phosphate

Fibroblast cells were suspended within 1.5 ml or 2 ml of a 1 mg/ml collagen solution, containing 0.2 mM L-ascorbic acid 2-phosphate and in one case 30 μg/ml fibronectin. They were then seeded around the outside of a cloning cylinder placed upright in the middle of a 35 mm dish. Following gelation of the collagen solution, the cloning cylinder was removed, leaving a hole in the middle of the gel. The cells were then observed migrating out of the gel and across the exposed surface in the centre of the dish, using phase contrast microscopy.

For each gel assembled, the inside edge of the gel could clearly be seen immediately after the removal of the cloning cylinder, taken as 0 hours (Fig. 5.3), at both low and high magnifications. Also, there were few or no cells present upon the surface of the dish that had been exposed by the removal of the cylinder. Those cells that had gained access to the surface, were positioned close to the gel edge. It was therefore clear that the cloning cylinder represented a successful barrier to the gel and the cells contained within the gel.

The dish containing 2 ml of gel was monitored over a period of 15 days, until it was discarded. During that time, it was noted that cells had migrated from the gel, across the dish surface. The progress that the migrating cell edge had made after 48 hours, 7 days and 15 days incubation is shown in Fig. 5.4a. Here it was apparent that the migrating cells were aligning themselves with each other as they began to form a monolayer, appearing more tightly organised at the gel boundary by 7 days incubation, than at the earlier time-point of 48 hours. Although cells had migrated further by 15 days incubation, forming a monolayer covering all of the exposed surface (Fig. 5.4b), the density of cell coverage did not appear to be higher, nor were there any indications that multi-layering of cells was occurring.

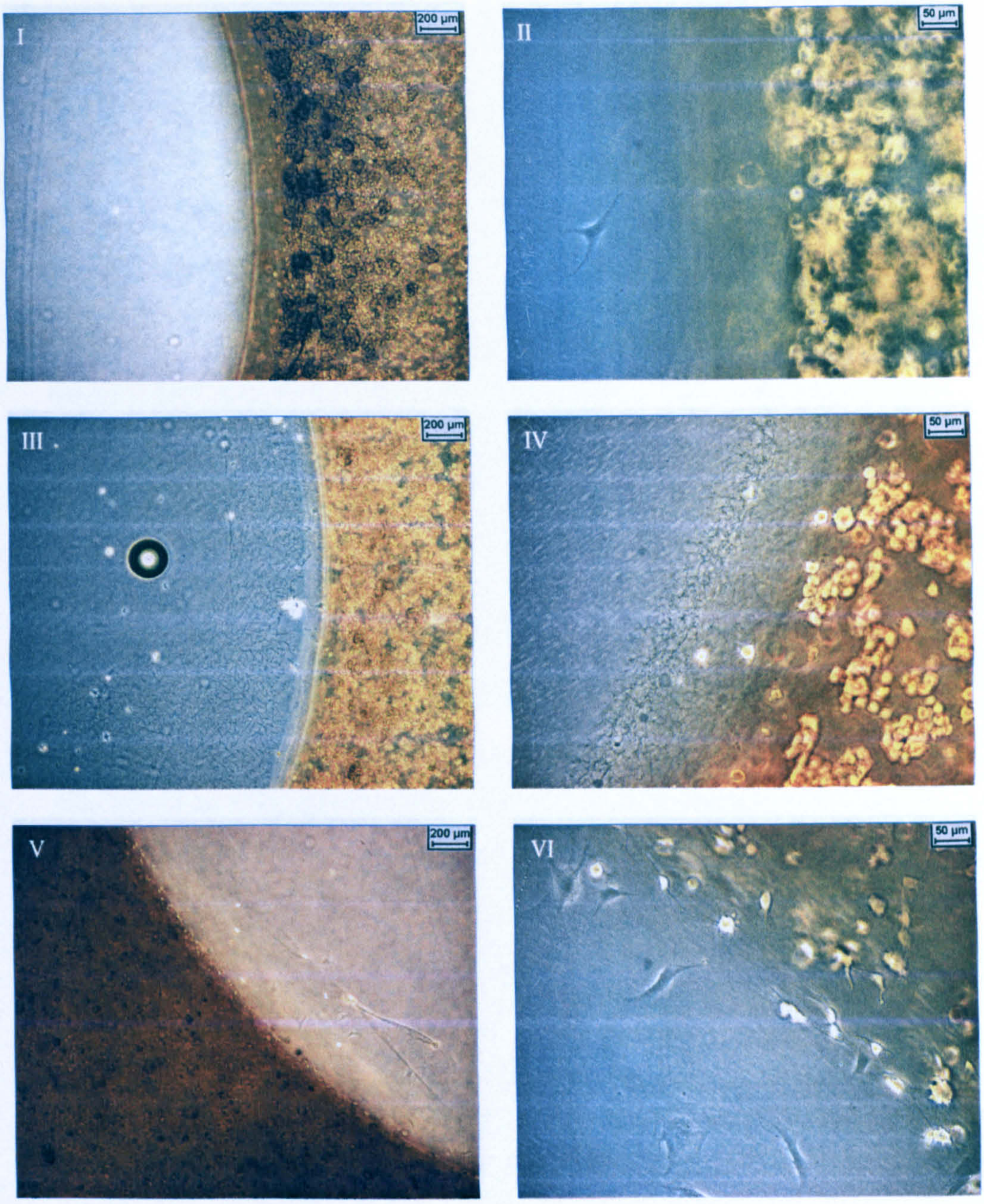

Figure 5.3 Boundary between fibroblast-populated gel and exposed dish surface immediately following removal of cloning cylinder (taken as 0 hours incubation). Sample containing: 2 ml gel (I, II); 1.5 ml gel (III, IV); 2 ml gel including 30 µg/ml fibronectin (V, VI).

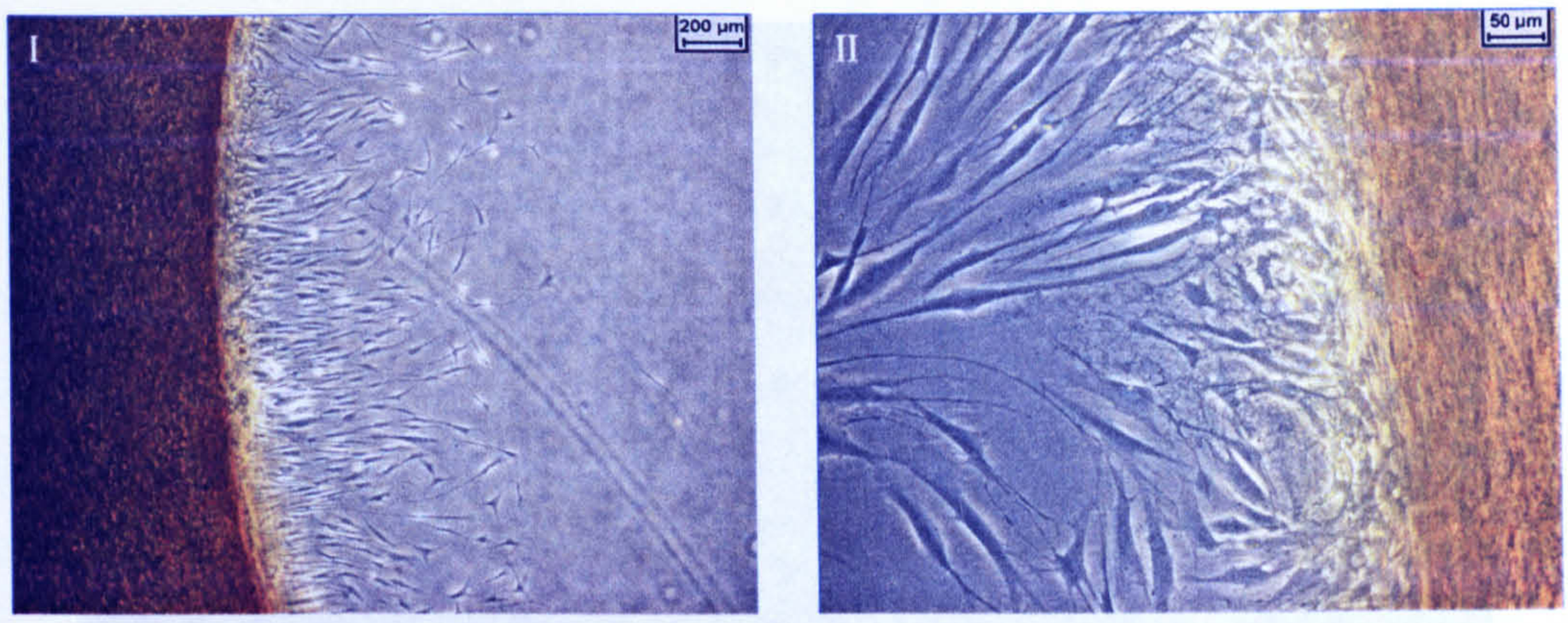

Figure 5.4a Boundary between 2 ml of fibroblast-populated gel and exposed dish surface following 48 hours incubation (I, II), 7 days incubation (III, IV) or 15 days incubation (V, VI) after removal of cloning cylinder.

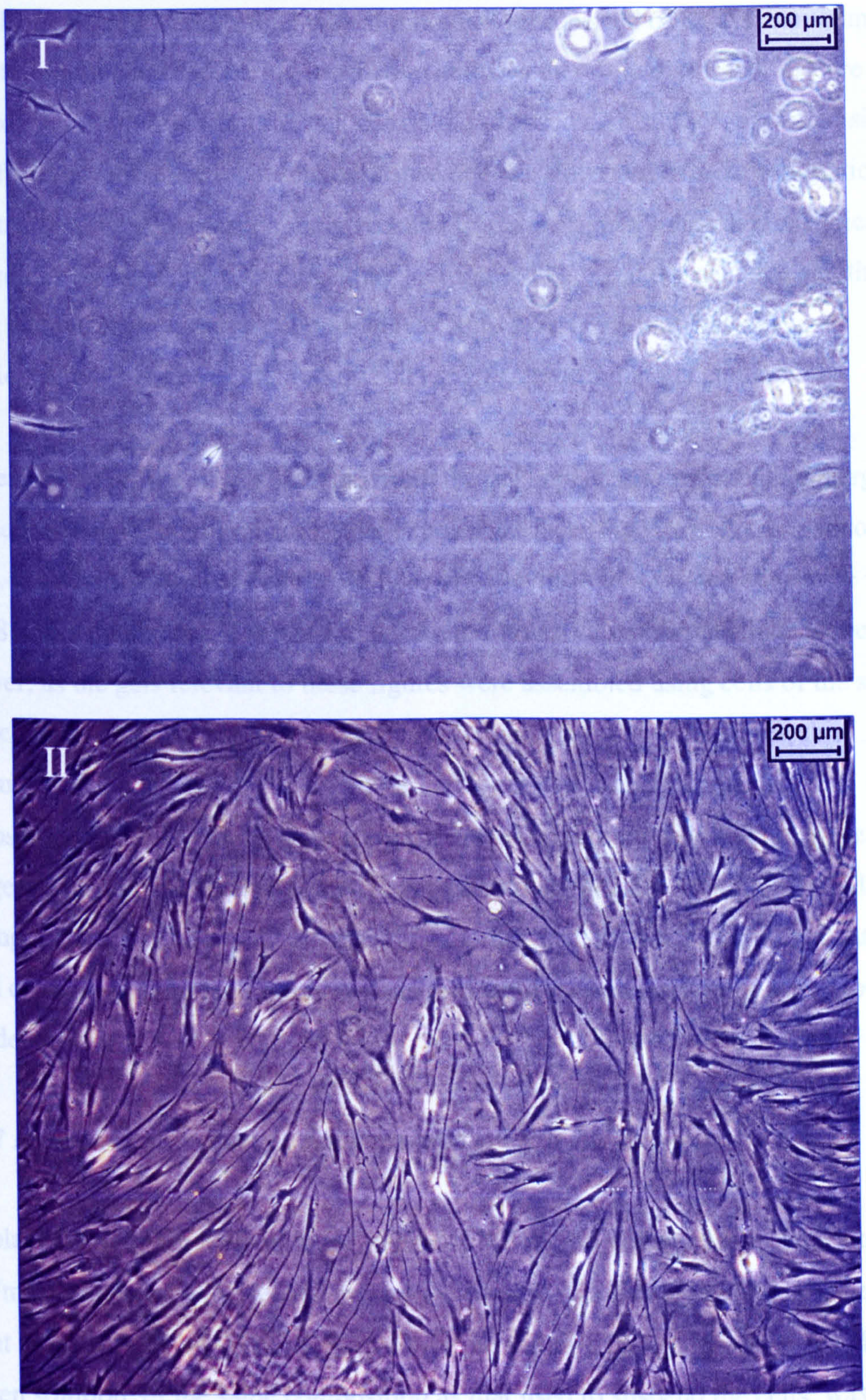

Figure 5.4b Centre of exposed surface of dish containing 2 ml fibroblast-populated gel. Progress of cells from gel towards centre of dish following 7 days incubation (I) and 15 days incubation (II) after removal of cloning cylinder.

The dish containing 1.5 ml of gel was monitored over a period of 8 days, sometime after which it became detached during incubation and was therefore discarded. Before this occurred, cell migration from the gel, across the exposed dish surface, appeared similar to that from the gel of 2 ml volume described above. However, at 8 days migration, it was noted that the gel had apparently receded from its original boundary, as indicated by the relatively large, irregular gaps that had formed between the gel edge and the trailing edge of the migrating cell monolayer (Fig. 5.5). This may have been an indication of collagen re-modelling by cells *in situ*, resulting in gel contraction.

The presence of 30 μg/ml fibronectin within the gel appeared to exert only a marginal influence upon cell migration across the exposed surface (Fig. 5.6). A comparison of Figs. 5.4a and 5.6, revealed that the number of cells that had migrated across the surface after 48 hours incubation, appeared to be slightly fewer when fibronectin was present. However, as the gels relevant to these figures were assembled using cells of the same passage number, but from separate trypsinisation and counting procedures, this difference may have been due to slight variability in cell number concentration. It was also observed that the cells migrating within the gel containing fibronectin appeared to be larger. This may be explained by the apparent lower density of migrating cells, reducing contact inhibition of cell spreading. Unfortunately, after 5 days incubation, the gel containing fibronectin became detached from the surface and was therefore discarded.

5.3.1.2 Fibroblast migration from a populated gel to a cell-free gel

Fibroblast cells suspended within a 1 mg/ml or 1.5 mg/ml collagen solution containing 30 μg/ml fibronectin, were seeded around the outside of a cloning cylinder placed upright in the middle of a 35 mm dish. Once the solution had gelled, a small volume of collagen solution, of the same composition as that used to suspend the cells, was placed into the centre of the cylinder until it had reached a similar height to that of the surrounding gel. Following partial gelation of the solution, the cloning cylinder was removed and the cell-populated and cell-free gels allowed to converge and gelling to complete. Cells were observed at the cell-populated/cell-free boundary using both phase contrast and confocal microscopy.

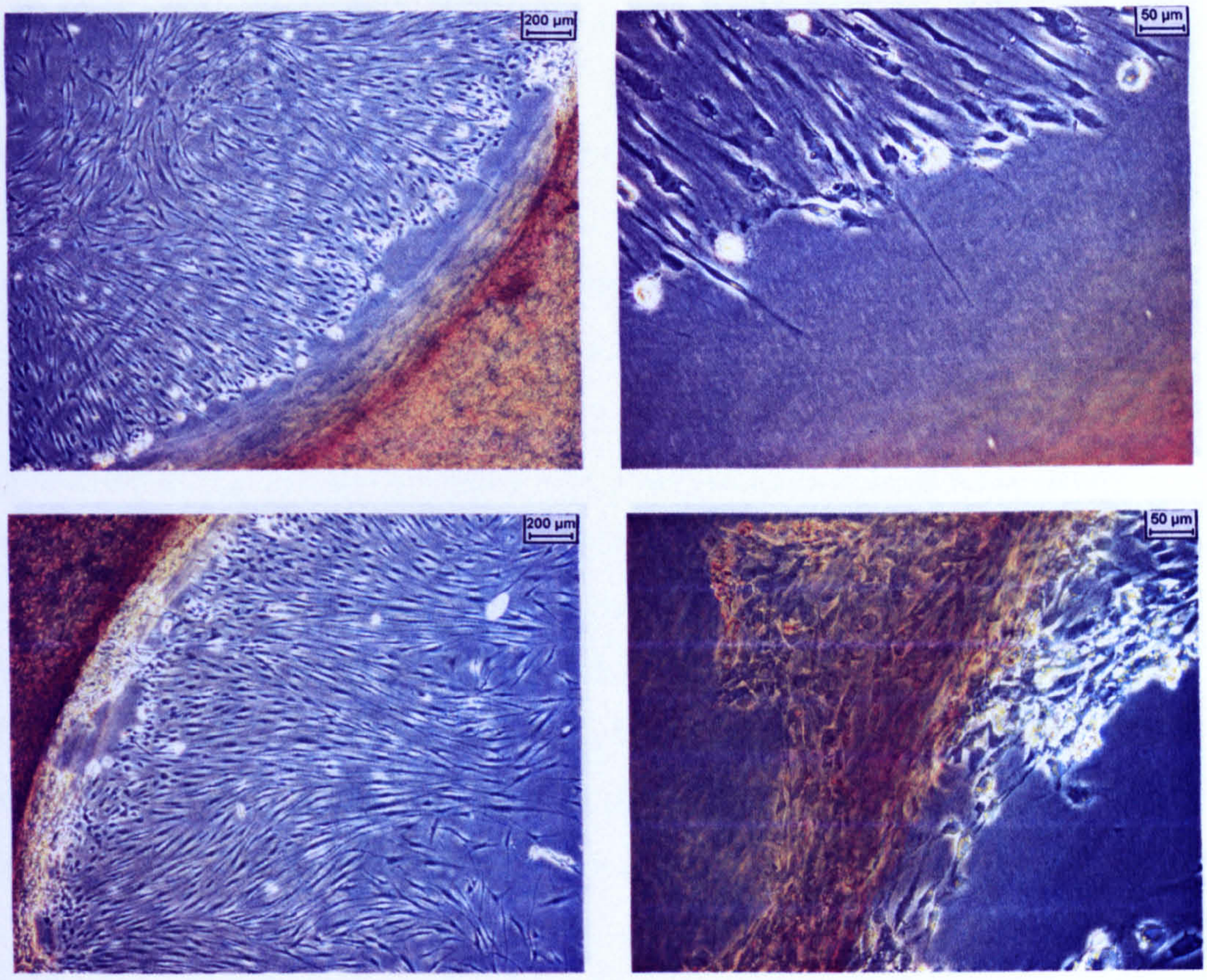

Figure 5.5 Boundary between fibroblast-populated gel and exposed dish surface following 8 days incubation after removal of cloning cylinder. Images demonstrate that the gel had receded from its original boundary over the incubation period. This is indicated by the relatively large, irregular gaps that are visible between the gel edge and the trailing edge of the migrating cell monolayer.

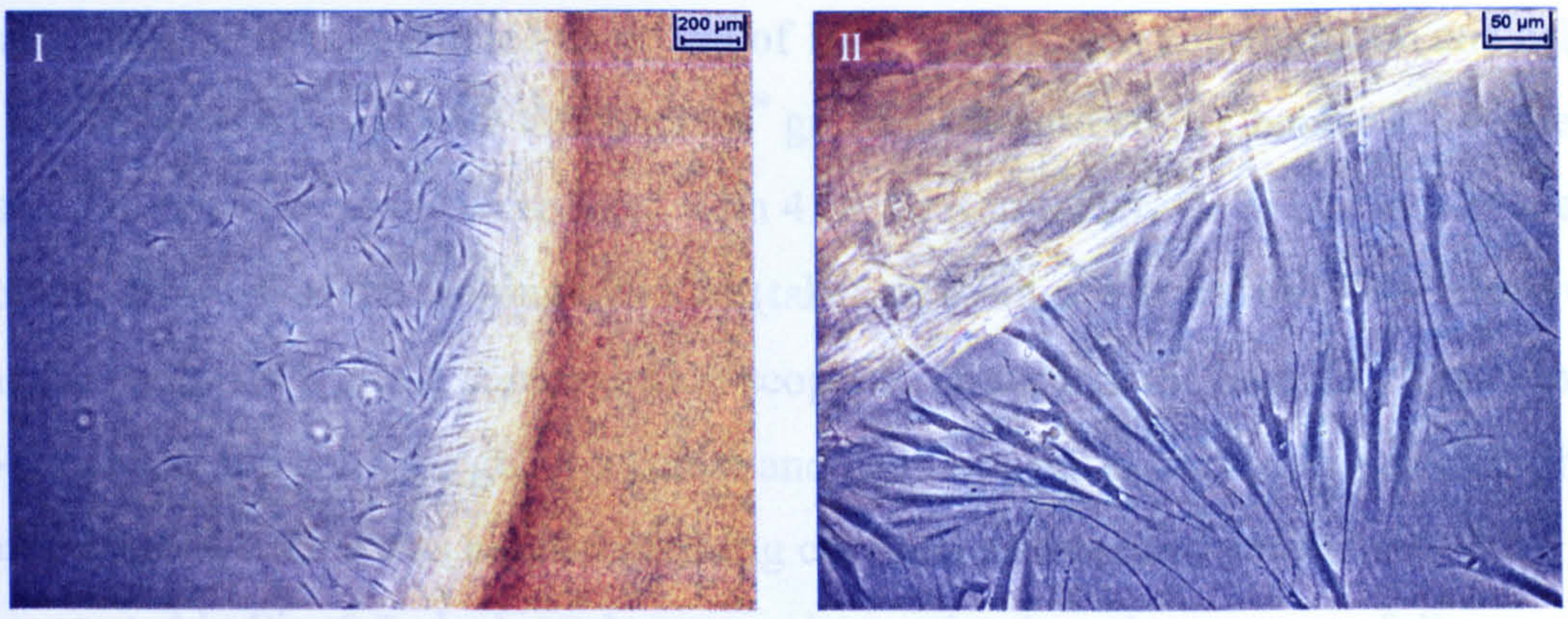

Figure 5.6 Boundary between 2 ml fibroblast-populated gel, containing 30 µg/ml fibronectin, and exposed dish surface following 48 hours (I, II) or 5 days incubation (III, IV) after removal of cloning cylinder.

Initially, assays were assembled using gel of 1 mg/ml collagen concentration and cells that had been pre-stained with Celltracker™ green, as described in Chapter 2.2.4. Here, cells within one such assay were fixed with 4 % paraformaldehyde *in situ* immediately following removal of the cloning cylinder (taken as 0 hours incubation). The assay was then observed, using phase contrast microscopy, to check that the boundary between cell-populated and cell-free gels was clear and had not been disrupted by removal of the cloning cylinder. This was confirmed using confocal microscopy where, as demonstrated in Fig. 5.7, the boundary was observed to have been successfully maintained throughout the complete depth of the gel. However, it was also noted that there appeared to be more cells at the bottom than at the top of the populated gel, indicating that sinking of cells had occurred. In general, once gels containing 1 mg/ml collagen had set, they remained quite weak, being easily dislodged. They were also easily deformed by the lens of the confocal microscope during focusing. As such, images had to be taken with extreme care in order to ensure their reliability.

A similar assay was fixed following 24 hours incubation, in order to assess cell migration across the gel boundaries. Confocal microscopy revealed that cells had indeed migrated out of the populated gel (Fig. 5.8). However, as shown in the series of images taken vertically through the gel boundaries, cells had only migrated at the bottom of the gel (Fig. 5.9). It is possible that the cells had migrated on the tissue culture plastic surface underneath the cell-free gel section. This pattern of migration might have occurred because the cell-free gel may have lifted off the surface of the dish upon removal of the cloning cylinder. This in turn would have allowed cells from the populated gel to undermine the cell-free gel and therefore migrate in two dimensions along the dish surface. Considering how easily gels of 1 mg/ml collagen concentration can be dislodged, as noted above, this explanation appears likely.

In order to overcome the difficulties described above, further assays were assembled using gel of a higher collagen concentration (1.5 mg/ml). In addition, cells were stained with FITC-phalloidin and PI following fixation to allow a more detailed observation of cellular morphology. In one such assay, the cells were fixed and stained *in situ* immediately following removal of the cloning cylinder in order to assess the clarity of the cell-populated/cell-free boundary. As shown in Fig. 5.10, the boundary could clearly be discerned, indicating that it had been successfully maintained. Other assays

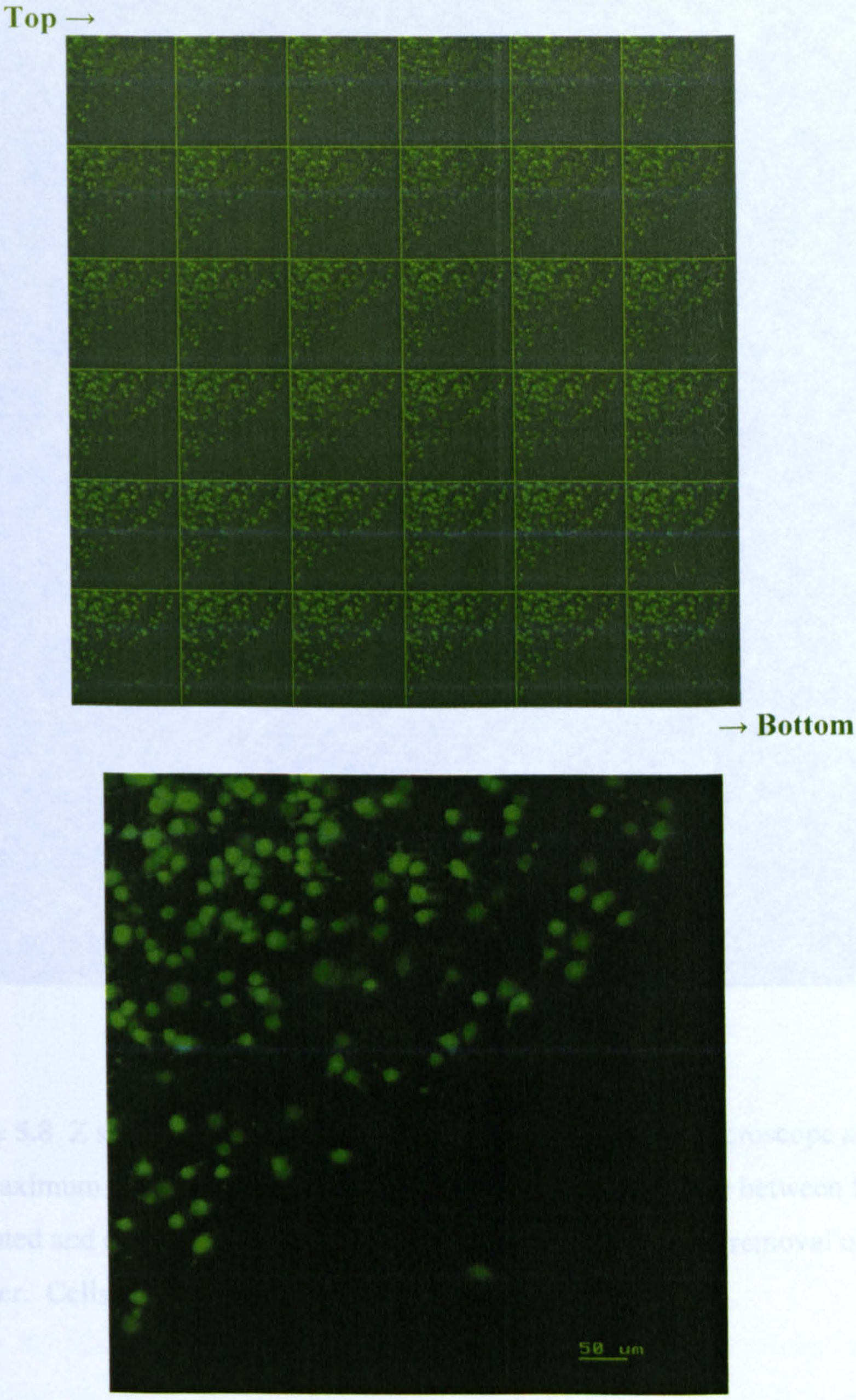

Figure 5.7 Z series of optical sections, taken using confocal microscope and displayed in a gallery, from left to right, moving from top to bottom (*above*) and as a maximum intensity projection of all the sections (*below*). These show the boundary between fibroblast-populated and cell-free gels through ~50 μm depth. Cells, stained with Celltracker™ green, fixed immediately following removal of cloning cylinder (0 hours incubation).

Figure 5.8 Z series of optical sections, taken using confocal microscope and displayed as a maximum intensity projection of all the sections. Boundary between fibroblast-populated and cell-free gels following 24 hours incubation after removal of cloning cylinder. Cells stained with Celltracker™ green.

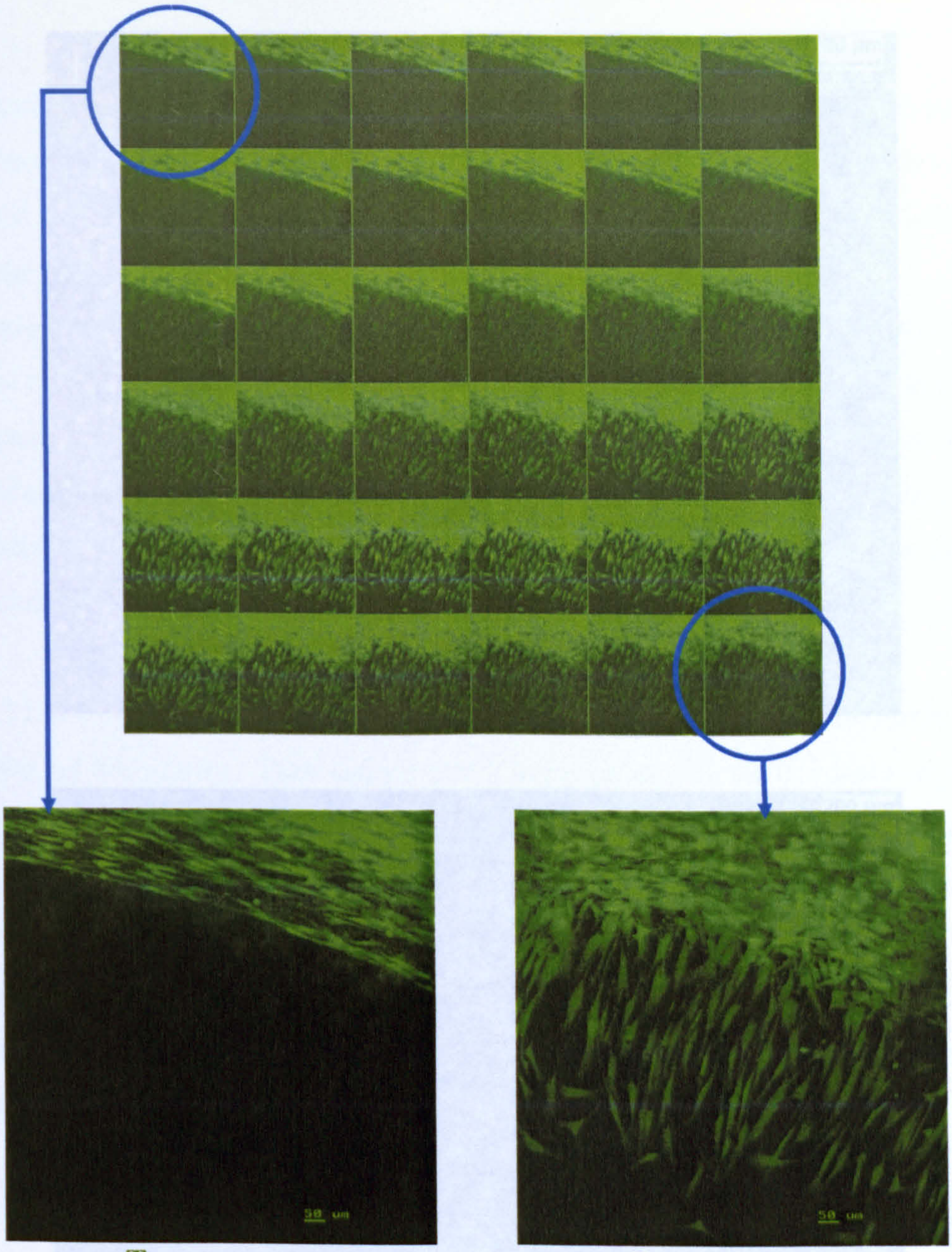

Top

Bottom

Figure 5.9 Z series of optical sections, taken using confocal microscope and displayed in a gallery, from left to right, moving from top to bottom. Boundary between fibroblast-populated and cell-free gels following 24 hours incubation after removal of the cloning cylinder. Sections taken from top and bottom of series are highlighted and demonstrate that cell migration was occurring only at the bottom of the gel. Cells stained with Celltracker™ green.

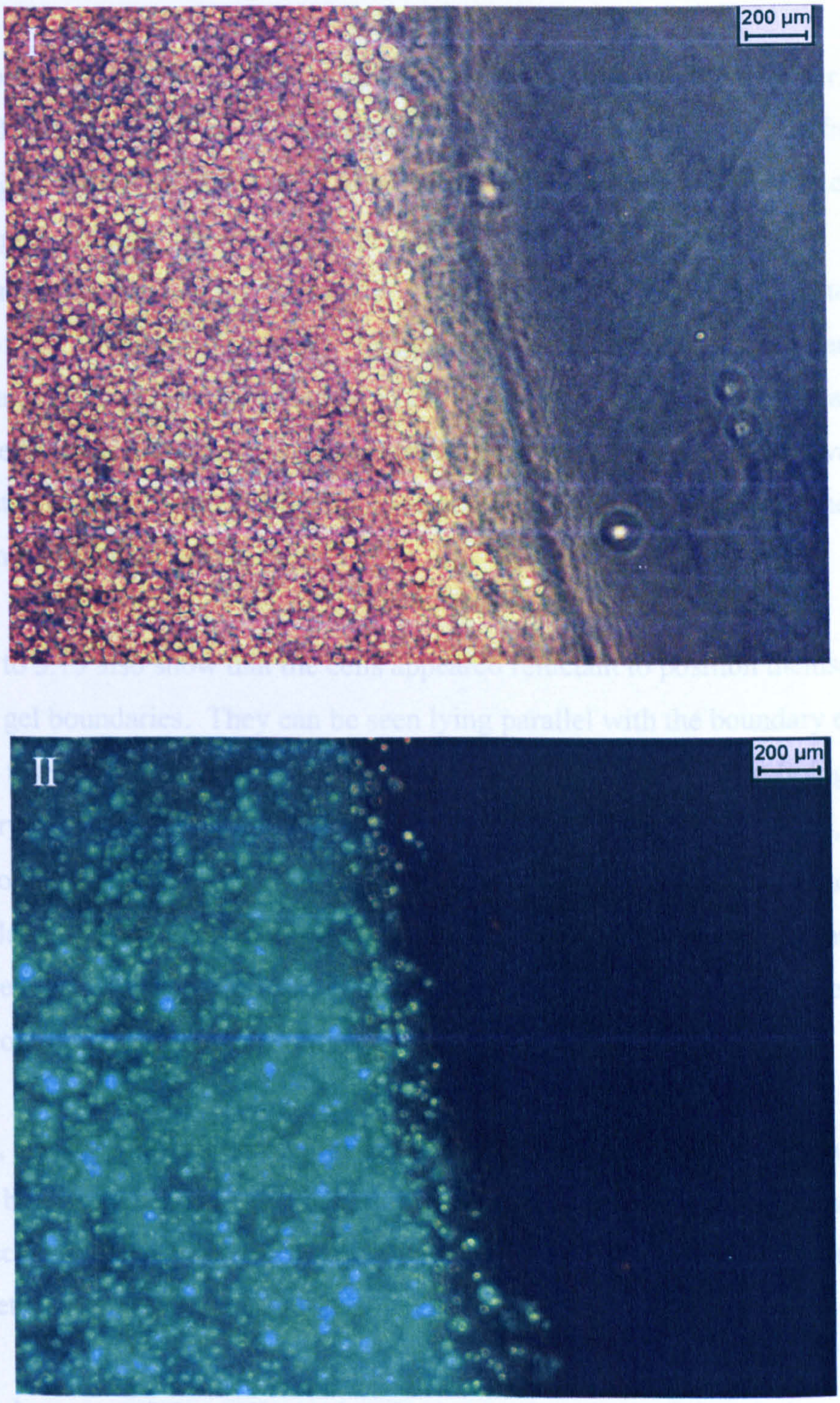

Figure 5.10 Boundary between fibroblast-populated and cell-free gels, immediately after removal of the cloning cylinder. A demarcation between the two can clearly be seen when imaged using phase contrast microscopy (I) or fluorescence microscopy through a standard fluorescein filter set (II).

were incubated for either 48 hours or 5 days following removal of the cylinder, before being fixed and stained, so as to establish whether cells were able to migrate from the populated gel. As shown in Fig. 5.11, there appeared to be little migration of cells across the gel boundary after 48 hours incubation. This image was typical of observations made at this time. Even after 5 days incubation, there appeared to be no evidence of cell migration (Fig. 5.12). In addition, one image suggests that part of the cell-populated gel had become detached from the boundary edge, as it shows an isolated group of cells present within the cell-free gel which did not appear to have invaded from the populated gel (Fig. 5.13). This may have occurred during incubation of the gel, replenishment of media or fixing.

Figs. 5.11 to 5.13 also show that the cells appeared reluctant to position themselves across the gel boundaries. They can be seen lying parallel with the boundary edge, projecting few, if any, extensions into the cell-free gel. Comparing morphologies of cells at very high magnification yielded similar conclusions (Fig. 5.14). Here, the images show that cells positioned within the populated gel, away from its edge, projected lamellipodia and fine, dendritic-like extensions in all directions. Those at the boundary edge however, remained parallel with it and projected very few extensions in the direction of the cell-free gel.

As before, problems in assay assembly remained, with a number of assays having to be discarded before analysis. Unfortunately, the gel assembly remained fragile and, on several occasions during removal of the cloning cylinder, the cell-free gel section became detached from the dish surface.

5.3.2 Development of three-dimensional assays using the 'cell droplet' method

Here, assays were assembled throughout, using gels made from a 1.5 mg/ml collagen solution, containing 30 μg/ml fibronectin. Fibroblast cells, suspended within a droplet of such a solution, were placed on top of a layer of gel. Following the droplet's gelation another layer of gel was then added to cover it. Cell migration out of the droplet and into the surrounding matrix was observed using both phase contrast and confocal microscopy.

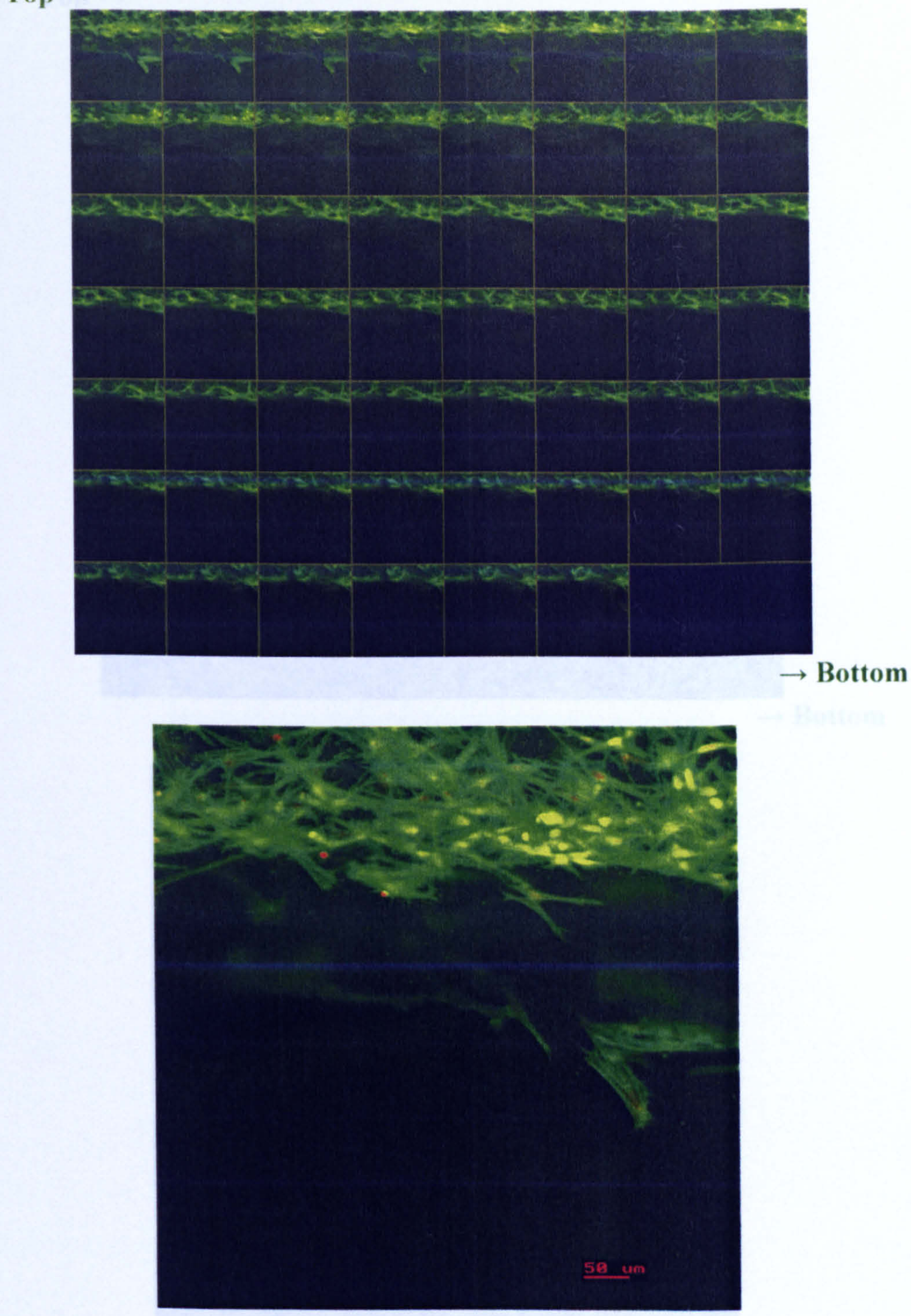

Figure 5.11 Z series of optical sections, taken using confocal microscope and displayed in a gallery, from left to right, moving from top to bottom (*above*) and as a maximum intensity projection of all the sections (*below*). This series shows the boundary between fibroblast-populated and cell-free gels through ~166 μm depth. Cells fixed following 48 hours incubation after removal of cloning cylinder and stained with FITC-phalloidin and propidium iodide.

Top →

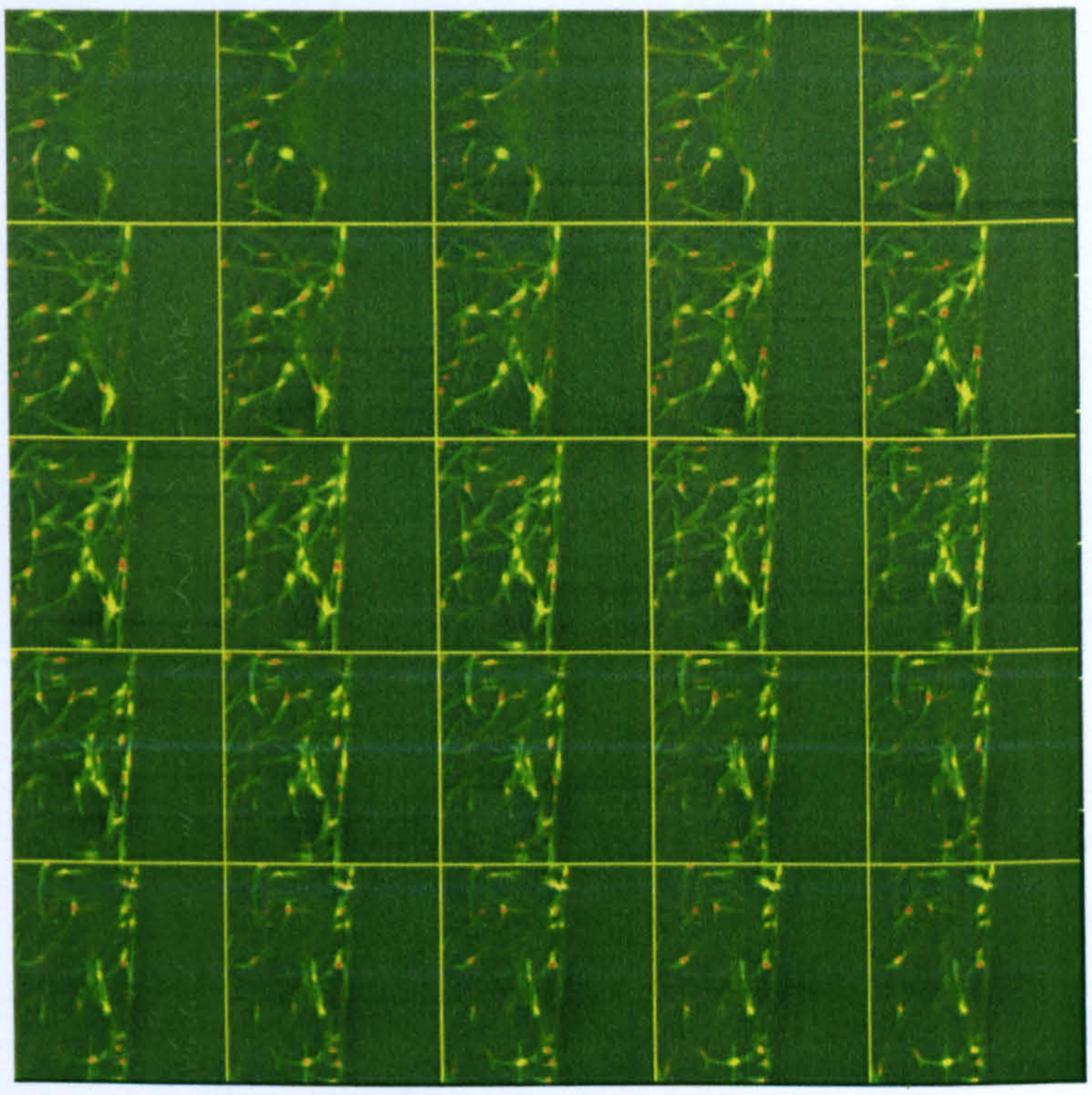

→ Bottom

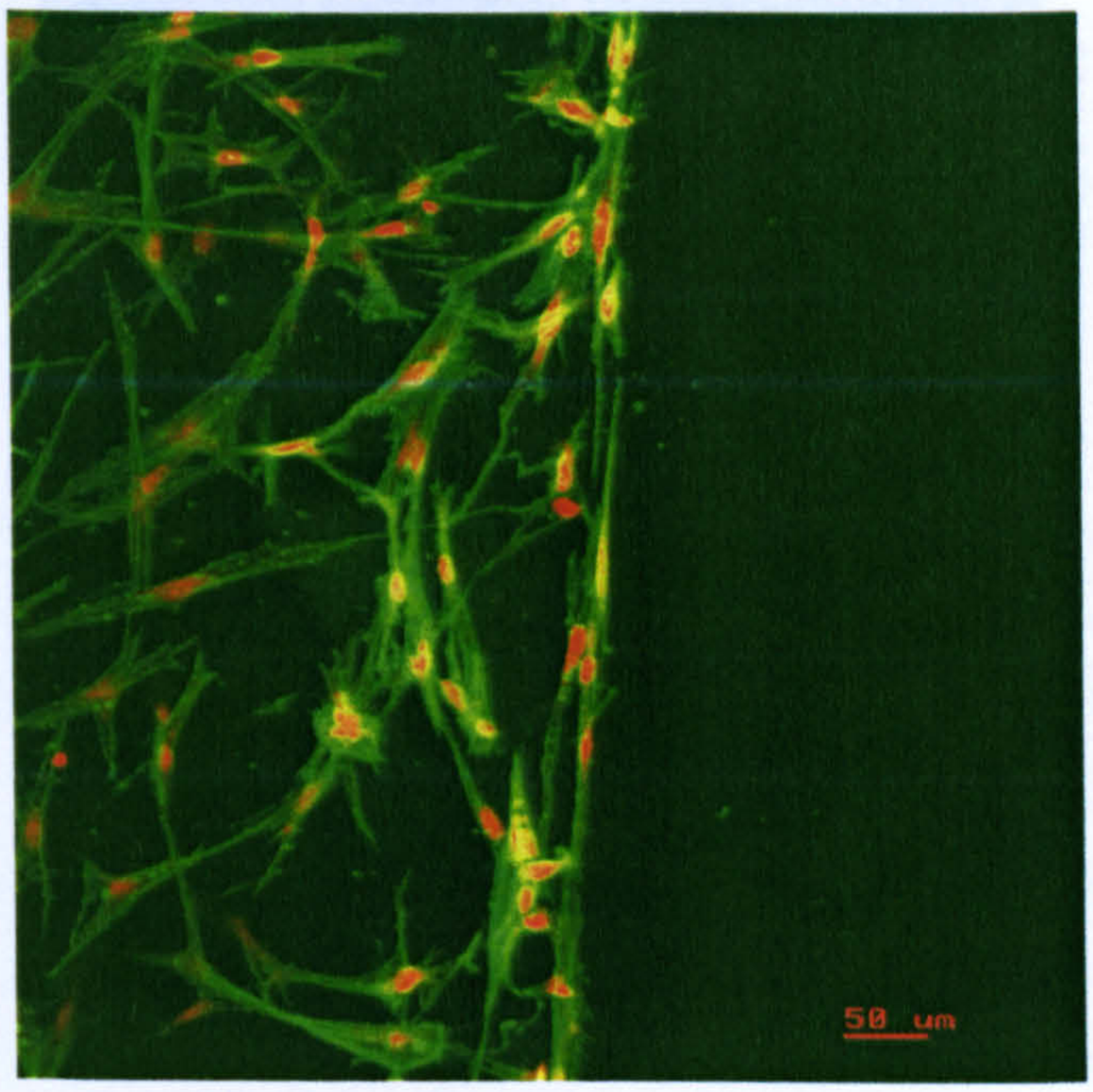

Figure 5.12 Z series of optical sections, taken using confocal microscope and displayed in a gallery, from left to right, moving from top to bottom (*above*) and as a maximum intensity projection of all the sections (*below*). This series shows the boundary between fibroblast-populated and cell-free gels. Cells fixed following 5 days incubation from removal of the cloning cylinder and stained with FITC-phalloidin and propidium iodide.

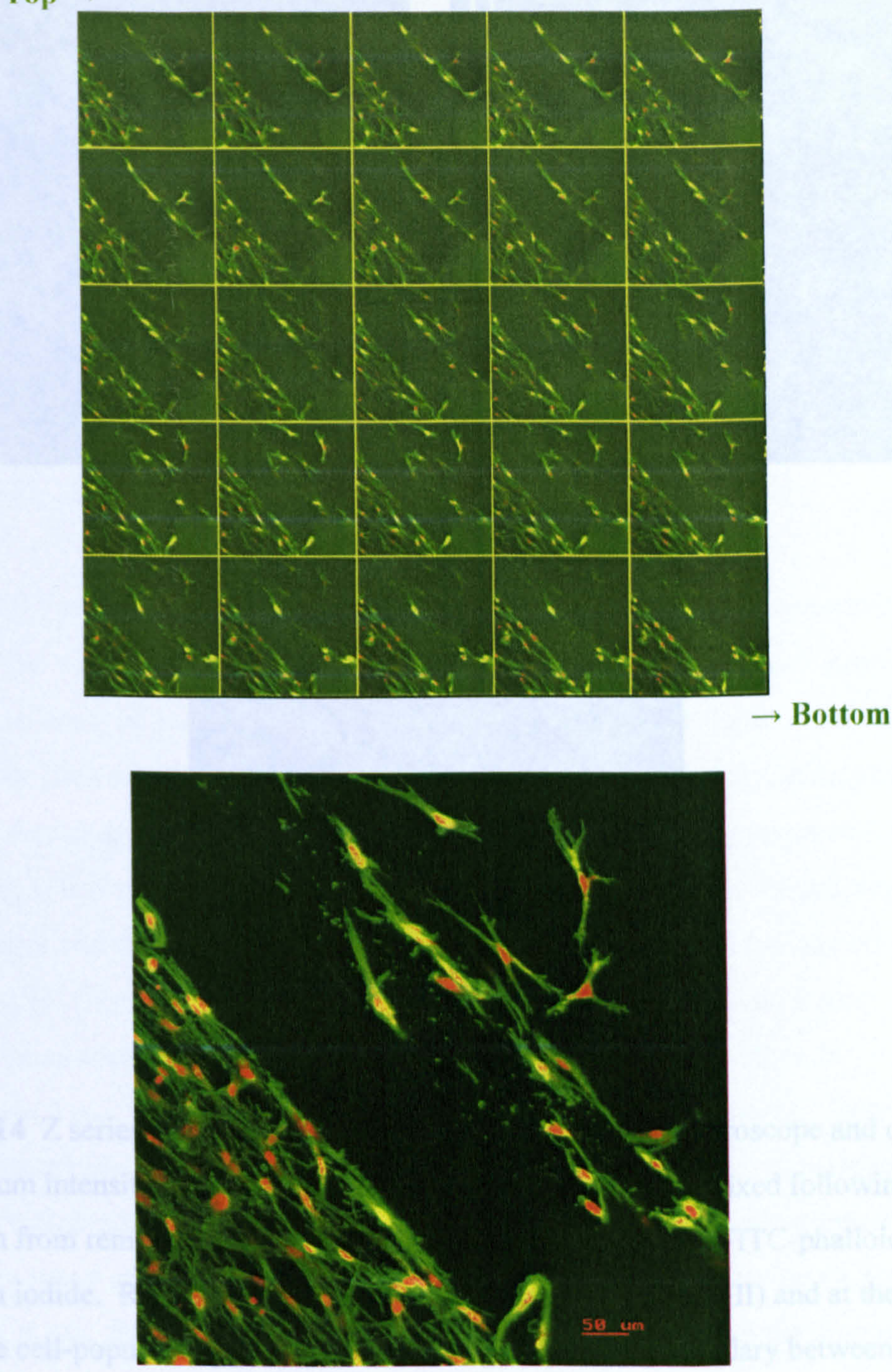

Figure 5.13 Z series of optical sections, taken using confocal microscope and displayed in a gallery, from left to right, moving from top to bottom (*above*) and as a maximum intensity projection of all the sections (*below*). These show the boundary between fibroblast-populated and cell-free gels through ~75 μm depth. Part of the cell-populated gel appears to have become detached from the boundary edge. Cells fixed following 5 days incubation from removal of the cloning cylinder and stained with FITC-phalloidin and propidium iodide.

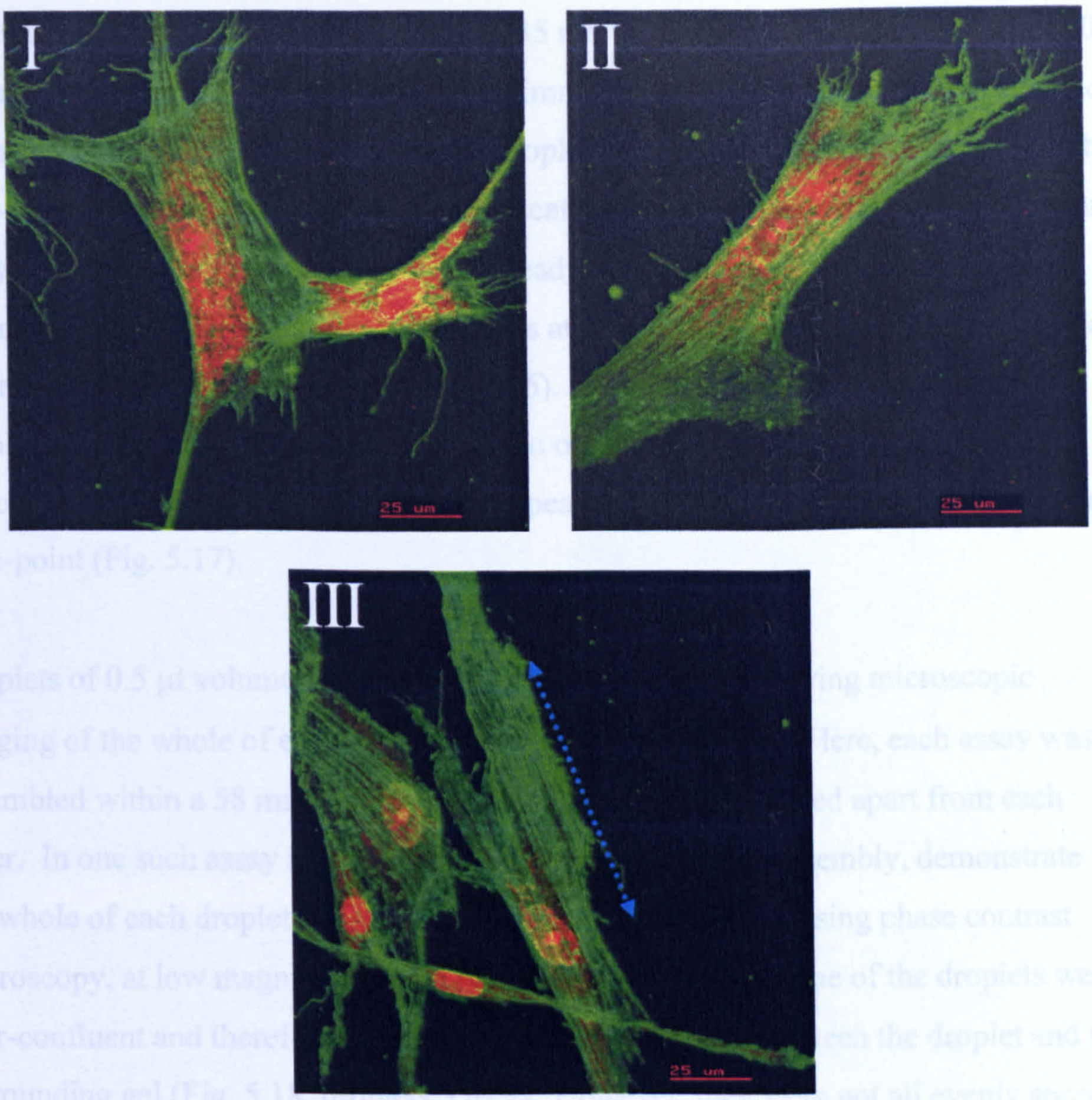

Figure 5.14 Z series of optical sections, taken using confocal microscope and displayed as maximum intensity projections of all the sections. Fibroblasts fixed following 5 days incubation from removal of the cloning cylinder and stained with FITC-phalloidin and propidium iodide. Representative images of cells in the middle (I, II) and at the edge (III) of the cell-populated gel. Blue, dotted arrow represents boundary between cell-populated gel and cell-free gel.

At first, the assay was assembled within a 35 mm dish and included one droplet of 20 µl volume. As shown, at 0 hours incubation, immediately after the assay was assembled, a boundary defined by cells within the gel droplet could clearly be seen (Fig. 5.15). The cells were confluent and none were found scattered around the outside of the boundary. They also appeared viable as they were already beginning to project dendritic-like extensions. After 48 hours incubation, cells at the droplet's edge were observed to have extended into the surrounding gel (Fig. 5.16). Some had migrated away from the droplet completely. Cell migration was also observed following 5 days incubation, although the distances travelled by cells appeared similar to those observed at the earlier time-point (Fig. 5.17).

Droplets of 0.5 µl volume were then used, with the aim of allowing microscopic imaging of the whole of each droplet's circumference at once. Here, each assay was assembled within a 58 mm dish and included five droplets, placed apart from each other. In one such assay images, taken immediately after its assembly, demonstrate that the whole of each droplet could be viewed in one image when using phase contrast microscopy, at low magnifications (Fig. 5.18). Cells within some of the droplets were near-confluent and therefore provided for a clear boundary between the droplet and the surrounding gel (Fig. 5.18, droplets 3 to 5). However, they were not all evenly spread, with some areas containing higher densities of cells than others. In other droplets (Fig. 5.18, droplets 1 to 2), very few cells were present and appeared scattered. Here no distinct droplet boundaries could be discerned. These problems were thought to be associated with practical difficulties in accurately pipetting such small volumes of solution. In many cases the solution gelled within the pipette. Following 48 hours incubation, it was observed that cells had successfully migrated from the droplets in both horizontal and vertical orientations (Fig, 5.18 to 5.20), indicating the potential of the 'cell droplet' method.

The assay was then repeated in an attempt to improve the pipetting of the droplets. In this case three assays were assembled, one of which served as a control (no ES), while the remainder contained either 1 µg/ml ES or 10 µg/ml ES throughout the media, gel and droplets present. Unfortunately, it proved even more difficult to pipette each droplet successfully. In most cases, a droplet failed to release from the pipette upon the

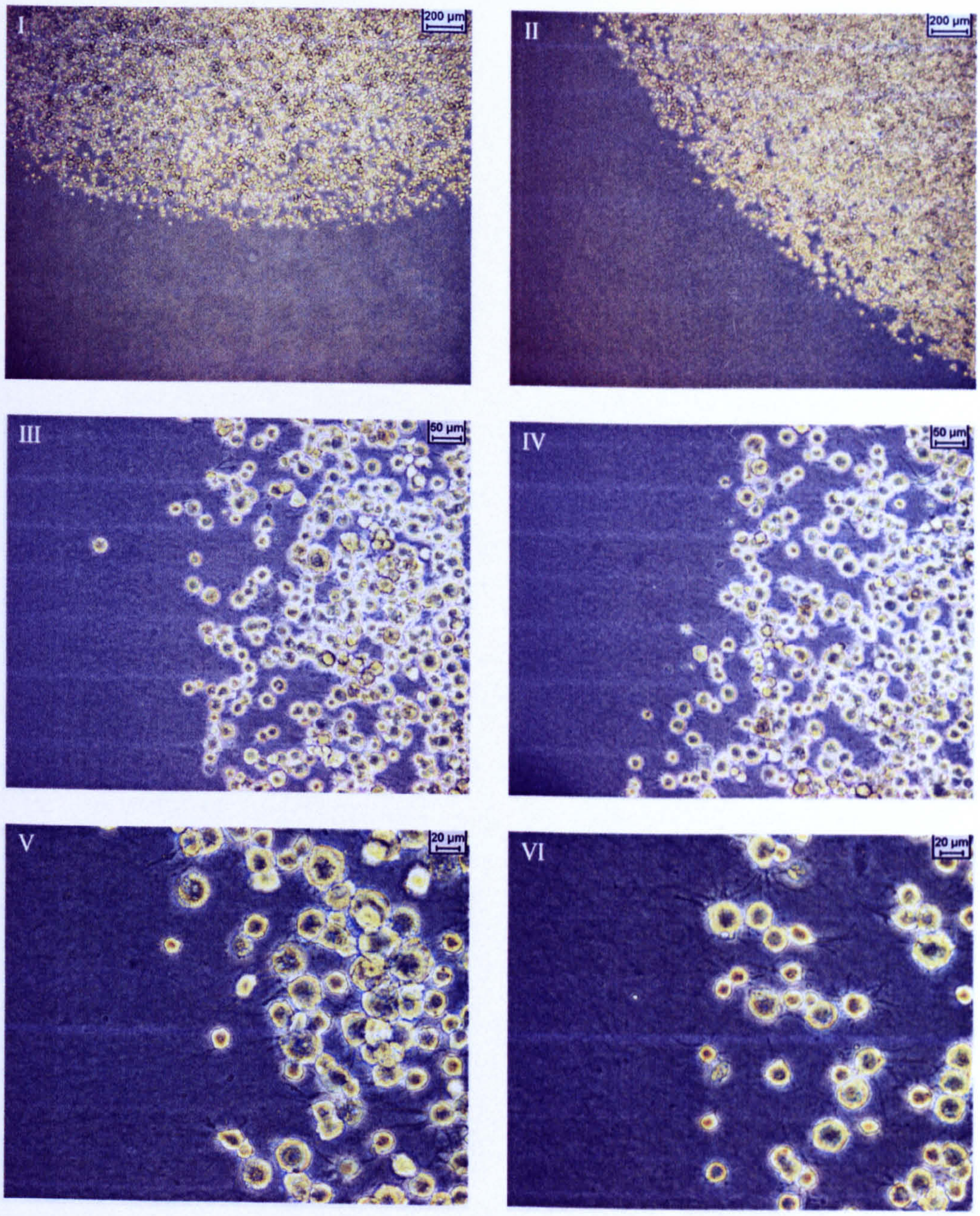

Figure 5.15 Edge of a 20 µl fibroblast-seeded gel droplet embedded within a cell-free gel. Throughout, gel contained 1.5 mg/ml collagen and 30 µg/ml fibronectin. Phase contrast images taken immediately after assay assembly (0 hours incubation). Cells appear confluent and a clear cell boundary can be seen (I - IV). When observed at high magnification (V - VI), cells are shown to have already started developing dendritic-like extensions.

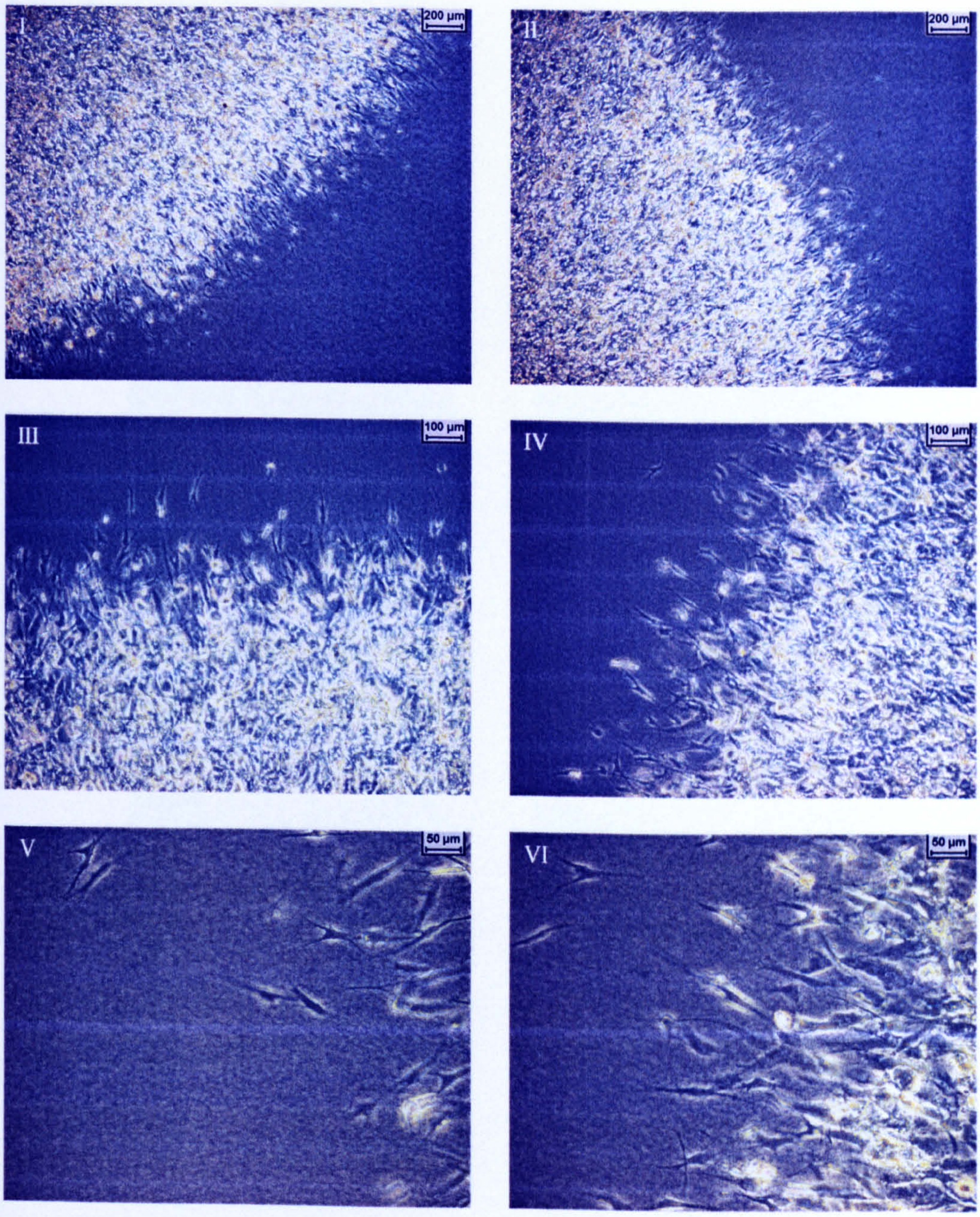

Figure 5.16 Edge of a 20 µl fibroblast-seeded gel droplet embedded within a cell-free gel. Throughout, gel contained 1.5 mg/ml collagen and 30 µg/ml fibronectin. Phase contrast images taken after 48 hours incubation of assembled assay. Cells at the periphery of the droplet are shown extending into the surrounding gel (I – II). Cells have also migrated away from the droplet (III – VI).

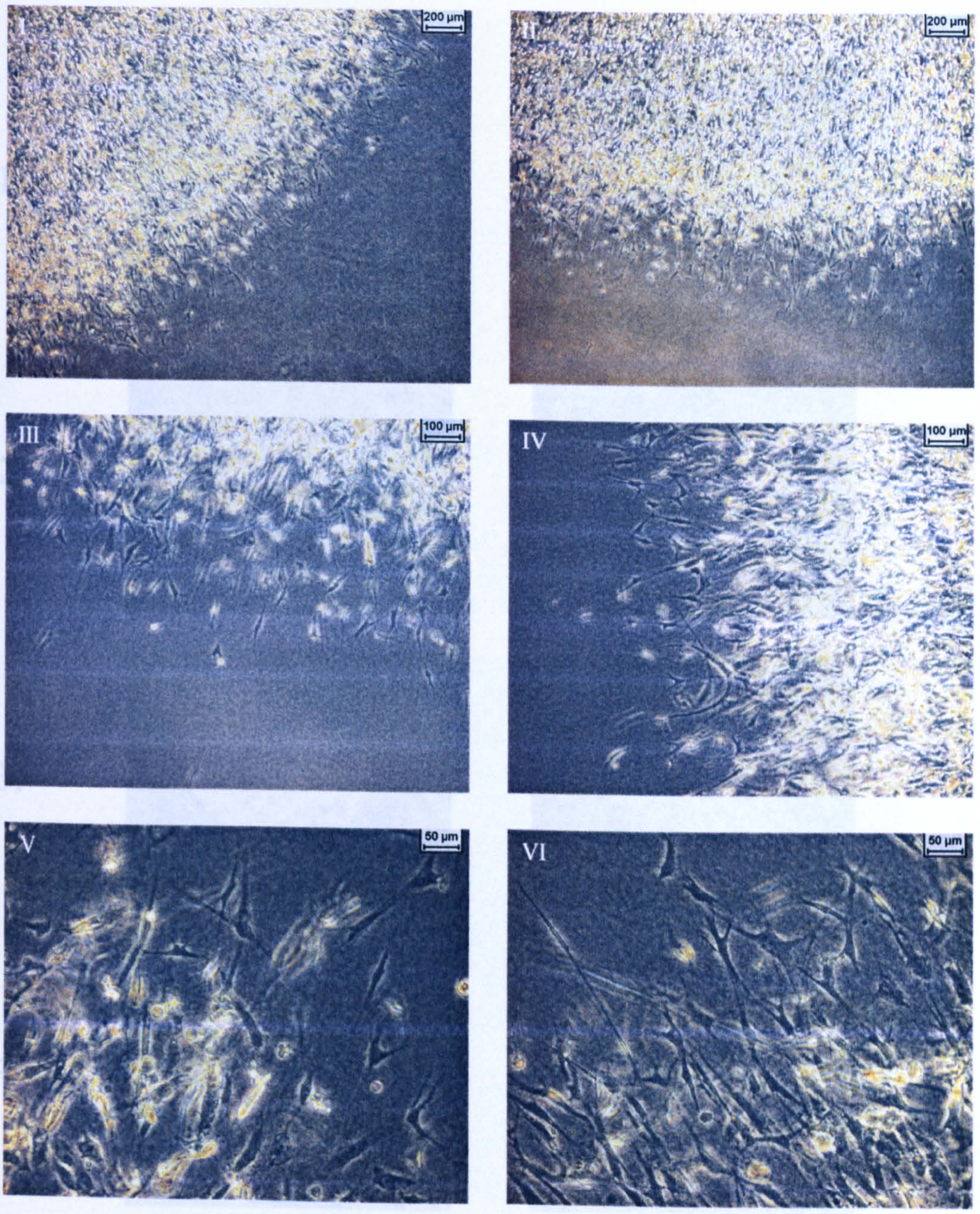

Figure 5.17 Edge of a 20 µl fibroblast-seeded gel droplet embedded within a cell-free gel. Throughout, gel contained 1.5 mg/ml collagen and 30 µg/ml fibronectin. Phase contrast images taken after 5 days incubation of assembled assay. Cells at the periphery of the droplet are shown migrating into the surrounding gel.

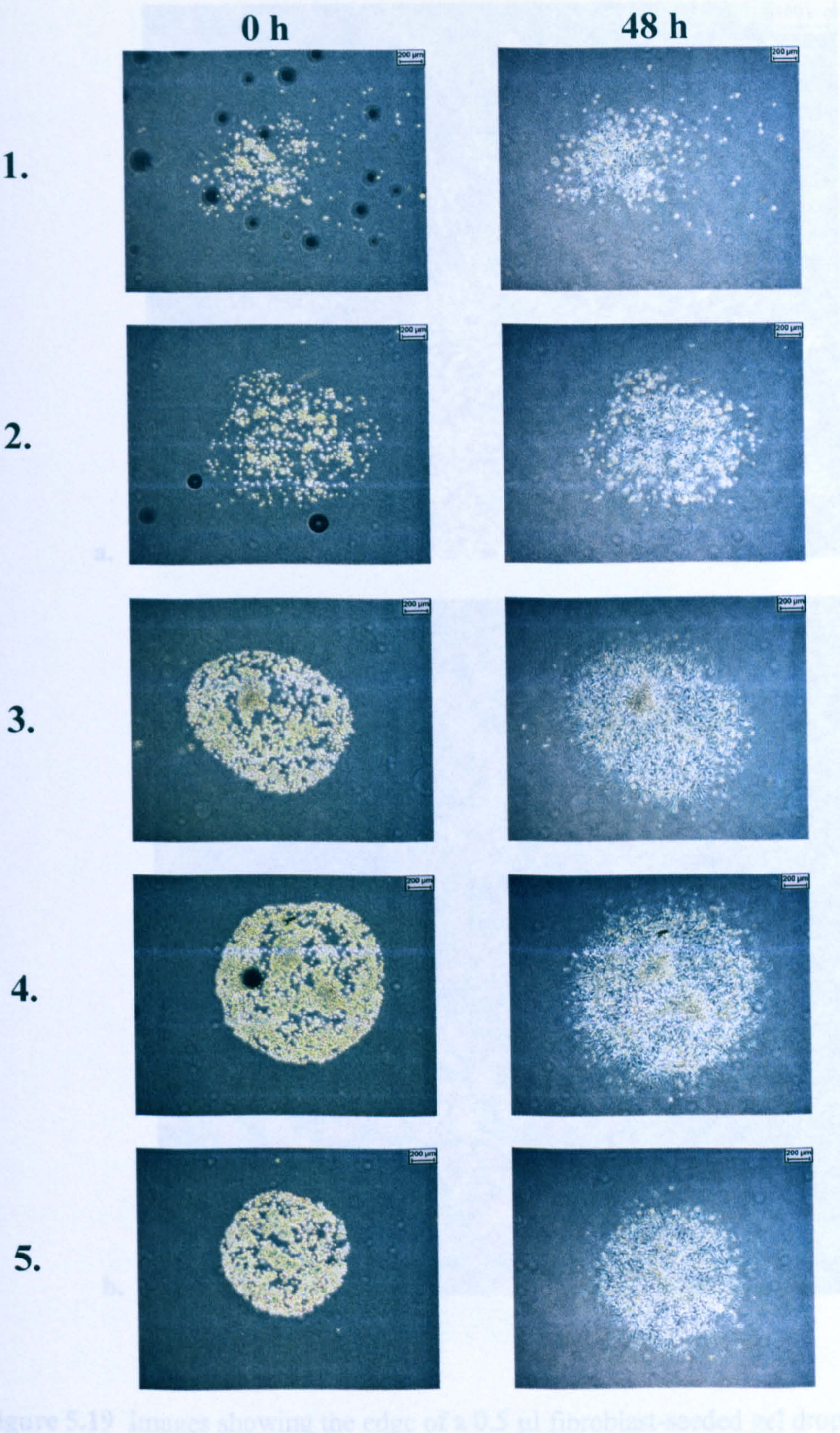

Figure 5.18 Phase contrast images of 0.5 µl fibroblast-seeded gel droplets embedded within a cell-free gel. Images taken immediately after assay assembly (0 h) or after 48 hours incubation.

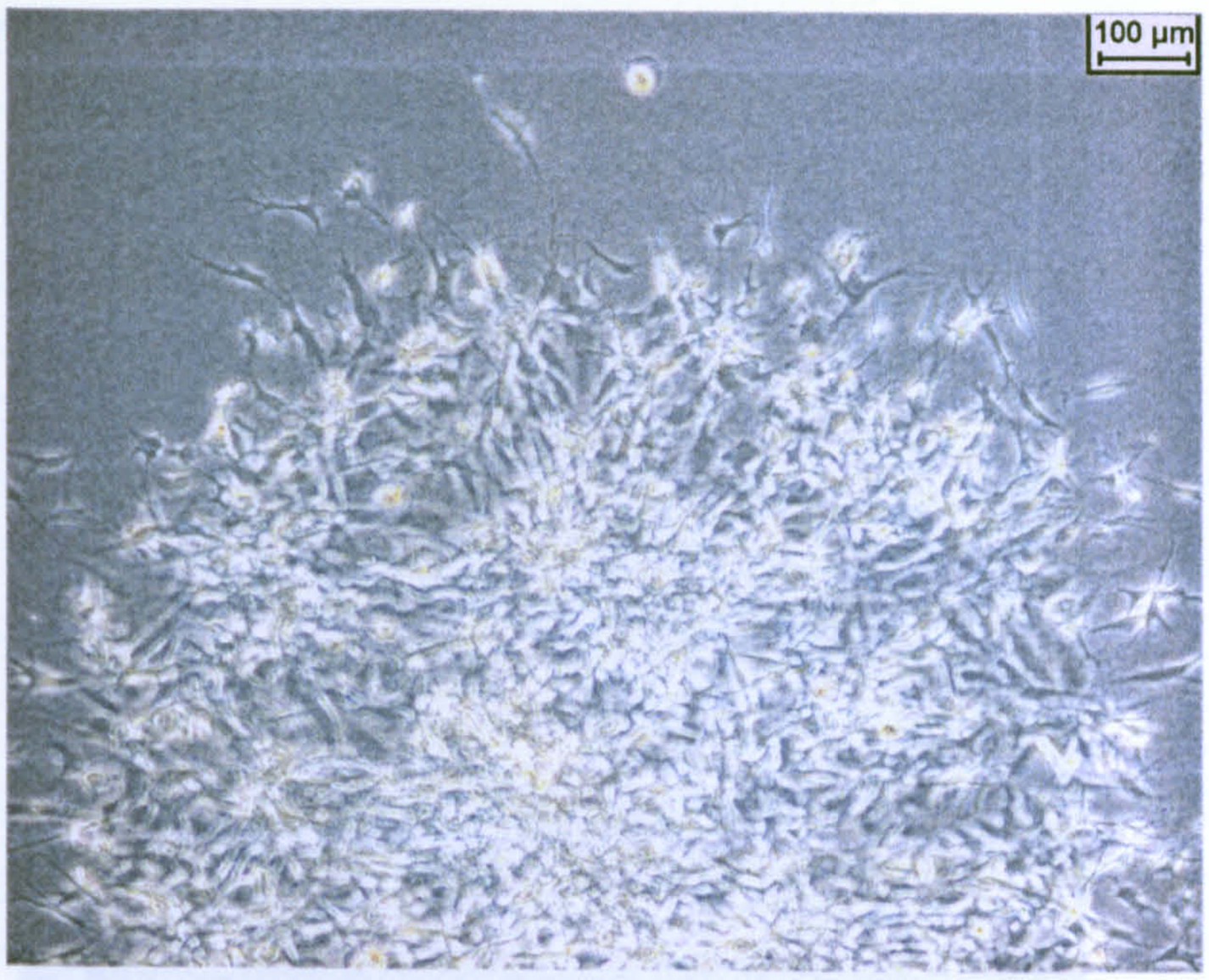

a.

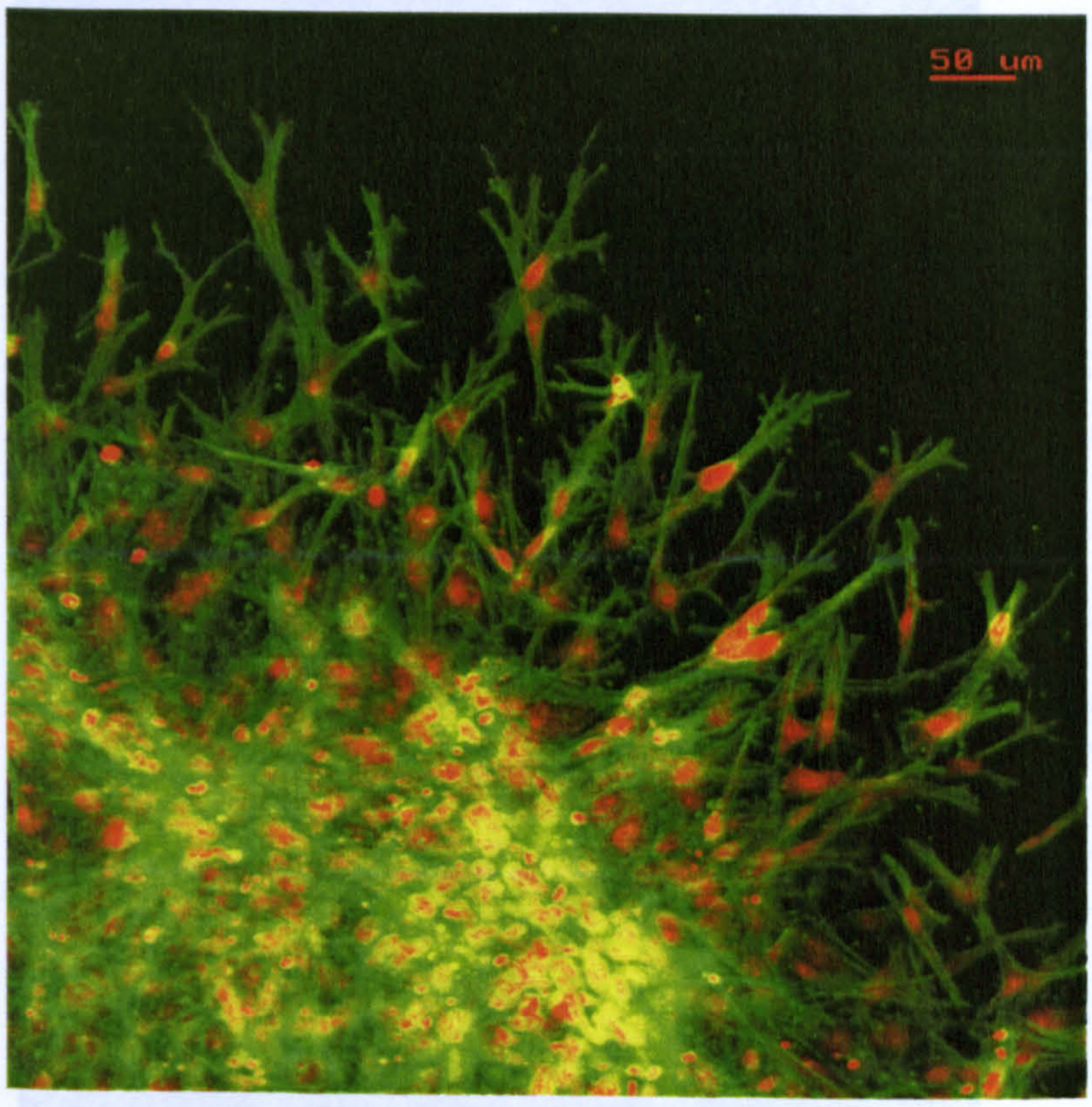

b.

Figure 5.19 Images showing the edge of a 0.5 µl fibroblast-seeded gel droplet following 48 hours incubation. **a.** Phase contrast image of droplet, recognised as #5 in Fig. 5.18. **b.** Z series of optical sections, taken using confocal microscope and displayed as a maximum intensity projection of all the sections. Cells fixed and stained with FITC-phalloidin and propidium iodide. Droplet identified as #3 in Fig. 5.18.

a. Top →

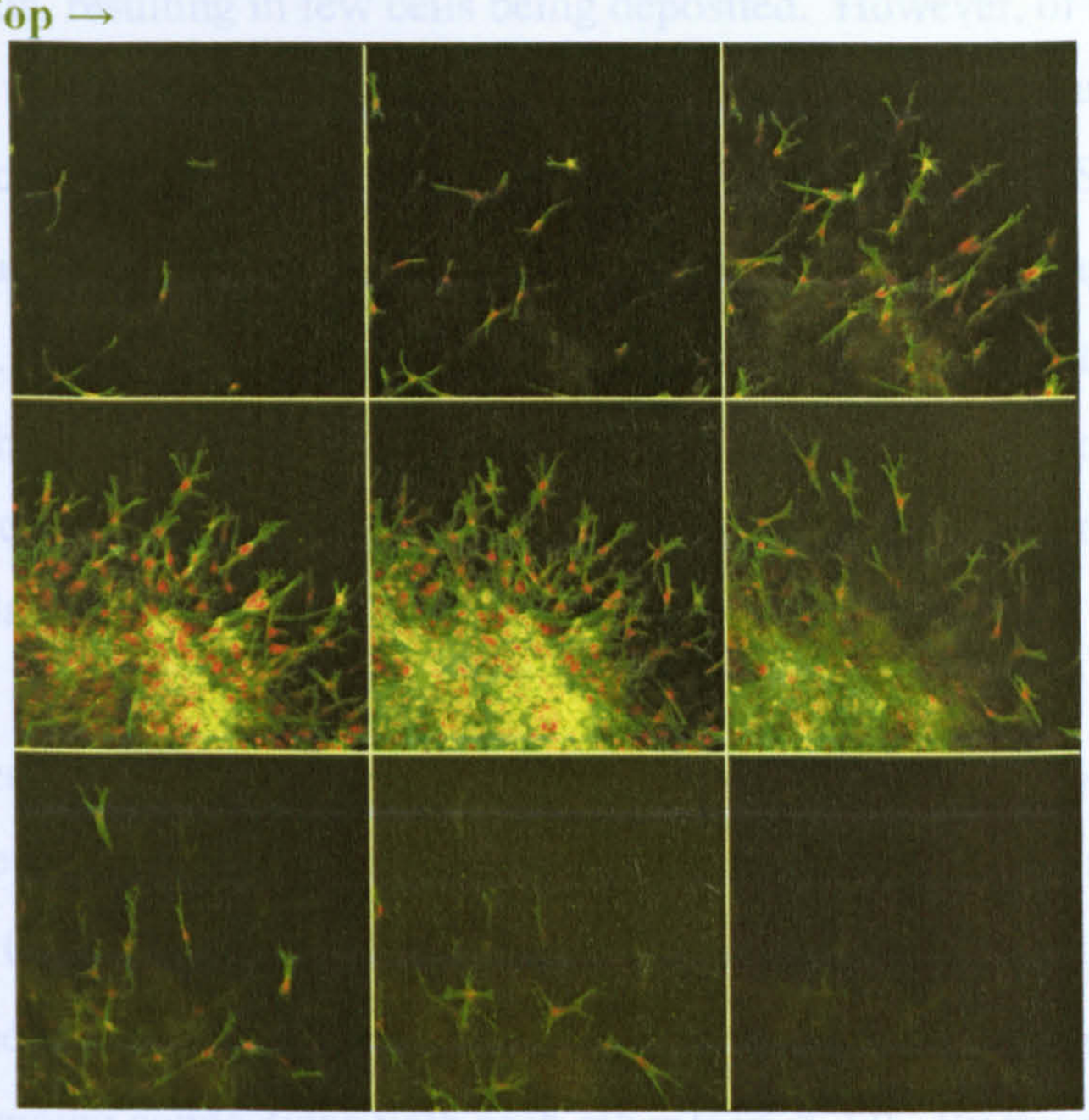

→ Bottom

b. Top →

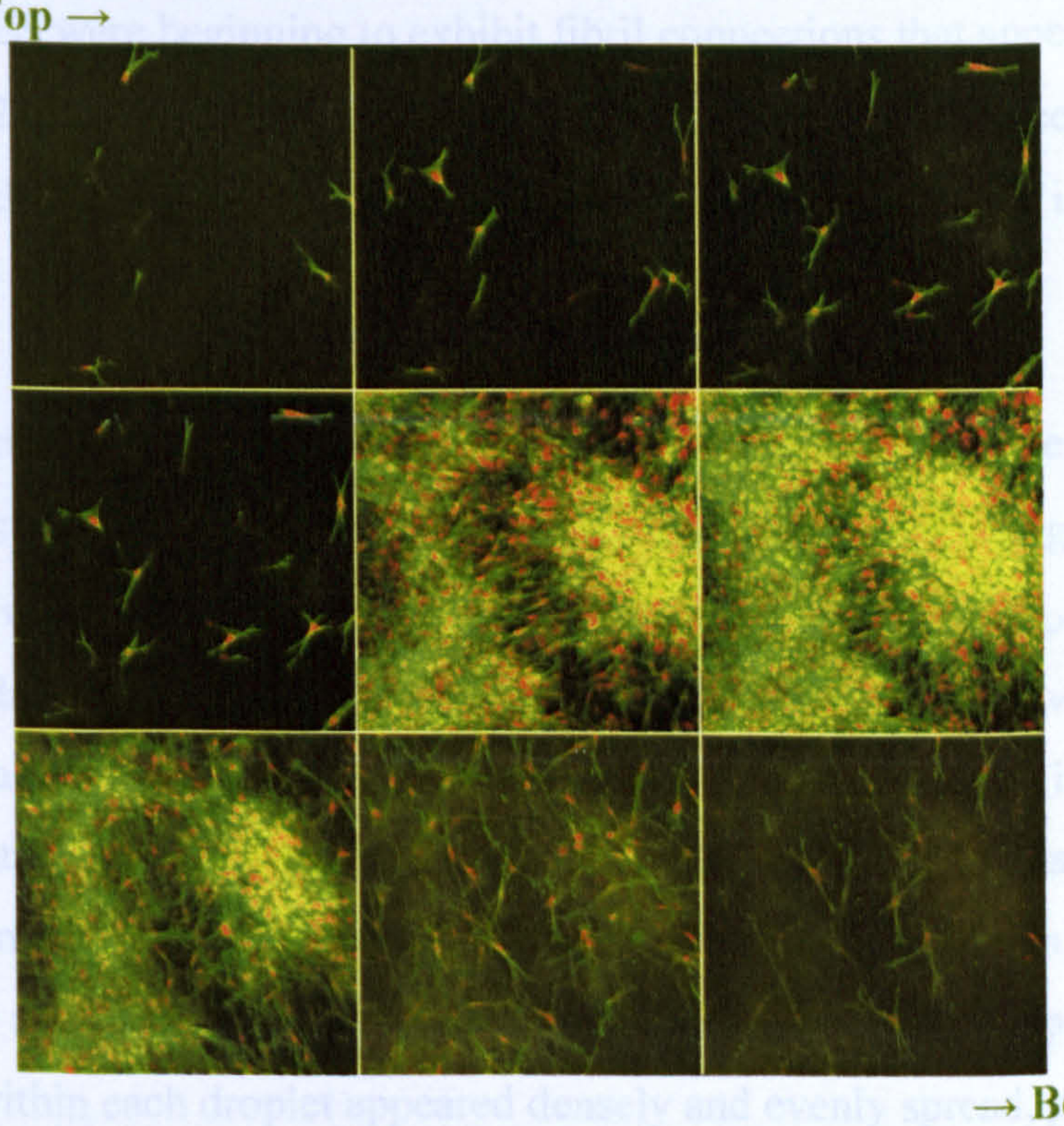

→ Bottom

Figure 5.20 Z series of optical sections, taken using confocal microscope and displayed in a gallery, from left to right, moving from top to bottom. Each tiled image in the gallery represents a composite of 6 sequential optical sections. Edge (a) or centre (b) of a 0.5 µl fibroblast-seeded gel droplet (#3 in Fig. 5.18) shown through ~144 µm depth. Cells fixed after 48 hours incubation and stained with FITC-phalloidin and propidium iodide.

solution's ejection, resulting in few cells being deposited. However, of those cells present, distinct morphological differences were observed, which appeared dependent upon the presence of ES. After 24 hours incubation, cells in 1 μg/ml ES and particularly 10 μg/ml ES appeared well spread and many were extending long projections (Fig. 5.21). Those exposed to 10 μg/ml ES also exhibited strand-like fibril connections with adjacent cells, even when they lay quite far apart. In contrast, many cells within the control had failed to spread at such a low seeding density, remaining rounded. Cellular debris also appeared to be present.

It was also noticed that the gels exposed to both concentrations of ES were more translucent in appearance. This increased over time, until, by 48 hours incubation, the gel containing 10 μg/ml ES had transformed to a clear, viscous, liquid-like state. As a consequence, the cells contained within had adopted a more rounded morphology, but were still maintaining connections with each other (Fig. 5.22). By this time, cells within 1 μg/ml ES were beginning to exhibit fibril connections that appeared similar to those observed 24 hours earlier in the higher ES concentration. Many cells in the control remained rounded and cellular debris continued to be observed, indicating a loss of cell viability.

Due to the difficulties associated with accurately pipetting small volumes of solution, such as 0.5 μl as described above, the assay was modified to include slightly larger droplets of 2 μl volume. This was with the aim of providing for easier pipetting, whilst still producing droplets that would each be small enough to be viewed within one microscopic image. In one such assay, images taken immediately after its assembly demonstrate that the whole of each droplet could indeed be viewed in its entirety using phase contrast microscopy, albeit at very low magnifications (Fig. 5.23a). The cells appeared viable as dendritic-like extensions were already beginning to protrude (Fig. 5.23b). Cells within each droplet appeared densely and evenly spread, providing for clear boundaries between droplets and the surrounding gel. Confocal microscopy revealed the boundary to be consistent throughout the depth of the droplet, with no cells scattered outside of it (Fig. 5.24). Images taken after assays had been incubated for 24 hours demonstrated that cells had successfully migrated from the droplets in both horizontal and vertical orientations (Fig. 5.25).

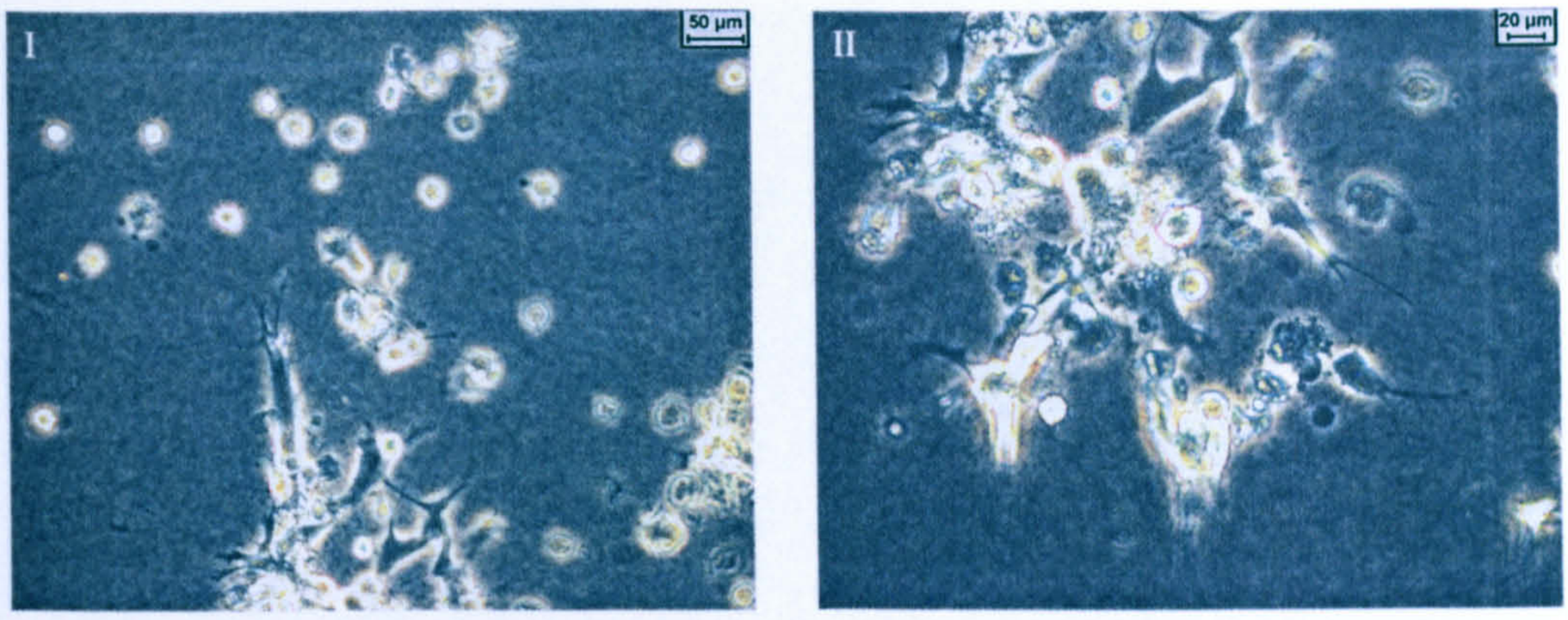

Figure 5.21 Representative phase contrast images of 0.5 µl fibroblast-seeded gel droplets embedded within a cell-free gel. Images taken following 24 hours incubation. Appearance of cells in the absence of ES (control) (I, II) or in the presence of 1 µg/ml ES (III, IV) or 10 µg/ml ES (V, VI). Many cells in the control have failed to spread, remaining rounded. Cellular debris is also present. The presence of strand-like fibres between cells exposed to 10 µg/ml can be discerned. Examples of these are indicated by arrows.

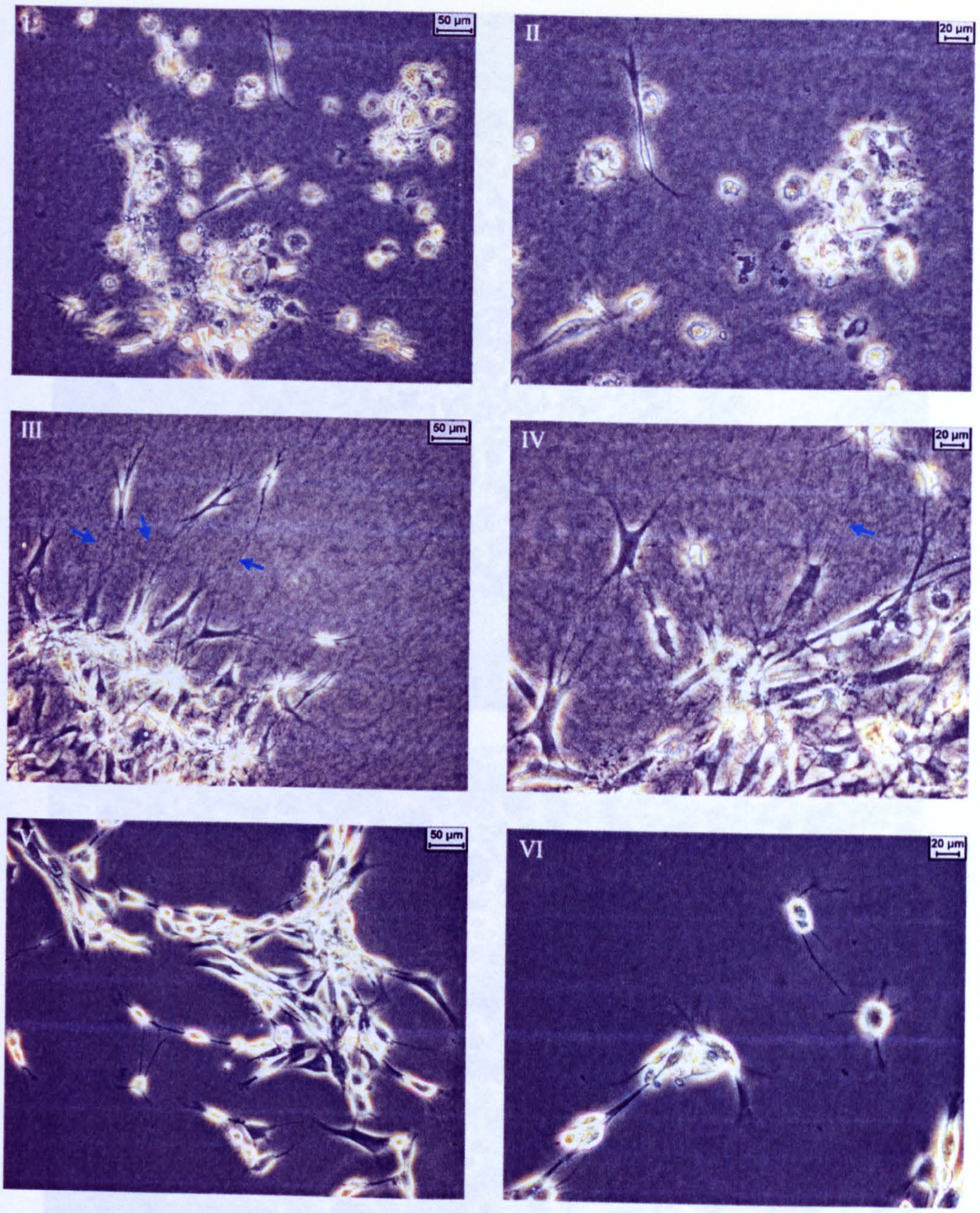

Figure 5.22 Representative phase contrast images of 0.5 µl fibroblast-seeded gel droplets embedded within a cell-free gel. Images taken following 48 hours incubation. Appearance of cells in the absence of ES (control) (I, II) or in the presence of 1 µg/ml ES (III, IV) or 10 µg/ml ES (V, VI). Many cells in the control have failed to spread and cellular debris is present. The presence of strand-like fibres between cells exposed to 1 µg/ml ES can just be observed, as indicated by the arrows. Cells in 10 µg/ml ES have rounded up, but thin, intercellular connections are maintained.

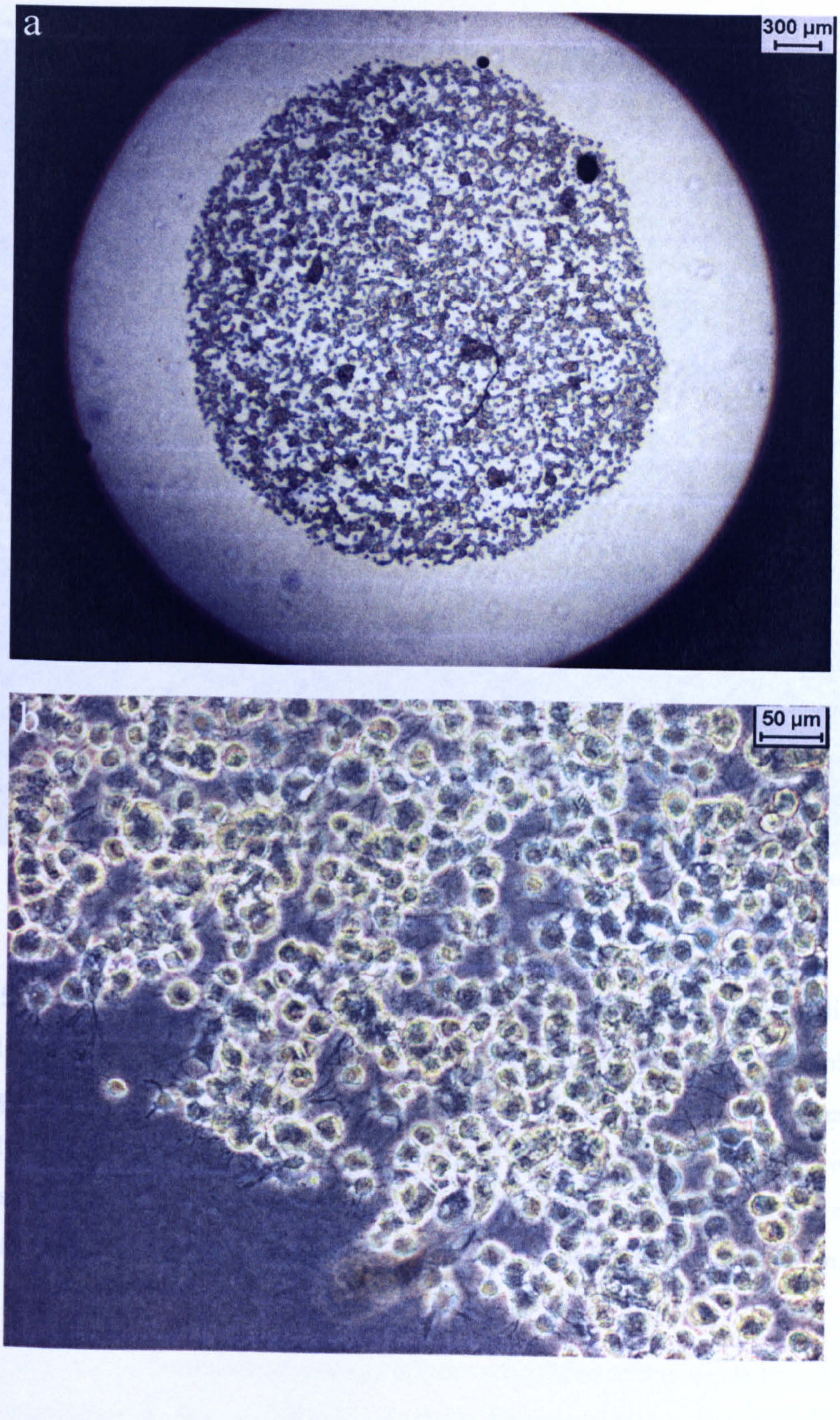

Figure 5.23 A 2 µl fibroblast-seeded gel droplet embedded within a cell-free gel. Phase contrast images taken shortly after assay assembly. **a.** Image taken at low magnification to illustrate that the whole droplet could be viewed simultaneously. **b.** Image taken at higher magnification to show that the cells were already developing dendritic-like extensions, thus demonstrating their viability.

Top →

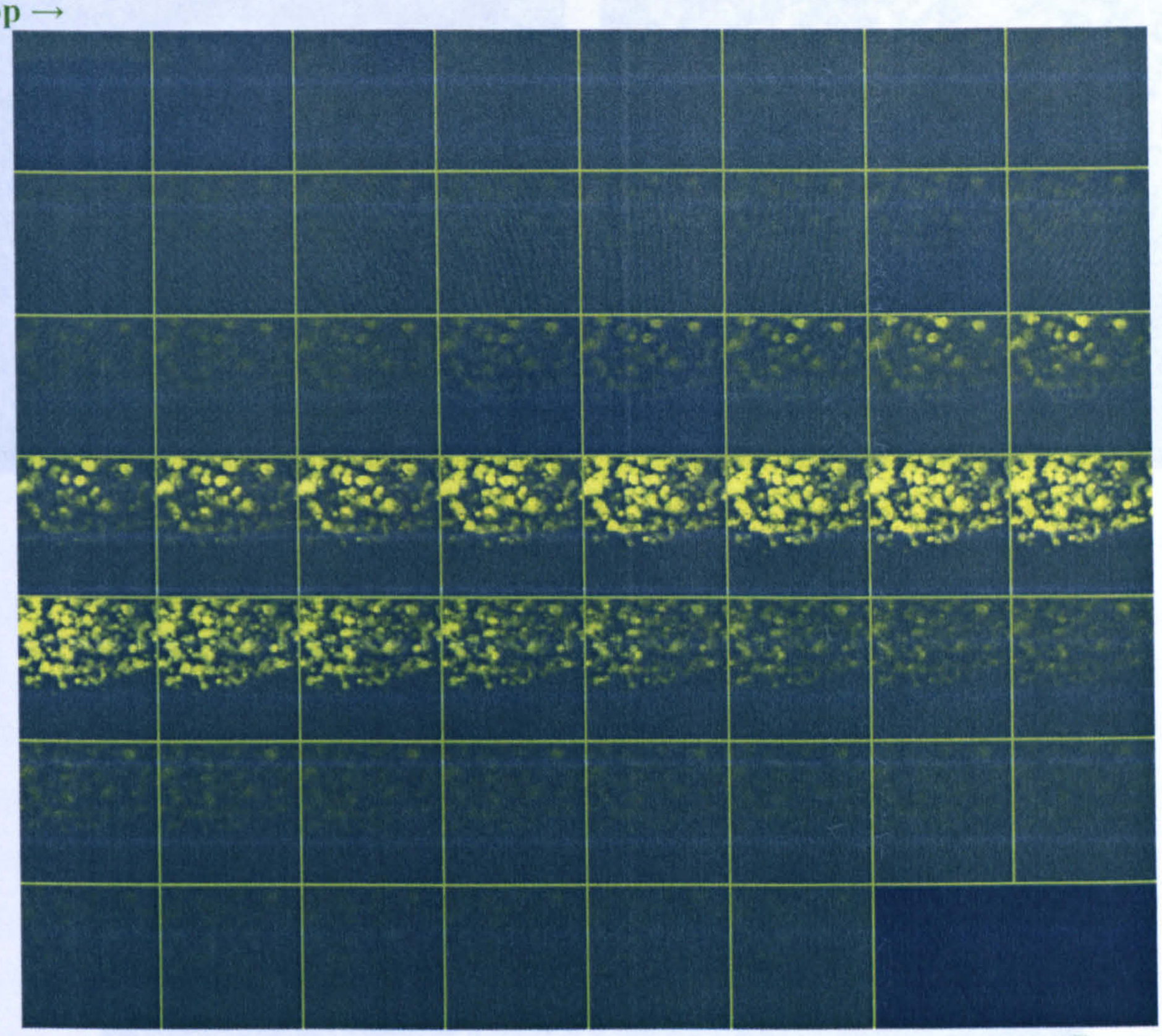

→ Bottom

Figure 5.24 Z series of optical sections, taken using confocal microscope and displayed in a gallery, from left to right, moving from top to bottom. Edge of a 2 μl fibroblast-seeded gel droplet embedded within a cell-free gel. Cells fixed immediately after assay assembly (0 hours incubation) and stained with FITC-phalloidin and propidium iodide. Sections through the gel show that the cell droplet boundary was consistent and no cells were scattered away from the droplet in either a vertical or horizontal orientation.

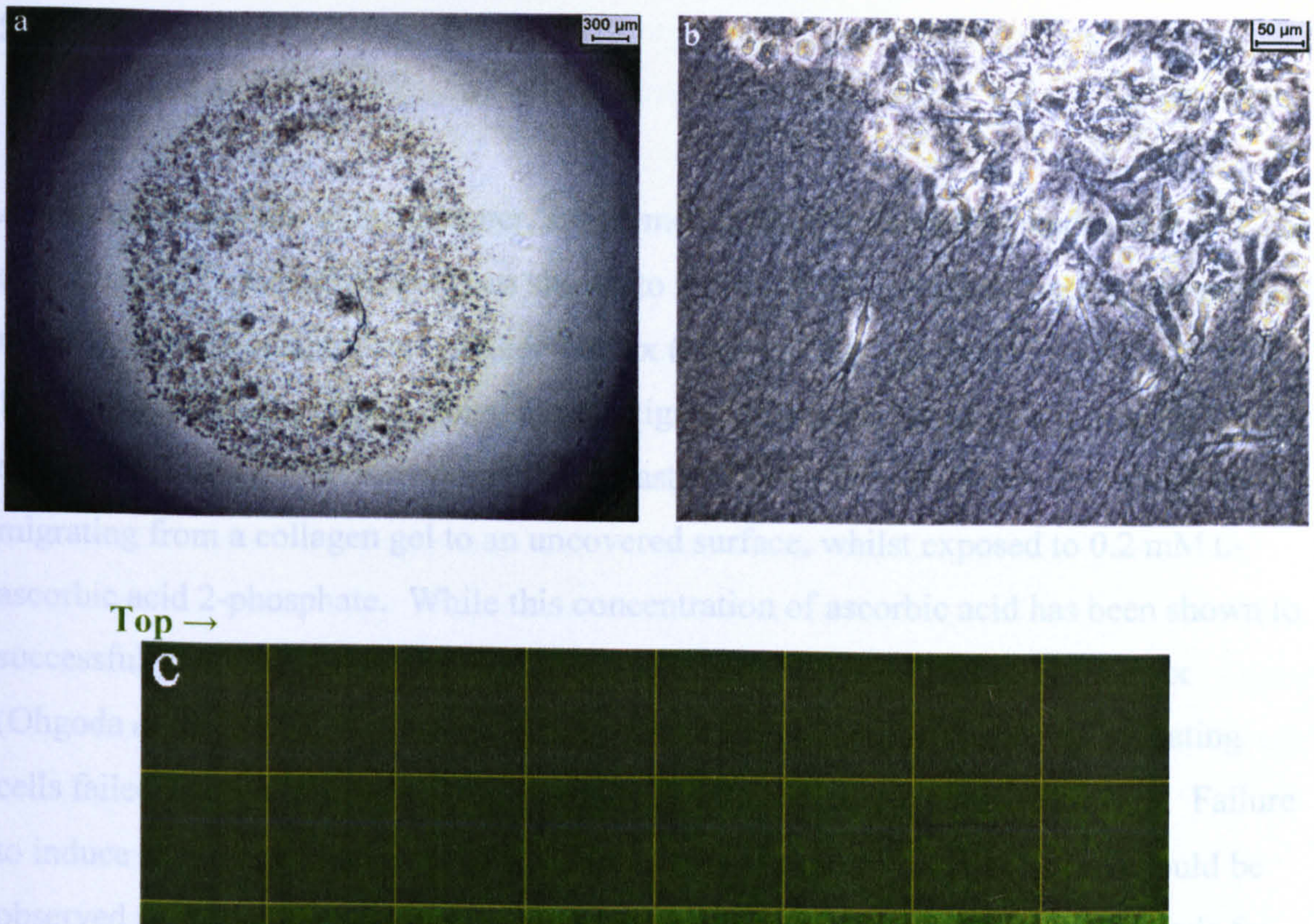

Figure 5.25 A 2 µl fibroblast-seeded gel droplet embedded within a cell-free gel. Images taken after 24 hours incubation. **a.** and **b.** Phase contrast images demonstrating that cells had migrated in a horizontal orientation from the droplet. **c.** z series of optical sections, taken using confocal microscope and displayed in a gallery, from left to right, moving from top to bottom. This image demonstrates that cells had migrated in a vertical orientation, above and below the droplet. Cells stained with FITC-phalloidin and propidium iodide.

5.4 Discussion

As discussed already in this chapter, supplementation of cell culture media with L-ascorbic acid 2-phosphate has been shown to induce fibroblasts to arrange themselves in multi-layers and accumulate collagen matrix (Hata and Senoo, 1989; Ishikawa *et al.*, 1997; Ohgoda *et al.*, 1998). Thus, to investigate the possibility of developing three-dimensional assays that incorporate fibroblast-derived matrices, cells were observed migrating from a collagen gel to an uncovered surface, whilst exposed to 0.2 mM L-ascorbic acid 2-phosphate. While this concentration of ascorbic acid has been shown to successfully induce fibroblasts to produce a three-dimensional tissue-like matrix (Ohgoda *et al.*, 1998), the same was not observed here. Multi-layering of migrating cells failed to occur during the time periods in which the assays were observed. Failure to induce any noticeable levels of fibroblast-derived matrices, in which cells could be observed in three dimensions, resulted in the decision to investigate other methods for allowing the viewing of fibroblasts in three-dimensional environments. Externally-derived collagen/fibronectin gel matrices were therefore included in subsequent assays. In order to ensure continuity with previous work, in which cell adhesion and migration was observed in the absence of ascorbic acid, it was decided to omit L-ascorbic acid 2-phosphate from these assays.

Assays designed to observe cells embedded within collagen/fibronectin gel matrices were first assembled using cloning cylinders to separate cell-free from cell-populated gels. These assays proved difficult to assemble throughout, with much wastage resulting from disruption of the gels during removal of the cylinders. Initially, gels of 1 mg/ml collagen concentration were used. These proved particularly fragile and were prone to being distorted by the lens of the confocal microscope. Cells embedded within these gels also tended to sink through them by gravity, either because gelling took too long to complete and/or because the resulting gels were too weak to support each cell's position. In addition, no cells were observed migrating across the cell-populated/cell-free boundaries. Although increasing the collagen concentration to 1.5 mg/ml relieved some of these problems, assays still proved difficult to assemble. The cells also remained reluctant to cross cell-populated/cell-free boundaries. It therefore appeared that this assay design, although successful in separating a cell-populated from a cell-free

gel, failed to provide the conditions necessary for the two gels to form a continuous matrix that cells could traverse when migrating.

Ensuing difficulties with assays assembled using cloning cylinders led to the decision to assemble alternative three-dimensional assays. The result was the development of the 'cell droplet' method of assembly in which droplets of cells suspended within a gel solution were placed upon a cell-free gel layer and then covered with another layer of cell-free gel. The migration of cells out of each droplet could then be observed in a horizontal orientation, using phase contrast microscopy and in a vertical orientation, using confocal microscopy. These assays proved far easier to assemble and cells within the droplets were able to infiltrate the surrounding, cell-free gel by migration. Problems that were encountered, concerned determining the volume and therefore the size of each cell droplet suitable for allowing the whole of its circumference to be viewed simultaneously under the phase contrast microscope. This was with the aim of facilitating an estimation of the total number of cells migrating into the surrounding cell-free gel at any given moment. Although easier to view, very small droplets, each of 0.5 μl volume, proved difficult to deliver, with such small gel volumes being prone to gelling within the pipette tips. Droplets of 2 μl volume were easier to pipette, yet remained small enough to be viewed in their entirety. Both phase contrast and confocal microscopy revealed clear demarcations between cell-populated and cell-free areas at the beginning of each observed assay's incubation period. This provided evidence that the cells were not drifting out of the droplets before the gel solutions had been given sufficient time to set. Thus, any cells observed outside of the droplet perimeter after a given period of incubation could be attributed to active cell migration.

Some interesting observations worth reiterating originated from one assay containing cell droplets of 0.5 μl volume and larval ES at concentrations of 1 μg/ml and 10 μg/ml. Here, it was noted that the presence of ES facilitated the spreading of cells that were present at a very low population density. The higher ES concentration in particular appeared to alter the morphologies of the cells observed, increasing the lengths of cellular extensions protruding into the gel. Fine, strand-like fibrils could also be seen connecting cells, some of which lay a considerable distance apart. The appearance of these fibril-like structures may have been related to the observed partial degradation of

the gels into viscous, liquid states. Presumably, such degradation was caused by proteolytic enzymes present within the ES. As these structures also appeared to be connecting cells, they may also have resulted from modified fibroblast behaviour.

5.5 Conclusions

Three-dimensional assays assembled using the 'cell droplet' method proved to be the most successful of those that were investigated. Of the cell droplet volumes tested, 2 μl was confirmed as large enough to dispense with ease. This volume also produced droplets that were small enough to be viewed in their entirety under the phase contrast microscope. It was therefore decided to continue using this method of assembly, incorporating 2 μl cell droplets into three-dimensional assays for quantifying the effects of larval ES upon fibroblast migration. It was also decided to investigate further the findings of one experiment when 0.5 μl cell droplets were used, resulting unintentionally in very low population densities. As described above, the presence of ES in these assays exerted a considerable effect upon cell morphology and the structure of the matrix between cells.

CHAPTER 6

Fibroblast Migration in Three Dimensions

6.1 Introduction

Results within Chapter 4 demonstrated *L. sericata* larval ES to enhance fibroblast migration across a fibronectin-coated surface. However, existing evidence suggests that cells behave very differently within two dimensions than within their familiar three-dimensional *in vivo* environment (Elsdale and Bard, 1972; Breathnach, 1978; Trinkaus, 1984; Van Exan and Hardy, 1984; Omagari and Ogawa, 1990; Zamir *et al.*, 1999; Beertsen, McCulloch and Sodek, 2000; Friedl and Bröcker, 2000 Cukierman *et al.*, 2001; Tamariz and Grinnell, 2002; Grinnell *et al.*, 2003). With this in mind, further research was directed towards developing a three-dimensional *in vitro* wound assay in which to observe fibroblast migration in response to ES. As shown in the previous chapter, this objective was first addressed by attempting to induce fibroblasts, using L-ascorbic acid 2-phosphate, to produce substantial volumes of their own ECM. As these attempts proved unsuccessful, externally derived gel matrices were utilised. Based upon the fibroblast-populated collagen lattice, first introduced by Ehrmann and Gey (1956), this procedure involved embedding fibroblasts within a collagen gel matrix. Fibronectin (30 μg/ml) was also added to the matrix, as previous research has found this concentration optimal for migration (Greiling and Clark, 1997). After experimenting with assay assembly methods designed to allow cells to be observed migrating from a cell-populated to a cell-free section of gel, the 'cell droplet' method of assembly was deemed the most suitable.

Here, this chapter presents the effects that ES exerted upon fibroblast migration within three-dimensional assays, assembled using the 'cell droplet' method. Also presented are findings resulting from the observation of cells that were embedded at much lower population densities within these assays. Here, the influence of ES upon fibroblast morphology and matrix structure was noted and inferences were drawn.

6.2 Methods

6.2.1 Three-dimensional *in vitro* wound assay – fibroblast migration

A stock solution containing 1.5 mg/ml collagen and 30 μg/ml fibronectin was prepared as described in Chapter 5.2.1.2. Larval ES (from batch E – see Table 2.1) was also added to the concentration indicated. For the controls, an equivalent volume of PBS was added in place of ES. Three-dimensional *in vitro* wound assays were then assembled following the 'cell droplet' method described in the Chapter 5.2.3. Here for each assay, five droplets of the above stock solution, of 2 μl volume containing $1x10^7$ fibroblast cells/ml, were placed on top of a pre-prepared gel layer within a 58 mm tissue culture dish. Following gelation of the droplets, stock solution was poured over the top to completely cover them and left to gel. Finally, serum-free cell culture medium, from the same source that was used to make the gel solution stock, was diluted to 1 x concentration using distilled water and either larval ES or, where appropriate, an equivalent volume of PBS. When ES was present, this was added to the same concentration as that which was present within the gel. This medium (2 ml) was then poured into each dish to cover the gels. The assembled assay was incubated at 37°C in a humidified 5 % (v/v) CO_2 atmosphere for the time stated. Medium was replaced every 24 hours.

Phase contrast images, showing the whole area of each cell droplet embedded within each gel, were taken following 0 hours, 24 hours and where possible 48 hours incubation. At 48 hours, it was observed that the gel containing 5 μg/ml ES had detached from the well surface, whilst that containing 10 μg/ml ES had dissolved

completely to a viscous liquid state. Fibroblast migration within the gels was therefore quantified following 24 hours incubation, when each assay was still intact.

Using Microsoft Paint Shop Pro 6 the image of each cell droplet at 0 hours was superimposed over the same droplet's image after 24 hours incubation, as shown in Fig. 6.1. These composite images were then analysed using Leica QUIPS software. Firstly, the perimeter distance of the original cell droplet was calculated. This was followed by quantifying the number of fibroblasts that had migrated horizontally, away from the cell droplet, over the 24 hour period. In order to correct for variable droplet perimeter distances, the number of migrating cells was expressed as cells per μm perimeter of the original cell droplet boundary. The linear distance each cell had migrated was also estimated. Analysis by the viewer was performed blind.

After 48 hours incubation, fibroblasts within intact gels were fixed *in situ* by the addition of 4 % paraformaldehyde, as described in Chapter 5.2.2.2, and then stained with FITC-phalloidin and PI following the method outlined in Chapter 2.2.4. Following staining, gels were carefully blotted to remove excess liquid and then mounted with Bio-Rad fluorescence mounting medium and a coverslip. They were then visualised using a confocal microscope, as described in Chapter 2.2.4. Maximum intensity images of cell droplet edges were taken to observe migrating cell morphology. In addition, series' of images showing focal planes through the z-axis of the gel, including above, through and below each cell droplet, were taken and examined to quantify the number of cells that had migrated in a vertical direction. These images were compared with each other and also with those taken from replicate assays that had been treated in a similar way but had not been allowed to incubate following their assembly (*ie* the cells had been fixed following 0 hours incubation). This was undertaken to confirm that the probability of cells drifting out of the droplets during assay assembly was low.

6.2.1.1 Statistical analysis

Values, representing the number of migrating cells per μm perimeter of each cell droplet replicate within each treatment, were transformed to their square roots to ensure normal distribution within treatments. The transformed values were then subjected to one-way analysis of variance (ANOVA) and Dunnett's Multiple Comparison Tests,

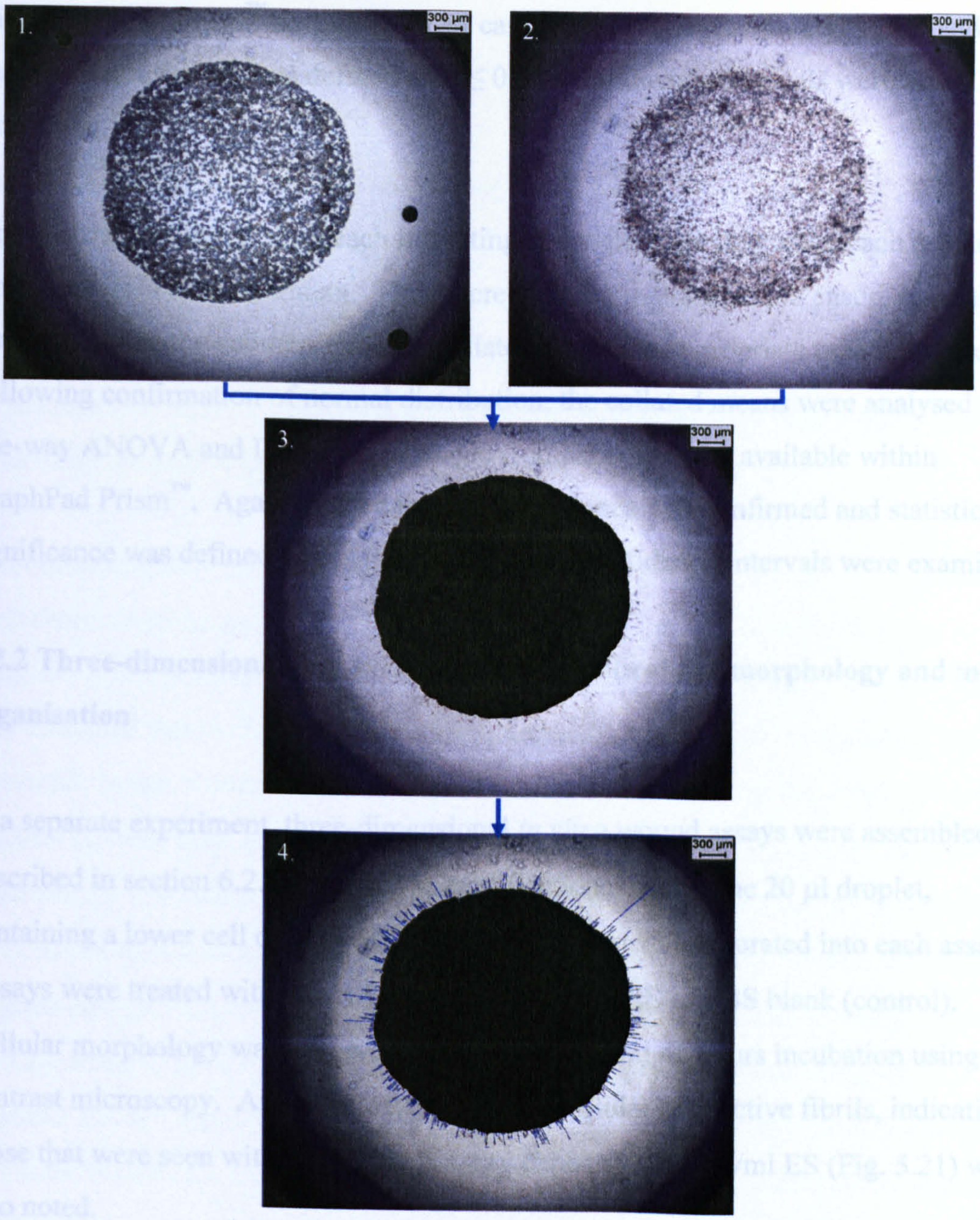

Figure 6.1 A demonstration of how fibroblast migration from gel droplets within three-dimensional *in vitro* wound assays was quantified from phase contrast microscopic images. **1.** Fibroblast-seeded droplet immediately after assay assembly (0 hours incubation). **2.** The same droplet after 24 hours incubation. **3.** Fibroblast-seeded droplet at 0 hours incubation, coloured black for contrast, superimposed upon image from 24 hours incubation. **4.** Only those cells that had migrated from the droplet over the 24 hour period are left showing, thus allowing them to be counted. The distance each cell had travelled was estimated by measuring the lengths of vectors (shown in blue), drawn from the leading edge of each cell, to the perimeter of the superimposed 0 hours image. The perimeter distance of the fibroblast-seeded droplet at 0 hours incubation was also measured by drawing around the superimposed 0 hours image. These measurements were performed using Leica QUIPS software.

using GraphPad Prism™ software. In all cases, equal variance was confirmed and statistical significance was defined as $P \leq 0.05$. Confidence Intervals were also scrutinised.

Linear distances travelled by each migrating cell were compiled under each droplet replicate within each treatment. They were then log transformed to ensure normal distribution and the geometric means collated under the appropriate treatment category. Following confirmation of normal distribution, the collated means were analysed using one-way ANOVA and Dunnett's Multiple Comparison Tests, available within GraphPad Prism™. Again, in all cases, equal variance was confirmed and statistical significance was defined as $P \leq 0.05$. Similarly, Confidence Intervals were examined.

6.2.2 Three-dimensional *in vitro* wound assay – fibroblast morphology and matrix organisation

In a separate experiment, three-dimensional *in vitro* wound assays were assembled, as described in section 6.2.1, with minor modifications. Here, one 20 µl droplet, containing a lower cell density of 3×10^5 cells/ml, was incorporated into each assay. Assays were treated with either 1 µg/ml ES, 5 µg/ml ES or PBS blank (control). Cellular morphology was observed following 0, 24 and 48 hours incubation using phase contrast microscopy. Any development of intercellular connective fibrils, indicative of those that were seen within a previous assay exposed to 10 µg/ml ES (Fig. 5.21) was also noted.

6.3 Results

6.3.1 Three-dimensional *in vitro* wound assay – fibroblast migration

Three-dimensional *in vitro* wound assays were assembled according to the 'cell droplet' method described in Chapter 5.2.3. Here, five droplets of 2 µl volume containing $1x10^7$ cells/ml were incorporated into each assay. The migration of cells out of each droplet,

whilst exposed to 0.1, 1.0, 5 and 10 μg/ml larval ES was quantified and cellular morphology assessed.

Two separate experiments were performed. One compared the effects of 0.1 μg/ml ES and 5 μg/ml ES against a control, where ES was absent. The other examined the effects of 1 μg/ml ES and 10 μg/ml ES, when compared with another control. As typified in Fig. 6.2, the droplet edges within assays from both experiments were clearly demarcated by the presence of cells. The cells also appeared viable, as they were already beginning to develop dendritic-like extensions soon after assay assembly.

As demonstrated by the representative images shown in Fig. 6.3 and 6.4 the whole of each droplet within each assay, from both experiments, could be viewed in one image when the phase contrast microscope was used at a low magnification. These images also indicated that by 24 hours incubation, cell migration into the surrounding gel had occurred. Initial observations suggested that cell migration from the droplets exposed to 5 μg/ml ES was more extensive than within the control (Fig. 6.3). Differences between other assays were more difficult to distinguish. By 48 hours incubation, it was clear that cells within the controls or exposed to 0.1 μg/ml ES or 1 μg/ml ES had continued to migrate into the surrounding gel (Figure 6.5 and Figure 6.6). Cells within 1 μg/ml ES also appeared to have migrated further than in the respective control (Figure 6.6). In contrast, the cell droplets exposed to 10 μg/ml ES appeared to have been degraded over this time because the circumference of the main population of cells within each droplet, as shown in the example image, appeared to be smaller (Figure 6.6). In addition, the cells within each droplet were more scattered than what they had been 24 hours earlier. Some areas of cells had also contracted into tight, dark masses. The gel exposed to 5 μg/ml ES had unfortunately become detached from the dish surface, causing disruption of the cell droplets (Figure 6.5).

Phase contrast images, taken at higher magnifications after the assays had been incubated for 24 hours, revealed differences in the morphologies of cells at the droplet edges (Fig. 6.7 and 6.8). These differences were dependent on the concentration of larval ES present. In the representative images shown, no clear morphological differences could be discerned between cells in the relevant control and those in 0.1

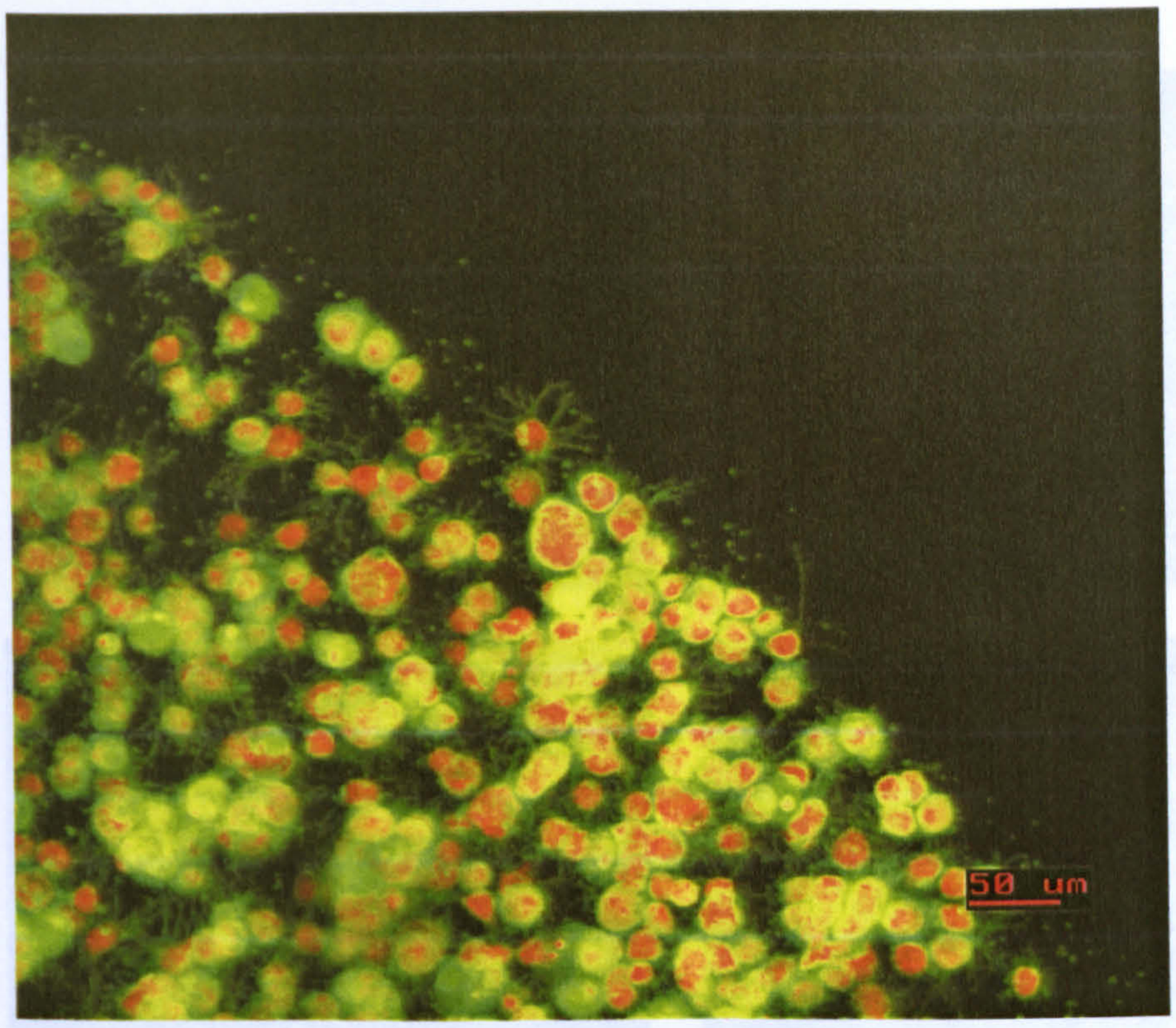

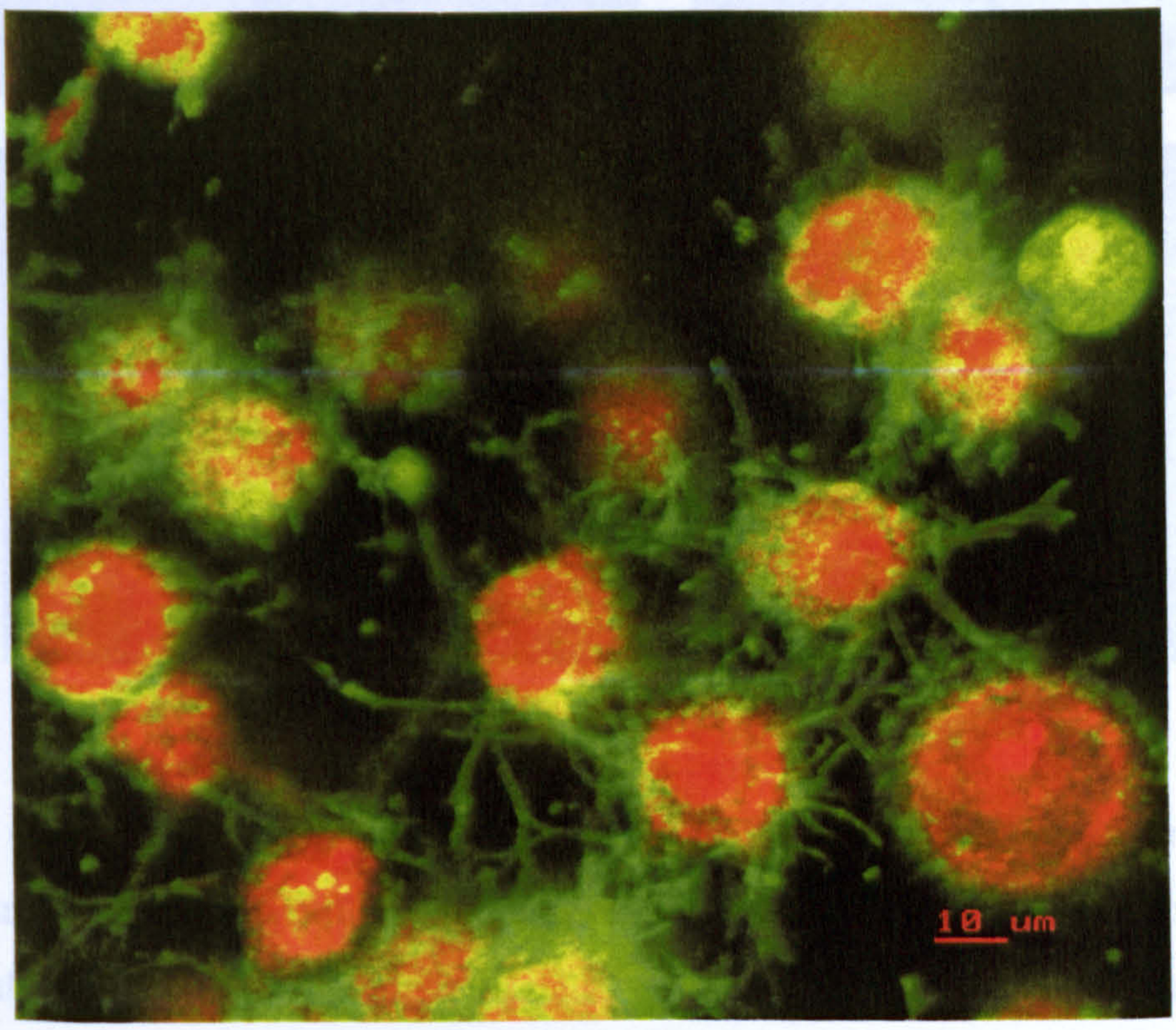

Figure 6.2 Z series of optical sections, taken using confocal microscope, and displayed as maximum intensity projections of all the sections. Images show the edge of a fibroblast-seeded gel droplet embedded within a cell-free gel. Dendritic-like extensions can be observed protruding from the cells. Cells fixed and stained with FITC-phalloidin and propidium iodide soon after assay assembly (0 hours incubation).

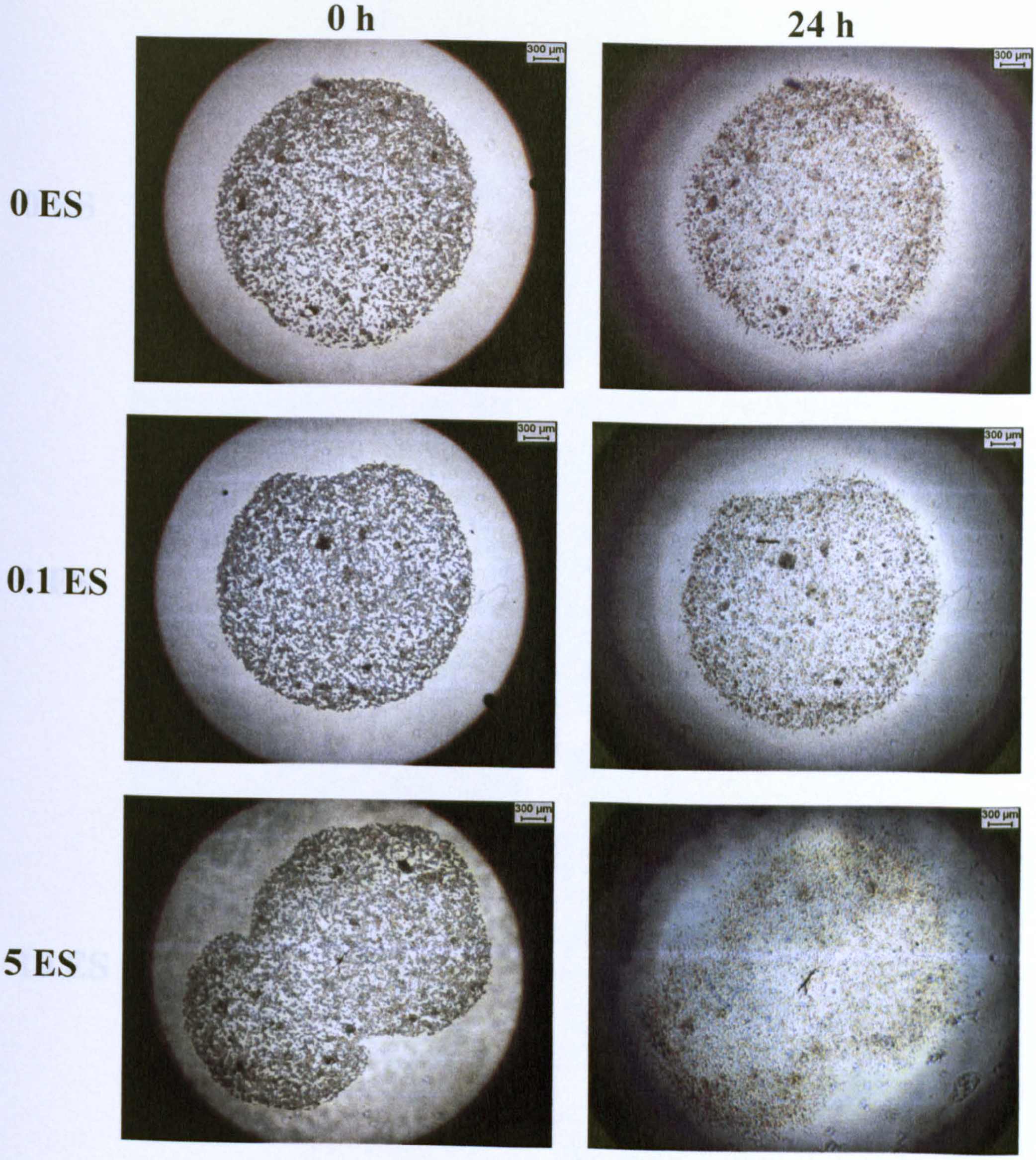

Figure 6.3 Representative phase contrast images of fibroblast-seeded gel droplets, of 2 µl volume, immediately following their placement within a cell-free gel (0 h) or 24 hours after their placement within the cell-free gel. Numerals on the left hand side of the images refer to the concentration of larval ES (µg/ml) present within the assay. 0 ES refers to the control where ES was absent.

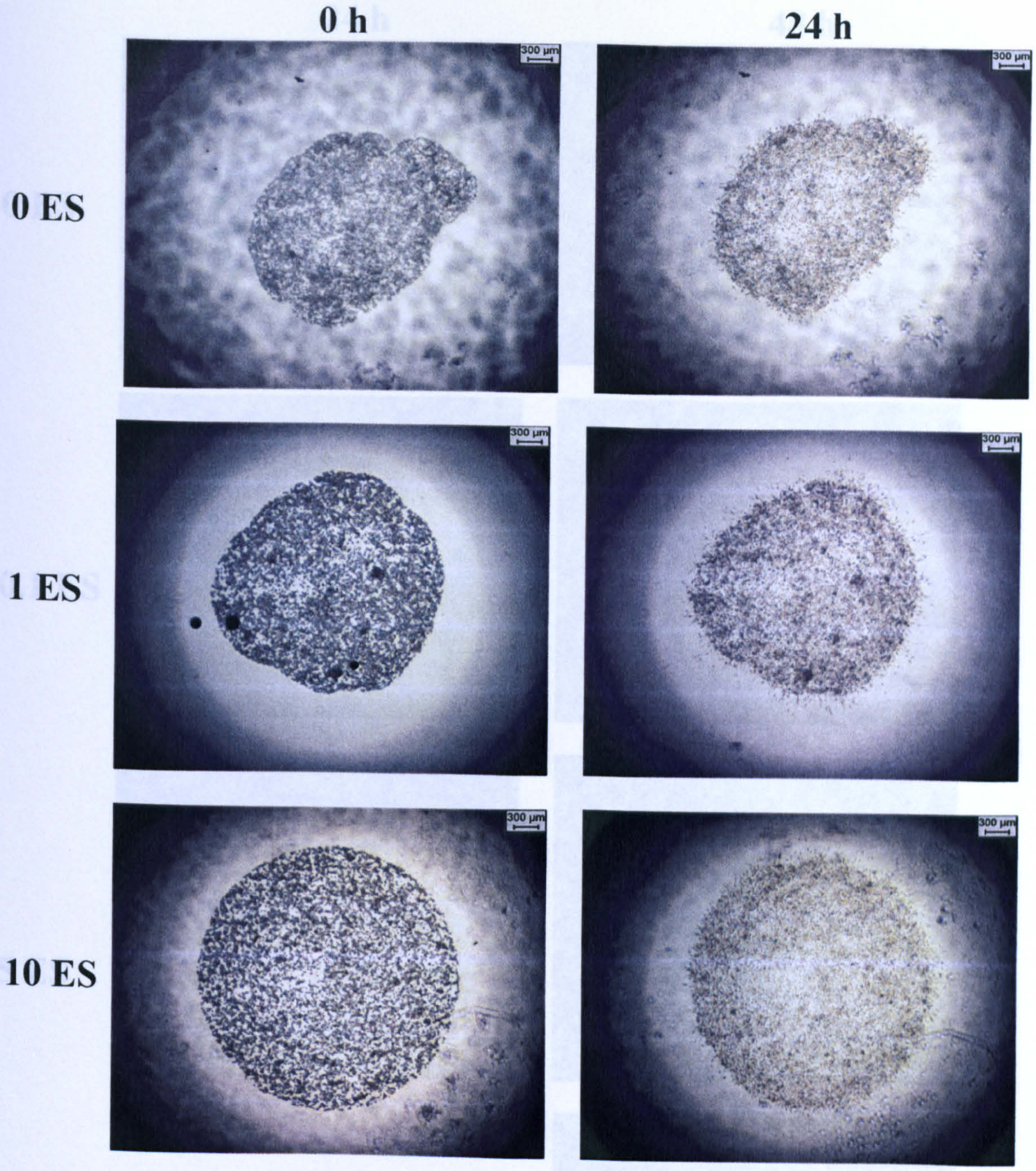

Figure 6.4 Representative phase contrast images of fibroblast-seeded gel droplets, of 2 µl volume, immediately following their placement within a cell-free gel (0 h) or 24 hours after their placement within the cell-free gel. Numerals on the left hand side of the images refer to the concentration of larval ES (µg/ml) present within the assay. 0 ES refers to the control where ES was absent.

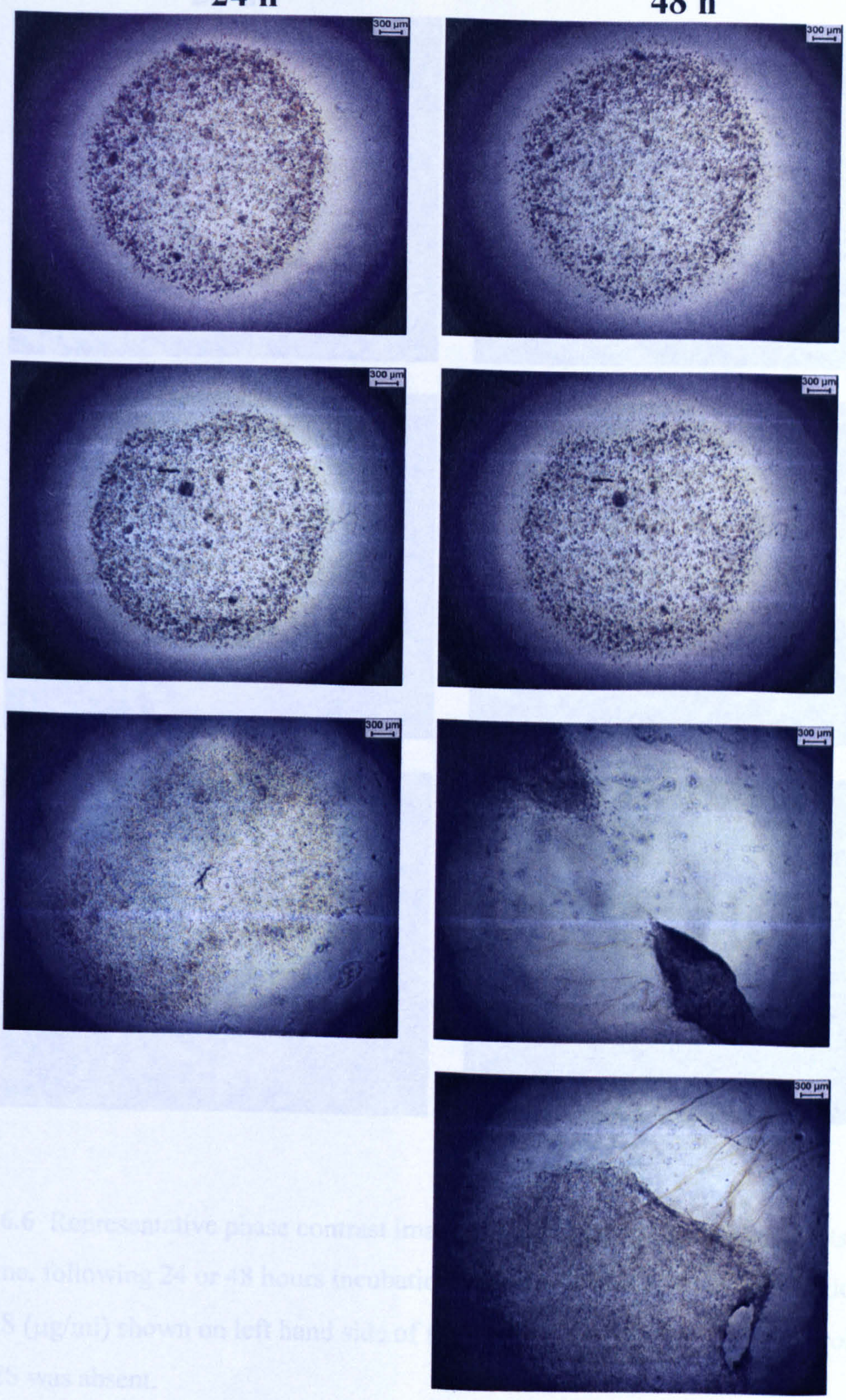

Figure 6.5 Representative phase contrast images of fibroblast-seeded gel droplets, of 2 µl volume, following 24 or 48 hours incubation within cell-free gels. Concentration of larval ES (µg/ml) shown on left hand side of the images. 0 ES refers to the control where ES was absent. Note that after 48 hours, the gel exposed to 5 µg/ml ES became detached from the dish surface.

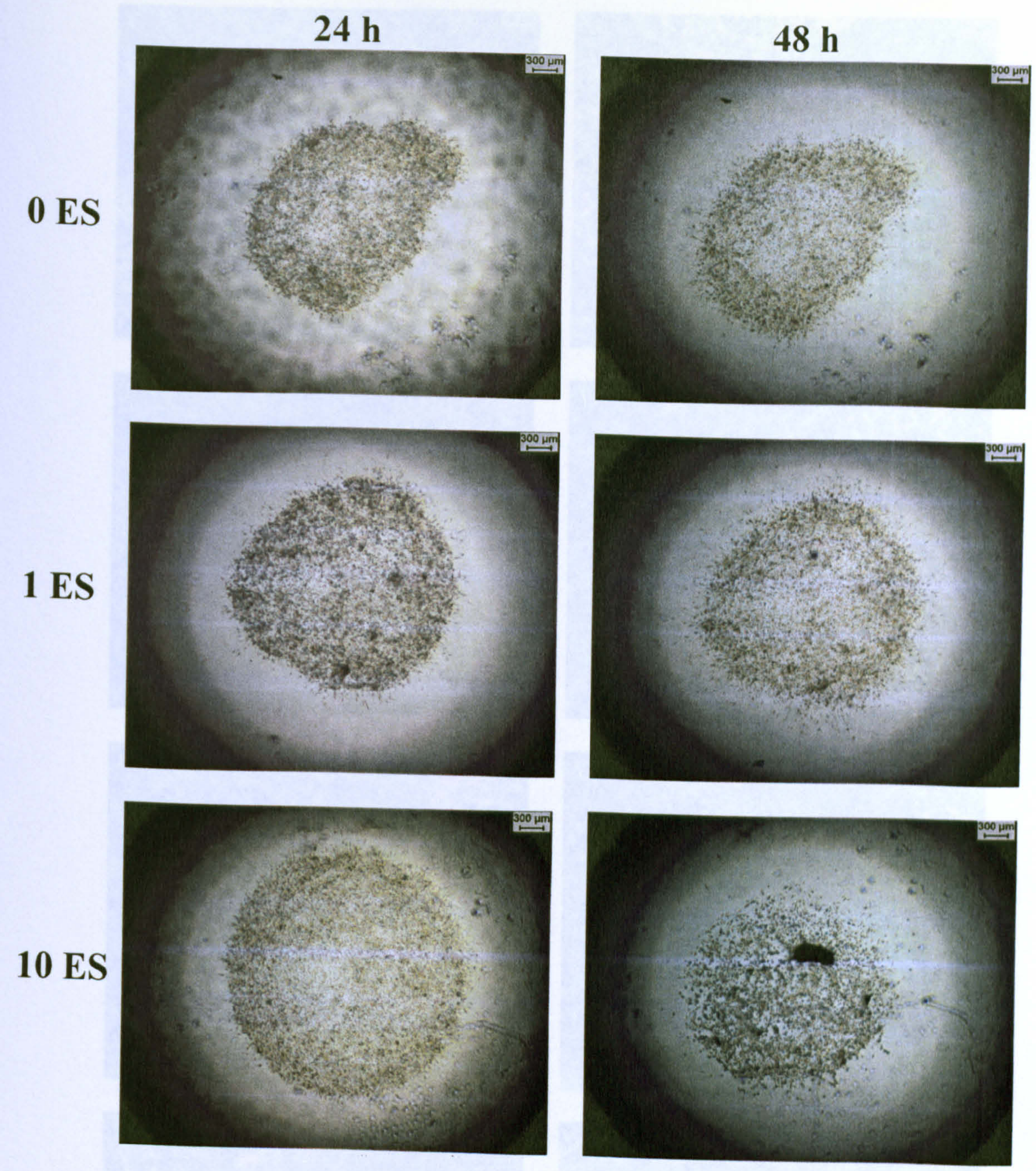

Figure 6.6 Representative phase contrast images of fibroblast-seeded gel droplets, of 2 µl volume, following 24 or 48 hours incubation within cell-free gels. Concentration of larval ES (µg/ml) shown on left hand side of the images. 0 ES refers to the control where ES was absent.

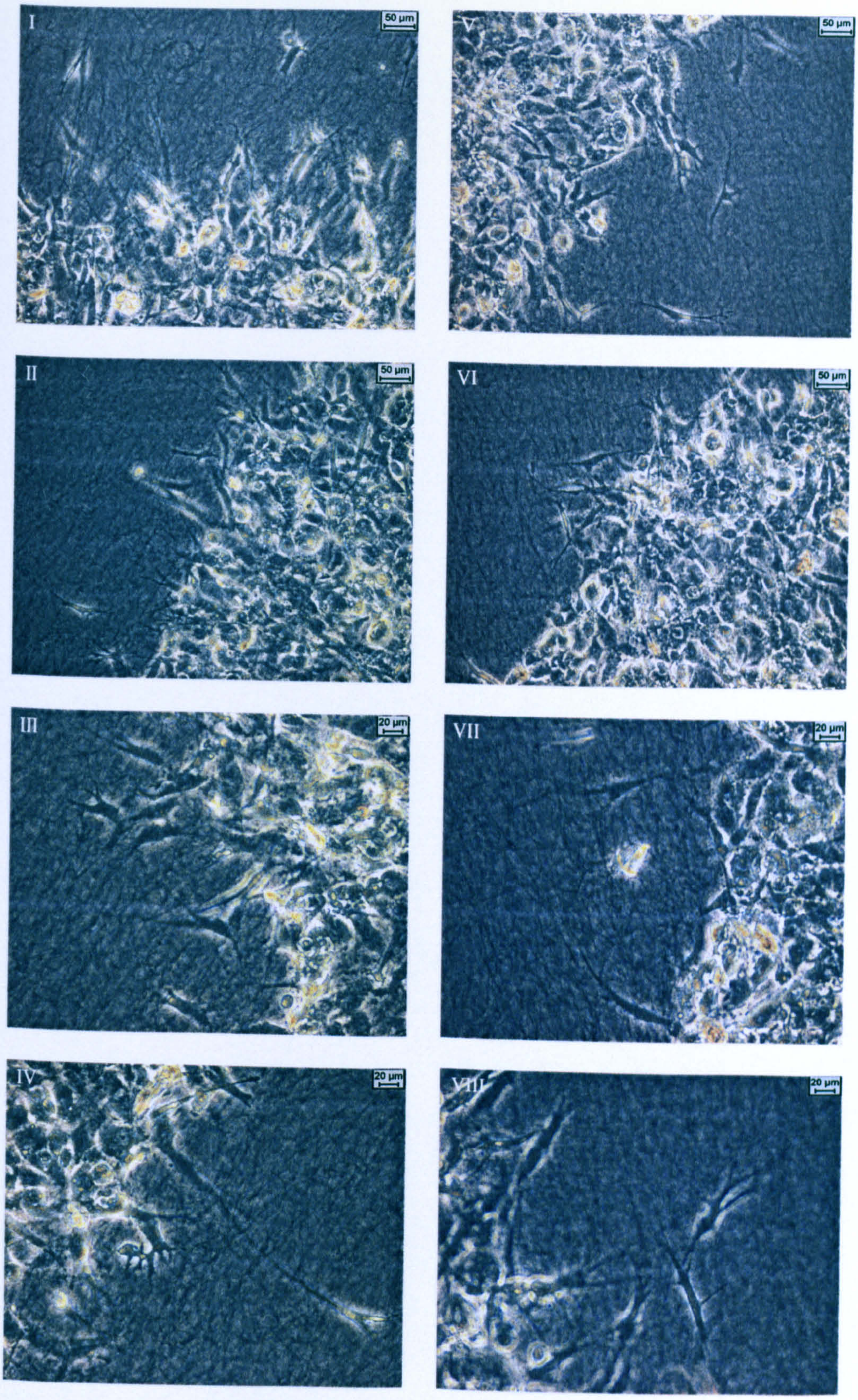

Figure 6.7a Representative phase contrast images of the edges of fibroblast-seeded gel droplets following 24 hours incubation within a cell-free gel. Comparison between cells in the control where ES was absent (I to IV) and cells exposed to 0.1 µg/ml ES (V to VIII).

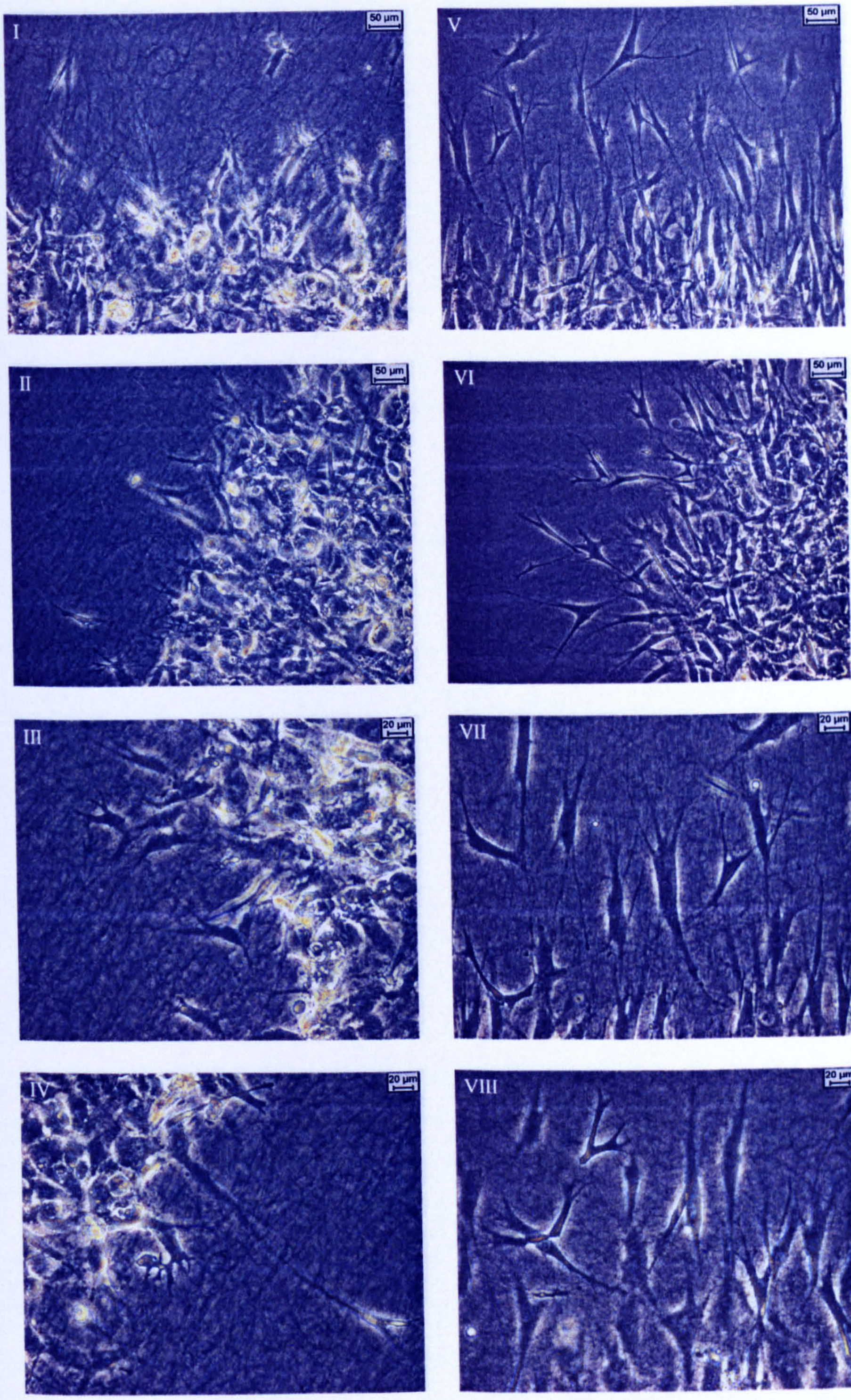

Figure 6.7b Representative phase contrast images of the edges of fibroblast-seeded gel droplets following 24 hours incubation within a cell-free gel. Comparison between cells in the control where ES was absent (I to IV) and cells exposed to 5 µg/ml ES (V to VIII).

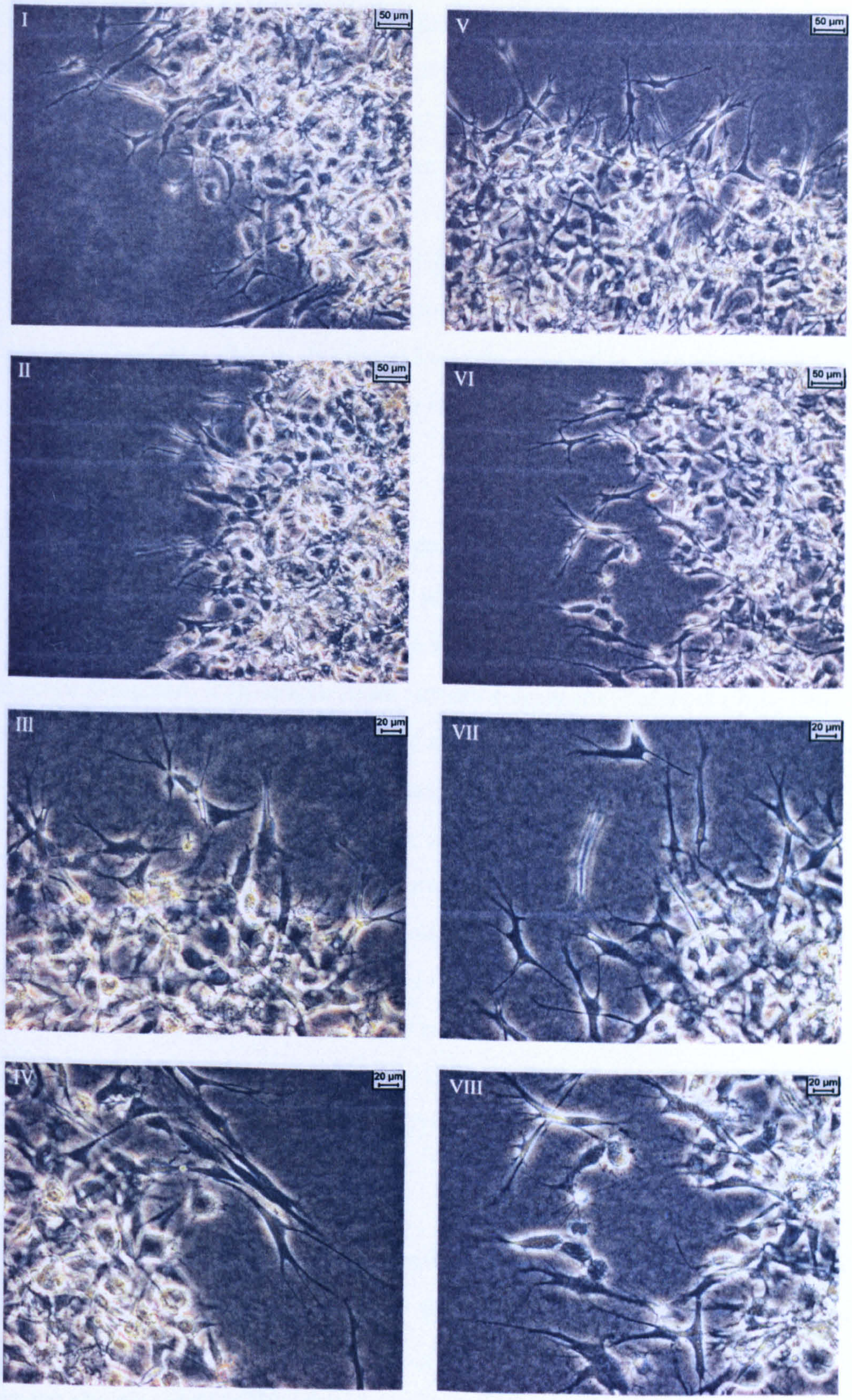

Figure 6.8a Representative phase contrast images of the edges of fibroblast-seeded gel droplets following 24 hours incubation within a cell-free gel. Comparison between cells in the control where ES was absent (I to IV) and cells exposed to 1 µg/ml ES (V to VIII).

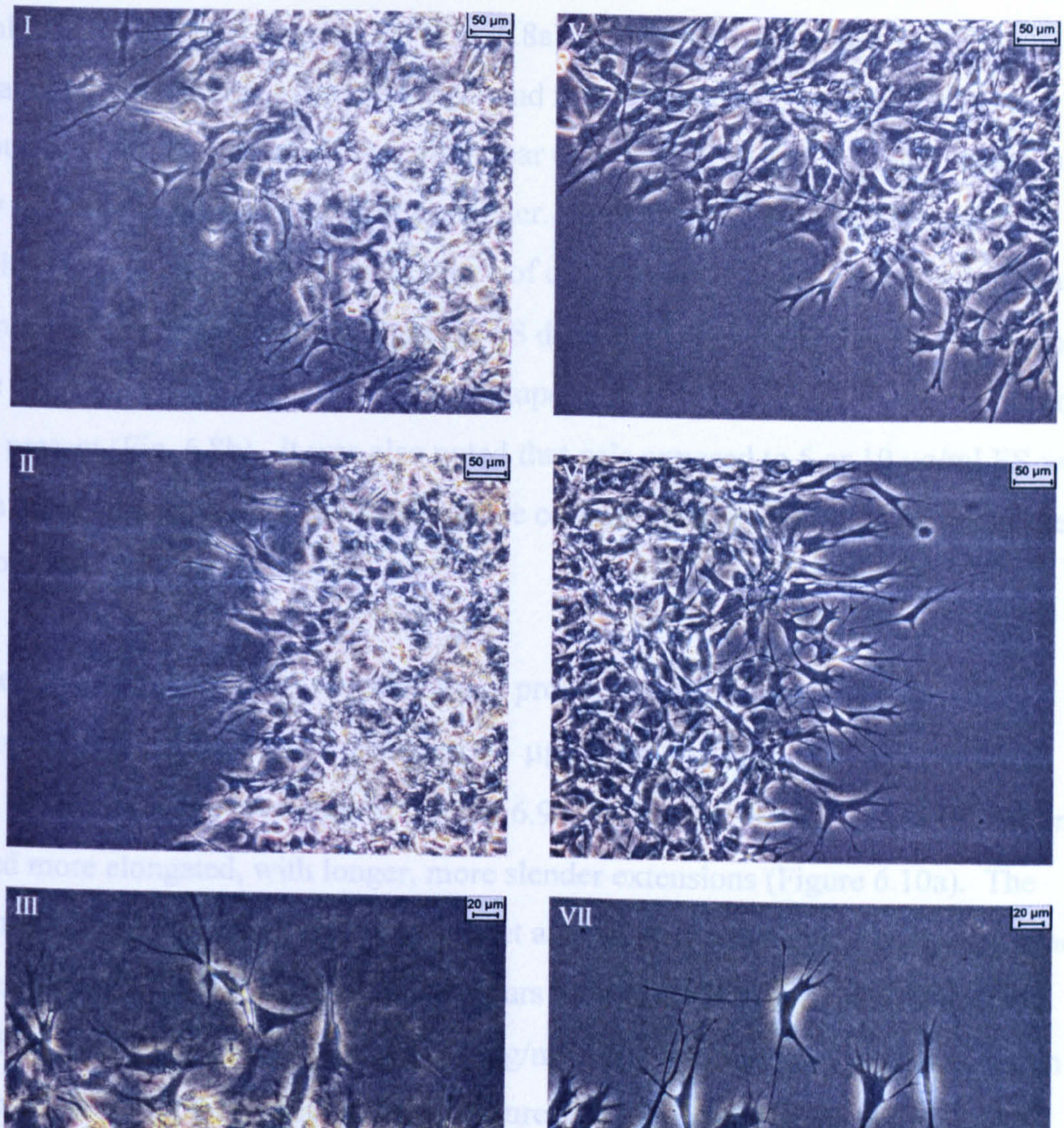

Figure 6.8b Representative phase contrast images of the edges of fibroblast-seeded gel droplets following 24 hours incubation within a cell-free gel. Comparison between cells in the control where ES was absent (I to IV) and cells exposed to 10 µg/ml ES (V to VIII).

μg/ml ES (Fig. 6.7a) or 1 μg/ml ES (Fig. 6.8a). However, cells exposed to 5 μg/ml ES appeared larger and had projected longer and more numerous extensions into the surrounding gel (Fig. 6.7b). It was also clear that more cells had migrated across and away from the original cell droplet perimeter. In places, migrating cells exhibited parallel alignment indicating some degree of organisation. Many cells positioned at the perimeter of the droplet within 10 μg/ml ES displayed numerous, slender extensions, some of which were exceptionally long compared to those seen when other conditions were present (Fig. 6.8b). It was also noted that gels exposed to 5 or 10 μg/ml ES were much more transparent than their respective controls, improving visibility under the microscope.

Images taken after 48 hours revealed more pronounced differences between cells (Figure 6.9 and 6.10). Cells exposed to 0.1 μg/ml ES still appeared very similar to those within the respective control (Figure 6.9a). However, cells exposed to 1 μg/ml ES looked more elongated, with longer, more slender extensions (Figure 6.10a). The distance of migration away from the droplet also appeared to be greater. Despite the gel having become dislodged before the 48 hours incubation was complete, it was still possible to view some cells exposed to 5 μg/ml ES in their original positions within the matrix. The example images shown in Figure 6.9b revealed that the cells that had migrated out of the droplet appeared elongated, with numerous, long extensions. The gel exposed to 10 μg/ml ES had by 48 hours incubation, turned into a viscous liquid. The cells within the droplets appeared to be more rounded than those in the control, having lost many of their slender extensions (Figure 6.10b). However, a significant proportion of these cells had remained in physical contact with others by maintaining long, slender intercellular extensions.

Confocal microscopic images, taken after assays had been incubated for 48 hours, also revealed differences in cellular morphology and migration. As shown in Fig. 6.11, cells within 1 μg/ml ES appeared longer and had migrated further from the droplet edge than those in the absence of ES. This observation is in agreement with those made when the relevant phase contrast images were examined (Figure 6.10a).

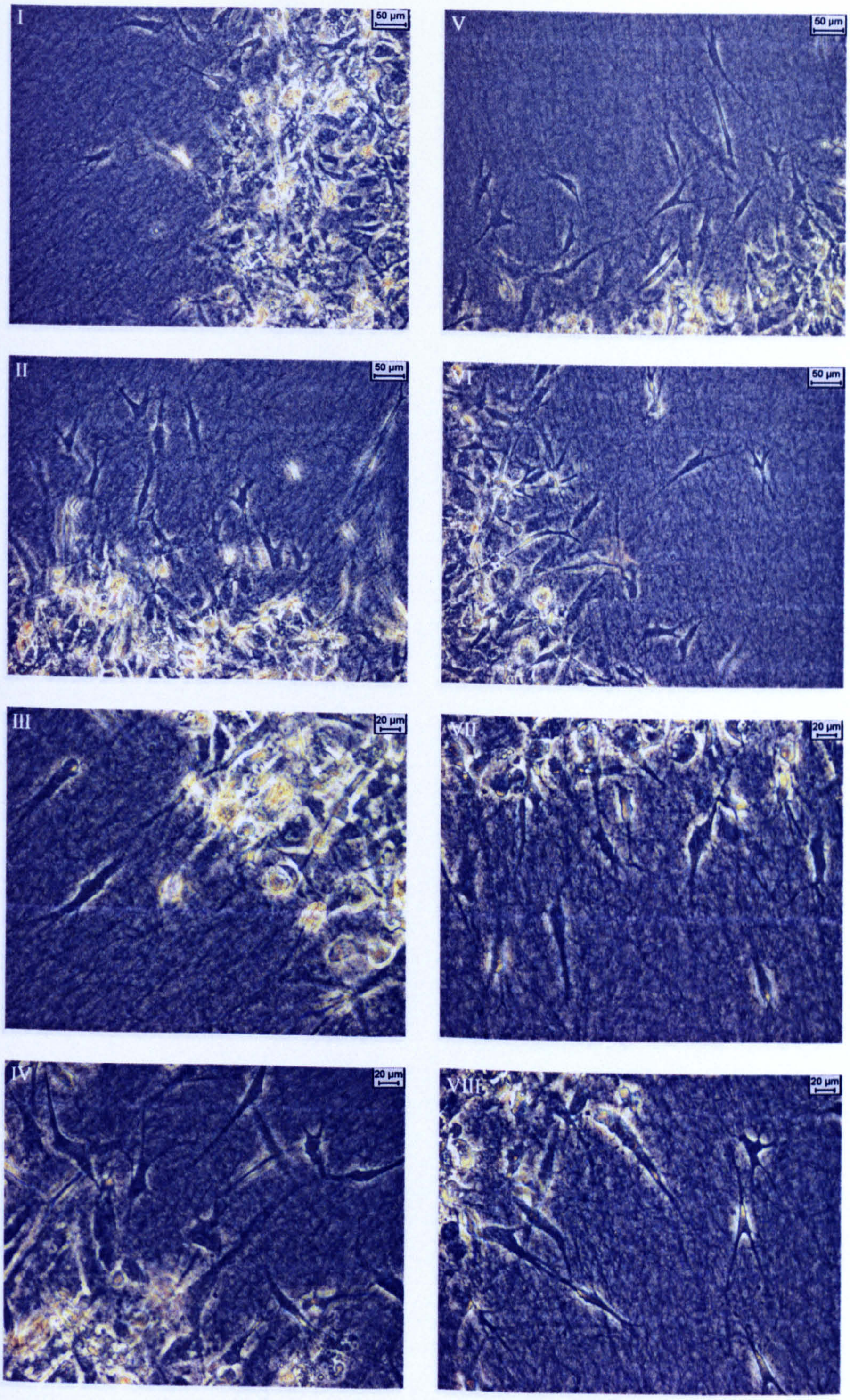

Figure 6.9a Representative phase contrast images of the edges of fibroblast-seeded gel droplets following 48 hours incubation within a cell-free gel. Comparison between cells in the control where ES was absent (I to IV) and cells exposed to 0.1 µg/ml ES (V to VIII).

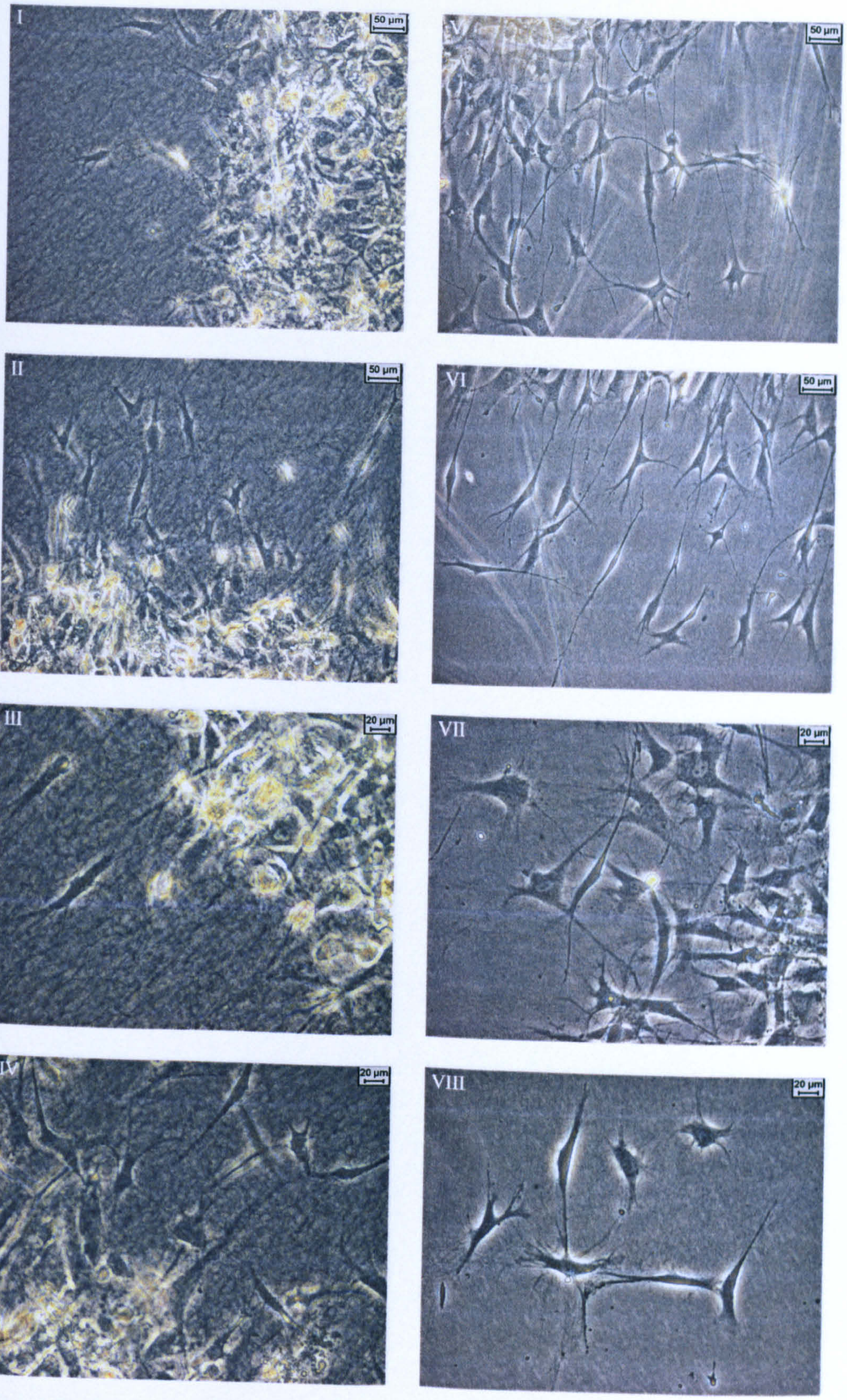

Figure 6.9b Representative phase contrast images of the edges of fibroblast-seeded gel droplets following 48 hours incubation within a cell-free gel. Comparison between cells in the control where ES was absent (I to IV) and cells exposed to 5 µg/ml ES (V to VIII).

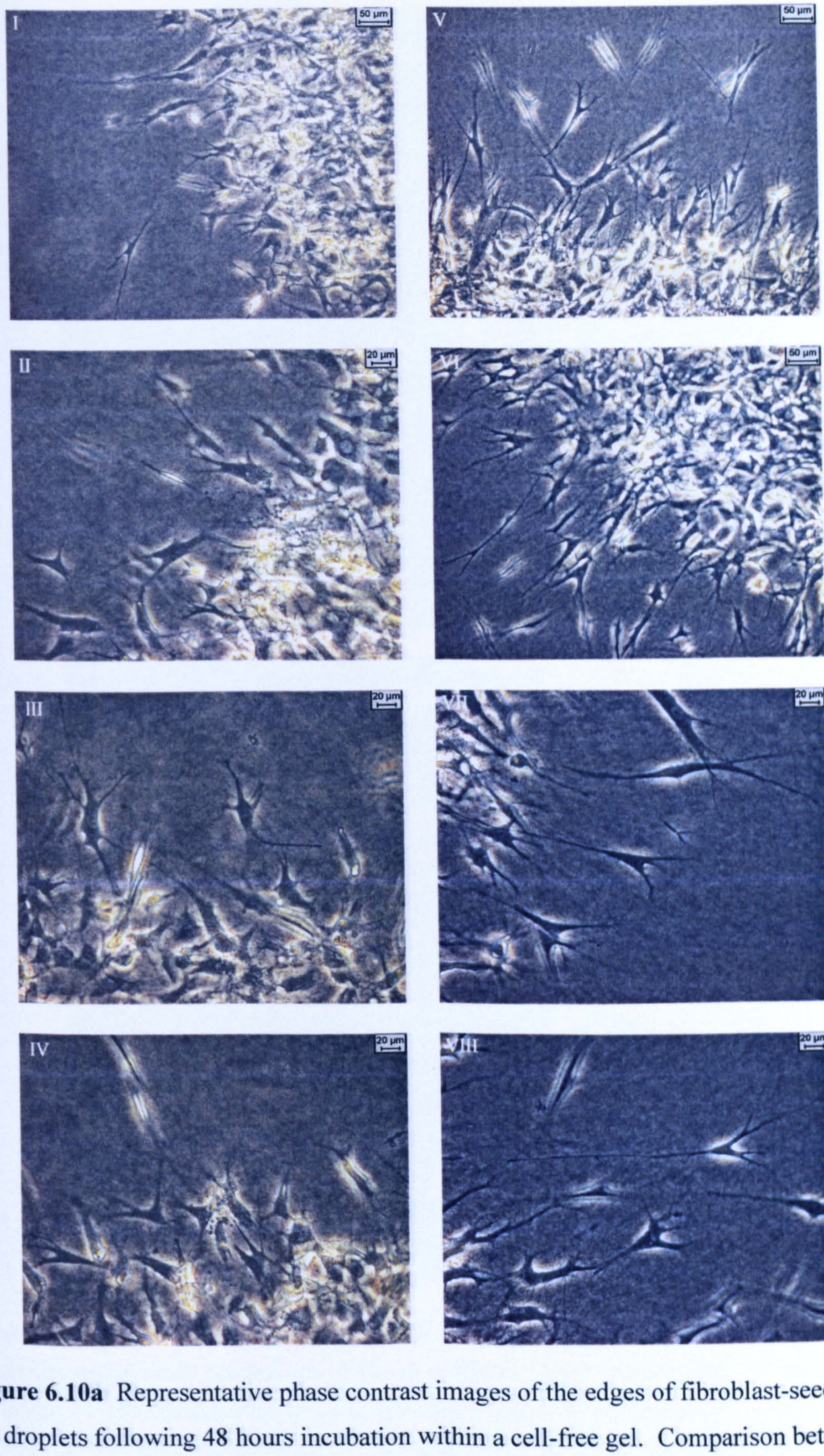

Figure 6.10a Representative phase contrast images of the edges of fibroblast-seeded gel droplets following 48 hours incubation within a cell-free gel. Comparison between cells in the control where ES was absent (I to IV) and cells exposed to 1 µg/ml ES (V to VIII).

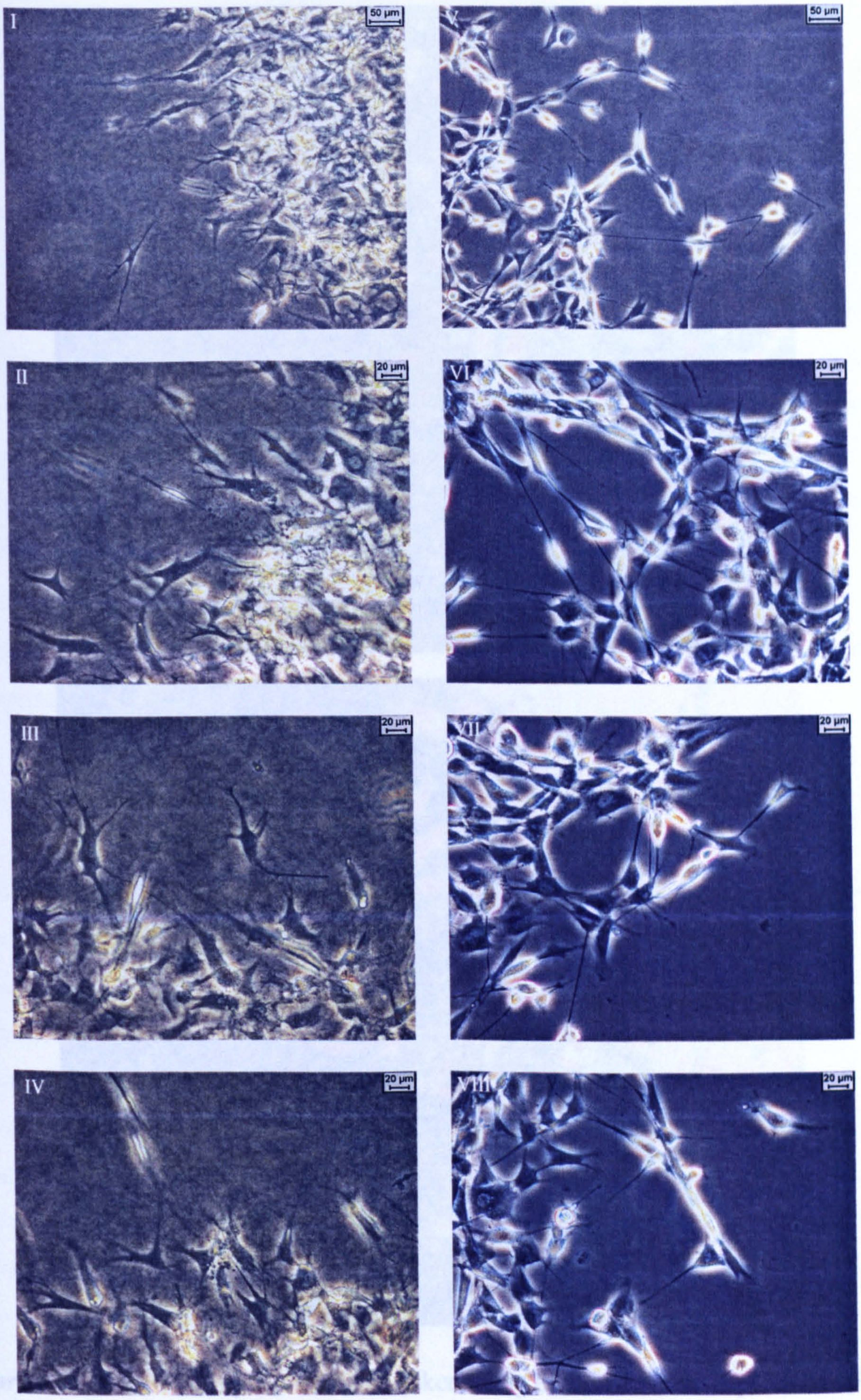

Figure 6.10b Representative phase contrast images of the edges of fibroblast-seeded gel droplets following 48 hours incubation within a cell-free gel. Comparison between cells in the control where ES was absent (I to IV) and cells exposed to 10 µg/ml ES (V to VIII).

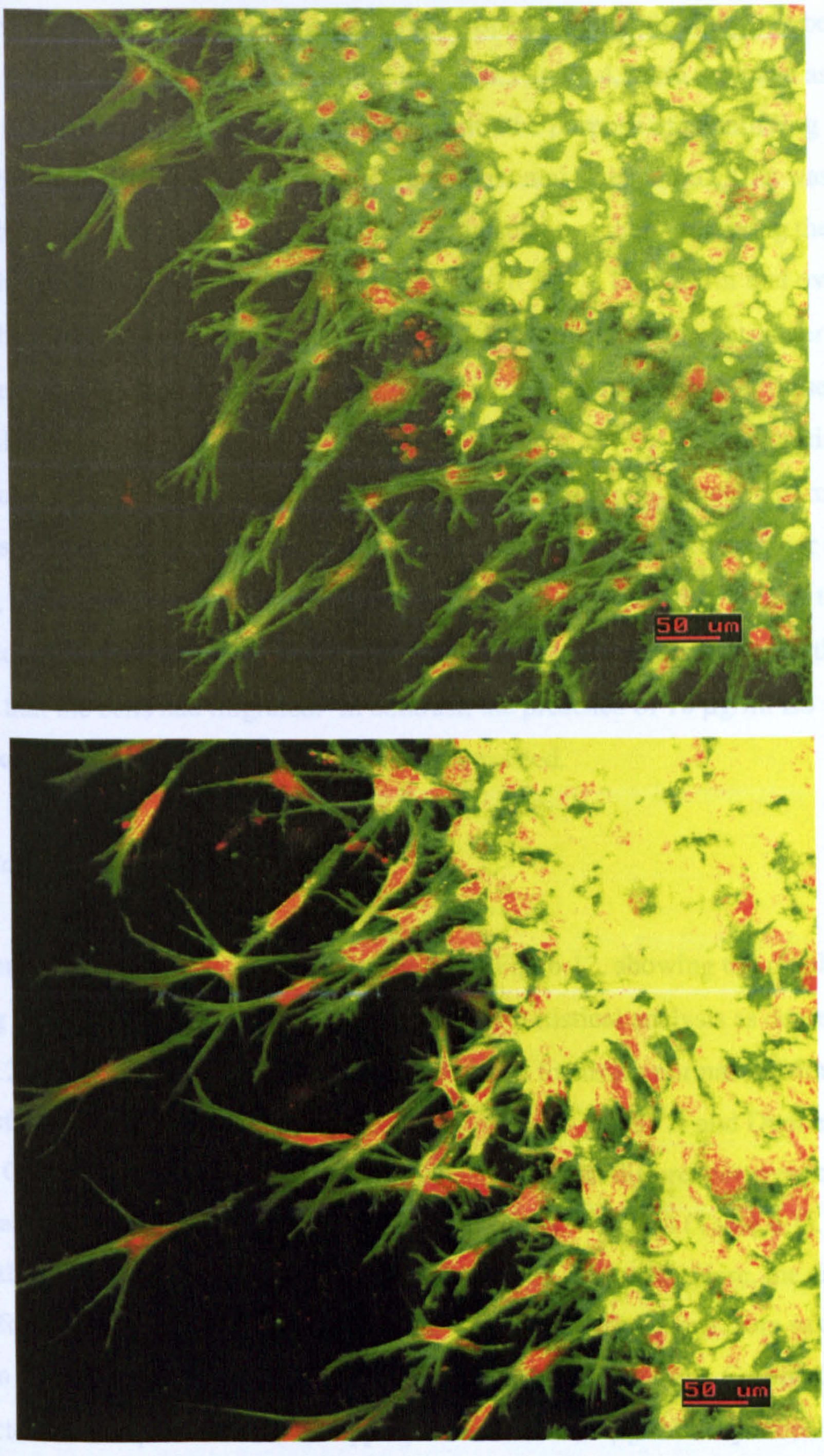

Figure 6.11 Z series of optical sections, taken using confocal microscope and displayed as maximum intensity projections of all the sections. Representative images showing the edges of fibroblast-seeded gel droplets following 48 hours incubation embedded within cell-free gels. Appearance of cells in the absence of ES (control) (*top*) or in the presence of 1 μg/ml ES (*bottom*). Cells fixed and stained with FITC-phalloidin and propidium iodide.

Low magnification phase contrast images of all droplets, taken after they had been incubated for 0 or 24 hours, as exemplified in Fig. 6.3 and 6.4, were analysed as described in section 6.2 and Fig. 6.1. This was with the purpose of quantifying the extent of cell migration out of each droplet in a horizontal orientation. This was achieved by first counting the number of migrating cells and then measuring the linear distance that each had travelled. The results shown in Fig. 6.12 confirm that over the 24 hour incubation period, the number of cells that had migrated per μm perimeter of each cell droplet was highest in the presence of 5 μg/ml ES. The distances that these cells had travelled were also amongst the highest recorded (Fig. 6.13). Cells migrating in the presence of 1 μg/ml ES were more numerous than those migrating under control conditions. They also appeared to have travelled slightly further. The number of cells migrating in the presence of 0.1 μg/ml ES was slightly lower than that seen in the relevant control, where ES was absent. There appeared to be no difference in the distances that the cells had migrated. In contrast, the presence of 10 μg/ml ES inhibited the number of migrating cells and the distances travelled.

6.3.1.1 Statistical analysis

In addition to visual observations, data taken from Fig. 6.12, showing the number of migrating cells per μm perimeter, were subjected to statistical analysis as described in section 6.2.1.1. Firstly, all the data was square rooted to ensure normal distribution. The transformed data were then compared using one-way ANOVA and Dunnett's Multiple Comparison Test. In both experiments, significant differences were observed between all larval ES-treated assays and their controls ($P < 0.001$) (Table 6.1). The distance that each cell had migrated (Fig. 6.13) was also analysed. Here, the data were log transformed to ensure normal distribution. The Geometric means from each dataset were then compared using one-way ANOVA and Dunnett's Multiple Comparison Test. As expected, in comparison with the appropriate controls, 5 μg/ml ES yielded statistically significantly higher migration ($P < 0.001$), while 0.1 μg/ml ES had no effect ($P > 0.05$) (Table 6.2). In contrast, 10 μg/ml ES exerted a significant inhibitory effect ($P < 0.001$), while 1 μg/ml ES promoted migration ($P < 0.05$).

a.

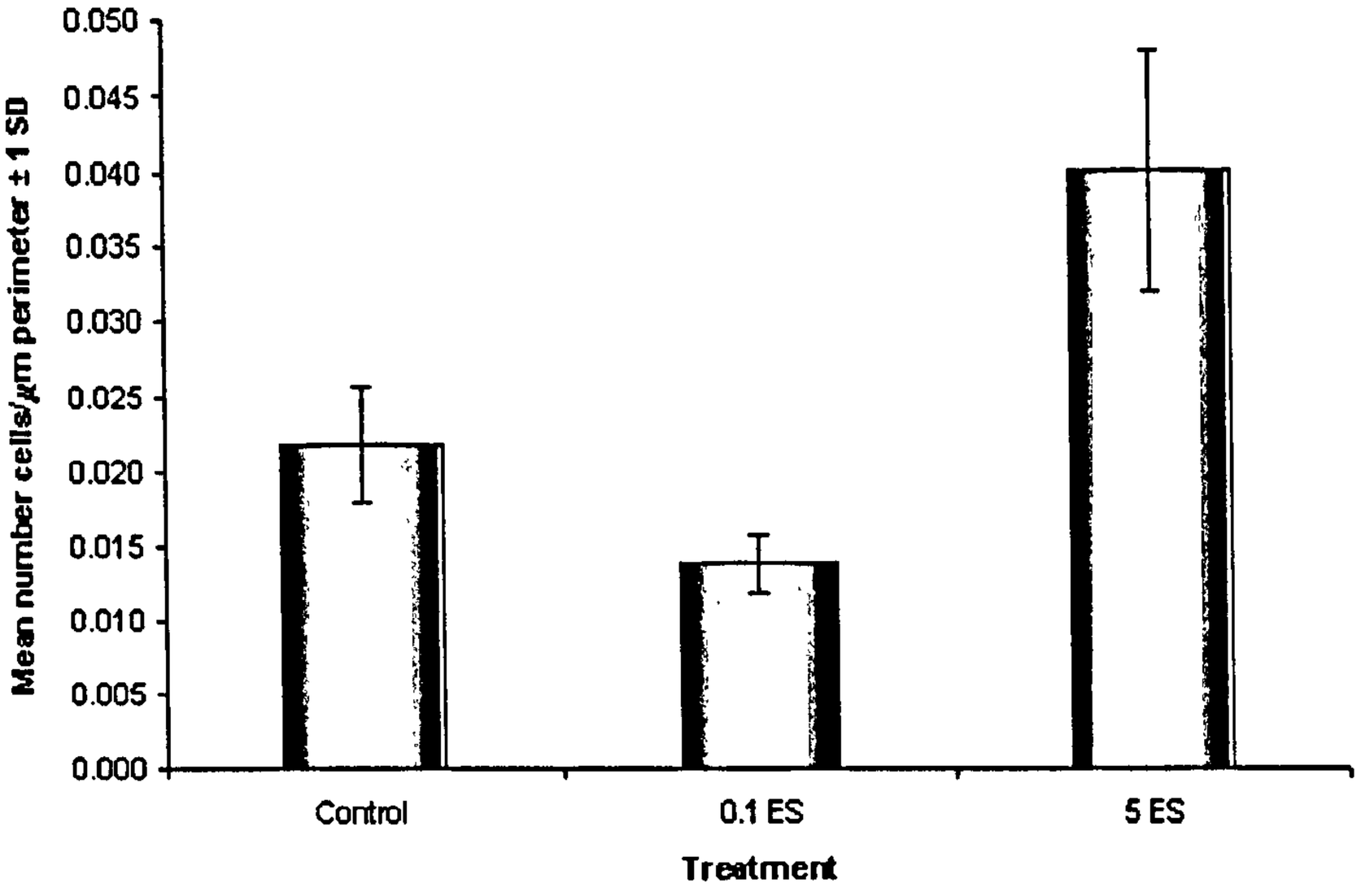

b.

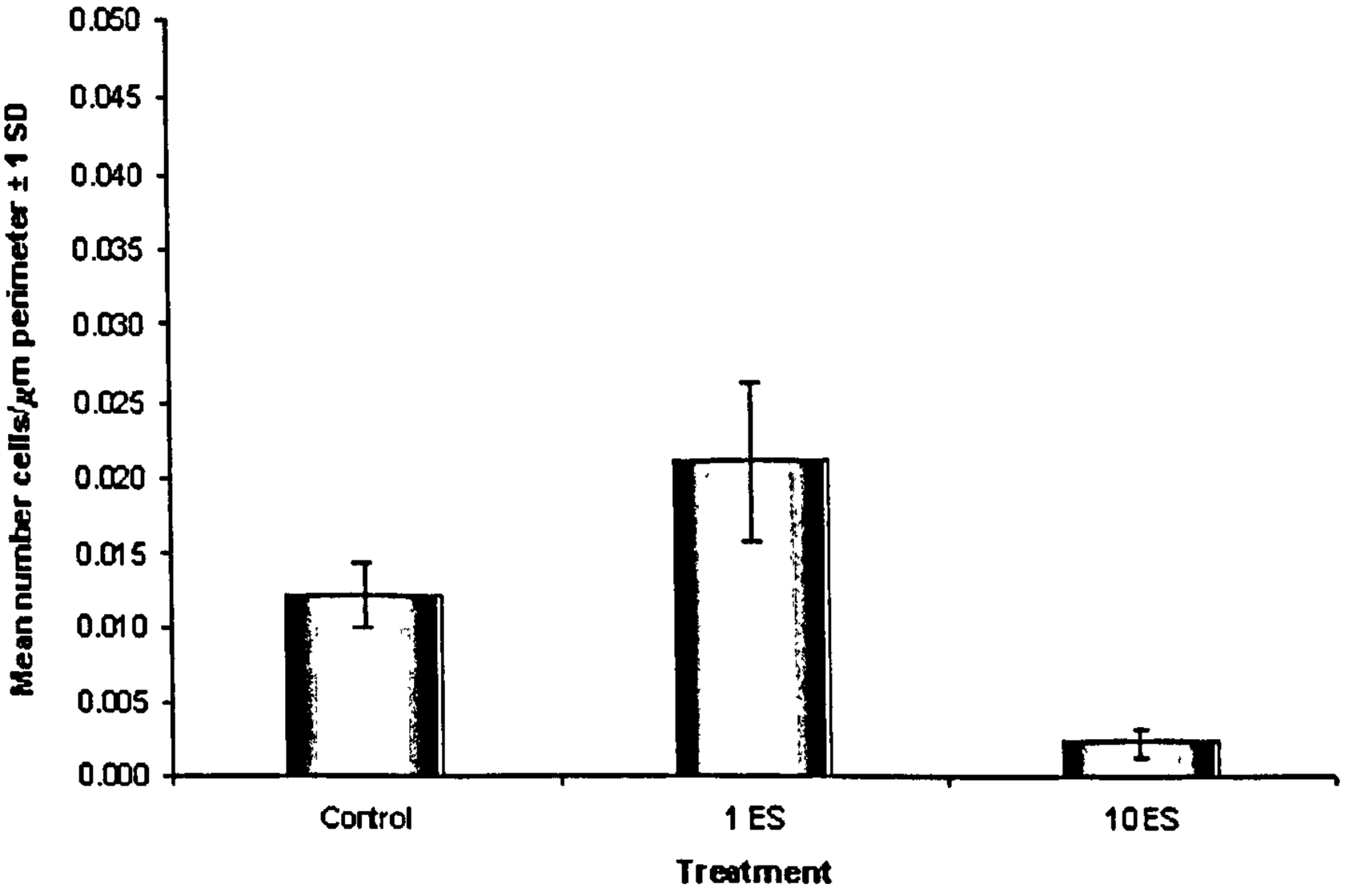

Figure 6.12 Fibroblast migration from 2 μl cell-seeded gel droplets within three-dimensional *in vitro* wound assays over 24 hours. Results expressed as number of migrating cells per μm perimeter of droplet. Each value represents the mean of five replicate droplets ± 1 standard deviation. **a.** Migration in the absence of ES (control) or in the presence of 0.1 μg/ml ES (0.1 ES) or 5 μg/ml ES (5 ES). **b.** Migration in the absence of ES (control) or in the presence of 1 μg/ml ES (1 ES) or 10 μg/ml ES (10 ES).

a.

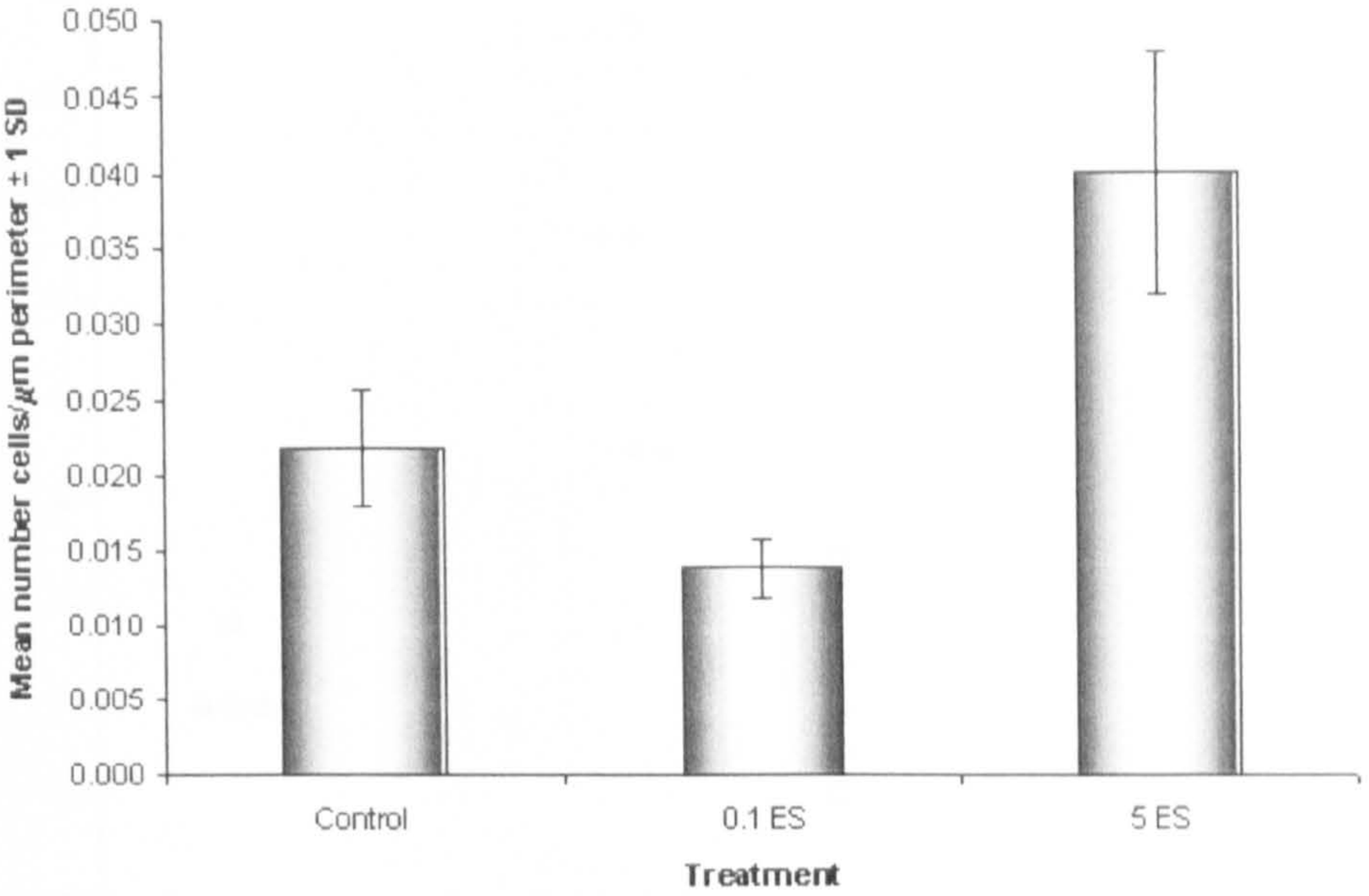

b.

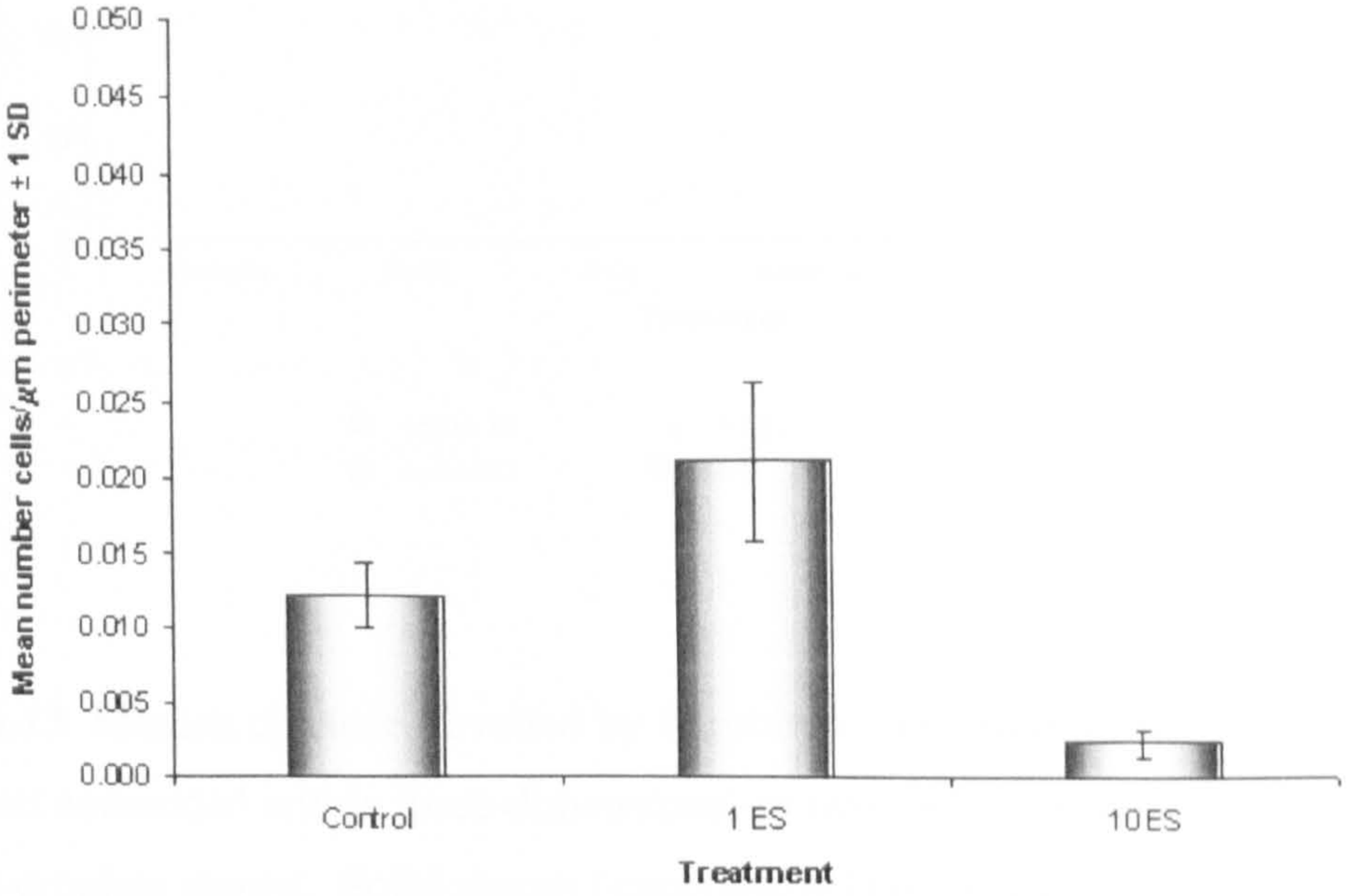

Figure 6.12 Fibroblast migration from 2 μl cell-seeded gel droplets within three-dimensional *in vitro* wound assays over 24 hours. Results expressed as number of migrating cells per μm perimeter of droplet. Each value represents the mean of five replicate droplets ± 1 standard deviation. **a.** Migration in the absence of ES (control) or in the presence of 0.1 μg/ml ES (0.1 ES) or 5 μg/ml ES (5 ES). **b.** Migration in the absence of ES (control) or in the presence of 1 μg/ml ES (1 ES) or 10 μg/ml ES (10 ES).

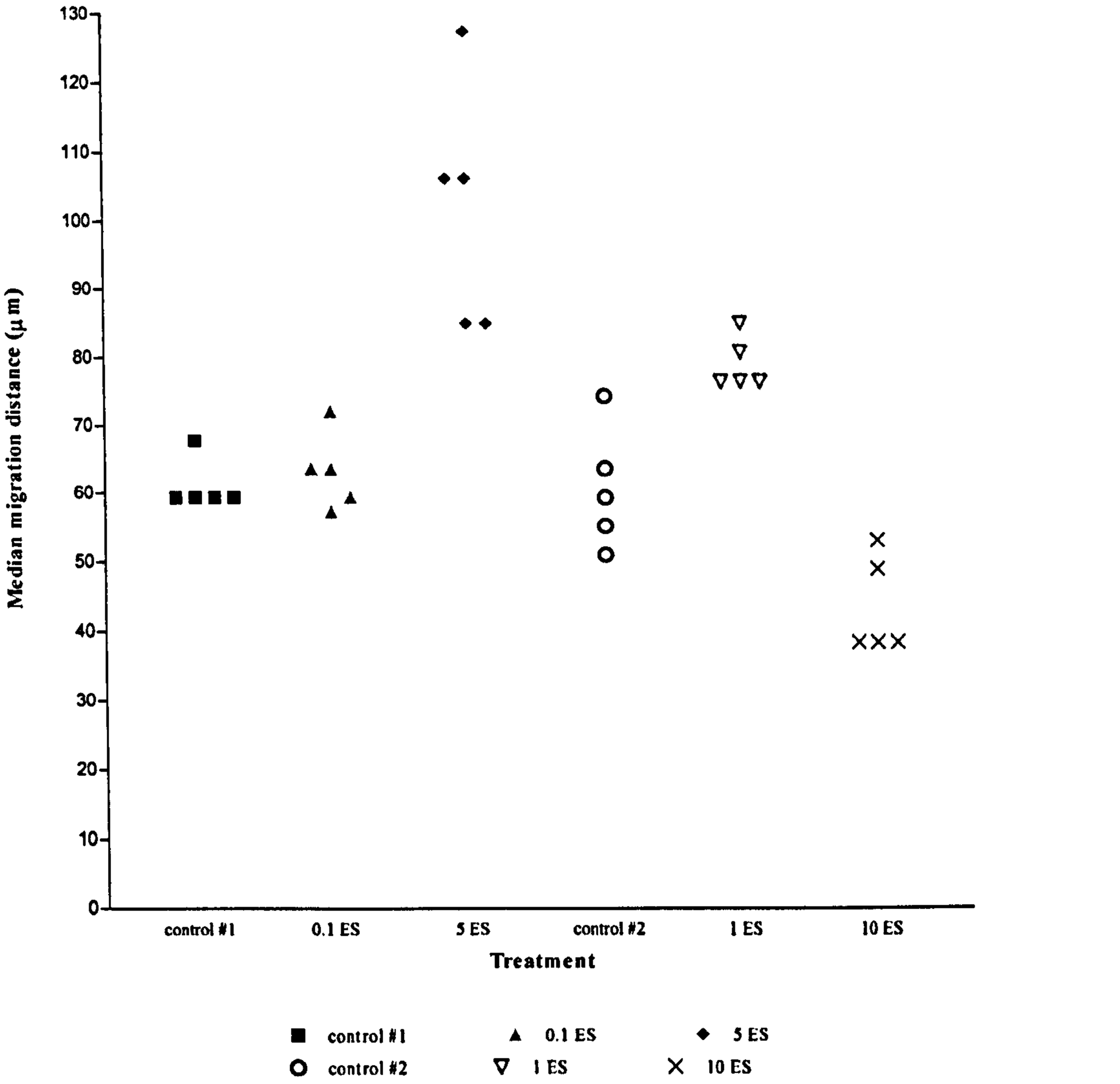

Figure 6.13 Median distance travelled by fibroblasts migrating from each cell-seeded gel droplet embedded within three-dimensional *in vitro* wound assays. Values from five replicate droplets shown. Solid shapes (experiment 1) represent distance travelled in the absence of ES (control #1) or in the presence of 0.1 μg/ml ES or 5 μg/ml ES. Open shapes (experiment 2) represent distance travelled in the absence of ES (control #2) or in the presence of 1 μg/ml ES or 10 μg/ml ES.

Experiment 1. One-way ANOVA: P < 0.0001. Bartlett's: P > 0.05, equal variance.

Larval ES (μg/ml)	Control (ES absent)	
	P value	95 % CI of difference
0.1	< 0.001	0.008 to 0.053
5	< 0.001	-0.074 to -0.029

Experiment 2. One-way ANOVA: P < 0.0001. Bartlett's: P > 0.05, equal variance.

Larval ES (μg/ml)	Control (ES absent)	
	P value	95 % CI of difference
1	< 0.001	-0.056 to -0.012
10	< 0.001	0.043 to 0.0869

Table 6.1 Statistical analysis of fibroblast migration data from three-dimensional *in vitro* wound assays. Comparison between larval ES-treated and control assays in the number of migrating cells per μm droplet perimeter using one-way ANOVA and Dunnett's Multiple Comparison Test. Confidence Interval referred to as CI. $P \leq 0.05$ taken as significant. Bartlett's test for equal variance yielded P values > 0.05. Therefore, equal variance assumed.

Experiment 1. One-way ANOVA: P = 0.0001. Bartlett's: P > 0.05, equal variance.

Larval ES	Control (ES absent)	
(μg/ml)	P value	95 % CI of difference
0.1	ns	-0.130 to 0.035
5	< 0.001	-0.288 to -0.124

Experiment 2. One-way ANOVA: P < 0.0001. Bartlett's: P > 0.05, equal variance.

Larval ES	Control (ES absent)	
(μg/ml)	P value	95 % CI of difference
1	< 0.05	-0.139 to -0.004
10	< 0.001	0.051 to 0.187

Table 6.2 Statistical analysis of fibroblast migration data from three-dimensional *in vitro* wound assays. Comparison between larval ES-treated and control assays in the mean distance travelled by migrating cells from each droplet using one-way ANOVA and Dunnett's Multiple Comparison Test. Confidence Interval referred to as CI. $P \leq 0.05$ taken as significant. Bartlett's test for equal variance yielded P values > 0.05. Therefore, equal variance assumed.

The 95 % Confidence Intervals (CIs) of the differences between compared sample means, as shown in Table 6.1 and 6.2, provide a measure of the true differences between population means. These were therefore scrutinised in order to assess the importance of the significant differences described above. It was clear, just by viewing phase contrast images, that 5 μg/ml ES had a very positive influence upon cell migration. Hence, the CIs generated when results from this treatment were compared with those from the control, were regarded as indicating important significant differences.

With this in mind, it was clear that when the number of migrating cells was compared, between the control and the assay containing 0.1 μg/ml ES, the lower confidence limit of the CI generated was very low (Table 6.1). This indicated that although the means were different (as $P < 0.001$), the scientific relevance could not be stated without more data. However, in comparison with the control, no differences in cell morphology could be seen at the droplet edges, either by 24 or 48 hours incubation (Fig. 6.7a and 6.9a). In addition, there were no significant differences in terms of the distance that migrating cells had travelled (Table 6.2). It was therefore decided that within the three-dimensional assay environment, 0.1 μg/ml ES had no decisive influence over fibroblast migratory behaviour.

When the number of migrating cells and the distances travelled were compared between the control and the assay containing 1 μg/ml ES, the lower confidence limits of the CIs generated were also low (Table 6.1 and 6.2). This indicated the need for more data in order to make clear conclusions. However, the cells exposed to 1 μg/ml ES appeared to be morphologically different to those within the control, particularly after 48 hours incubation (Fig. 6.10a). In addition, it was visibly apparent that following 48 hours, the cells exposed to ES had migrated further (Fig. 6.6 and 6.10a. It may therefore be tentatively concluded that 1 μg/ml ES did exert a stimulatory effect upon migration.

When 10 μg/ml ES was tested against the control, the lower confidence limit of the CI, resulting from a comparison of the distance travelled by migrating cells, was low (Table 6.2). This indicated that, although the means were different (as $P < 0.001$), the scientific relevance could not be stated without more data. However, in comparing the number of

migrating cells, the lower confidence limit of the CI calculated (Table 6.1) was sufficiently high to suggest a scientifically important difference. In addition, the circumferences of the cell droplets exposed to 10 μg/ml ES had decreased in size. Here, it was noted that the image of each droplet at 0 hours incubation overlapped the circumference of the same droplet's image following 24 hours incubation (Fig. 6.14). Also, differences in cell morphology were clearly observed (Fig. 6.8b and Fig. 6.10b). It was therefore concluded that 10 μg/ml ES did exert an influence over fibroblast behaviour.

The extent of cell migration out of each droplet in a vertical orientation was also assessed using confocal microscopy. Here, a number of z series' of optical sections were taken of droplets after they had been incubated for 48 hours within the assays that had been analysed above. Confocal images were also taken of droplets that had been assembled within separate assays and immediately fixed without any incubation (0 hours incubation). All droplets within assays fixed at 0 hours were analysed. Of those incubated for 48 hours, droplets were selected at random by the microscope operator. The area imaged within each droplet was also chosen arbitrarily. Within each z series, sections were categorised into particular zones, depending on how far they lied from the main body of the droplet (Fig. 6.15a). Cells visible within each section were then allocated to the appropriate zone (Fig. 6.15b). As shown in the example image, no cells were found above or below the droplets that had been fixed at 0 hours incubation (Fig. 6.16a). This confirmed that any cells found outside of the droplets that had been incubated for 48 hours had most likely migrated to these locations. Evidence for the occurrence of migration is exemplified by Fig. 6.16b. As shown in Fig. 6.17 more cells, in both the control and 1 μg/ml ES, were found in zones closer to the droplet. However, there was little difference between treatments. As each z series image incorporated only a very small surface area it is reasonable to propose that more images were required to allow conclusions to be drawn.

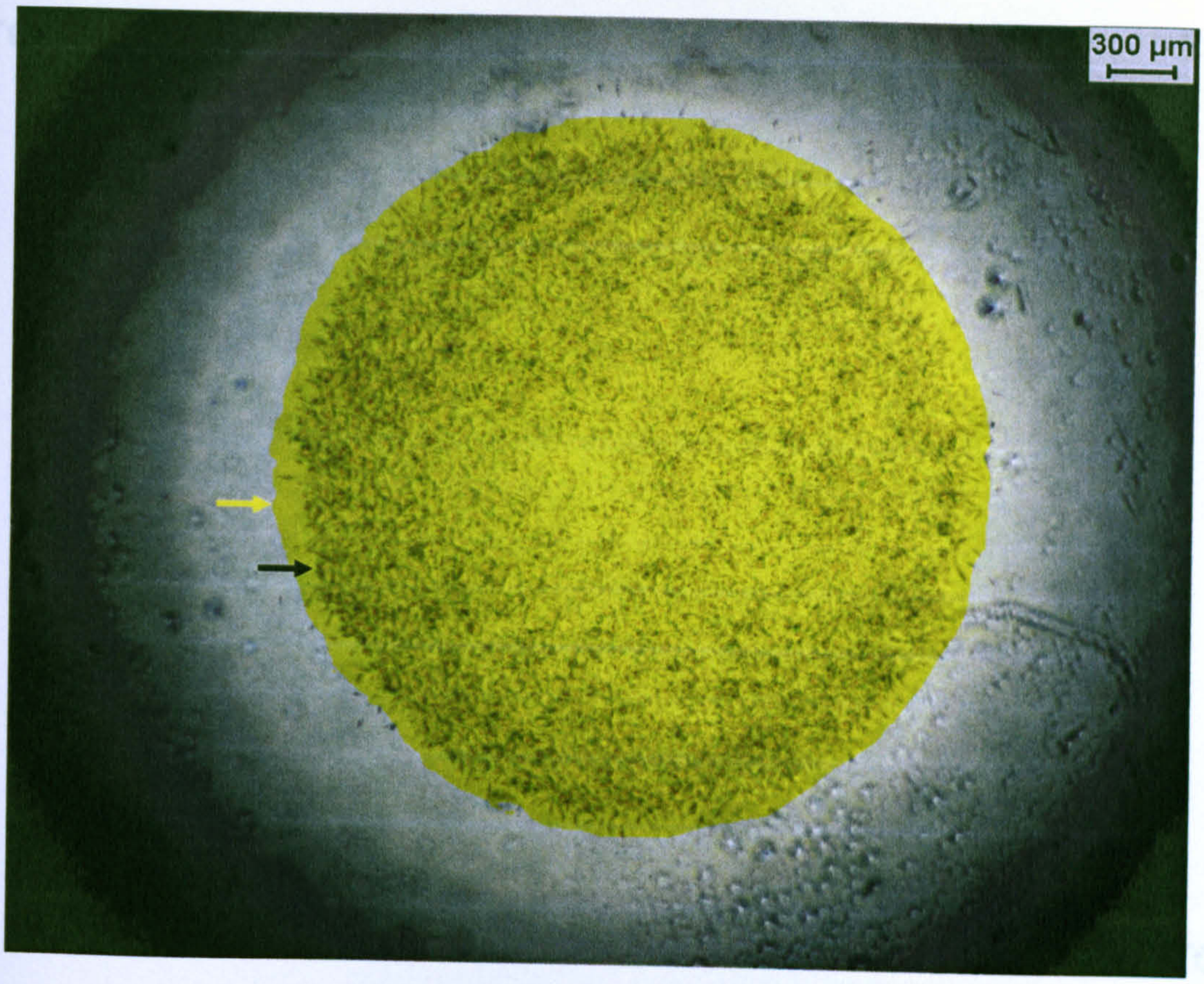

Figure 6.14 Fibroblast-seeded gel droplet within three-dimensional *in vitro* wound assay exposed to 10 µg/ml larval ES. Surface area coverage of droplet at 0 hours highlighted in yellow. Image of same droplet after 24 hours incubation seen underneath. Yellow arrow indicates border of droplet at 0 hours. Black arrow denotes border of droplet at 24 hours.

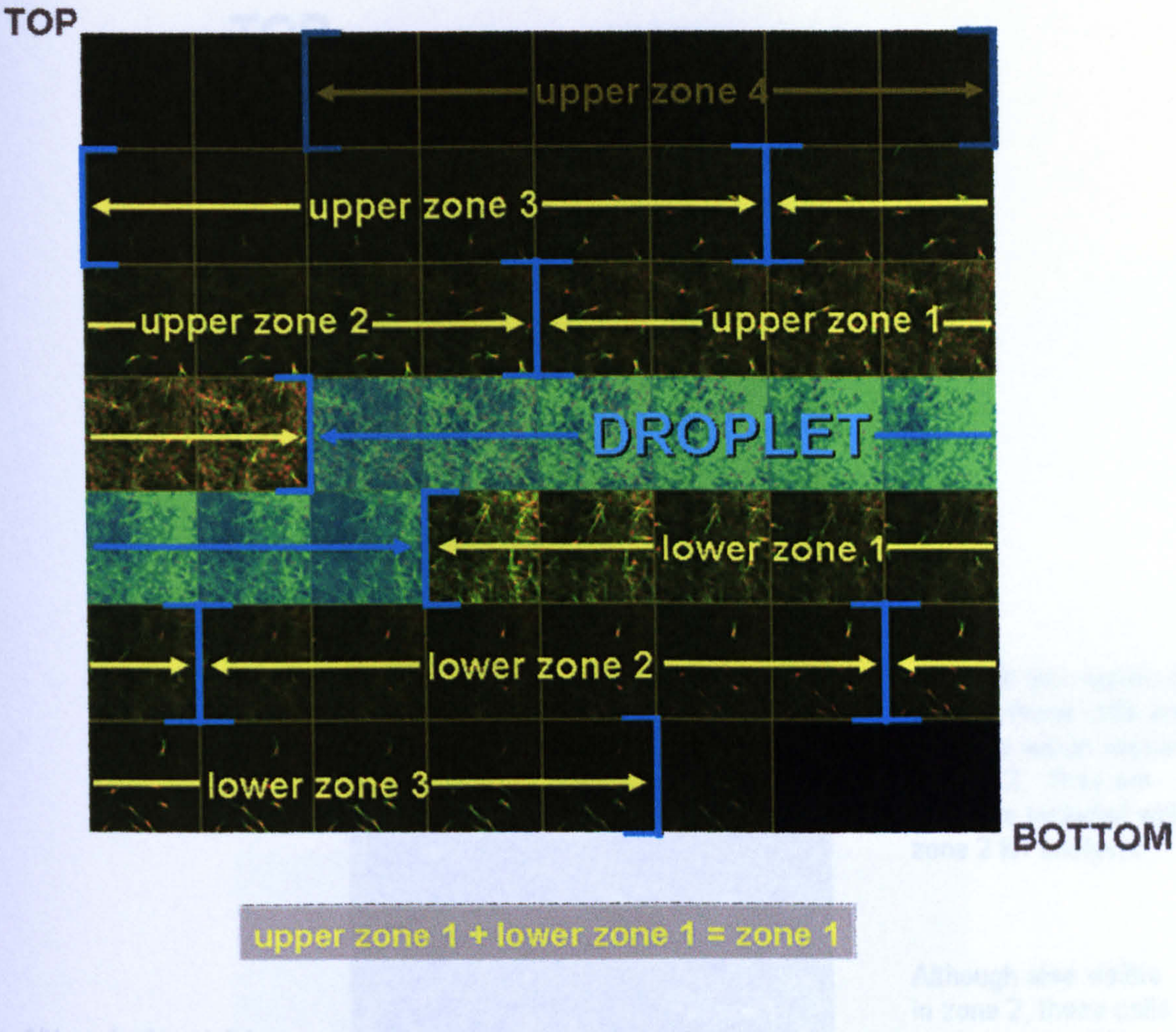

Figure 6.15a Illustration of how fibroblast migration in a vertical orientation, above and below the cell-seeded gel droplet, was quantified. A z series of optical sections was taken using a confocal microscope. These were then analysed to determine the position of cells contained within the droplet. The optical sections surrounding the droplet were categorised into zones that were 6 sections deep. Cells that were positioned within sections included in each zone were counted. Counts within the lower and upper regions of each zone were then combined. The presence of both upper and lower regions were required for the zone to be included in the analysis. In this example, only the upper region of zone 4 was visible. Zone 4 was therefore discounted.

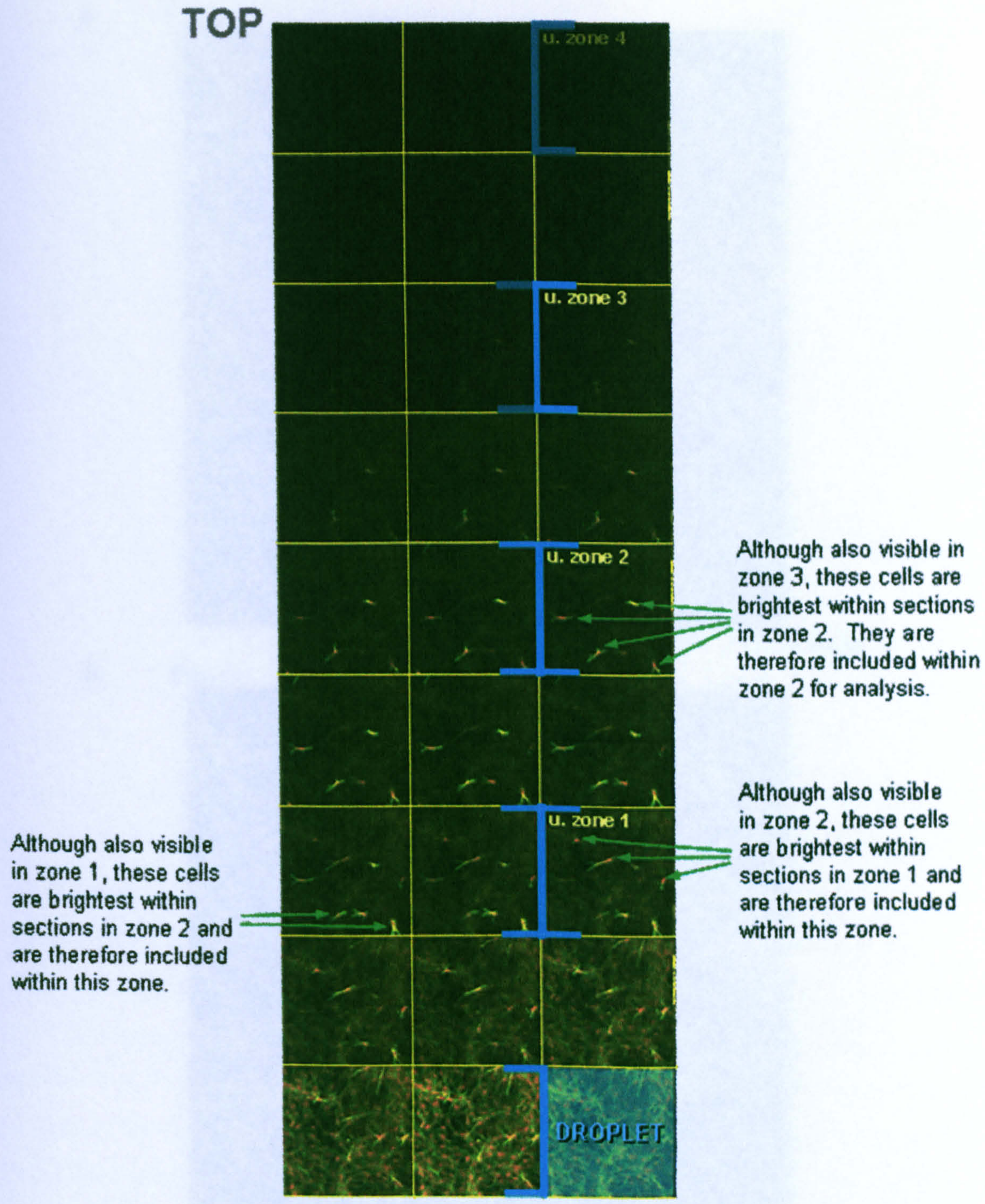

Figure 6.15b The top 27 optical sections taken from the z series of sections shown in Fig. 6.15a. Images taken using a confocal microscope. Illustration of how cells present within sections were allocated to particular zones. This was dependent upon the position of the section in which they appeared brightest.

a. Top →

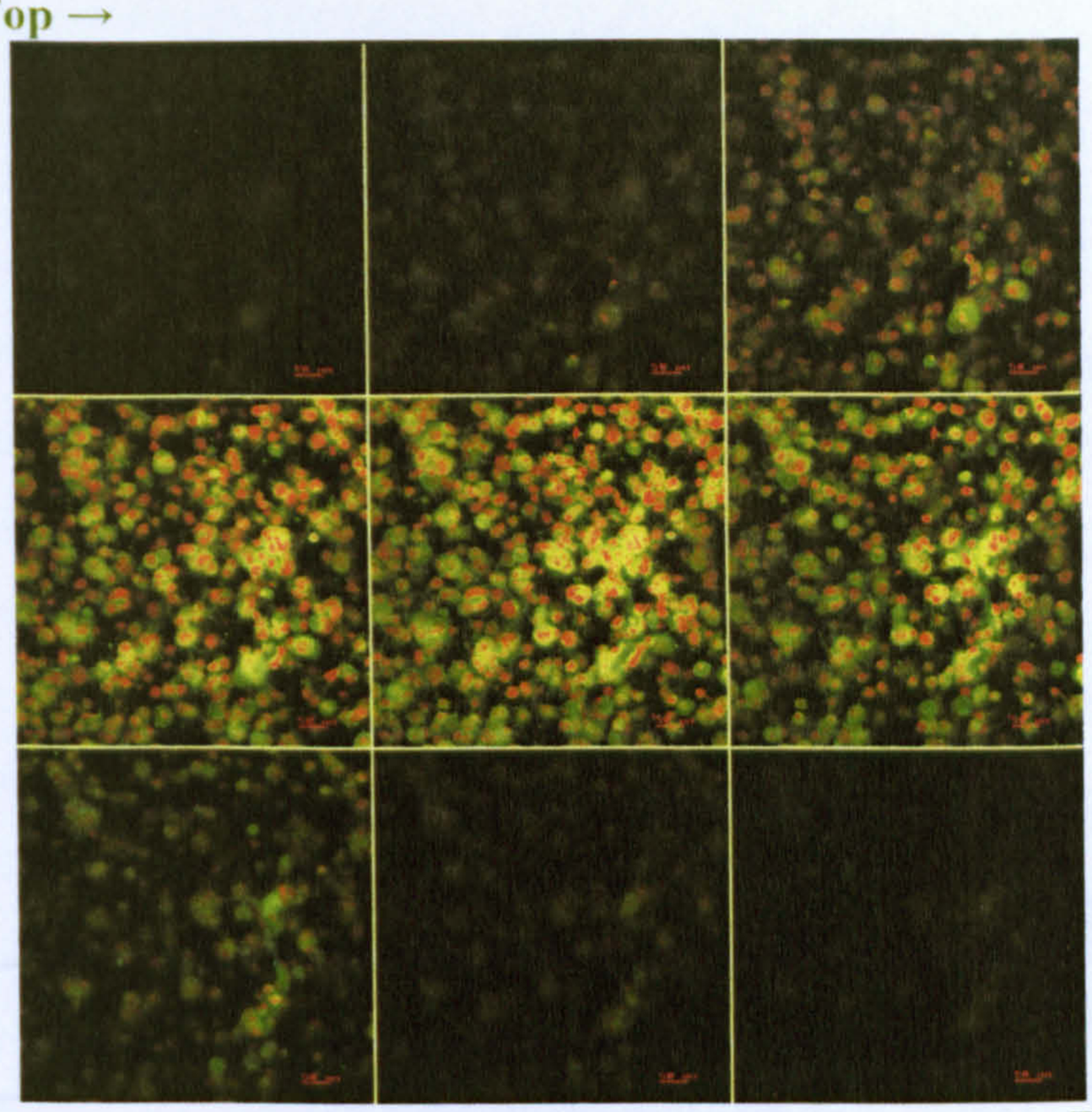

→ Bottom

b. Top →

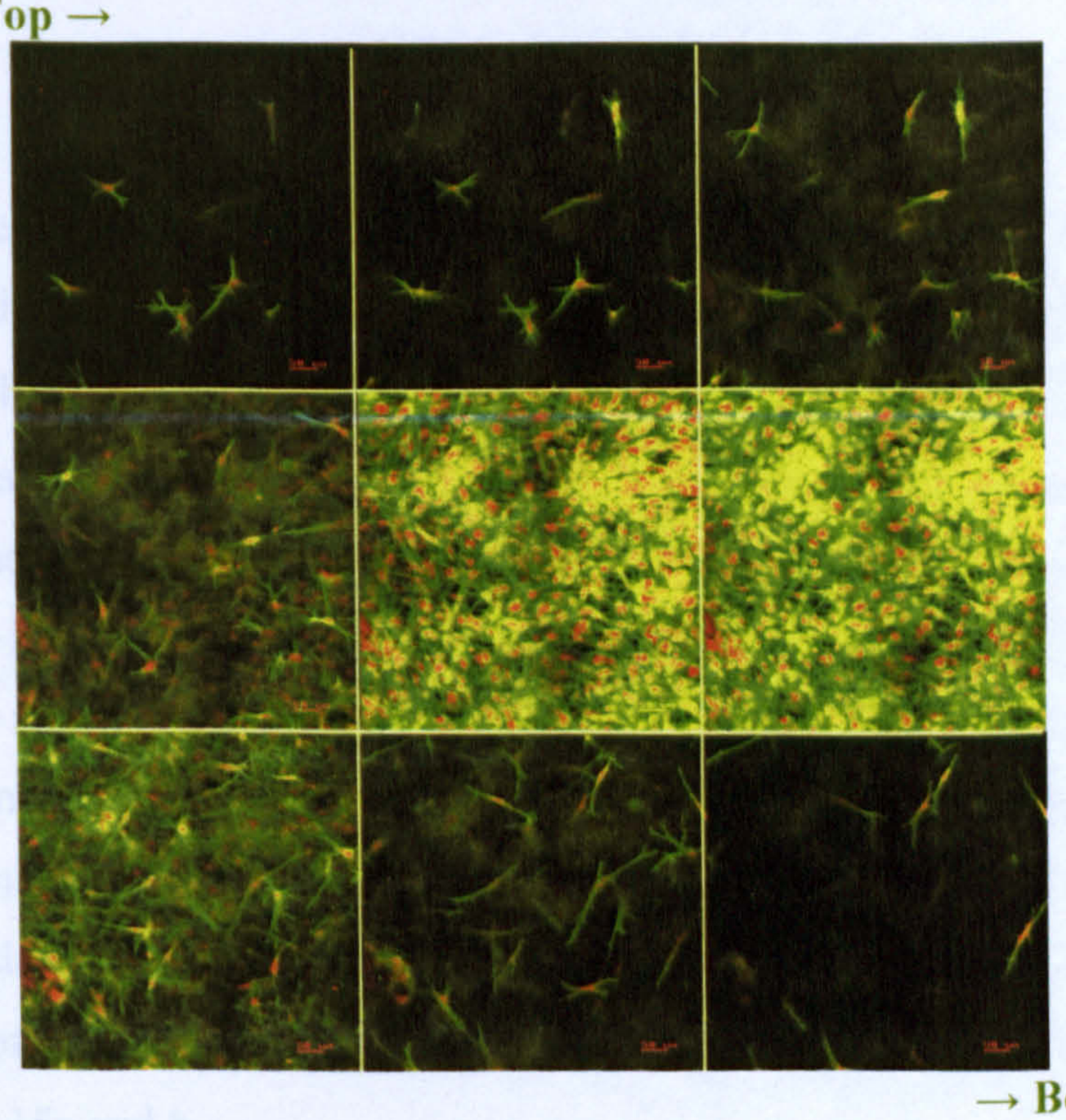

→ Bottom

Figure 6.16 Z series of 54 optical sections, taken using confocal microscope and displayed in a gallery, from left to right, moving from top to bottom. Each of the nine images in the gallery represents a composite of 6 sequential optical sections. Position of fibroblasts within, above or below a cell-seeded gel droplet embedded within a cell-free gel. **a.** Droplet exposed to 1 μg/ml ES and fixed immediately after assay assembly (0 hours incubation). **b.** Droplet in the absence of ES and fixed after 48 hours incubation. Cells stained with FITC-phalloidin and propidium iodide.

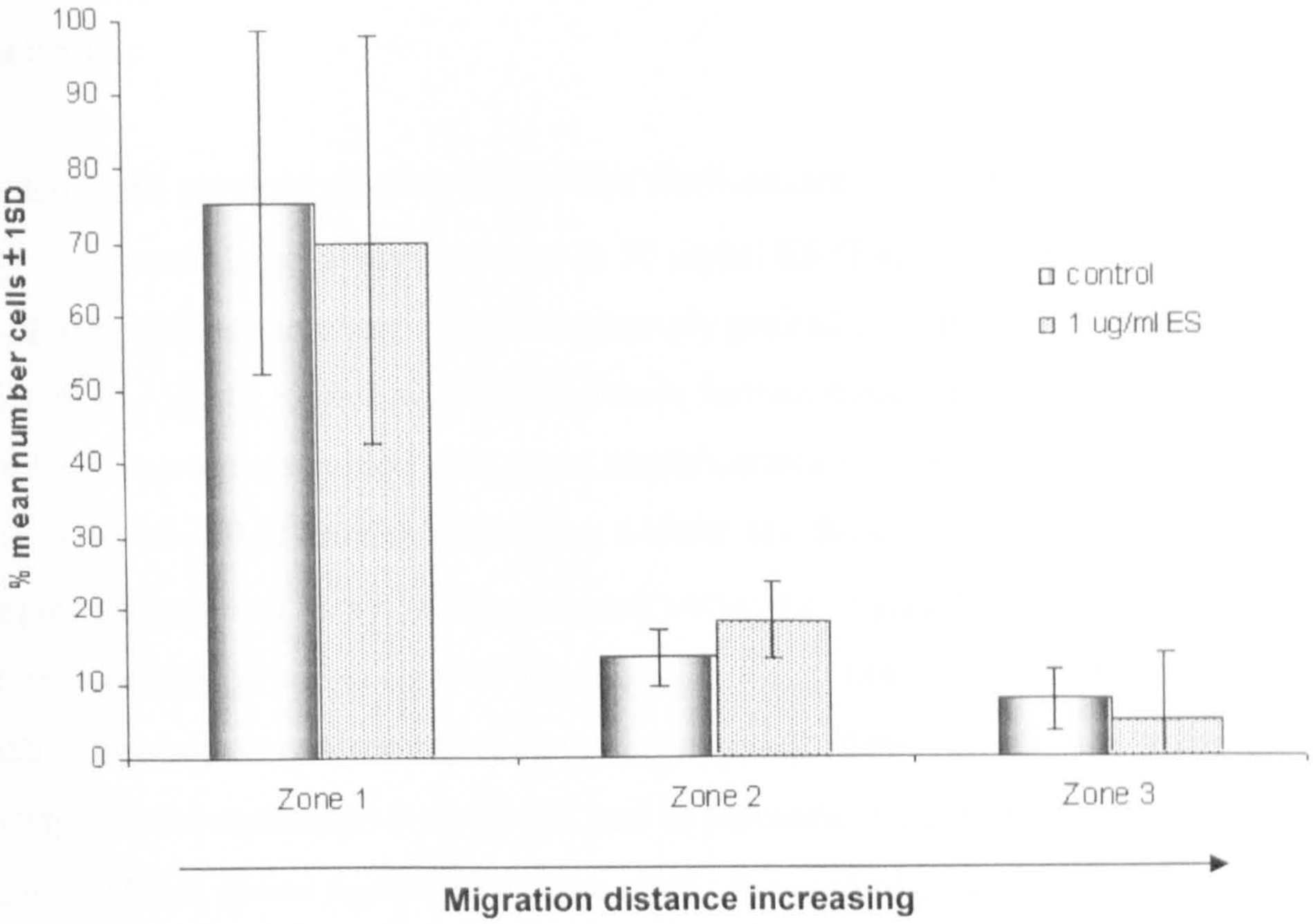

Figure 6.17 Mean number of fibroblasts that had migrated in a vertical orientation from cell-seeded gel droplets over 48 hours, either in the absence of ES (control) or in the presence of 1 μg/ml ES. For each treatment, four confocal z series images were analysed. For each z series image, the number of cells within each of the zones was counted. The mean number of cells within each zone was then derived using data from the four z series images analysed for each treatment. The total number of cells present within all of the zones within each image was also calculated and the mean total number of cells determined. In order to compare the distribution of migrating cells between zones, the percentage contribution of each zone's mean cell count to the mean total count was calculated as follows: (zone n mean cell count / mean total cell count) × 100. Determination of zones and the categorisation of cells into each zone was performed as shown in Fig. 6.15a and b.

6.3.2 Three-dimensional in vitro wound assay – fibroblast morphology and matrix organisation

As noted in the previous chapter, strand-like fibril connections were observed between adjacent cells within gel assays exposed to 10 μg/ml ES (Fig. 5.21). Such connections proved to be difficult to observe between densely packed cells in the assays described in section 6.3.1. Hence to investigate these fibrils further, three-dimensional *in vitro* wound assays were assembled with slight modifications to those utilised within section 6.3.1. Here, one 20 μl droplet, containing a lower cell density of 3×10^5 cells/ml, was incorporated into each assay. Assays treated with either 1 μg/ml ES or 5 μg/ml ES were tested and compared with a control. As shown in Fig. 6.18a, cells appeared to be similar following assay assembly (0 hours incubation). However, after 24 hours the majority of cells exposed to 1 μg/ml ES, and in particular 5 μg/ml ES, were less rounded and had spread further than those within the control (Fig. 6.18b). In places, within the assay containing 5 μg/ml ES, intercellular parallel-aligned connective fibrils could also be observed. By 48 hours (Fig. 6.18c), cells within the control were rounded. In contrast, cells within both concentrations of larval ES appeared to be well spread. Connective fibrils between many cells within 5 μg/ml ES could clearly be seen and the gel was more translucent than within the other assays.

6.4 Discussion

Results presented within Chapter 4 suggest that larval ES at a concentration of 0.1 μg/ml, enhances fibroblast migration across fibronectin-coated surfaces. However, as previously discussed, fibroblasts behave differently within two dimensions than within more familiar *in vivo*-like three-dimensional ECM environments. The migration of fibroblasts within collagen/fibronectin gels in response to various concentrations of ES was therefore examined. Results demonstrated that ES modified fibroblast migratory behaviour in a dose-dependent manner. In comparison with the relevant controls, ES concentrations of 1 and 5 μg/ml significantly increased both the number of migrating cells and the distances they had travelled away from the cell droplet. Out of the

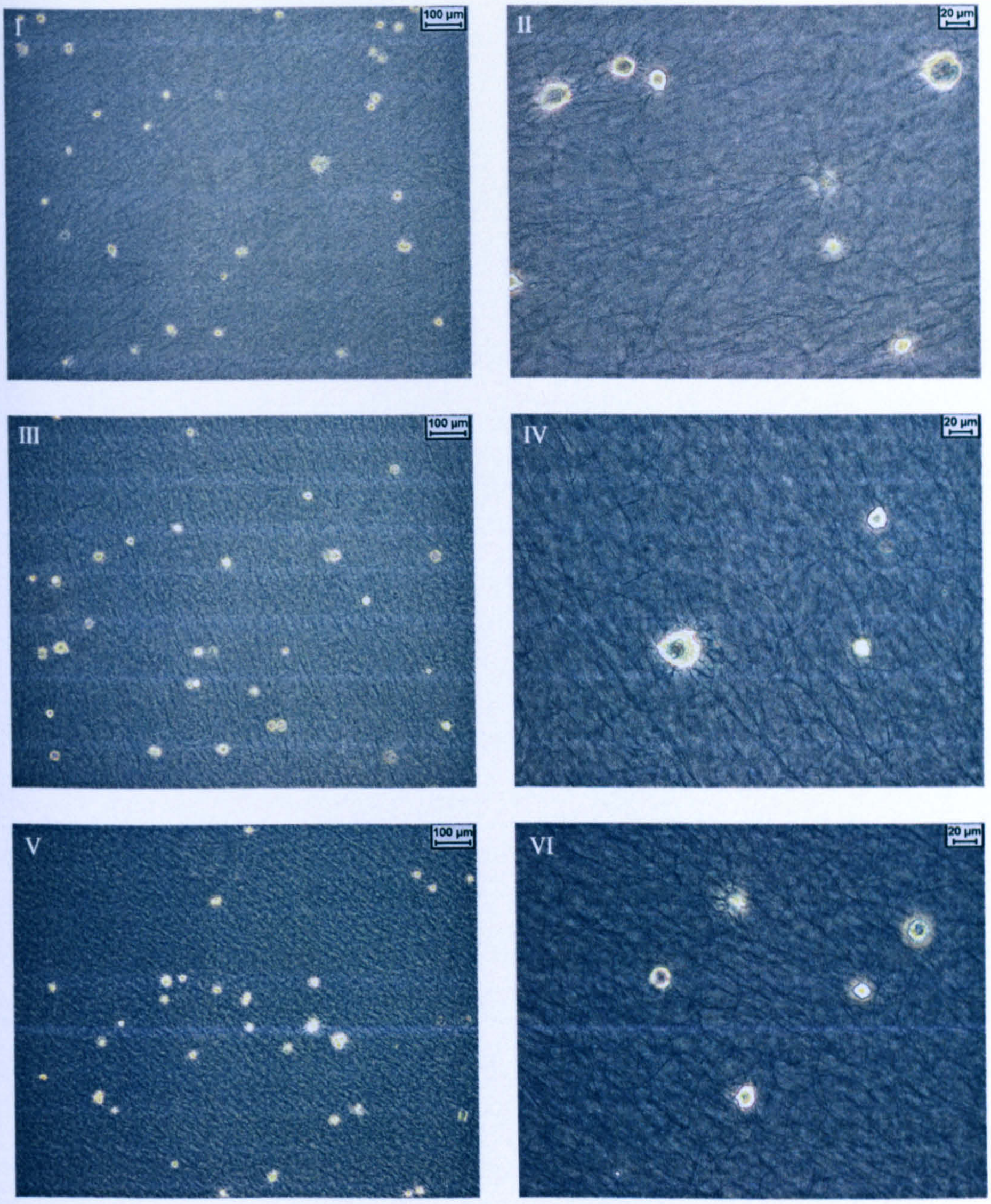

Figure 6.18a Representative phase contrast images showing fibroblasts within three-dimensional *in vitro* wound assays, at a seeding density of 3×10^5 cells/ml, immediately following assay assembly (0 hours incubation). Appearance of cells in the absence of ES (control) (I, II) or in the presence of 1 µg/ml ES (III, IV) or 5 µg/ml ES (V, VI).

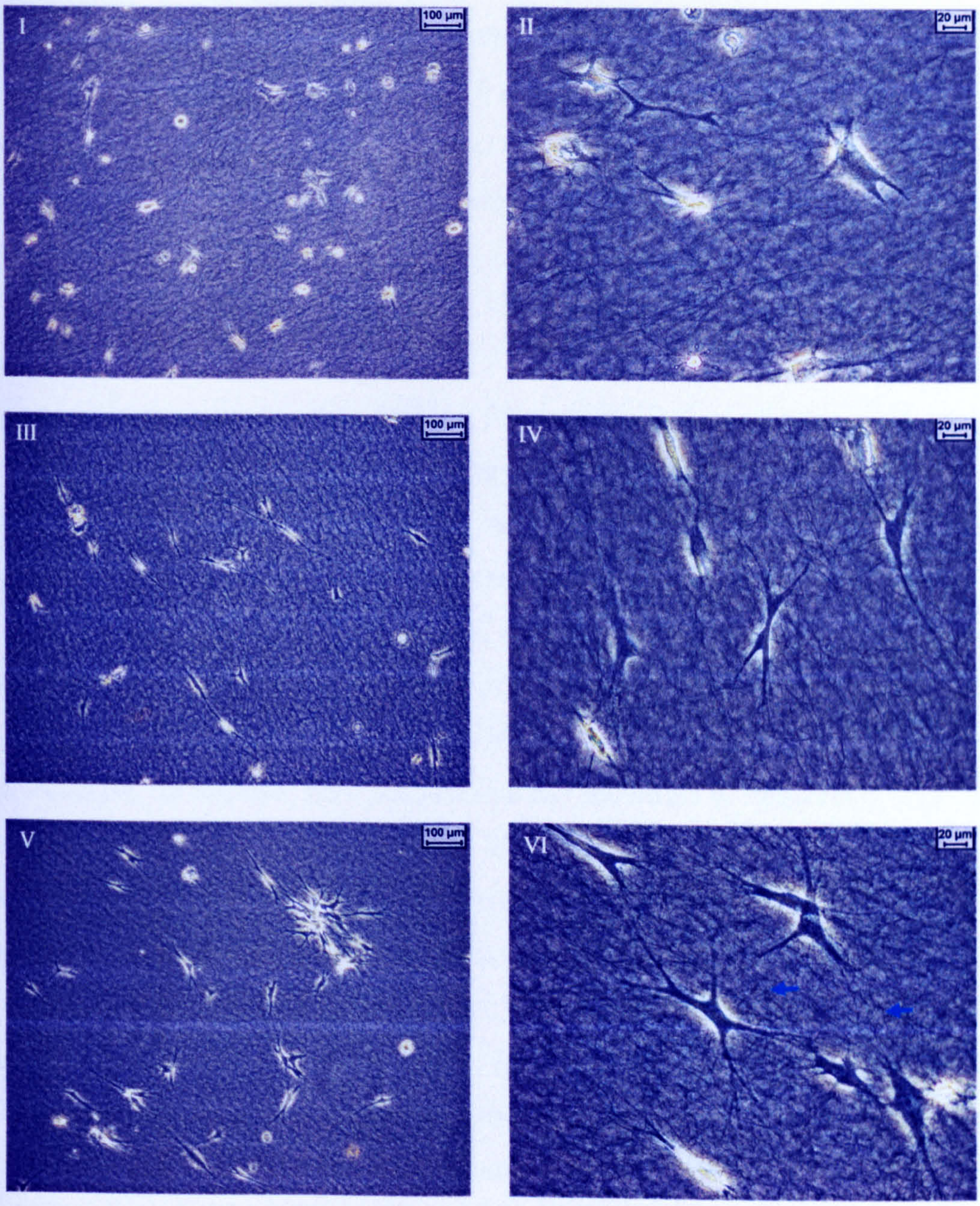

Figure 6.18b Representative phase contrast images showing fibroblasts within three-dimensional *in vitro* wound assays, at a seeding density of 3×10^5 cells/ml, following 24 hours incubation. Appearance of cells in the absence of ES (control) (I, II) or in the presence of 1 µg/ml ES (III, IV) or 5 µg/ml ES (V, VI). Aligned, strand-like connective fibrils have just become visible within the assay exposed to 5 µg/ml ES, as indicated by the blue arrows.

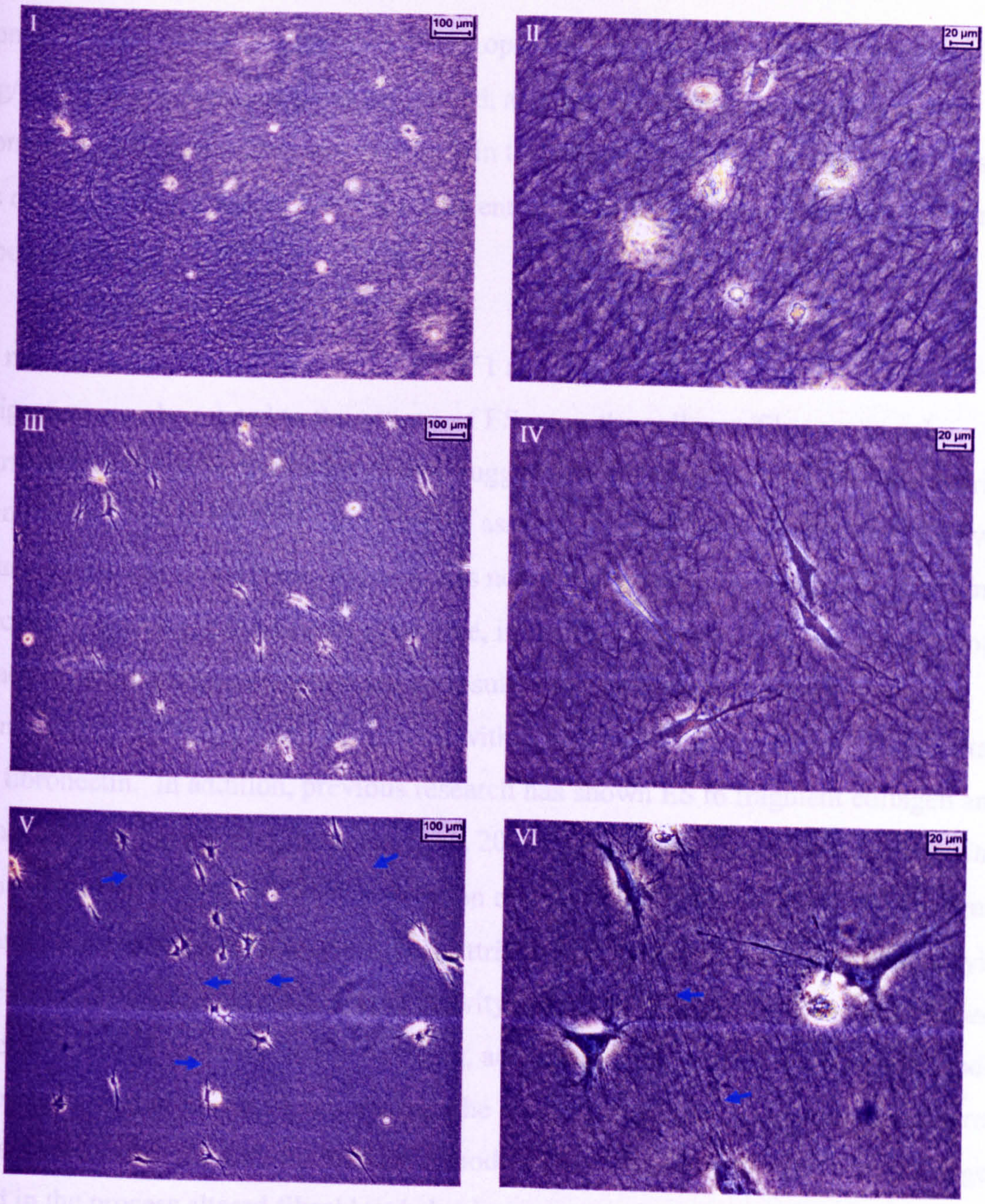

Figure 6.18c Representative phase contrast images showing fibroblasts within three-dimensional *in vitro* wound assays, at a seeding density of 3×10^5 cells/ml, following 48 hours incubation. Appearance of cells in the absence of ES (control) (I, II) or in the presence of 1 µg/ml ES (III, IV) or 5 µg/ml ES (V, VI). Aligned, strand-like connective fibrils visible within the assay exposed to 5 µg/ml ES, as indicated by the blue arrows.

concentrations tested, 5 μg/ml ES proved optimal for migration. In comparison, 10 μg/ml ES, the highest concentration tested, appeared to inhibit cell migration. In contrast to the results that were recorded in the two-dimensional *in vitro* wound assays, as documented in Chapter 4, ES at a concentration of 0.1 μg/ml exerted little effect upon migration.

A mechanism by which concentrations of 1 and 5 μg/ml ES promoted fibroblast migration may be related to the actions of ES upon the collagen/fibronectin gel surrounding the cells. Evidence, which suggests that ES may have altered the matrix components within the three-dimensional assays, is provided by observations that were made during the experiment. Here, it was noted that gels exposed to 5 and 10 μg/ml ES became increasingly translucent over time, indicating that modifications were taking place. Further evidence is provided by results presented within Chapter 3, which demonstrate that the proteolytic activity within ES causes the progressive fragmentation of fibronectin. In addition, previous research has shown ES to fragment collagen and other ECM components (Chambers *et al.*, 2003). Within the two-dimensional *in vitro* wound assays (Chapter 4), the acceleration of migration in the presence of 0.1 μg/ml ES was hypothesised to be at least partially attributed to ES proteolytic activity modifying the fibronectin-coated surface. Such activity may have changed the density of adhesive sites available to the cells and in so doing, according to the 'receptor saturation model', promoted migration (Fig. 4.7a). Within the three-dimensional assays described here, this same proteolytic activity may have modified the biophysical properties of the gel and in the process altered fibroblast behaviour.

In order to appreciate how ES may have promoted fibroblast migration by altering the matrix in which the cells were embedded, it is first necessary to understand the extent to which the biophysical properties of that matrix influence fibroblast behaviour. The stiffness or degree of mechanical tension present within the matrix has been shown to control fibroblast phenotype. This is thought to be related to the functions of fibroblasts in wound healing because evidence suggests that the cells not only contribute to granulation tissue formation, but also initiate wound closure. Although fibroblasts migrate slowly compared with other cells, such as keratinocytes and leukocytes, they exert much greater tractional forces (Harris, Stopak and Wild, 1981; Fray *et al.*, 1998).

Harris, Stopak and Wild (1981) have estimated that the strength of traction exerted by fibroblasts is at least two or three orders of magnitude higher than what is required for the cells' normal pace of locomotion. This indicates that for fibroblasts, traction fulfills a function that remains distinct from migration. Ehrlich and Rajaratnam (1990) have proposed that the tractional forces generated by fibroblasts migrating into the granulation tissue are sufficient to precipitate wound closure. In addition however, fibroblasts have also been shown to differentiate into a contractile phenotype (Gabbiani, Ryan and Majno, 1971). Triggered by a rise in mechanical tension, probably caused by tractional forces exerted by migrating fibroblasts, the cells develop features of the protomyofibroblast (Tomasek *et al*, 2002). This contractile cell phenotype expresses actin stress fibres, focal adhesion complexes and organises the formation of fibronectin fibrils on the cell surface. Composed of both fibronectin from its surrounds and secreted cellular fibronectin, these fibrils contain a splice variant to normal adult fibronectin, which only appears during embryogenesis and wound healing (French-Constant, Dvorak and Hynes, 1989; Brown *et al.*, 1993; Serini *et al.*, 1998). The presence of this splice variant, termed ED-A (refer to Fig. 1.2 in Chapter 1), together with a continuing rise in mechanical tension and the presence of TGF-β1, which promotes further ED-A fibronectin expression, leads to the emergence of the myofibroblast (Hinz *et al.*, 2001; Serini *et al.*, 1998; Desmouliere *et al.*, 1993; Vaughan, Howard and Tomasek, 2000). Expressing α-smooth muscle actin, myofibroblasts exert even greater contractile force and are believed to be involved in the latter stages of wound healing, when the wound is finally closed. The role that fibronectin fibril formation plays in the induction of a more contractile fibroblast phenotype is perhaps highlighted by the work of Hocking, Sottile and Langenbach (2000). These researchers found that fibronectin polymerisation within a free-floating fibroblast-populated collagen gel increased fibroblast-mediated contraction.

It is therefore clear that the degree of mechanical tension within the matrix influences fibroblast phenotype. From the tractional forces exerted by the migrating fibroblast to the strong contractility of the myofibroblast, it is also clear that the cell itself exerts a major influence upon the stiffness of the matrix around it, initiating a positive feedback loop. Within the wound, it may be hypothesised that the tractional forces generated by fibroblasts migrating into the granulation tissue, causes re-modelling of the matrix.

This results in a rise in the tension of the matrix, encouraging the protomyofibroblast phenotype to emerge. In turn, the myofibroblast predominates.

Considering that fibroblasts exert strong tractional forces, it is perhaps unsurprising that they exert considerable mechanical tension within collagen gels that are tethered to the dish surface. It is conceivable that in such a situation, the resident fibroblasts may differentiate into the protomyofibroblast state. Indeed, Tomasek *et al.* (2002) believe this to be the case. The question remains as to what occurs upon the release of this mechanical tension, when the collagen gel is freed from its tethers by the investigator's intervention. Such studies have shown fibroblasts to rapidly contract the gel following its release. It is also believed that the cells upregulate MMP production. For instance, release of collagenase is thought to be associated with re-organisation of the actin cytoskeleton, which occurs when the cell experiences a change in mechanical loading (Unemori and Werb, 1986; Lambert *et al.*, 2001). This reaction may represent an attempt by the cells to re-instate mechanical tension by enhancing localised matrix modification (Lambert, Lapière and Nusgens, 1998). Further evidence, which suggests that fibroblasts react to oppose the relaxation of mechanical tension, is provided by Brown *et al.* (1996, 1998), Eastwood, McGrouther and Brown (1994) and Eastwood *et al.* (1996). These researchers developed the tensional culture force monitor to measure the reaction of fibroblasts embedded within collagen gels, to changes in externally applied mechanical loads. Their results revealed that fibroblasts maintain an active tensional homeostasis, reacting to modify the endogenous matrix tension in the opposite direction to externally applied loads. Hence, an increase in the externally applied load and therefore an increase in mechanical tension, elicits a decrease in cell-mediated contraction and *vice versa*. In support of this evidence, it is interesting to note that within the body, almost all connective tissues, including the dermis are held in tensional homeostasis (Tomasek *et al.*, 2002).

Reports have shown stress relaxation within collagen gels to cause other modifications in fibroblast behaviour. For example, Lee *et al.* (1993) have observed that fibroblasts within an anchored collagen matrix retract their pseudopodia when the gel is freed. This change in the environment also triggers ectocytosis of plasma membrane vesicles containing actin, annexins II and VI and β_1 integrin receptors. Jenkins *et al.* (1999)

have found that fibroblasts upregulate α_2 integrin subunit mRNA expression when the anchored collagen gel in which they are embedded is released.

There is therefore considerable evidence to show that the strength of mechanical tension within fibroblast-populated *in vitro* collagen gels influences fibroblast behaviour. Hence, it is reasonable to assume that within the three-dimensional assays undertaken here, ES proteolytic modification of the collagen/fibronectin gel may have contributed to the enhancement of fibroblast migration. This is because it was noted that the gels exposed to 5 and 10 μg/ml ES were more translucent than their respective controls. They were also more fragile and over time, the gel exposed to the highest concentration of ES actually degraded into a viscous liquid state. This suggests that the presence of ES reduces the stiffness of collagen/fibronectin gels and in so doing, dissipates the mechanical load imposed upon any embedded cells. If this is the case, an upregulation of MMP expression by the resident cells may have resulted. The cells may also have reacted by escalating tractional force, in order to maintain tensional homeostasis. As a consequence of both these reactions, matrix re-modelling around the cells may have been enhanced. Increased cellular traction would also have been reflected by changes in cell morphology. As Harris, Stopak and Wild (1981) observed, fibroblast traction '...is distinct from simple contraction like that of a muscle...' because '...the cells elongate instead of shorten as they compress and stretch the collagen around them'.

Evidence that the fibroblasts responded to the presence of ES by increasing the exertion of traction is provided by another experiment that was performed. Here, the morphology of fibroblasts in the absence of ES or in the presence of 1 μg/ml ES or 5 μg/ml ES was investigated. In order to avoid any contact inhibition, the cells were embedded within the gels at a much lower population density than in the previous experiments, when fibroblast migration was quantified. The presence of considerable space between cells also allowed for the observation of any intercellular connective fibrils that may have formed, as was reported in the previous chapter, when cells were exposed to 10 μg/ml ES. As described within this chapter's results (section 6.3.2), cells within 1 and 5 μg/ml ES exhibited an enhanced degree of spreading compared with the control, which became increasingly apparent as the incubation time increased. By 48 hours, most cells within the control had become rounded, whilst cells exposed to either

concentration of ES remained well spread. This may have been indicative of increased cellular traction in response to ES because, as mentioned above, fibroblasts elongate instead of shorten when exerting traction (Harris, Stopak and Wild, 1981).

Within this same experiment, intercellular connective fibrils were also observed in gels exposed to 5 μg/ml ES. Although it was not possible to identify these fibrils as being composed of collagen or fibronectin, it is interesting to note that they bore an intriguing resemblance to structures that were first reported by Harris, Stopak and Wild (1981) and later by Sawhney and Howard (2002). Both these groups of researchers found that over a period of time, patterns of aligned collagen formed between explants of fibroblasts that were embedded approximately 1.5 cm or 1 mm apart within tethered collagen gels. These aligned fibrils, as shown in the example image recorded by Sawhney and Howard (2002) (Fig. 6.19, image I), appear similar to the structures that were observed between individual cells exposed to 5 μg/ml ES (Fig. 6.18bc and 6.19, image VI) and within a previous experiment, to 10 μg/ml ES (Fig. 5.21). They also appear remarkably similar to structures that were observed between cell droplets within a collagen/fibronectin gel exposed to 0.1 μg/ml ES (Fig. 6.19, images II to V). These images were taken from a preliminary assay that was assembled in a similar way to the three-dimensional assays that were used to quantify fibroblast migration. Kept under observation, it was noted that following the gel's accidental detachment from the dish surface, cell droplets within the gel appeared to be connected by parallel-aligned fibrils. The cells appeared to be in direct contact with these fibrils, indicating cellular involvement in fibril alignment. Fig. 6.19, image IV, even shows one cell apparently pulling on one of the fibrils, drawing the fibril towards the cell body. Sawhney and Howard (2002) named the fibril structures they observed as 'ligament-like collagen straps'. In agreement with the conclusions of Harris, Stopak and Wild (1981) these researchers believed that the 'straps' had been formed by cellular traction forces. They then went on to demonstrate that the effects of small local movements of the collagen fibres, caused by the actions of cells, can be transmitted a great distance to cause global re-alignment. This is owing to the interconnected matrix or mesh-like network that the collagen forms. Using a nylon net as an analogy, Sawhney and Howard (2002) showed that a small pull from two fixed points results in a small displacement of points located on the axis of tension, but a much larger displacement of points located at right angles to the axis of tension.

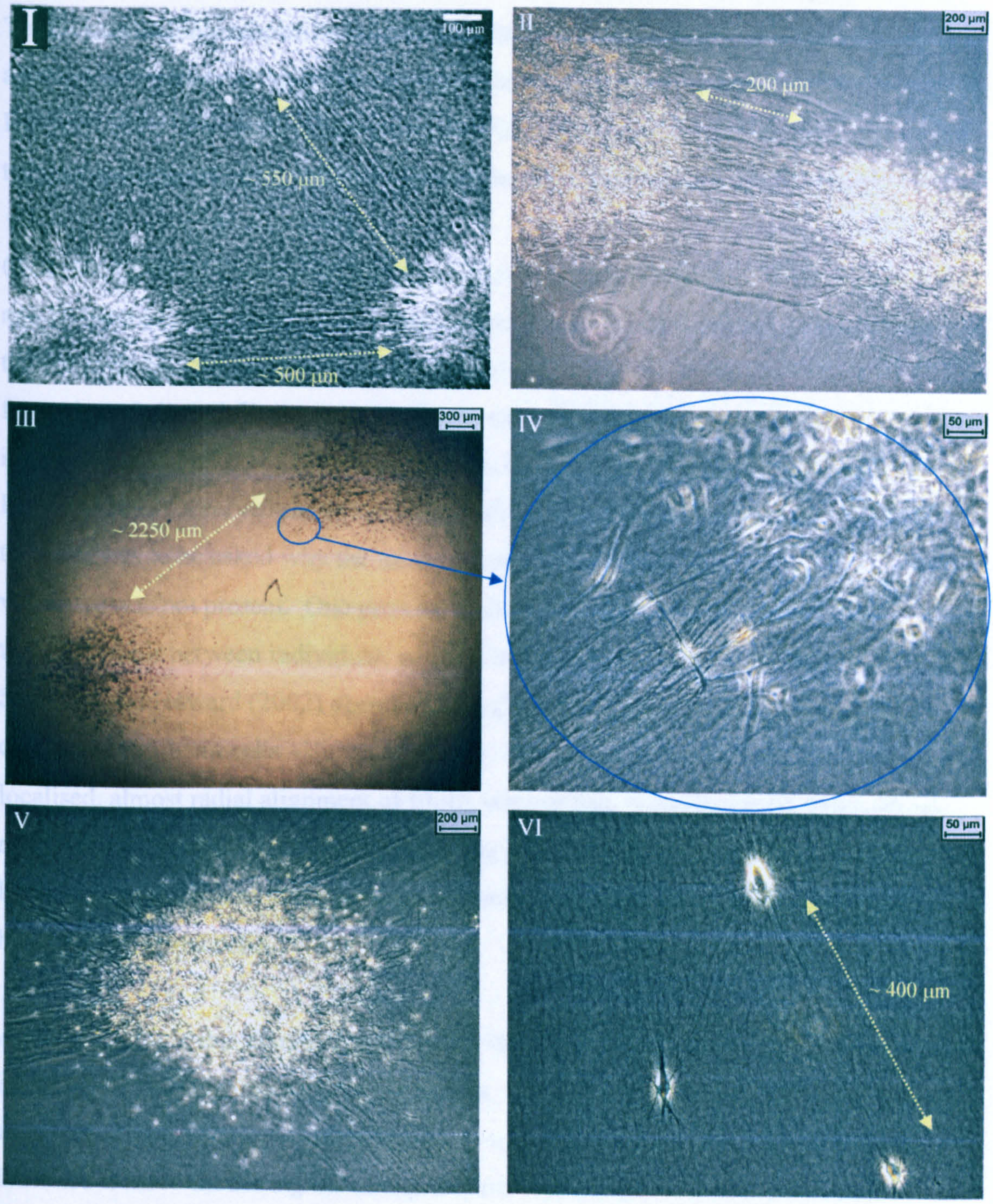

Figure 6.19 Formation of collagen 'straps' between cell populations and individual cells within three-dimensional assays – comparison with research by Sawhney and Howard (2002). **I** Mouse dermal fibroblast explants after 8 hours incubation within 1.7 mg/ml type I collagen gel, containing 10% FCS. Picture adapted from Fig.1 in Sawhney and Howard (2002). **II** to **V** 2 µl fibroblast-seeded gel droplets within three-dimensional *in vitro* assay containing 1.5 mg/ml type I collagen, 30 µg/ml fibronectin and 0.1 µg/ml ES, following 5 days incubation and accidental detachment of the gel. Note that image **IV** displays an area within image **II** at a higher magnification. **VI** Fibroblast cells within three-dimensional *in vitro* assay, containing 1.5 mg/ml type I collagen, 30 µg/ml fibronectin and 5 µg/ml ES following 48 hours incubation. Droplet seeding density of 3×10^5 cells/ml. Distances between cells indicated by yellow dotted lines.

Termed 'orthogonal amplification of mesh distortion', this phenomenon potentiates the alignment of collagen fibrils over relatively large distances. As stated by Sawhney and Howard (2002), this implies that tractional forces may provide the driving force behind the patterning of collagen in connective tissues during development and wound healing.

Considering the comparative evidence of Harris, Stopak and Wild (1981) and Sawhney and Howard (2002), it may be concluded that within the experiments conducted here, the presence of ES caused enhanced matrix re-modelling as exemplified by the formation of aligned fibrils, presumably composed of collagen, between cells (Fig. 6.19, image VIII and Fig. 6.18). However, Harris, Stopak and Wild (1981) and Sawhney and Howard (2002) observed the occurrence of fibril alignment in the absence of ES. It therefore has to be asked why the same was not observed here in the control sample where ES was not present. One possible reason is that fibril alignment does not typically occur between individual, isolated cells. Harris, Stopak and Wild (1981) and Sawhney and Howard (2002) observed collagen 'strap' formation between isolated clusters of confluent cells. However, Harris, Stopak and Wild (1981) did observe a localised, almost radial alignment of fibrils surrounding individual cells, although no mention was made of these fibrils interacting with neighbouring cells on a one-to-one basis. It is possible that the presence of ES may have allowed fibril alignment to occur between individual cells.

Another reason is that Harris, Stopak and Wild (1981) and Sawhney and Howard (2002) included 10 % FCS within their gel matrices. No serum was present in the experiments undertaken here. It may be that without the stimulatory effects of serum, fibroblasts are inhibited from re-modelling the collagen matrix effectively. Evidence for this is provided by Tomasek *et al.* (1992). These researchers discovered that removing serum just prior to the release of tethered fibroblast-populated collagen gels, inhibited the extent of subsequent gel contraction by the resident cells. This suggests that ES contains agents that indirectly initiate a cellular response by altering the biophysical properties of the gel matrix and/or, by directly stimulating the cells to respond to their environment. As discussed above there is considerable evidence to suggest that fibroblasts are capable of sensing and responding to mechanical signals from the matrix. In addition, it is possible that there are also mechanisms by which fibroblasts may be directly stimulated by components that are already known to exist within ES. One such

mechanism involves the activation of certain membrane-bound receptors. It has been shown that fibroblasts express proteinase-activated receptors (PARs) (reviewed by Déry and Bunnett, 1999). As discussed within Chapter 1.5, this family of G-protein-coupled receptors are activated by thrombin and trypsin-like enzymes. These serine proteinases cleave specific sites located on the extracellular side of the receptor, exposing N-terminal tethered ligands which then bind and activate the cleaved receptors. Synthetic peptides corresponding to the tethered ligands also directly activate these receptors (Maryanoff *et al.*, 2001). Coupled to signalling pathways that are related to growth and inflammation, activation of PAR receptors may elicit a range of cellular responses. For example, PAR-1 activation by thrombin has been shown to induce mitogenesis in fibroblasts (Déry and Bunnett, 1999). As discussed previously within Chapter 1.5, larval ES contains trypsin-like serine proteinases. Hence, in addition to eliciting cellular responses through proteolytic modification of the matrix, these enzymes may also directly interact with fibroblast signalling mechanisms.

Another mechanism by which ES enhanced matrix re-modelling may have involved substances with actions similar to those of plasmin, the activated form of plasminogen. Using fluorogenic substrates specific to certain classes of enzymes, previous research has demonstrated that ES may contain plasmin-like serine proteases (Chambers *et al.*, 2003). Plasmin is known to activate zymogen pre-cursors of various MMPs secreted by cells (Mignatti *et al.*, 1996). Although plasmin does not degrade collagen directly, the plasmin-like activity of ES may have enhanced the localised degradation of the collagen/fibronectin matrix surrounding the fibroblasts by increasing the activity of the MMPs that the cells may have secreted.

How enhanced matrix re-modelling by the actions of ES is translated into accelerated fibroblast migration, as observed in the quantitative assays when cell droplets were exposed to 1 and 5 μg/ml ES, may be explained by the way fibroblasts use collagen fibrils to assist migration. In the mechanism termed 'contact guidance', fibroblasts align themselves along discontinuities in the surrounding substrata (McCarthy, Iida and Furcht, 1996). Thus, alignment of collagen fibrils by enhanced matrix re-modelling may promote directional cell migration. Indeed, Sawhney and Howard (2002) found that collagen 'strap' formation between clusters of cells precipitated the advancement of cells and also directed cell migration towards neighbouring cell clusters.

Relaxation of the matrix and a specific kind of proteolytic activity that may be present within ES may also have interacted to stimulate migration. In addition to its plasmin-like activity, ES also appears to contain urokinase-like activity (Chambers *et al.* (2003). Referred to as urokinase plasminogen activators (uPAs), urokinases convert plasminogen into its active form, plasmin. They also bind with urokinase plasminogen activator receptors (uPARs), which studies have shown to be expressed by fibroblasts (Ellis, Behrendt and Dano, 1993; Behrendt *et al.*, 1993; Mignatti *et al.*, 1996). Once bound, these receptors localise to focal adhesion sites through binding with β_1, β_2 and β_3 integrins. (Chapman and Wei, 2001; Porter and Hogg, 1998). It is believed that as a consequence integrin-mediated function is modulated, perhaps by the induction of a conformational change in the ECM receptor (Chapman and Wei, 2001). As a result, the affinity of the integrin receptors for ECM ligand sites may be altered and a more motile cell phenotype promoted. Indeed, uPAR has been reported to have a signalling role in cell migration, adhesion and chemotaxis (Odekon, Sato and Rifkin, 1992; Waltz, Sailor and Chapman, 1993; Gyetko *et al.*, 1994). Evidence suggests that protein kinase C may play a role in the uPAR signal transduction pathway associated with cell migration (Busso *et al.*, 1994). uPARs also appear to be physically linked to actin microfilaments within the cell (Wang *et al.*, 1995). This may perhaps explain ligated uPAR localisation to focal adhesion sites. Bayraktutan and Jones (1995) have found that disruption of the actin cytoskeleton results in an upregulation of uPAR expression in human, dermal fibroblasts. On this point, it is interesting to note that fibroblasts embedded within collagen gels re-organise their cytoskeletons in response to the relaxation of mechanical tension (Unemori and Werb, 1986). Hence, it seems logical that as a consequence, uPAR expression may be enhanced. Considering this evidence, it is reasonable to speculate that urokinase-like activity within ES may have resulted in the ligation of uPARs expressed by the fibroblasts, and their subsequent localisation to integrin receptors. In turn, this may have modulated integrin-mediated function, thereby promoting migration. Relaxation of the collagen/fibronectin gels by ES proteolytic activity may also have promoted further uPAR-mediated control of fibroblast phenotype through causing changes in the actin cytoskeleton, thus upregulating uPAR expression.

Another related mechanism by which urokinase-like activity may enhance migration is dependent upon the presence of plasminogen. Upon binding to uPAR, uPA is activated to convert plasminogen into plasmin. This is part of a self-maintained feedback loop as

plasmin also activates uPA. Once produced, plasmin goes on to activate MMP zymogens. Hence, in the presence of plasminogen, localisation of uPAR to integrins may focus proteolytic degradation of the matrix to focal adhesion sites because pro-MMPs released at these sites will be activated. This in turn, allows for fine control of matrix re-modelling to areas within the immediate vicinity of the cell where contact with the ECM is made. Although it is not clear whether the *in vitro* assays here contained plasminogen, originating from either the ES or as impurities in the matrix componments, it would almost certainly be present within the actual wound. This is because circulating plasminogen is quite readily transported to extravascular sites. As such, the presence of uPA-like activity within ES may have a profound effect upon the levels of active plasmin within the wound and may represent another mechanism by which ES stimulates fibroblast migration. Plasmin is also believed to mobilise stores of bFGF complexed with proteoglycans in the extracellular matrix (Mignatti *et al.*, 1996). As such, raising the plasmin levels may increase the availability of this important growth factor to the cells, which again may enhance migration. In addition, bFGF may also contribute to fibroblast proliferation and angiogenesis. Stimulatory mechanisms originating from the conversion of plasminogen into plasmin may not however have played a role within the *in vitro* assays here, as plasminogen may not have been present. Nevertheless, it is interesting to note that relaxation of mechanical tension within collagen gels stimulates fibroblast expression of MMPs in conjunction with actin cytoskeleton re-organisation and subsequent upregulation of uPAR expression. As MMPs are activated by plasmin and uPA increases the levels of plasmin when bound to uPAR, it may well be that fibroblasts release MMPs in anticipation of higher levels of plasmin. There is after all, little point in increasing MMP expression if there was not the capacity to activate these molecules.

As fibroblasts are capable of detecting and responding to changes in mechanical tension, it is clear from the images shown in Fig. 6.18 that however ES stimulated fibroblasts to remodel the matrix, the enhancement of intercellular communication may have resulted. This is because each cell would presumably have been able to detect local differences in mechanical tension due to opposing tractional forces from other cells causing fibril alignment. Cells lying a considerable distance apart may have been capable of detecting each other's physical presence. For example, within Fig. 6.19, image VI, the length of the fibrils aligned between two cells was approximately 400

μm. Such an enhanced awareness of neighbouring cells, even over comparatively long distances, may have resulted in the improved co-ordination of action between cells. This in turn may also have contributed to enhanced migration within the quantitative three-dimensional assays. This may be relevant in the chronic wound situation where isolated clusters of healthy, viable cells may be made aware of each other's presence across areas of tissue that have been freshly debrided of non-viable, necrotic tissue by the actions of maggots and their secretions. Indeed, Sheetz , Felsenfeld and Gabraith (1998) propose a similar mechanism of co-ordinated cell migration, where the cells direct their movement according to the orientation and rigidity of the ECM protein fibres. This is based upon their own research which demonstrates that cells are capable of sensing the stiffness of individual surface contacts (Choquet, Felsenfeld and Sheetz, 1997) and the research of Wang and Ingber (1994) which shows that cytoskeletal stiffness increases in proportion to the force applied to integrins.

Another mechanism by which fibroblast migration was enhanced may be related to the production of bio-active peptides through the proteolytic degradation of the collagen and/or fibronectin constituents of the gel. Both these matrix components have been shown to release bio-active peptides upon their fragmentation. These peptides then go on to influence fibroblast adhesion and migration (Pierschbacher and Ruoslahti, 1984; Woods *et al.*, 1993; Livant *et al.*, 2000; Schor *et al.*, 1996). Of particular interest is the finding that a 120 kDa fibronectin fragment, containing the central cell-binding domain, induces a net increase in matrix-degradative activity in fibrocartilaginous cells (Hu *et al*, 2000). It appears to do this by inducing both MMPs and their activator uPA while at the same time inhibiting TIMPs. Co-operative signalling by $\alpha_5\beta_1$ and $\alpha_4\beta_1$ integrin receptors may be involved in this (Huhtala *et al.* (1995). In addition, some matrix-derived peptides may mimic ligands that activate PARs.

Apart from facilitating the migration of cells into the wound space, promotion of a migratory fibroblast phenotype by the direct or indirect actions of ES may also confer another benefit. Research has shown that induction of migration is associated with tyrosine phosphorylation of p130 Crk-associated substrate (CAS), which then complexes with the adaptor protein c-CrkII (Crk) (Klemke *et al.*, 1998). Through the assembly of signal-generating complexes, this adaptor protein is involved in co-ordinating a cascade of biochemical signals initiated by integrin or cytokine receptor

ligation. In addition to inducing migration, CAS/Crk coupling is also associated with the suppression of apoptosis (Cho and Klemke 2000). Hence, the presence of ES within the wound may promote cell survival, thereby providing further assistance to new tissue growth.

Despite the supposed benefits of ES proteolytic activity in enhancing migration, it is important that proteolysis is not excessive. Unlike the carefully controlled localised MMP expression and activation around cells, the addition of ES causes global breakdown of the matrix irrespective of where the cells are. Sufficient fibril structure needs to remain in order to facilitate contact guidance and translocation. This point is perhaps illustrated by the results that were obtained from the quantitative three-dimensional assays that were exposed to the highest ES concentration. Here, 10 μg/ml ES not only inhibited migration, but also rapidly degraded the gel into a viscous liquid state. Over periods of time longer than when migration was quantified, 5 μg/ml ES may also have eventually inhibited migration, due to progressive matrix degradation. It would therefore be interesting to measure the concentration gradient of ES proteolytic activity through the depth of chronic wounds treated by maggots. It would also be interesting to determine the influence of wound exudates upon this gradient. As the exudates are expelled to the wound surface, ES may be washed out of the wound. Perhaps an as yet undetermined intermediate level of ES activity is optimal for enhancing fibroblast migration and wound healing.

As displayed previously within Chapter 4, ES at a concentration of 0.1 μg/ml increased fibroblast migration within a two-dimensional *in vitro* wound assay. However, this concentration apparently had little influence within the three-dimensional assay described here. This may have been due to requirements for cell translocation differing between two-dimensional and three-dimensional environments. Cell migration in two dimensions is predominantly a function of adhesion and de-adhesion events because resistance to the advancing cell body above the planar surface is lacking. This explains why research presented here in Chapter 4 and in other studies has found that the concentration of fibronectin coating a surface exerts a major influence upon the speed of cell migration. Noted for its adhesive properties, the greater the concentration of fibronectin present, the more adhesive the surface will be to fibroblasts. Within three

dimensions however, cells have to overcome resistance from the matrix that completely surrounds them. Unlike the two-dimensional environment, cells have to create or find a passage through the fibrous network of the matrix before forward movement can be initiated (Haas *et al.*, 1998; Friedl and Bröcker, 2000). In addition, it may be hypothesised that the cell's detachment from the matrix for the purpose of migration is more difficult in the three-dimensional than the two-dimensional environment. This is because in three dimensions the cell is in contact with the matrix at all angles. As presented within Chapter 3, ES substantially modifies fibroblast adhesion to planar surfaces. It is therefore logical to assume that fibroblast migration will be more sensitive to ES when the cells are located upon a planar surface than when they are embedded within a three-dimensional matrix environment. Hence, higher concentrations of ES would be required to promote fibroblast migration within gel matrices than upon two-dimensional surfaces.

Another reason why 0.1 μg/ml ES promoted fibroblast migration in the two-dimensional assay but not in the three-dimensional assay may have been due to the different batches of ES that were used. As shown in Chapter 3, ES that had been heat-treated to remove its proteolytic activity exerted a much lower influence upon fibroblast adhesion to fibronectin than untreated ES. It may therefore be assumed that the proteolytic activity of ES plays a role in enhancing fibroblast migration because, as discussed above, the strength of cell adhesion influences migration. With a specific activity of 6.04×10^6 units per mg protein (ES batch E), the ES applied here in the three-dimensional assays demonstrated 0.61 of the proteolytic activity of the ES employed within the two-dimensional assays (with a specific activity of 9.87×10^6 units per mg protein – ES batch D), as measured using FITC-casein substrate assays (see Table 2.1 in Chapter 2). This difference can only be explained by variation between the batches of larvae that were obtained. Reasons for this variability remain to be elucidated.

6.5 Conclusions

Within the time periods examined, ES concentrations of 1 and 5 μg/ml promoted fibroblast migration within collagen/fibronectin gels. Evidence suggested that this might have been associated with enhanced matrix re-modelling. Partial proteolytic degradation of the matrix components by the actions of ES may have been one contributory factor. This may have relaxed mechanical tension within the matrix thereby stimulating opposing cellular traction forces that have been shown to re-organise the surrounding collagen fibril network. Proteolytic degradation may also have released bio-active peptides. Particular enzymatic activities within ES may also have activated MMP zymogens produced by the cells, thus enhancing localised matrix degradation around the cells. In addition, these activities may have been involved in directly stimulating membrane-bound receptors expressed by the cells, including PARs and uPARs. In turn, this may have activated a variety of responses, including changes in fibroblast adhesion, migration, proliferation and chemotaxis. Promotion of fibroblast migration may have also promoted cell survival through the inhibition of apoptosis.

The presence of ES within the wound may confer additional benefits. For instance, the possibility of plasmin-like activity within ES and the conversion of plasminogen to plasmin may lead to the mobilisation of growth factor stores held within the matrix. It may also stimulate angiogenesis. Furthermore, increased cellular traction forces and matrix re-modelling may facilitate intercellular communication between isolated clusters of viable cells.

CHAPTER 7

Final Conclusions

Maggots placed within chronic wounds, in the procedure termed 'biosurgery', have been observed to debride the wound of necrotic tissue, cleanse the wound of infection and promote granulation tissue formation. However, little is known about the mechanisms by which they initiate these beneficial effects upon the wound. The work presented within this thesis was directed towards elucidating how the maggots may promote new tissue formation. Fibroblast migration was therefore examined as this aspect of the cell's behaviour directs the expansion and invasion of granulation tissue into the wound space. Fibroblast adhesion was also examined as this plays an integral role in determining the cell's ability to translocate. Both these features of fibroblast behaviour were observed in the presence of common extracellular matrix proteins as these have been shown to be controlling factors. For the purpose of determining the influence that maggots may exert upon the cells, these studies included the presence of maggot secretions as these have been shown to modify ECM proteins that are present at the wound site, thus providing a possible avenue by which maggots may influence healing.

As shown in Chapter 3, the secretions (more properly termed excretions/secretions or ES) modulated fibroblast adhesion to collagen-coated and, in particular, fibronectin-coated surfaces. Studies showed that this was related to proteolytic modification of the ECM protein coating by enzymes present within ES. Fibroblast adhesion to uncoated tissue culture plastic was also modified in the presence of ES in a dose-dependent manner. This suggests that ES may be targeting the integrin receptor-surface complex directly, in addition to modifying the ECM protein.

Work presented in Chapter 4 showed that the presence of just 0.1 μg/ml ES accelerated fibroblast migration over a fibronectin-coated surface. This may be attributed to the modulatory effects that ES was shown to exert upon fibroblast adhesion. However, at 10 μg/ml, the concentration of ES used to study fibroblast adhesion to collagen and fibronectin, ES had a negative impact upon migration. These results show that while modification of the strength of fibroblast adhesion may be necessary to promote migration, a reduction in the number of fibroblasts adhering to the surface, as was seen in Chapter 3, will induce the opposite effect. This indicates the importance by which the concentration of larval secretions present within the wound influences the progress of healing.

As was noted within this thesis, results presented within Chapter 4 were based upon two-dimensional assays. Cells *in vivo* interact within a three-dimensional environment, with ECM surrounding them on all sides. Research has shown that cells behave very differently within the three-dimensional environment than upon planar surfaces, displaying different morphologies and receptor-surface interactions. Chapter 5 was therefore devoted to the development of three-dimensional *in vitro* wound assays incorporating collagen gel/fibronectin composites. Chapter 6 contains work resulting from the study of fibroblast migration and morphology within these assays whilst the cells were exposed to different concentrations of ES. Hence, the effects of ES upon fibroblast behaviour were observed while the cells were experiencing an environment more akin to the *in vivo* state. Here, larval ES was found to promote fibroblast migration. Of the concentrations tested, 5 μg/ml ES was optimal for migration over a 24 hour period. Evidence suggested that this may have been associated with enhanced matrix re-modelling, arising from the partial proteolytic degradation of the gel matrix. Cell morphological studies revealed that the cells themselves may also have been stimulated to re-organise the matrix in response to the actions of ES. As with the two-dimensional assay, 10 μg/ml ES had a negative effect upon migration. This appeared to be related to the excessive proteolytic degradation of the gel matrix into a liquid state, preventing the cells from gaining purchase upon any solid substratum. Over longer periods of time, the same may also have occurred with the gel exposed to 5 μg/ml ES because, by 48 hours incubation, it had become fragile and more transparent in appearance. Although 0.1 μg/ml ES exerted no noticeable effect upon fibroblast

migration in the time period studied, it may eventually have promoted migration. This is because, judging from results involving the higher concentrations of ES, it appears that ES modifies the gel matrix in a progressive dose- and time-dependent manner.

Before the onset of work that was included within this thesis, colleagues had recently discovered that larval ES is a rich source of proteolytic enzymes, incorporating serine proteinase (trypsin-like and chymotrypsin-like), aspartyl proteinase and metalloproteinase activities (Chambers *et al.*, 2003). In addition, the chymotrypsin-like activity within ES was shown to degrade ECM components, including fibrin clots, fibronectin, laminin and collagen. In the chronic wound such activity may transfer to the break-down of composite matrix cuffs which are believed to surround blood vessels and contribute to impaired healing. If this is the case, such activity may promote re-perfusion of the wound with oxygen, nutrients and growth factors. It may also contribute to wound debridement, aiding the removal of slough and eschar. Work presented within this thesis suggests that larval ES may also promote healing through enhancing matrix re-modelling and increasing the rate of fibroblast migration, thus promoting the recruitment of cells to the wound space and accelerating granulation tissue formation. A model of wound healing under the influence of ES is proposed in Fig. 7.1. This combines the findings of the thesis presented here and of Chambers *et al.* (2003). However, the model does not include the reported anti-microbial effects of biosurgery which provides a whole new exciting area for research. Future work leading on from this thesis may include the identification of the particular proteolytic enzymes, or indeed other as yet unidentified substances, which are responsible for promoting fibroblast migration and enhancing matrix re-modelling. Once these have been identified, they may then form the basis for developing new wound healing products which may prove to be more versatile than applying the whole, live maggot. They may also prove to be a more 'palatable' alternative for clinicians and patients alike.

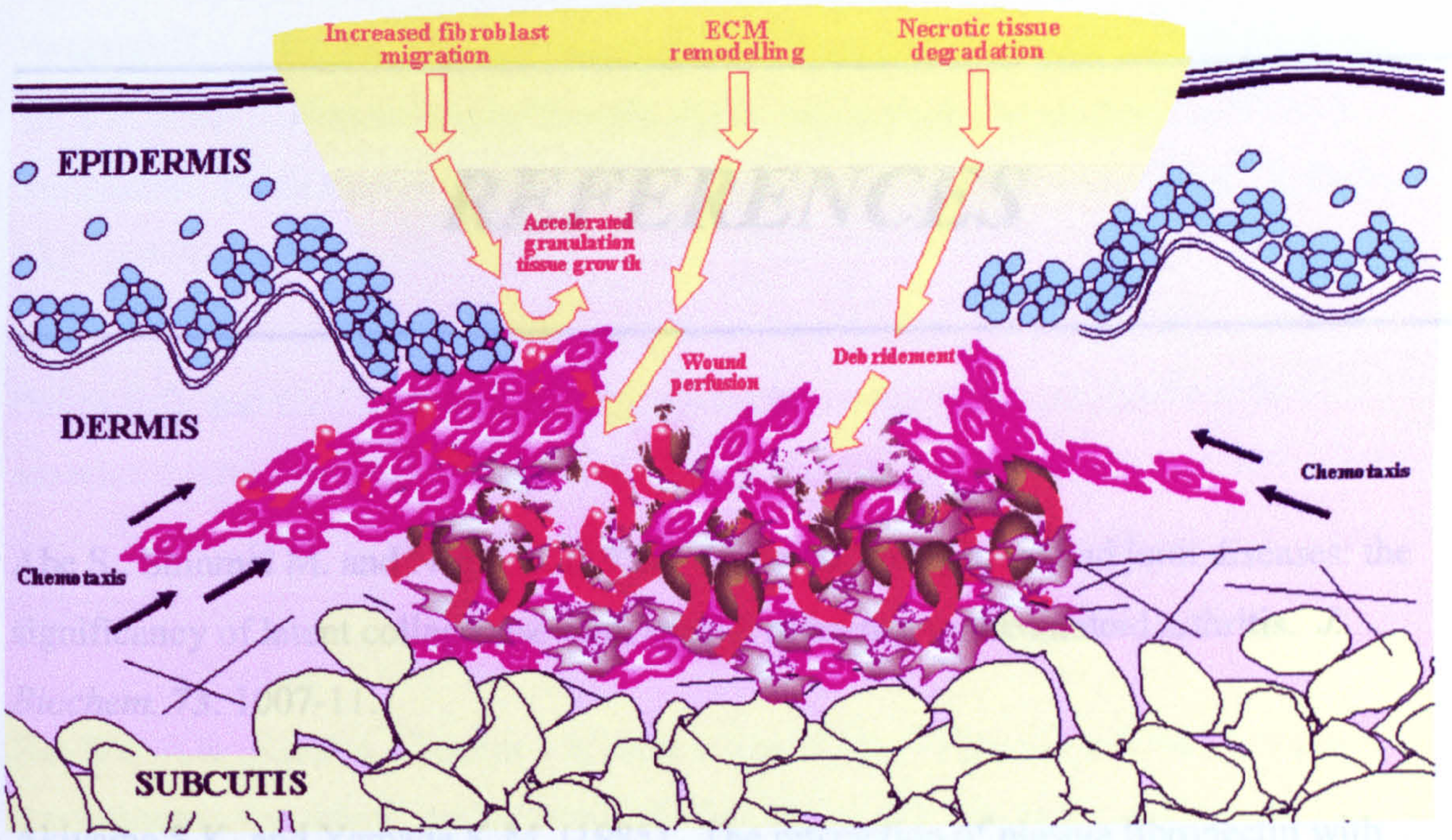

Figure 7.1 Proposed model for the advancement of wound healing under the influence of *L. sericata* larval ES. Infiltration of larval ES, indicated in yellow, into the open chronic wound initiates debridement. It also promotes matrix re-modelling, assisting the degradation of components found within composite matrix cuffs which block blood vessels, thus aiding re-perfusion of the wound. Fibroblast migration is also assisted, promoting the recruitment of cells to the wound, possibly through additional chemotaxic effects. As a result of the actions of ES, non-viable tissue is removed, oxygenation of the wound is improved and granulation tissue growth is enhanced.

REFERENCES

Abe S., Shinmei M. and Nagai Y. (1973). Synovial collagenase and joint diseases: the significancy of latent collagenase with special reference to rheumatoid arthritis. *J. Biochem.* **73**: 1007-11.

Akiyama S.K. and Yamada K.M. (1985). The interaction of plasma fibronectin with fibroblastic cells in suspension. *J. Biol. Chem.* **260**: 4492-500.

Albini A. and Adelmann-Grill B.C. (1985). Collagenolytic cleavage products of collagen type I as chemoattractants for human dermal fibroblasts. *Eur. J. Cell Biol.* **36**: 104-7.

Albini A., Pontz B., Pulz M., Allavena G., Mensin H. and Muller P.K. (1988). Decline of fibroblast chemotaxis with age of donor and cell passage number. *Collagen Rel. Res.* **1**: 23-37.

Andreasen P.A., Kjoller L., Christensen L. and Duffy M.J. (1997). The urokinase-type plasminogen activator system in cancer metastasis: a review. *Int. J. Cancer* **72**: 1-22.

Aota S., Nagai T. and Yamada K.M. (1991). Characterisation of regions of fibronectin besides the arginine-glycine-aspartic acid sequence required for adhesive function of the cell-binding domain using site-directed mutagenesis. *J. Biol. Chem.* **266**: 15938-43.

Aota S., Nomizu M. and Yamada K.M. (1994). The short amino acid sequence Pro-His-Ser-Arg-Asn in human fibronectin enhances cell-adhesive function. *J. Biol. Chem.* **269**: 24756-61.

Ashcroft G.S., Herrick S.E., Tarnuzzer R.W., Horan M.A., Schultz G.S. and Ferguson M.W.J. (1997). Human ageing impairs injury-induced *in vivo* expression of tissue inhibitor of matrix metalloproteinase (TIMP)-1 and -2 proteins and mRNA. *J. Pathol.* **183**: 169-76.

Ballas C.B. and Davidson J.M. (2001). Delayed wound healing in aged rats is associated with increased collagen gel remodelling and contraction by skin fibroblasts, not with differences in apoptotic or myofibroblast cell populations. *Wound Rep. Reg.* **9**: 223-37.

Bar-Shavit R., Kahn A., Fenton J.W. and Wilner G.D. (1983). Chemotactic response of monocytes to thrombin. *J. Cell Biol.* **96**: 282-5.

Bayraktutan U. and Jones P. (1995). Expression of the human gene encoding urokinase plasminogen activator receptor is activated by disruption of the cytoskeleton. *Exp. Cell Res.* **221**:486-95.

Beertsen W., McCulloch C.A. and Sodek J. (2000). The periodontal ligament: a unique, multifunctional connective tissue. *Periodontology* **13**: 20-40.

Behrendt N., Ploug M., Ronne E., Høyer-Hansen G. and Dano K. (1993). Cellular receptor for urokinase-type plasminogen activator: protein structure. *Methods Enzymol.* **223**: 207-222.

Bell E., Ivarsson B. and Merrill C. (1979). Production of a tissue-like structure by contraction of collagen lattices by human fibroblasts of different proliferative potential *in vitro*. *Proc. Natl. Acad. Sci. USA* **76**: 1274-8.

Benecke B.-J., Ben-Ze'ev A. and Penman S. (1978). Control of messenger-RNA production, translation and turnover in suspended and reattached anchorage-dependent fibroblasts. *Cell* **14** (4): 931-9.

Beningo K.A., Dembo M., Kaverina I., Small V. and Wang Y. (2001). Nascent focal adhesions are responsible for the generation of strong propulsive forces in migrating fibroblasts. *J. Cell Biol.* **153** (4): 881-7.

Beningo K.A. and Wang Y. (2002). Flexible substrata for the detection of cellular traction forces. *Trends Cell Biol.* **12** (2): 79-84.

Bernfield M., Kokenyesi R., Kato M., Hinkes M.T., Spring J., Gallo R.L. and Lose E.J. (1992). Biology of the syndecans: a family of transmembrane heparan sulphate proteoglycans. *Annu. Rev. Cell Biol.* **8**: 365-93.

Bhargava S., Chapple C.R., Bullock A.J., Layton C. and MacNeil S. (2004). Tissue-engineered buccal mucosa for substitution urethroplasty. *BJU Int.* **93**: 807-11.

Bizot-Foulon V., Bouchard B., Horneback W., Dubertret L. and Bertaux B. (1995). Uncoordinate expression of type I and III collagens, collagenase and tissue inhibitor of matrix metalloproteinase 1 along in vitro proliferative life span of human skin fibroblasts. Regulation by all-*trans* retinoic acid. *Cell Biol. Int.* **19**: 129-34.

Bonn D. (2000). Maggot therapy: an alternative for wound infection. *Lancet* **356**: 1174 (single page).

Bowditch R.D., Hariharan M., Tominna E.F., Smith J.W., Yamada K.Y.,Getzoff E.D and Ginsberg M.H. (1994). Identification of a novel integrin binding site in fibronectin. Differential utilisation by β3 integrins. *J. Biol. Chem.* **269**: 10856-63.

Bradford M. M. (1976). A rapid and sensitive method for the quantitation of microgram quantities of protein utilising the principle of protein-dye binding. *Analyt. Biochem.* **72**: 248-54.

Breathnach A.S. (1978). Development and differentiation of dermal cells in man. *J. Invest. Dermatol.* **71**: 2-8.

Brommer E.J.P. and van Bocke L.J.H. (1992). Composition and susceptibility to thrombolysis of human arterial thrombi and the influence of their age. *Blood Coagul. Fibrinolysis* **3**: 717-25.

Brown L.F., Dubin D., Lavigne L., Logan B., Dvorak H.F. and van de Water L. (1993). Macrophages and fibroblasts express embryonic fibronectins during cutaneous wound healing. *Am. J. Pathol.* **142** (3): 793-801.

Brown R.A., Talas G., Porter R., McGrouther D.A. and Eastwood M. (1996). Balanced mechanical forces and microtubule contribution to fibroblast contraction. *J. Cell Physiol.* **169**: 439-47.

Brown R.A., Prajapati R., McGrouther D.A., Yannas I.V. and Eastwood M. (1998). Tensional homeostasis in dermal fibroblasts: mechanical responses to mechanical loading in three-dimensional substrates. *J. Cell Physiol.* **75**: 323-32.

Browse N.L. and Burnand K.G. (1982). The cause of venous ulceration. *Lancet* **2**: 243-5.

Buchman J. and Blair J.E. (1932). Maggots and their use in the treatment of chronic osteomyelitis. *Surg. Gyn. Obst.* **55**:177-90.

Buckley C.D., Pilling D., Lord J.M. Akbar A.N., Scheel-Toellner D. and Salmon M. (2001). Fibroblasts regulate the switch from acute resolving to chronic persistent inflammation. *Trends Immunol.* **22** (4): 199-204.

Busso N., Masur S.K., Lazega D., Waxman S. and Ossowski L. (1994). Induction of cell migration by pro-urokinase binding to its receptor: possible mechanisms for signal transduction in human epithelial cells. *J. Cell Biol.* **126** (1): 259-70.

Chakrabarty K.H., Heaton M., Dalley A.J., Dawson R.A., Freedlander E., Khaw P.T. and MacNeil S. (2001). Keratinocyte-driven contraction of reconstructed human skin. *Wound Rep. Reg.* **9** (2): 95-106.

Chambers L., Woodrow S., Brown A.P., Harris P.D., Phillips D., Hall M., Church J.C.T. and Pritchard D.I. (2003). Degradation of extracellular matrix components by defined proteases from the greenbottle fly larva *Lucilia sericata* used for chemical debridement of non-healing wounds. *Br. J. Dermatol.* **148**: 14-23.

Chapman H.A. and Wei Y. (2001). Protease crosstalk with integrins: the urokinase receptor paradigm. *Thromb. Haemost.* **86**: 124-9.

Chen W.T. (1981). Mechanism of retraction of the trailing edge of during fibroblast movement. *J. Cell Biol.* **90**: 187-200.

Chen W.Y.J. and Abatangelo G. (1999). The functions of hyaluronan in wound repair – a review. *Wound Rep. Reg.* **7**: 79-89.

Cho S.Y. and Klemke R.L. (2000). Extracellular-regulated kinase activation and CAS/Crk coupling regulate cell migration and suppress apoptosis during invasion of the extracellular matrix. *J. Cell Biol.* **149** (1): 223-36.

Choquet D., Felsenfeld D.P. and Sheetz M.P. (1997). Extracellular matrix rigidity causes strengthening of integrin-cytoskeleton linkages. *Cell* **88**:39-48.

Church J.C.T. (1999). Larva therapy in modern wound care: a review. *Primary Intention* **7**: 63-8.

Clark R.A.F., Wikner N.E., Doherty D.E. and Norris D.A. (1988). Cryptic chemotactic activity of fibronectin for human monocytes resides in the 120kDa fibroblastic cell-binding fragment. *J. Biol. Chem.* **263**: 12115-23.

Clark R.A.F., Nielsen L.D., Welch M.P. and McPherson J.M. (1995). Collagen matrices attenuate the collagen synthetic response of cultured fibroblasts to TGF-β. *J. Cell Sci.* **108**: 1251-61.

Clark R.A.F. (1996). Wound repair: overview and general considerations. In: Clark R.A.F., editor. *The molecular and cellular biology of wound repair*. Second Edition. New York: Plenum Press: 3-50.

Cleary E.G. (1996). Skin. In: Comper W.D., editor. *Extracellular matrix, volume 1: tissue function*. Amsterdam, NL: Harwood Academic Publishers: 77-109.

Coleridge Smith P.D., Thomas P., Scurr J.H. and Dormandy J.A. (1988). Causes of venous ulceration: a new hypothesis. *Br. Med. J.* **296**: 1726-7.

Cook H., Stephens P., Davies K.J., Harding K.G. and Thomas D.W. (2000). Defective extracellular matrix reorganization by chronic wound fibroblasts is associated with alterations in TIMP-1, TIMP-2, and MMP-2 activity. *J. Invest. Dermatol.* **115**: 225-33.

Cox E.A., Sastry S.K., Huttenlocher A. (2001). Integrin-mediated adhesion regulates cell polarity and membrane protrusion through the Rho family of GTPases. *Mol Biol Cell* **12** (2): 265-77.

Cukierman E., Pankov R., Stevens D.R. and Yamada K.M. (2001). Taking cell-matrix adhesions to the third dimension. *Science* **294**: 1708-12.

Dalton S.L., Marcantonio E.E. and Assoian R.K. (1992). Cell attachment controls fibronectin and $\alpha 5\beta 1$ integrin levels in fibroblasts. *J. Biol. Chem.* **267** (12): 8186-91.

Dealey C. (1999). *The care of wounds: a guide for nurses*. Second Edition. Oxford: Blackwell Science Ltd.

Dean J.W. and Blankenship J.A. (1997). Migration of gingival fibroblasts on fibronectin and laminin. *J. Periodontol.* **68**: 750-7.

Dembo M. and Bell G.I. (1987). The thermodynamics of cell adhesion. In: Bronner F and Kleinzeller A, editors. Current topics in membranes and transport, vol. 29. New York: Academic Press: 71-89.

Denholm E.M., Cauchon E., Poulin C. and Silver P.J. (2000). Inhibition of human dermal fibroblast proliferation by removal of dermatan sulphate. *Eur. J. Pharm.* **400**: 145-53.

Déry O. and Bunnett N.W. (1999). Proteinase-activated receptors: a growing family of heptahelical receptors for thrombin, trypsin and tryptase. *Biochem. Soc. Trans.* **27**: 146-254.

Desmouliere A., Geinoz A., Gabbiani F. and Gabbiani G. (1993). Transforming growth-factor-beta-1 induces alpha-smooth muscle actin expression in granulation-tissue myofibroblasts and in quiescent and growing cultured fibroblasts. *J. Cell Biol.* **122** (1): 103-11.

DiMilla P.A., Stone J.A., Quinn J.A., Albelda S.M. and Lauffenburger D.A. (1993). Maximal migration of human smooth muscle cells on fibronectin and type IV collagen occurs at an intermediate attachment strength. *J. Cell Biol.* **122**: 729-737.

Dimri G.P., Lee X., Basile G., Acosta M., Scott G., Roskelley C., Medrano E.E., Linskens M., Rubelj I., Pereira-Smith O., Peacocke M. and Campisi J. (1995). A biomarker that identifies senescent human cells in culture and in aging skin *in vivo*. *Proc. Natl. Acad. Sci. USA* **92**: 9363-7.

DiPietro L.A. (1995). Wound healing: the role of the macrophage and other immune cells. *Shock* **4** (4): 233-40.

Dissemond J., Kopperman M., Esser S., Schultewolter T., Goos M. and Wagner S.N. (2002). Treatment of methicillin-resistant *Staphylococcus aureus* (MRSA) as part of biosurgical management of a chronic leg ulcer. *Hautarzt* **53** (9): 608-12.

Drake S.L., Klein D.J., Mickelson D.J., Oegema T.R., Furcht L.T. and McCarthy J.B. (1992). Cell surface phosphatidylinositol-anchored heparan sulphate proteoglycan initiates mouse melanoma cell adhesion to a fibronectin-derived, heparin-binding synthetic peptide. *J. Cell Biol.* **117**: 1331-41.

Eastwood M., McGrouther D.A. and Brown R.A. (1994). A culture force monitor for measurement of contraction forces generated in human dermal fibroblast cultures: evidence for cell-matrix mechanical signalling. *Biochim. Biophys. Acta* **1201**:186-92.

Eastwood M., Porter R., Khan U., McGrouther G. and Brown R. (1996). Quantitative analysis of collagen gel contractile forces generated by dermal fibroblasts and the relationship to cell morphology. *J. Cell Physiol.* **166** (1): 33-42.

Eckes B., Aumailley M. and Krieg T. (1996). Collagens and the reestablishment of dermal integrity. In: Clark R.A.F., editor. *The molecular and cellular biology of wound repair*. Second Edition. New York: Plenum Press: 493-512.

Eckes B., Zigrino P., Kessler D., Holtkötter O., Shephard P., Mauch C. and Krieg T. (2000). Fibroblast-matrix interactions in wound healing and fibrosis. *Matrix Biol.* **19**: 325-32.

Ehrlich H.P. and Rajaratnam J.B.M. (1990). Cell locomotion forces versus cell contraction forces for collagen lattice contraction – an in vitro model of wound contraction. *Tissue Cell* **22**: 407-17.

Ehrlich H.P., Gabbiani G. and Meda P. (2000). Cell coupling, CX 43 expression and fibroblast populated collagen lattice contraction. *J. Cell. Physiol.* **184**: 86-92.

Ehrlich H.P. and Rittenberg T. (2000). Differences in the mechanism for high- versus moderate-density fibroblast-populated collagen lattice contraction. *J. Cell. Physiol.* **185**: 432-9.

Ehrmann R.L. and Gey G.O. (1956) The growth of cells on a transparent gel of reconstituted rat-tail collagen. *J. Natl. Cancer Inst.* **16**: 1375-1403.

Ellis V., Behrendt N. and Dano K. (1993). Cellular receptor for urokinase-type plasminogen activator: function in cell-surface proteolysis. *Methods Enzymol.* **223**: 223-33.

Elsdale T. and Bard J. (1972). Collagen substrata for studies on cell behaviour. *J. Cell Biol.* **54**: 626-37.

Falanga V. and Eaglestein W.H. (1993). The 'trap' hypothesis of venous ulceration. *Lancet* **341**: 1006-8.

Falanga V., Carson P., Greenberg A., Hasan A., Nichols E. and McPherson J. (1996). Topically applied recombinant tissue plasminogen activator for the treatment of venous ulcers. *Dermatol. Surg.* **22**: 643-4.

Fine J.D. and Couchman J. (1988). Chondroitin-6-sufate-containing proteoglycan as a new component of human skin dermoepidermal junction. *J. Invest. Dermatol.* **90**: 283-8.

Fray T.R., Molloy J.E., Armitage M.P. and Sparrow J.C. (1998). Quantification of single human dermal fibroblast contraction. *Tissue Eng.* **4** (3): 281-91.

French-Constant C., Dvorak H.F. and Hynes R.O. (1989). Reappearance of an embryonic pattern of fibronectin splicing during wound-healing in the adult-rat. *J. Cell Biol.* **109**: 903-14.

Friedl P. and Bröcker E.-B. (2000). The biology of cell locomotion within three-dimensional extracellular matrix. *Cell. Mol. Life Sci.* **57**: 41-64.

Gabbiani G., Ryan G.B. and Majno G. (1971). Presence of modified fibroblasts in granulation tissue and their possible role in wound contraction. *Experientia* **27**: 549-550.

Gailit J. and Clark R.A.F. (1996). Studies *in vitro* on the role of alpha v and beta 1 integrins in the adhesion of human dermal fibroblasts to provisional matrix proteins fibronectin, vitronectin, and fibrinogen. *J. Invest. Dermatol.* **106** (1): 102-8.

Gallo R.L. (2000). Proteoglycans and cutaneous vascular defense and repair. *J. Invest. Dermatol. Sympos. Proc.* **5**: 55-60.

Gallo R.L. and Bernfield M. (1996). Proteoglycans and their role in wound repair. In: Clark R.A.F., editor. *The molecular and cellular biology of wound repair*. Second Edition. New York: Plenum Press: 475-92.

Garcia A.J., Ducheyne P. and Boettiger D. (1997). Cell adhesion strength increases linearly with adsorbed fibronectin surface density. *Tissue Eng.* **3**: 197-206.

Gaudet C., Marganski W.A., Kim S., Brown C.T., Gunderia V., Dembo M. and Wong J.Y. (2003). Influence of type I collagen density on fibroblast spreading, motility, and contractility. *Biophys. J.* **85**: 3329-35.

Ghosh M.M., Boyce S., Layton C., Freedlander E. and MacNeil S. (1997). A comparison of methodologies for the preparation of human epidermal-dermal composites. *Ann. Plastic Surg.* **39**: 390-404.

Giancotti F.G. and Ruoslahti E. (1999). Integrin signalling. *Science* **285**: 1028-32.

Goldstein A.S. and DiMilla P.A. (2002). Effect of adsorbed fibronectin concentration on cell adhesion and deformation under shear on hydrophobic surfaces. *J. Biomed. Mat. Res.* **59** (4): 665-75.

Grant G.A, Eisen A.Z., Marmer B.L., Roswit W.T. and Goldberg G.I. (1987). The activation of human skin fibroblast procollagenase. Sequence identification of the major conversion products. *J. Biol. Chem.* **262**: 5886-9.

Greiling D. and Clark R.A.F. (1997). Fibronectin provides a conduit for fibroblast transmigration from collagenous stroma into fibrin clot provisional matrix. *J. Cell Sci.* **110**: 861-70.

Grinnell F. (1994). Fibroblasts, myofibroblasts, and wound contraction. *J. Cell Biol.* **124**: 401-4.

Grinnell F., Ho C.-H., Tamariz E., Lee D.J. and Skuta G. (2003). Dendritic fibroblasts in three-diemsional collagen matrices. *Mol. Biol. Cell* **14**: 384-95.

Gyetko M.R., Todd III R.F. Wilkinson C.C. and Sitrin R.G. (1994). The urokinse receptor is required for human monocyte chemotaxis *in vitro*. *J. Clin. Invest.* **93**: 1380-7.

Haas T.L., Davis S.J. and Madri J.A. (1998). Three-dimensional type I collagen lattices induce coordinate expression of matrix metalloproteinases MT-1MMP and MMP-2 in microvascular endothelial cells. *J. Biol. Chem.* **273** (6): 3604-10.

Hansbrough J.F. (2001). The use of bioengineered skin for burn patients. In: Falanga V., editor. *Cutaneous wound healing*. London: Martin Dunitz Ltd: 433-55.

Harris A.K., Stopak D. and Wild P. (1981). Fibroblast traction as a mechanism for collagen morphogenesis. *Nature* **290**: 249-51.

Harris P.A., Leigh I.M. and Navsaria H.A. (2001). Keratinocyte biology and dermal-epidermal interactions. In: Falanga V., editor. *Cutaneous wound healing*. London: Martin Dunitz Ltd: 39-56.

Hansbrough J.F., Doré C. and Hansbrough W.B. (1992). Clinical trials of a living dermal tissue replacement beneath meshed, split-thickness skin grafts on excised burn wounds. *J. Burn Care Rehabil.* **13**: 519-29.

Hata R.I. and Senoo H. (1989). L-ascorbic-acid 2-phosphate stimulates collagen accumulation, cell-proliferation, and formation of a 3-dimensional tissue-like substance by skin fibroblasts. *J.Cell Physiol.* **138**: 8-16.

Health Protection Agency (HPA). (2003). Staphylococcus aureus bacteraemia laboratory reports and methicillin susceptibility: England and Wales, 1992-2002. Available at: http://www.hpa.org.uk/infections/topics_az/staphylo/lab_data_staphyl.htm. [accessed 9th July, 2004]

Hehenberger K., Kratz G., Hansson A. and Brismar K. (1998). Fibroblasts derived from human chronic diabetic wounds have a decreased proliferation rate, which is recovered by the addition of heparin. *J. Dermatol. Sci.* **16**: 144-51.

Herrick S.E., Sloan P., McGurk M., Freak L., McCollum C.N. and Ferguson M.W.J. (1992). Sequential changes in histologic pattern and extracellular matrix deposition during the healing of chronic venous ulcers. *Am. J. Pathol.* **141** (5): 1085-95.

Herrick S.E., Ireland G.W., Simon D., McCollum C.N. and Ferguson M.W.J. (1996). Venous ulcer fibroblasts compared with normal fibroblasts show differences in collagen but not fibronectin production under both normal and hypoxic conditions. *J. Invest. Dermatol.* **106**: 187-93.

Hinshaw J. (2000). Larval Therapy: a review of clinical human and veterinary studies. *World Wide Wounds* [online]. Available at: <http://www.worldwidewounds.com/2000/oct/Janet-Hinshaw/Larval-Therapy-Human-and-Veterinary.html#References.> [accessed 31 October, 2000].

Hinz B., Mastrangelo D., Iselin C.E. Chaponnier C. and Gabbiani G. (2001). Mechanical tension controls granulation tissue contractile activity and myofibroblast differentiation. *Am. J. Pathol.* **159** (3): 1009-20.

Hocking D.C., Sottile J. and Langenbach K.J. (2000). Stimulation of integrin-mediated cell contractility by fibronectin polymerisation. *J. Biol. Chem.* **275** (14): 10673-82.

Horobin A.J., Shakesheff K.M., Woodrow S., Robinson C. and Pritchard D.I. (2003). Maggots and wound healing: an investigation of the effects of secretions from *Lucilia sericata* larvae upon interactions between human dermal fibroblasts and extracellular matrix components. *Br. J. Dermatol.* **148** (5): 923-933.

Hsieh P. and Chen L.B. (1983). Behaviour of cells seeded on isolated fibronectin matrices. *J. Cell Biol.* **96**: 1208-17.

Hu B., Kapila Y.L., Buddhikot M., Shiga M. and Kapila S. (2000). Coordinate induction of collagenase-1, stromelysin-1 and urokinase plasminogen activator (uPA) by the 120-kDa cell-binding fibronectin fragment in fibrocartilaginous cells: uPA contributes to activation of procollagenase-1. *Matrix Biol.* **19**: 657-69.

Huang Q.H., Dawson R.A., Pegg D.E., Kearney J.N. and MacNeil S. (2004). Use of peracetic acid to sterilize human donor skin for production of acellular dermal matrices for clinical use. *Wound Rep. Reg.* **12** (3): 276-87.

Huhtala P., Humphries M.J., McCarthy J.B., Tremble P.M., Werb Z. and Damsky C.H. (1995). Cooperative signalling by α5β1 and α4β1 integrins regulates metalloproteinase gene expression in fibroblasts adhering to fibronectin. *J. Cell Biol.* **129** (3): 867-79.

Humphries M.J. and Ayad S.R. (1983). Stimulation of DNA synthesis by cathepsin D digests of fibronectin. *Nature* **305**: 811-3.

Ignotz R.A. and Massague J. (1986). Transforming growth factor-β stimulates the expression of fibronectin and collagen and their incorporation into the extracellular matrix. *J. Biol. Chem.* **261**: 4337-40.

Iocono J.A., Ehrlich H.P., Gottrup F. and Leaper D.J. (1998). The biology of healing. In: Leaper D.J. and Harding K.G., editors. *Wounds: biology and management.* New York: Oxford University Press: 10-22.

Iozzo R.V. (1998). Matrix proteoglycans: from molecular design to cellular function. *Ann. Rev. Biochem.* **67**: 609-52.

Ishikawa O., Kondo A., Okada K., Miyachi Y. and Furumura M. (1997). Morphological and biochemical analyses on fibroblasts and self-produced collagens in a novel three-dimensional culture. *Brit. J. Dermatol.* **136**: 6-11.

Jenkins G., Redwood K.L., Meadows L. and Green M.R. (1999). Effect of gel re-organization and tensional forces on alpha 2 beta 1 integrin levels in dermal fibroblasts. *Eur. J. Biochem.* **263** (1): 93-103.

Kakibuchi M., Hosokawa K., Fujikawa M. and Yoshikawa K. (1996). The use of cultured epidermal cell sheets in skin grafting. *J. Wound Care* **5** (10): 487-90.

Klein C.E., Dressel D., Steinmacher T., Mauch C., Eckes B., Krieg T., Baukert R.B. and Weber L. (1991). Integrin α2β1 is upregulated in fibroblasts and highly aggressive melanoma cells in three-dimensional collagen lattices and mediates the reorganization of collagen I fibrils. *J. Cell Biol.* **115**: 1427-36.

Klemke R.L., Leng J., Molander R., Brooks P.C., Vuori K. and Cheresh D.A. (1998). CAS/Crk coupling serves as a "molecular switch" for induction of cell migration. *J. Cell Biol.* **140** (4): 961-72.

Knight C.G., Morton L.F., Peachey A.R., Tuckwell D.S., Farndale R.W. and Barnes M.J. (2000). The collagen-binding A-domains of integrin α1β1 and α2β1 recognize the same specific amino acid sequence, GFOGER, in native (triple helical) collagens. *J. Biol. Chem.* **7**: 35-40.

Kuhn M.A., Smith P.D., Hill D.P., Ko F., Meltzer D.D., Vande Berg J.S. and Robson M.C. (2000). In vitro fibroblast populated collagen lattices are not good models of in vivo clinical wound healing. *Wound Repair Regen.* **8** (4): 270-6.

Laemmli U.K. (1970). Cleavage of structural proteins during the assembly of the head of bacteriophage T4. *Nature* **227**: 680-5.

Lambert C.A., Soudant E.P., Nusgens B.V. and Lapière C.M. (1992). Regulation of extracellular matrix macromolecules and collagenase synthesis at a pre-translational level by mechanical forces in collagen lattices. *Lab. Invest.* **66**: 444-51.

Lambert C.A., Lapière C.M. and Nusgens B.V. (1998). An interleukin-1 loop is induced in human skin fibroblasts upon stress relaxation in a three-dimensional collagen gel but is not involved in the up-regulation of matrix metalloproteinase 1. *J. Biol. Chem.* **273**: 23143-9.

Lambert C.A., Colige A.C., Munaut C., Lapière C.M. and Nusgens B.V. (2001). Distinct pathways in the over-expression of matrix metalloproteinases in human fibroblasts by relaxation of mechanical tension. *Matrix Biol.* **20**: 397-408.

Lee T.L., Lin Y.C., Mochitate K. and Grinnell F. (1993). Stress-relaxation of fibroblasts in collagen matrices triggers ectocytosis of plasma membrane vesicles containing actin, annexins II and VI, and beta 1 integrin receptors. *J. Cell Sci.* **105** (1): 167-77.

Livant D.L., Brabec R.K., Kurachi K., Allen D.L., Wu Y., Haaseth R., Andrews P., Ethier S.P. and Markwart S. (2000). The PHSRN sequence induces extracellular matrix invasion and accelerates wound healing in obese diabetic mice. *J. Clin. Invest.* **105**: 1537-45.

Lobmann R., Pittasch D., Muhlen I. and Lehnert H. (2003). Autologous human keratinocytes cultured on membranes composed of benzyl ester of hyaluronic acid for grafting in nonhealing diabetic foot lesions: a pilot study. *J. Diabetes Comp.* **17** (4): 199-204.

Maheshwari G., Wells A., Griffith L.G. and Lauffenburger D.A. (1999). Biophysical integration of effects of epidermal growth factor and fibronectin on fibroblast migration. *Biophys. J.* **76**: 2814-23.

Maize J.C. (1998). *Cutaneous Pathology.* Philadelphia, USA: Churchill Livingstone

Malinda K.M. and Wysocki A.B. (2000). Acute and chronic wound fluids stimulate cell migration. *Mol. Biol. Cell* **11**: 245 Suppl S.

Martin D.E., Reece M.C., Maher J.E. and Reese A.C. (1988). Tissue debris at the injury site is coated by plasma fibronectin and subsequently removed by tissue macrophages. *Arch Dermatol.* **124**: 226-9.

Maryanoff B.E., Santulli R.J., McComsey D.F., Hoekstra W.J., Hoey K., Smith C.E., Addo M., Darrow A.L. and Andrade-Gordon P. (2001). Protease-activated receptor-2 (PAR-2): structure-function study of receptor activation by diverse peptides related to tethered-ligand epitopes. *Arch. Biochem. Biophys.* **386** (2): 195-204.

Mauch C., Adelmanngrill B., Hatamochi A. and Krieg T. (1989). Collagenase gene expression in fibroblasts is regulated by a three-dimensional contact with collagen. *FEBS Lett.* **250**:301-5.

Mauviel A. (1993). Cytokine regulation of metalloproteinase gene expression. *J. Cell. Biochem.* **53**: 288-95.

McCarthy J.B., Chelberg M.K., Mickelson D.J. and Furcht L.T. (1988). Localisation and chemical synthesis of fibronectin peptides with melanoma adhesion and heparin binding activities. *Biochemistry* **27**: 1380-8.

McCarthy J.B., Skubitz A.P.N., Zhao Q., Yi X-Y., Mickelson D.J., Klein D.J. and Furcht L.T. (1990). RGD-independent cell adhesion to the carboxyl-terminal heparin-binding fragment of fibronectin involves heparin-dependent and independent activities. *J. Cell Biol.* **110**: 777-87.

McCarthy J.B., Iida J. and Furcht L.T. (1996). Mechanisms of parenchymal cell migration into wounds. In: Clark R.A.F., editor. *The molecular and cellular biology of wound repair*. Second Edition. New York: Plenum Press: 373-390.

Mendez M.V., Stanley A., Park H.-Y., Shon K., Phillips T. and Menzoian J.O. (1998). Fibroblasts cultured from venous ulcers display cellular characteristics of senescence. *J. Vasc. Surg.* **28**: 876-83.

Mendez M.V., Raffetto J.D., Phillips T., Menzoian J.O. and Park H.-Y. (1999). The proliferative capacity of neonatal skin fibroblasts is reduced after exposure to venous ulcer wound fluid: a potential mechanism for senescence in venous ulcers. *J. Vasc. Surg.* **30**: 734-43.

Mignatti P., Rifkin D.B., Welgus H.G. and Parks W.C. (1996). Proteinases and tissue remodelling. In: Clark R.A.F., editor. *The molecular and cellular biology of wound repair*. Second Edition. New York: Plenum Press: 427-74.

Mohri H. (1997). Interaction of fibronectin with integrin receptors: evidence by use of synthetic peptides. *Peptides* **18** (6): 899-907.

Mosesson M.W., Siebenlist K.R., Amrani D.L. and DiOrio J.P. (1989). Identification of covalently linked trimeric and tetrameric D domains in cross-linked fibrin. *Proc. Natl. Acad. Sci. USA.* **86**: 1113.

Mumcuoglu K.Y. (2001). Clinical applications for maggots in wound care. *Am. J. Clin. Dermatol.* **2** (4): 219-27.

Mumcuoglu K.Y., Miller J., Mumcuoglu M., Friger M. and Tarshis M. (2001). Destruction of bacteria in the digestive tract of the maggot of *Lucilia sericata* (*Diptera*: *Calliphoridae*). *J. Med. Entomol.* **38** (2): 161-6.

Munevar S., Wang Y. and Dembo M. (2001a). Traction force microscopy of migrating normal and H-ras transformed 3T3 fibroblasts. *Biophys. J.* **80**: 1744-57.

Munevar S., Wang Y. and Dembo M. (2001b). Distinct roles of frontal and rear cell-substrate adhesions in fibroblast migration. *Mol. Biol. Cell* **12** (12): 3947-54.

Murphy G. and Gavrilovic J. (1999). Proteolysis and cell migration: creating a path? *Curr. Opin. Cell Biol.* **11**: 614-21.

NNIS System (1999). National Nosocomial Infections Surveillance (NNIS) System report data summary from January 1990 – May 1999, issued June 1999. *Am. J. Infect. Control* **27** (6): 520-32.

Nathan C. and Sporn M. (1991). Cytokines in context. *J. Cell. Biol.* **113**: 981-6.

Neurath H. (1989). The diversity of proteolytic enzymes. In: Beynon R.J. and Bond J.S., editors. *Proteolytic enzymes: a practical approach.* First edition. Oxford, England: IRL Press: 1-13.

Newman S.A., Frenz D.A., Tomasek J.J. and Rabuzzi D.D. (1985). Matrix-driven translocation of cells and non-living particles. *Science* **228**: 885-889.

Nowak G. and Schnellmann R.G. (1996). L-ascorbic acid regulates growth and metabolism of renal cells: improvements in cell culture. *Am. J. Physiol.* **271**:C2072-80

Nusrat A.R. and Chapman H.A. (1991). An autocrine role for urokinase in phorbol ester-mediated differentiation of myeloid cell lines. *J. Clin. Invest.* **87**: 1091-7.

Obara M., Kang M.S. and Yamada K.M. (1988). Site-directed mutagenesis of the cell-binding domain of human fibronectin: separable, synergistic sites mediate adhesive function. *Cell* **53**: 649-57

Odekon L.E., Sato Y. and Rifkin D.B. (1992). Urokinase-type plasminogen-activator mediates basic fibroblast growth factor-induced bovine endothelial-cell migration independent of its proteolytic activity. *J. Cell Physiol.* **150** (2): 258-63.

Ohgoda O., Sakai A., Koga H., Kanai K., Miyazaki T. and Hiwano Y. (1998). Fibroblast-migration in a wound model of ascorbic acid-supplemented three-dimensional culture system: the effects of cytokines and malotilate, a new wound healing stimulant, on cell migration. *J. Dermatol. Sci.* **17**: 123-31.

Oksala O., Salo T., Tammi R., Hakkinen L., Jalkanen M., Inki P. and Larjava H. (1995). Expression of proteoglycans and hyaluronan during wound healing. *J. Histochem. Cytochem.* **43** (2): 125-135.

Omagari N. and Ogawa K. (1990). Three-dimensional arrangement of fibrocytes in the dermal papilla of the human sole skin. *Okajimas Folia Anat. Jpn.* **67**: 195-202.

Ongenae K.C., Phillips T.J. and Park H.-Y. (2000). Level of fibronectin mRNA is markedly increased in human chronic wounds. *Dermatol. Surg.* **26**: 447-51.

Paladini R.D., Takahashi K., Bravo N.S. and Coulombe P.A. (1996). Onset of re-epithelialization after skin injury correlates with a reorganization of keratin filaments in wound edge keratinocytes: defining a potential role for keratin. *J. Cell Biol.* **132**: 381-97.

Pardes J.B., Tonnesen M.G., Falanga V., Eaglestein W.H. and Clark R.A.F. (1990). Skin capillaries surrounding chronic venous ulcers demonstrate smooth muscle hyperplasia and increased laminin and type IV collagen. *Clin. Res.* **38**: 628A.

Pelham R.J. and Wang Y. (1999). High resolution detection of mechanical forces exerted by locomoting fibroblasts on the substrate. *Mol. Biol. Cell* **10** (4): 935-45.

Penc S.F., Pomahac B., Winkler T., Dorschner R.A., Eriksson E., Herndon M. and Gallo R.L. (1998). Dermatan sufate released after injury is a potent promoter of fibroblast growth factor-2 function. *J. Biol. Chem.* **273** (43): 28116-21.

Pepper M.S. and Montesano M. (1992). Proteolytic balance and capillary morphogenesis. *Cell Diff. Dev.* **32**: 319-28.

Petroll W.M., Ma L., Jester J.V. (2003). Direct correlation of collagen matrix deformation with focal adhesion dynamics in living corneal fibroblasts. *J Cell Sci* **116**: 1481-91.

Pierschbacher M.D. and Ruoslahti E. (1984). Cell attachment activity of fibronectin can be duplicated by small synthetic fragments of the molecule. *Nature* **309**: 30-3.

Planus E., Barlovatz-Meimon G., Rogers R.A., Bonavaud S., Ingber D.E. and Wang N. (1997). Binding of urokinase to plasminogen activator inhibitor type-1 mediates cell adhesion and spreading. *J. Cell Sci.* **110**: 1091-8.

Porter J.C. and Hogg N. (1998). Integrins take partners: cross-talk between integrins and other membrane receptors. *Trends Cell Biol.* **8**: 390-6.

Postlethwaite A.E. and Kang A.H. (1976). Collagen and collagen peptide-induced chemotaxis of human blood monocytes. *J. Exp. Med.* **143**: 1299-1307.

Postlethwaite A.E, Seyer J.M. and Kang A.H. (1978). Chemotactic attraction of human fibroblasts to type I and III collagen and collagen-derived peptides. *Proc. Natl. Acad. Sci. USA* **75**: 871-4.

Postlethwaite A.E., Keski-Oja J., Balian G. and Kang A.H. (1981). Induction of fibroblast chemotaxis by fibronectin: localization of the chemotactic region to a 140,000-molecular weight non-gelatin-binding fragment. *J. Exp. Med.* **153**: 494-499.

Prete P.E. (1997). Growth effects of *Phaenicia sericata* larval extracts on fibroblasts: mechanism for wound healing by maggot therapy. *Life Sci.* **60** (8): 505-10.

Püschel H.-U., Chang J., Müller P.K. and Brinchmann J. (1995). Attachment of intrinsically and extrinsically aged fibroblasts on collagen and fibronectin. *J. Photochem. Photobiol. B* **27**: 39-46.

Quax P.H.A., Frisdal E., Pedersen N., Bonavaud S., Thibert P., Martelly I., Verheijen J.H., Blasi F. and Barlovatz-Meimon G. (1992). Modulation of activities and RNA level of the components of the plasminogen activation system during fusion of human myogenic satellite cells *in vitro*. *Dev. Biol.* **151** (1): 166-75.

Raffetto J.D., Mendez M.V., Marien B.J., Byers R., Phillips T.J., Park H.Y. and Menzoian J.O. (2001). Changes in cellular motility and cytoskeletal actin in fibroblasts from patients with chronic venous insufficiency and in neonatal fibroblasts in the presence of chronic wound fluid. *J. Vasc. Surg.* **33**: 1233-41.

Ramundo J. and Wells J. (2000). Wound debridement. In: Bryant R.A., editor. *Acute and chronic wounds – nursing management*. Second Edition. Missouri, USA: Mosby Inc: 157-178.

Rapraeger A.C., Krufka A. and Olwin B.B. (1991). Requirement of heparan sulfate for bFGF-mediated fibroblast growth and myoblast differentiation. *Science* **253** (June 21): 1705-8.

Reames M.K., Christensen C. and Luce E.A. (1988). The use of maggots in wound debridement. *Ann. Plastic Surg.* **21**: 388-91.

Ridley A.J., Schwartz M.A., Burridge K., Firtel R.A., Ginsberg M.H., Borisy G., Parsons J.T. and Horwitz A.R. (2003). Cell migration: integrating signals from front to back. *Science* **302**: 1704-9.

Robinson W. and Norwood V.H. (1933). The role of surgical maggots in the disinfection of osteomyelitis and other infected wounds. *J. Bone Joint Surg.* **15**: 409-12.

Robinson W. and Norwood V.H. (1934). Destruction of pyogenic bacteria in the alimentary tract of surgical maggots implanted in infected wounds. *J. Lab. Clin. Med.* **19**: 581-6.

Robinson W. (1937). The healing properties of allantoin and urea discovered through the use of maggots in human wounds. *Annu. Rep. Smithson. Inst.* **1937**: 451-61.

Robinson W. (1940) Ammonium bicarbonate secreted by surgical maggots stimulates healing in purulent wounds. *Am. J. Surg.* **47**: 111-15.

Robson M.C. and Smith P.D. (2001). Topical use of growth factors to enhance healing. In: Falanga V., editor. *Cutaneous wound healing.* London: Martin Dunitz Ltd: 379-98.

Romanelli M. (2001). The use of systemic and topical agents for wound healing. In: Falanga V., editor. *Cutaneous wound healing.* London: Martin Dunitz Ltd: 357-67.

Root-Bernstein R.S. and Root-Bernstein M.R. (1999). *Honey, Mud, Maggots and Other Medical Marvels.* Second Edition. London: Macmillan Publishers Ltd.

Ruoslahti E. and Pierschbacher M.D. (1986). Arg-Gly-Asp: a versatile cell recognition signal. *Cell* **44**:517-8.

Ruoslahti E., and Yamaguchi Y. (1991). Proteoglycans as modulators of growth factor activities. *Cell* **64**: 867-9.

Sarath G., de la Motte R.S. and Wagner F.W. (1989) In: Beynon R.J. and Bond J.S., editors. *Proteolytic enzymes: a practical approach.* First edition. Oxford, England: IRL Press: 25-55.

Saus J., Quinones S., Otani Y., Nagase H, Harris Jr E.D. and Kurkinen M. (1988). The complete primary structure of human matrix metallo-proteinase-3. Identity with stromelysin. *J. Biol. Chem.* **263**: 6742-5.

Sawhney R.K. and Howard J. (2002). Slow local movements of collagen fibers by fibroblasts drive the rapid global self-organization of collagen gels. *J. Cell Biol.* **157** (6): 1083-91.

Schor S.L., Ellis I., Dolman C., Banyard J., Humphries M.J., Mosher D.F., Grey A.M., Mould A.P., Sottile J. and Schor A.M. (1996). Substratum-dependent stimulation of fibroblast migration by the gelatin-binding domain of fibronectin. *J. Cell Sci.* **109**: 2581-90.

Senior R.M., Griffin G.L. and Mecham R.P. (1980). Chemotactic activity of elastin-derived peptides. *J. Clin. Invest.* **66**: 859-62.

Serini G., Bochaton-Piallat M.L., Ropraz P., Geinoz A., Borsi L., Zardi L. and Gabbiani G. (1998). The fibronectin domain ED-A is crucial for myofibroblastic phenotype induction by transforming growth factor-beta 1. *J Cell Biol.* **142** (3): 873-81.

Shainoff J.R., Urbanic D.A. and DiBello P.M. (1991). Immunoelectrophoretic characterisation of the cross-linking of fibrinogen and fibrin by factor XIIIa and tissue transglutaminase. *J. Biol. Chem.* **166**: 6429-37.

Sheetz M.P., Felsenfeld D.P. and Gabraith C.G. (1998). Cell migration: regulation of force on extracellular-matrix-integrin complexes. *Trends Cell Biol.* **8**: 51-4.

Sherman R.A. (2000). The Maggot Therapy Project [online]. Available at: <www.ucihs.uci.edu/path/sherman/home_pg.htm> [accessed 31 October, 2000].

Sherman R.A., Hall M.J.R. and Thomas S. (2000). Medicinal maggots: an ancient remedy for some contempory afflictions. *Annu. Rev. Entomol.* **45**: 55-81.

Siebenlist K.R. and Mosesson M.W. (1992). Factors effecting γ-chain multimer formation in cross-linked fibrin. *Biochemistry* **31**: 936.

Singer A.J. and Clark R.A.F. (1999). Cutaneous wound healing. *N. Eng. J. Med.* **341**: 738-45.

Smith B.D. (2001). Expression and regulation of the collagen family in skin. In: Falanga V., editor. *Cutaneous wound healing.* London: Martin Dunitz Ltd: 57-80.

Smith L.T., Holbrook K.A. and Madri J.A. (1986). Collagen types I, III and V in human embryonic and fetal skin. *Am. J. Anat.* **175**: 507-521.

Stanley A. and Osler T. (2001). Senescence and the healing rates of venous ulcers. *J. Vasc. Surg.* **33**: 1206-11.

Stetler-Stevenson W.G., Krutzsch H.C., Wacher M.P., Margulies I.M.K. and Liotta L.A. (1989). The activation of human type IV collagenase proenzyme. Sequence identification of the major conversion product following organomercurial activation. *J. Biol. Chem.* **264**: 1353-6.

Stoker M., O'Neill C., Berryman S. and Waxman V. (1968). Anchorage and growth regulation in normal and virus-transformed cells. *Int. J. Cancer* **3** (5): 683-93.

Streuli C.H., Schmidhauser C., Kobrin M., Bissell M.J. and Derynck R. (1993). Extracellular matrix regulates expression of the TGF-beta 1 gene. *J. Cell Biol.* **120**: 253-60.

Stryer L. (1995). *Biochemistry*. Fourth Edition. New York: W.H. Freeman and Co.

Tamariz E, and Grinnell F. (2002). Modulation of fibroblast morphology and adhesion during collagen matrix remodelling. *Mol. Biol. Cell* **13**: 3915-29.

Thomas S., Jones M., Shutler S. and Jones S. (1996). Using larvae in modern wound management. *J. Wound Care* **5** (2): 60-9.

Thomas S. and Andrews A.M., Hay N.P. and Bourgoise S. (1999). The anti-microbial activity of maggot secretions: results of a preliminary study. *J. Tissue Viability* **9** (4): 127-32.

Timpl R., Wiedemann H., van Delden V., Furthmayr H. and Kuhn K. (1981). A network model for the organization of type IV collagen molecules in basement membranes. *Eur. J. Biochem.* **120**: 203-11.

Tomasek J.J. and Akiyama S.K. (1992). Fibroblast-mediated collagen gel contraction does not require fibronectin-alpha-5-beta-1 integrin interaction. *Anat. Rec.* **234** (2): 153-160.

Tomasek J.J., Haaksma C.J., Eddy R.J, and Vaughan M.B. (1992). Fibroblast contraction occurs on release of tension in attached collagen lattices: dependency on an organized actin cytoskeleton and serum. *Anat. Rec.* **232**: 359-68.

Tomasek J.J., Gabbiani G., Hinz B., Chaponnier C. and Brown R.A. (2002). Myofibroblasts and mechanoregulation of connective tissue remodelling. *Nature Rev.* **3**: 349-63.

Trinkaus J. (1984). Cells into organs: the forces that shape the embryo. Englewood Cliffs, NJ: Prentice-Hall Inc.

Turnbull J., Powell A. and Guimond S. (2001). Heparan Sulfate: decoding a dynamic multifunctional cell regulator. *Trends Cell Biol.* **11** (2): 75-82.

Twining S.S. (1984). Fluorescein isothiocyanate-labeled casein assay for proteolytic enzymes. *Anal. Biochem.* **143**: 30-4.

Unemori E.N. and Werb Z. (1986). Reorganization of polymerised actin – a trigger for induction of procollagenase in fibroblasts cultured in and on collagen gels. *J. Cell Biol.* **103**: 1021-31.

Vaalamo M., Weckroth M., Puolakkainen P., Kere J., Saarinen P., Lauharanta J. and SaarialhoKere U.K. (1996). Patterns of matrix metalloproteinase and TIMP-1 expression in chronic and normally healing human cutaneous wounds. *Brit. J. Dermatol.* **135** (1): 52-9.

Van Exan R.J. and Hardy M.H. (1984). The differentiation of the dermis in the laboratory mouse. *Am. J. Anat.* **169**: 149-64.

Vaughan M.B., Howard E.W. and Tomasek J.J. (2000). Transforming growth factor-beta 1 promotes the morphological and functional differentiation of the myofibroblast. *Exp. Cell Res.* **257** (1): 180-9.

Vlodavsky I., Fuks Z., Ishai-Michaeli R., Bashkin P., Levi E., Korner G., Bar-Shavit R. and Klagsbrun M. (1991). Extracellular matrix-resident basic fibroblast growth factor: implication for the control of angiogenesis. *J. Cell. Biochem.* **45**: 167-76.

Wahl S.M., Hunt D.A., Wakefield L.M., McCartney-Francis N., Wahl L.M., Roberts A.B. and Sporn M.B. (1987). Transforming growth factor type beta induces monocyte chemotaxis and growth factor production. *Proc. Natl. Acad. Sci. USA* **84**: 5788-92.

Waldrop J. and Doughty D. (2000). Wound-healing physiology. In: Bryant R.A., editor. *Acute and chronic wounds – nursing management.* Second Edition. Missouri, USA: Mosby Inc: 17-39.

Waltz D.A., Sailor L.Z. and Chapman H.A. (1993). Cytokines induce urokinase-dependent adhesion of human myeloid cells. *J. Clin. Invest.* **91**: 1541-52.

Wang N. and Ingber D.E. (1994). Control of cytoskeletal mechanics by extracellular-matrix, cell-shape, and mechanical tension. *Biophys. J.* **66** (6): 2181-9.

Wang N., Planus E., Pouchelet M., Fredberg J.J. and Barlovatzmeimon G. (1995). Urokinase receptor mediates mechanical force transfer across the cell-surface. *Am. J. Physiol. – Cell Physiol.* **37** (4): C1062-6.

Weckroth M., Vaheri A., Lauharanta J., Sorsa T. and Konttinen Y.T. (1996). Matrix metalloproteinases, gelatinase and collagenase, in chronic leg ulcers. *J. Invest. Dermatol.* **106** (5): 1119-24.

Weckroth M., Vaheri A., Myohanen H., Tukiainen E. and Siren V. (2001). Differential effects of acute and chronic wound fluids on urokinase-type plasminogen activator, urokinase-type plasminogen activator receptor, and tissue-type plasminogen activator in cultured human keratinocytes and fibroblasts. *Wound Repair Regen.* **9** (4): 314-22.

Welch M.P., Odland G.F. and Clark R.A.F. (1990). Temporal relationships of F-actin bundle formation, collagen and fibronectin matrix assembly, and fibronectin receptor expression to wound contraction. *J. Cell Biol.* **110**: 133-45.

West M.D., Pereira-Smith O.M. and Smith J.R. (1989). Replicative senescence of human skin fibroblasts correlates with a loss of regulation and overexpression of collagenase activity. *Exp. Cell Res.* **184**: 138-47.

Wilhelm S.M., Collier I.E., Kronberger A., Eisen A.Z., Marmer B.L. Grant G.A., Bauer E.A. and Goldberg G.I. (1987). Human skin fibroblast stromelysin: structure, glycosylation, substrate specificity and differential expression in normal and tumorigenic cells. *Proc. Natl. Acad. Sci. USA* **84**: 6725-9.

Wilson E.H., Doan C.A. and Miller D.F. (1932). The Baer maggot treatment of osteomyelitis. Preliminary report of 26 cases. *JAMA* **98**:1149-52.

Witt D.P. and Lander A.D. (1994). Differential binding of chemokines to glycosaminoglycan subpopulations. *Curr. Biol.* **4**: 394-400.

Woessner Jr J.F. (1991). Matrix metalloproteinases and their inhibitors in connective tissue remodelling. *Faseb J.* **5**: 2145-54.

Wolff H. and Hansson C. (1999). Larval therapy for a leg ulcer with methicillin-resistant *Staphyloccocus aureus*. *Acta Derm-Venereol.* **79**: 320-1.

Woods A., McCarthy J.B., Furcht L.T., Couchman J.R. (1993). A synthetic peptide from the COOH-terminal heparin-binding domain of fibronectin promotes focal adhesion formation. *Mol. Biol. Cell* **4**: 605-13.

Woods A., Longley R.L., Tumova S. and Couchman J.R. (2000). Syndecan-4 binding to the high affinity heparin-binding domain of fibronectin drives focal adhesion formation in fibroblasts. *Arch. Biochem. Biophys.* **374** (1): 66-72.

Wolfe S.L. (1995). *An Introduction to Cell and Molecular Biology.* Belmont, CA: Wadsworth Publishing Company.

Wollina U., Liebold K., Schmidt W., Hartmann M. and Fassler D. (2002). Biosurgery supports granulation and debridement in chronic wounds – clinical data and remittance spectroscopy measurement. *Int. J. Dermatol.* **41**: 635-639.

Woods A. and Couchman J.R. (1998). Syndecans: synergistic activators of cell adhesion. *Trends Cell Biol.* **8** (May): 189-192.

Woods A., McCarthy J.B., Furcht L.T. and Couchman J.R. (1993). A synthetic peptide from the COOH-terminal heparin-binding domain of fibronectin promotes focal adhesion formation. *Mol. Biol. Cell* **4**: 605-13.

Wysocki A.B. (2000). Anatomy and physiology of skin and soft tissue. In: Bryant R.A., editor. *Acute and chronic wounds – nursing management.* Second Edition. Missouri, USA: Mosby Inc: 1-16.

Xu J. and Clark R.A.F. (1995). Extracellular matrix alters PDGF regulation of fibroblast integrins. *J. Cell Biol.* **132**: 239-49.

Yamada K.M. and Clark R.A.F. (1996). Provisional matrix. In: Clark R.A.F., editor. *The molecular and cellular biology of wound repair*. Second Edition. New York: Plenum Press: 51-93.

Yamada K.M., Gailit J. and Clark R.A.F. (1996). Integrins in wound repair. In: Clark R.A.F., editor. *The molecular and cellular biology of wound repair*. Second Edition. New York: Plenum Press: 311-38.

Zamir E., Katz B.Z., Aota S., Yamada K.M., Geiger B. and Kam Z. (1999). Molecular diversity of cell-matrix adhesions. *J. Cell Sci.* **112** (11): 1655-69.

APPENDIX

A.1. Phosphate buffered saline (PBS) composition

The following was made up in distilled H_2O:

Component	Concentration (M)
NaCl	0.160
KCl	0.003
Na_2HPO_4	0.008
KH_2PO_4	0.001

A.2. Preparation of fluorescein isothiocyanate (FITC)-casein conjugate

- 1 g casein dissolved in 100 ml of 50 mM Na_2CO_3 / $NaHCO_3$ buffer (pH 9.5) containing 150 mM NaCl. pH adjusted after dissolution if necessary.

- 40 mg fluorescein isothiocyanate (FITC) then added and mixed gently for 1 hour at RT.

- Solution dialysed twice against 2 L distilled H_2O containing 1 g/L activated charcoal. Solution then dialysed against 2 L 50 mM Tris-HCl (pH 8.5), followed by 2 L 50 mM Tris-HCl (pH 7.2).

- Protein concentration adjusted to 0.5 %. Solution aliquoted and stored at -20°C until required.

A.3. Preparation of 4 % paraformaldehyde

- 10 g paraformaldehyde added to 75 ml distilled H_2O and heated to 60°C.

- 1M NaOH added until solution became clear. Solution allowed to cool.

- Volume made up to 100 ml using distilled H_2O, thus producing 10 % paraformaldehyde solution. Solution then filtered through Whatman No.1 filter paper.

- 80 ml 10 % paraformaldehyde mixed with 100 ml 0.2 M NaH_2PO_4 / Na_2HPO_4 buffer (pH 7.4). pH adjusted after mixing if necessary.

- Volume made up to 200 ml using distilled H_2O, thus producing 4 % paraformaldehyde. pH adjusted after mixing if necessary. Solution aliquoted and stored at -20°C until required.

A.4. FITC-phalloidin staining procedure – solutions used

i. Preparation of permeabilising solution

The following was mixed in distilled H_2O, adjusted to pH 7.4 and then Triton X-100 added to 0.5 % concentration:

Component	Concentration (M)
HEPES	0.020
Sucrose	0.300
NaCl	0.050
$MgCl_2$	0.003

ii. Preparation of FITC-phalloidin

- FITC-phalloidin stock solution was made by mixing 100 µg FITC-phalloidin with 120 µl ethanol. Solution was stored at -20°C in 10 µl aliquots until required.

- FITC-phalloidin working solution was made by mixing 10 µl aliquot of the FITC-phalloidin stock solution with 1 ml 1 % BSA/PBS. Working solution was made up fresh, as and when required.

iii. Preparation of propidium iodide (PI)

- PI stock solution was made by mixing 10 mg PI with 1 ml PBS. Solution was stored at 4°C in the dark until required.

- PI working solution was made by mixing 10 µl of the PI stock solution with 10 ml 1 % BSA/PBS. Solution was stored at 4°C in the dark until required.

A.5. Preparation of samples and acrylamide gels for SDS-PAGE

Protein present within a sample was precipitated using ice-cold acetone. Supernatant was then removed and replaced with 20 µl reducing sample buffer, made up as follows:

Component	Amount added to make 10 ml total volume
0.5 M Tris/HCl pH 6.8	2 ml
Glycerol	2 ml
10 % (w/v) SDS*	4 ml
1 % Bromophenol blue	0.2 %
Dithiothreitol	0.154 g (for end concentration of 0.1 M)
Distilled H_2O	2 ml

For the gels, the following components were mixed at the volumes shown below. APS and TEMED were added immediately before pouring the solution between plates that had been assembled in the mini gel apparatus. Volumes made were sufficient for 2 gels.

Component	Stacking gel (4 % acrylamide). Volume added (ml)	Resolving gel (12 % acrylamide). Volume added (ml)
acrylamide/bisacrylamide (30 %:0.8 % w/v)	0.65	4.80
0.5 M Tris/HCl pH 6.8	1.25	-
1.5 M Tris/HCl pH 8.8	-	3.00
10 % (w/v) SDS*	0.05	0.12
Distilled H_2O	2.98	4.08
10 % (w/v) APS**	0.025	0.06
TEMED***	0.01	6×10^{-3}

The SDS-PAGE electrode buffer consisted of:

Component	Concentration (M)
Tris	0.025
Glycine	0.19
SDS*	3.5×10^{-3}

* SDS: sodium dodecyl sulphate.

** APS: ammonium persulphate.

*** TEMED: N,N,N,N- tetramethyl-ethylenediamine.

A.6. Preparation of collagen gels

i. Preparation for final collagen concentration of 1 mg/ml

Solution A – collagen stock	Solution B – 1.5 × cell culture medium
3 mg/ml acid-solubilised bovine collagen type I	20.07 g DMEM† powder 73.95 ml $NaHCO_3$ (7.5 % solution) 37.5 ml HEPES†† 15 ml AB/AM††† 15 ml L-Glutamine (0.2 M)
	Solution B made up to final volume of 955 ml with distilled H_2O and sterile-filtered

For 10 ml of 1 mg/ml collagen solution containing 1 × concentration of cell culture medium:

Solution A	3.333 ml
Solution B	6.366 ml
Distilled H_2O (or where specified, fibronectin at 1 mg/ml)	0.300 ml

Final component concentrations:

Collagen	1 mg/ml
DMEM†	1 × concentration
$NaHCO_3$	3.7 g/l
HEPES††	25 mM
AB/AM†††	100 units/ml penicillin G, 100 µg/ml streptomycin sulphate, 0.25 µg/ml amphotericin B
L-Glutamine	2 mM
Fibronectin (present where specified)	30 µg/ml

ii. Preparation for final collagen concentration of 1.5 mg/ml

Solution A – collagen stock	Solution B – 1.5 × cell culture medium
3 mg/ml acid-solubilised bovine collagen type I	26.76 g DMEM† powder 98.6 ml $NaHCO_3$ (7.5 % solution) 50 ml HEPES†† 20 ml AB/AM††† 20 ml L-Glutamine (0.2 M)
	Solution B made up to final volume of 940 ml with distilled H_2O and sterile-filtered

For 10 ml of 1.5 mg/ml collagen solution containing 1 × concentration of cell culture medium:

Solution A	5.000 ml
Solution B	4.700 ml
Distilled H_2O (or where specified, fibronectin at 1 mg/ml)	0.300 ml

Final component concentrations:

Collagen	1 mg/ml
DMEM†	1 × concentration
$NaHCO_3$	3.7 g/l
HEPES††	25 mM
AB/AM†††	100 units/ml penicillin G, 100 µg/ml streptomycin sulphate, 0.25 µg/ml amphotericin B
L-Glutamine	2 mM
Fibronectin (present where specified)	30 µg/ml

† DMEM: Dulbecco's Modified Eagle's Medium.

†† HEPES: N-(2-hydroxyethyl)piperazine-N'-(2-ethanesulphonic acid); 4-(2-hydroxyethyl)piperazine-1-ethanesulphonic acid.

††† AB/AM: antibiotic/antimycotic solution (10,000 units/ml penicillin G, 10 mg/ml streptomycin sulphate and 25 µg/ml amphotericin B).

A.7. Preparation of 1-4 diazabicyclo-2-2-2-octane (DABCO)

- DABCO stock solution was made by mixing 20 mg DABCO with 20 ml PBS. Solution was adjusted to pH 8.6 and stored at 4°C until required.

- DABCO working solution was made by mixing 2 ml of the DABCO stock solution with 18 ml glycerol, giving a final concentration of 2.5 % DABCO. Working solution was made up fresh as and when required.

THESIS CONTAINS CD ROM